Year : 2022

Structure-function study of PKS (Phytochrome Kinase Substrate) proteins

López Vázquez Ana

UNIL | Université de Lausanne

Faculté de biologie
et de médecine

Centre Intégratif de Génomique

Structure-function study of PKS (Phytochrome Kinase Substrate) proteins

Thèse de doctorat

présentée à la Faculté de biologie et de médecine de l'Université de Lausanne

pour l'obtention du grade de

Docteure ès sciences de la vie (PhD)

par

Ana López Vázquez

Master of Molecular Genetics and Biotechnology, University of Seville, Spain

Directeur de these

Prof. Christian Fankhauser

Jury

Prof. Alexandre Roulin, Président

Prof. Cyril Zipfel, Expert

Prof. Christian Hardtke, Expert

Lausanne 2022

Imprimatur

Vu le rapport présenté par le jury d'examen, composé de

Président·e	Monsieur	Prof.	Alexandre	**Roulin**
Directeur·trice de thèse	Monsieur	Prof.	Christian	**Fankhauser**
Expert·e·s	Monsieur	Prof.	Cyril	**Zipfel**
	Monsieur	Prof.	Christian	**Hardtke**

le Conseil de Faculté autorise l'impression de la thèse de
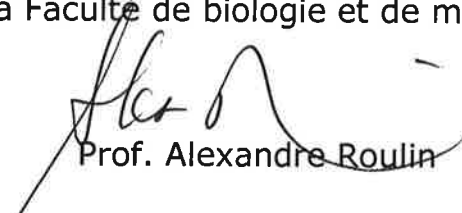
Ana López Vázquez

Master in Molecular genetics and biotechnology, Université de Séville, Espagne

intitulée

Structure-function study of PKS (Phytochrome Kinase Substrate) proteins

Lausanne, le 15 décembre 2022

pour le Doyen
de la Faculté de biologie et de médecine

Prof. Alexandre Roulin

THANK YOU

First of all, I would like to especially thank Prof. Christian Fankhauser for accepting me in his lab and allowing me to undertake a project that had a lot of interesting unresolved questions, which provided me with a broad field to build upon and fruitfully enabled this comprehensive PhD thesis work. I also thank him for his continuous guidance and support through the past five years and for being critical of my scientific writing, reasoning, and logic skills, and for teaching me the methodology to improve those weaknesses. This was very useful for my progress and I will always keep his advice in mind for future projects. I thank him for giving me the opportunity of writing together the submitted manuscript of the first chapter of this work and supervising a master's student, which allowed me to acquire very valuable skills.

I would also like to thank Prof. Alexandre Roulin, Prof. Christian Hardtke, and Prof. Cyril Zipfel for accepting to be part of my thesis jury and making interesting suggestions during my mid-term thesis exam to complete the continuation of my research work. I also thank my mentor Prof. Richard Benton for providing additional advice.

I especially thank Martine Trevisan and Laure Allenbach Petrolati for their continuous help and advice in the lab over the past five years. Special thanks to Martina Legris for making comments on the manuscript of this work and for helping with additional experiments required for the revision of the submitted work. Special thanks to Anne-Sophie Fiorucci for helping me with the French translation of the abstracts of this thesis. Special thanks to Alexandre Dudt, a master's student who I supervised during my 4th year of the doctorate, for his contribution to this work. I thank the rest of the past and current members of the Fankhauser lab for their help, support, and good atmosphere in the lab during the past years: Anne-Sophie Fiorucci, Vinicius Costa Galvao, Olivier Michaud,

association, which was an exciting experience on a side of my PhD studies. I thank many other from the dancing society, especially Andrea Guerrieri, Joana Filipa Vieira Duarte, and Gianrocco Lazzari for sharing good moments discovering the wonderful Swiss mountains and for their patience in teaching me how to stand up on the skies.

Finally, I would like to thank my parents, Javier López Sánchez and Esperanza Vázquez Becerra, for having made big efforts to support my studies and for being always there despite the distance. I thank my sister, Marina López Vázquez, for trusting me and for her support.

SUMMARY

Plants use light as a source of information to optimize their growth by driving numerous adaptive responses and developmental transitions. The determination of hypocotyl growth orientation results from the integration of phytochrome-mediated inhibition of gravitropism and phototropin-mediated phototropism. Phototropism arises from a phototropins (phot) activation gradient across the stem in response to unilateral blue light, which leads to an increase in growth on the shaded side of the stem resulting from asymmetric auxin accumulation.

phot form a protein complex at the plasma membrane (PM) with two families of PM-associated proteins that are possibly mediating the link between asymmetric phot activation and auxin gradient: (NONPHOTOTROPIC HYPOCOTYL 3 (NPH3) and ROOT PHOTOTROPISM 2 (RPT2) -like proteins) (NRL) and PHYTOCHROME KINASE SUBSTRATE (PKS). However, PKS molecular mechanisms in phot signaling remain unknown. *Arabidopsis thaliana* includes 4 PKS members, among which PKS4 and PKS1 are important for hypocotyl growth orientation, while PKS3 and PKS2 function in another phot-mediated response: leaf flattening.

Our phylogenetic and functional studies suggest that PKS4 is the protein family member appearing the earliest in evolution and whose function is conserved in monocots, while PKS3 and PKS2 have functionally diverged at different stages in evolution. PKS are intrinsically disordered proteins found in all angiosperms and characterized by six evolutionary conserved motifs (called A to F), whose functional importance was addressed in this work. Our data reveal that conserved Cys amino acids in motif C are required for PKS4 biological activity and association with the PM. Additionally, our work shows that motif D is essential for PKS4 function and identifies interactors of motif D in yeast that we are currently investigating to understand how PKS proteins regulate auxin asymmetric distribution to control plant organ growth orientation in response to light.

RÉSUMÉ

La lumière est une source d'informations pour les plantes, qui leur permet d'optimiser leur croissance en induisant de nombreuses réponses adaptatives et transitions développementales. Ainsi, l'orientation de la croissance de l'hypocotyle est déterminée par l'intégration de deux processus dépendants de la lumière: l'inhibition du gravitropisme médiée par les phytochromes d'une part, et le phototropisme médié par les phototropines d'autre part. Le phototropisme résulte d'un gradient d'activation des phototropines de part et d'autre de la tige en réponse à un signal lumineux bleu unilatéral. Cela entraîne une croissance accrue des cellules du côté non éclairé de la tige, conséquence d'une accumulation asymétrique d'auxine.

Les phototropines forment un complexe protéique à la membrane plasmique avec deux autres familles de protéines associées à la membrane, qui pourraient faire le lien entre l'activation asymétrique des phototropines et le gradient d'auxine : les protéines NRL (NONPHOTOTROPIC HYPOCOTYL 3 (NPH3) and ROOT PHOTOTROPISM 2 (RPT2) -like proteins) et les PKS (PHYTOCHROME KINASE SUBSTRATE). Cependant, la fonction moléculaire des PKS dans la signalisation via les phototropines est encore inconnue. *Arabidopsis thaliana* possède 4 protéines PKS, parmi lesquelles PKS4 et PKS1 sont importantes pour l'orientation de la croissance de l'hypocotyle, alors que PKS3 et PKS2 jouent un rôle dans la croissance plane des feuilles, une autre réponse développementale dépendante des phototropines.

Nos analyses phylogénétiques et fonctionnelles suggèrent que PKS4 est le membre de la famille PKS apparu le plus tôt au cours de l'évolution et que sa fonction est conservée chez les Monocotylédones, alors que PKS3 et PKS2 ont divergé fonctionnellement à plusieurs étapes au cours de l'évolution. Les PKS sont des protéines « intrinsèquement désordonnées » retrouvées chez

tous les Angiospermes et caractérisées par six motifs conservés (notés A à F), dont l'importance fonctionnelle a été analysée dans ce travail. Nos données révèlent que les acides aminés cystéines conservées dans le motif C sont nécessaires à l'activité biologique de PKS4 ainsi qu'à son association à la membrane plasmique. Par ailleurs, notre travail montre que le motif D est essentiel à la fonction de PKS4. Nous avons mis en évidence des partenaires protéiques du motif D en levure qui sont actuellement en cours d'étude afin de comprendre comment les protéines PKS régulent la distribution asymétrique d'auxine pour contrôler l'orientation de la croissance en réponse à la lumière.

Titre: Etude structure-function des protéines PKS (Phytochrome Kinase Substrate)

Projet de thèse de: Ana López Vázquez. Université de Lausanne - Centre Intégratif de Génomique

Résumé simplifié:

Contrairement aux animaux, les plantes ne peuvent se déplacer à la recherche des ressources nécessaires à leur survie. Mais nous avons tous déjà observé qu'une plante à proximité d'une fenêtre se tourne vers l'extérieur afin de recevoir plus de lumière. Ainsi, les organes végétaux peuvent bouger, ou plutôt se réorienter, de façon à trouver les conditions les plus favorables pour la photosynthèse, qui permet aux plantes de fabriquer leur propre matière organique.

Le processus de croissance orientée vers la lumière est appelé phototropisme et est dû à la présence de molécules photoréceptrices particulières appelées phototropines, qui convertissent le signal lumineux perçu en une information que la plante peut interpréter. Les phototropines sont plus actives du côté de la tige qui reçoit la lumière et elles vont diriger le transport d'une hormone de croissance, l'auxine, vers le côté non éclairé de la tige. C'est ainsi que la plante pousse dans la direction de l'éclairement. Néanmoins, nous ne comprenons pas encore bien le lien entre activation des phototropines et transport de l'auxine. Le professeur Christian Fankhauser a découvert une famille de protéines, les PKS, qui travaillent avec les phototropines et favorisent le transport de l'auxine, mais nous ne savons pas comment les PKS fonctionnent.

Dans ce travail de thèse, nous avons découvert qu'il existe des protéines PKS chez toutes les plantes à fleurs. Si chaque protéine PKS est différente des autres, elles ont toutes six segments en commun. Un de ces segments a pour rôle de maintenir PKS4 au bon endroit pour fonctionner, c'est-à-dire à la périphérie des cellules de la tige, là où se trouvent les phototropines. Un des autres segments permet à PKS4 de s'associer à d'autres protéines et cette association est importante pour l'orientation de la tige vers la lumière. Nous étudions maintenant comment ces autres protéines travaillent de concert avec PKS4 pour réguler le transport de l'auxine.

Contents

GENERAL INTRODUCTION

1. Plants use light as a source of information

Seed germination requires light, however, some seeds can germinate underground, which follows a rapid elongation of the embryonic stem (called hypocotyl), and a prominent apical hook protecting the shoot apical meristem. During this developmental stage, the seedling invests most of the energy in reaching the soil surface, therefore cotyledon expansion and leaf initiation are inhibited (Chen et al., 2004). This development in which young seedlings live from the seeds reserves after the germination in the dark is called skotomorphogenesis (etiolated growth). Once emerged from the soil, young seedlings acquire a photoautotrophic lifestyle in which plants use light as a source of energy to generate their organic material through photosynthesis. Besides, plants use light as a source of information to optimize their growth by driving numerous adaptive responses and developmental transitions, collectively known as photomorphogenesis (de-etiolated growth). Inhibition of hypocotyl and promotion of roots and cotyledons growth are rapid photomorphogenic responses after young seedlings emerge into the light (Chen et al., 2004, Gommers and Monte, 2018).

Plants in open habitats perceive direct sunlight (full sunlight situation) whose spectral composition, also called color or quality, is rather constant during the day but enriched in blue light (BL) and far-red light (FRL) during the sunset. In addition to these photoperiodic changes, plants are exposed to seasonal and latitude-related variations in light quality and to meteorological changes that cause differences in the amount (intensity) of light that they receive, for instance, clouds can reduce up to 90% of the incoming light. Light reaching plants is absorbed by pigments from the photosynthetic system and used as a source of energy to generate plant organic material through photosynthesis.

The photosynthetically active radiation (PAR) comprises the spectrum visible to the human eye (400-700 nm) but light absorption by the photosynthetic pigments primarily happens in the blue (400-500 nm) and red (600-700 nm). In addition, green plant tissues transmit or reflect FRL, which modifies the light environment in their surroundings (Fiorucci and Fankhauser, 2017).

In nature plants are often found within communities where competition for light between plants of the same height is high, as it is the case in meadows or agricultural fields. Plants detect the neighboring plants (neighbor detection situation) through the perception of an increase in FRL resulting from the reflected light by the surrounding plants which leads to a decreased red to far-red (R/FR) ratio (Franklin, 2008). In response to this neighbor detection, plants orchestrate a repertoire of morphological adaptations, collectively known as the shade-avoidance response (SAR), to outgrow competitors. SAR includes the stem and petiole elongation, leaves elevation (hyponasty), acceleration of flowering, and decrease of branching (Vandenbussche et al., 2005, Franklin, 2008, Ballaré and Pierik, 2017).

In denser canopies (canopy shade situation), the area covered by leaves increases, and the light quantity reaching the plants under the canopy decreases. The covering leaves absorb most of the BL, red (RL), and UV-B light while the filtered light is rich in green and FRL, which promotes elongation phenotypes in plants growing under the canopy. Different canopy densities and irregular leaves covering patterns allow unfiltered light to reach plants under the canopy, which inhibits SAR in addition to enabling a higher amount of light to do photosynthesis. Under these conditions, plants reorient their growth to reposition their photosynthetic organs towards favored light conditions to optimize photosynthesis (Figure 1) (Fiorucci and Fankhauser, 2017). This process known as phototropism mainly depends on BL directionality and it is the main response to light we are focusing on in this study.
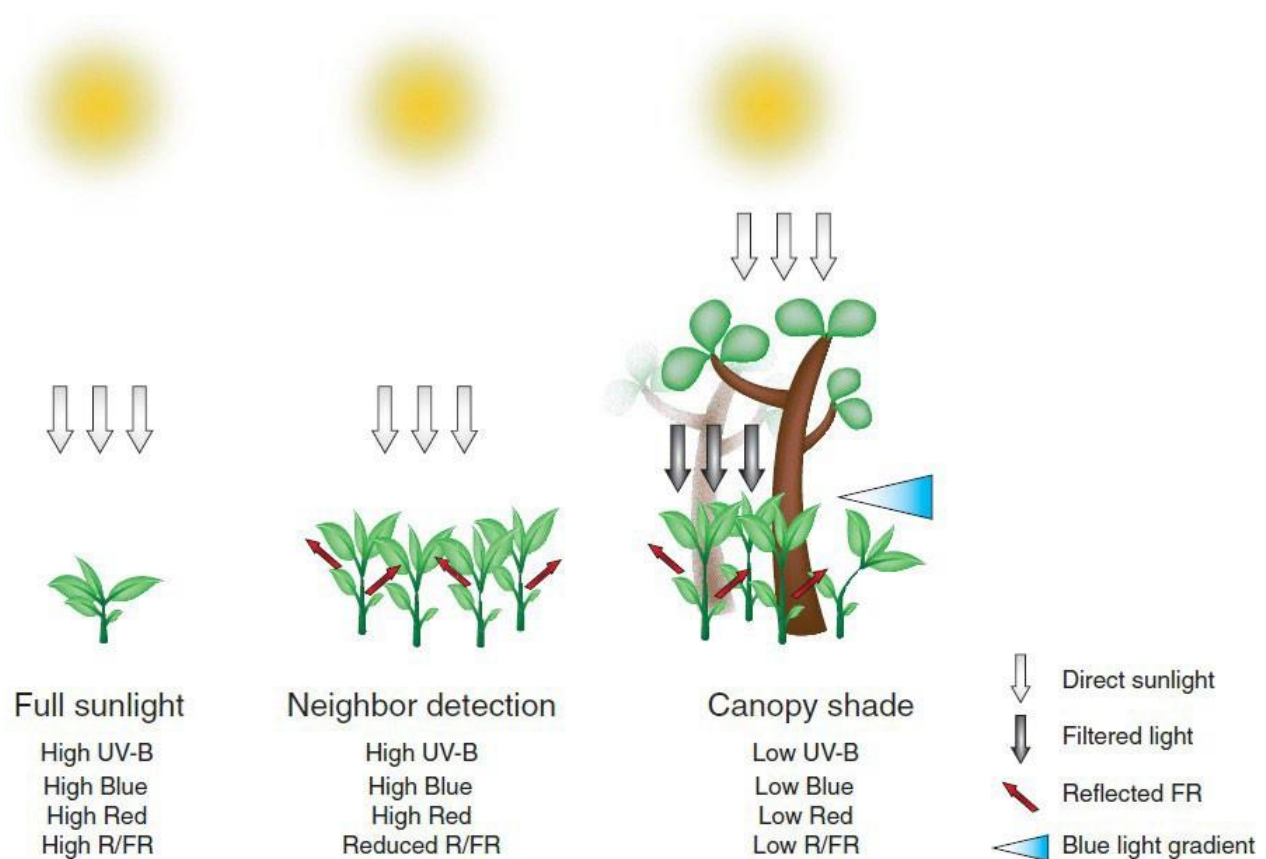
Figure 1. Plant adaptative responses to different light environments: full sunlight, neighbor detection, and canopy shade. Acquired from (Fiorucci and Fankhauser, 2017).

2. Plant photoreceptors and their involvement in different responses

Plants possess a repertoire of photoreceptors allowing them to sense changes in the amount, quality, photoperiod, and direction of light. Most of the photoreceptors are chromoproteins composed of an apo-protein bound to a variety of chromophores that determine the characteristic absorption spectra of the photoreceptors. In angiosperms, different classes of photoreceptors can be categorized based on the colors they perceive: sensors of UV-A / BL, including cryptochromes (cry), phototropins (phot), and members of the Zeitlupe family, sensors of RL and FRL, which comprise the phytochromes (phy) family, and sensors of UV-B light. In *Arabidopsis thaliana* (*A. thaliana*),

these families are represented by the members cry1 and cry2, phot1 and phot2, ztl, fkf1 and lkp2, phyA-phyE, and UVR8 respectively (Kami et al., 2010, Rizzini et al., 2011).

One single photoreceptor can be responsible for triggering some physiological responses to light, however, plants frequently integrate the information from different photoreceptors to orchestrate a coordinated response (Kami et al., 2010). For instance, important irreversible developmental transitions, such as induction of germination and transition to flowering, are controlled by phy, however, the second one is also controlled by cry and members of the Zeitlupe family (Franklin and Quail, 2010). Comparably, the combined action of phy and cry determines whether a seedling acquires an etiolated or de-etiolated development (Chen et al., 2004). Similarly, SAR and phototropism, two adaptative responses that confer plant plasticity to changes in the light environment, are mainly mediated by phy and phot respectively. However, some aspects of SAR are modulated by cry and phot, and phototropism is influenced by phy, cry, and UVR8 (Vandenbussche et al., 2005, Christie, 2007, Inoue et al., 2008, Millenaar et al., 2009, Goyal et al., 2013, Vanhaelewyn et al., 2019). Although less visible to the human eye, chloroplasts movements and opening of stomata are physiological responses for photosynthesis optimization that are mainly controlled by phot, however, cry, phy, and UVR8 also influence stomata opening (Christie, 2007, Kami et al., 2010, Galvão and Fankhauser, 2015).
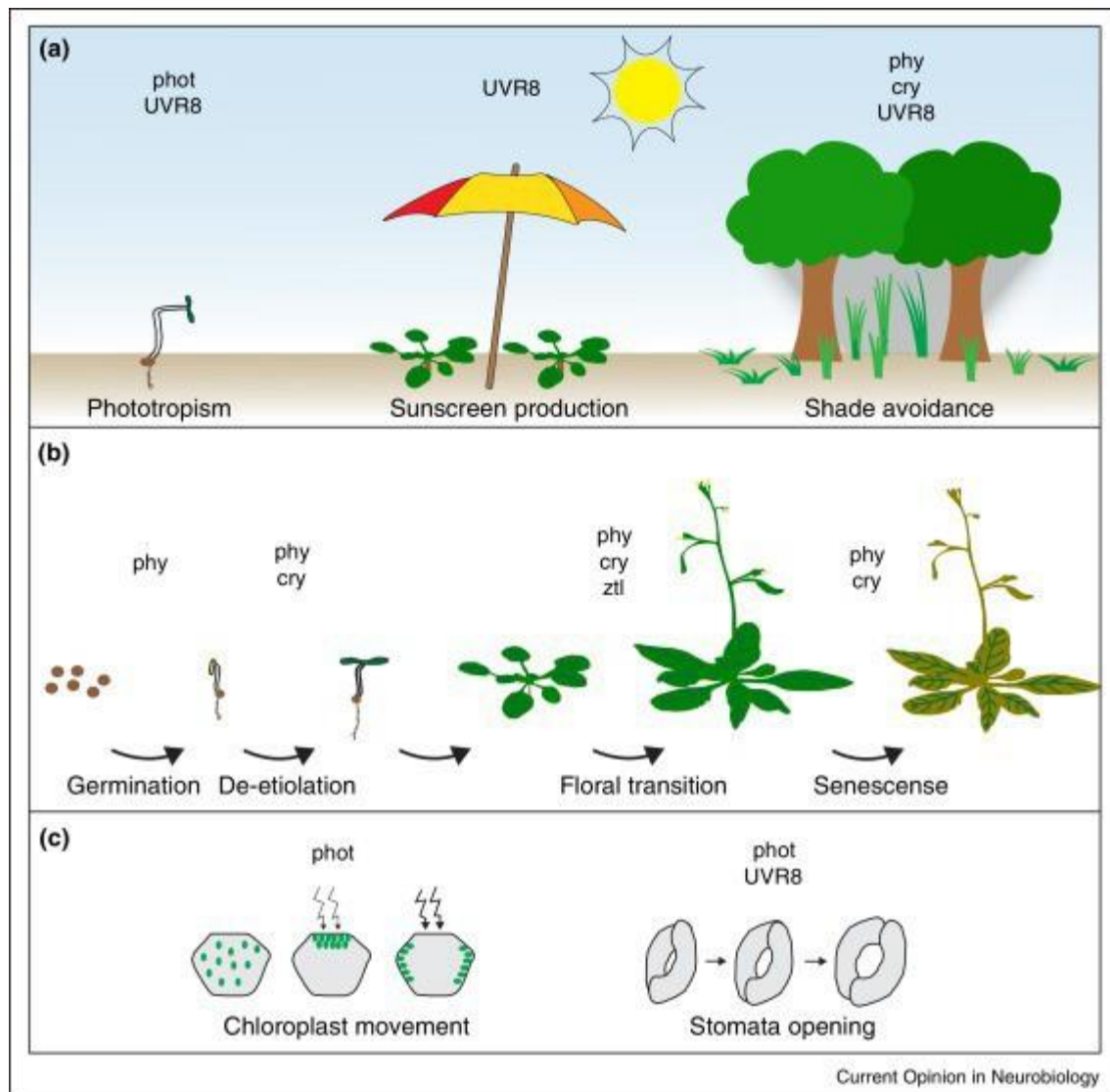
Figure 2. Importance of different photoreceptors controlling (a) different adaptative responses, (b) developmental transitions, and (c) microscopic physiological adaptations in response to light. Acquired from (Galvão and Fankhauser, 2015).

2.1 Cryptochromes

Cryptochromes are UV-A/BL photoreceptors present in bacteria, fungi, animals, and plants. *A. thaliana* cry are important in developmental transitions in response to BL, including germination,

de-etiolation, and transition to flowering (Figure 2) (Fankhauser and Christie, 2015). Both cry1 and cry2 have important functions during de-etiolation in BL. Cry2 is photo-labile and gets degraded within hours after BL exposure. Cry2 functions in response to dim BL while cry1 is light-stable and functions at higher fluence rates (Lin et al., 1998, Miao et al., 2022). Moreover, cry exhibits more specific functions, for instance, cry2 is more involved in the photoperiodic control of flowering while cry1 modulates phototropism in response to BL (Boccaccini et al., 2020, Ponnu and Hoecker, 2022). Additionally, cry function has been analyzed in some other angiosperms (eg. Barley and Soybean) and were found to control senescence in addition to germination, de-etiolation, and control of flowering time (Galvão and Fankhauser, 2015).

cry contain an N-terminal photolyase homology region (PHR) that binds the Flavin adenine dinucleotide (FAD) chromophore involved in light sensing and an intrinsically disordered C-terminal region (CCT) important for the interaction with proteins involved in signal transduction. cry exist as monomers in the darkness, however upon BL excitation, the reduction of the chromophore leads to homo- and hetero-oligomers, a process that can be inverted by thermal dark reversion (Figure 3b) (Liu et al., 2020). PHR interacts with a family of CRYPTOCHROME-INTERACTING bHLH (CIB) transcription factors to regulate flowering time and seedling de-etiolation (Wang and Lin, 2020).

The BLUE LIGHT INHIBITOR OF CHRYPTOCHROMES (BIC) BIC1 and BIC2 expression is induced by BL, RL, and UV-B light providing a negative feedback regulation of cry given that BIC1 and BIC2 can interact with the PHR inhibiting cry oligomerization and the signaling cascade leading to function (Wang et al., 2016, Miao et al., 2022, Ponnu and Hoecker, 2022). Additionally, cry signaling activation requires CCT, which involves cry phosphorylation and degradation (Wang et al., 2015). Cry2 phosphorylation by the PHOTOREGULATORY PROTEIN KINASES (PPK1-

PPK4) family is required for function. PPKs are constituted by an N-terminal region containing a Ser/Thr protein kinase domain and a C-terminal non-catalytic region that interacts with the CCT (Liu et al., 2017). Photo-activated and phosphorylated cry2 is degraded by the COP1/SPA E3 ubiquitin ligase. Moreover, Light-Response Brick-a-Brack/Trambrack/Broad (LRB) E3 ubiquitin ligases also rapidly degrade photo-activated cry2, a process depending on the PPK-mediated cry2 phosphorylation (Chen et al., 2021).

In the darkness, the E3 ubiquitin ligase COP1 mediates the poly-ubiquitination and degradation of transcription factors that activate gene expression promoting photomorphogenesis. Among COP1/SPA complex targets are ELONGATED HYPOCOTYL5 (HY5) and CONSTANS (CO), which promote de-etiolation and flowering respectively. BL-photo-activated cry interact with COP1 inhibiting the poly-ubiquitination and degradation of these transcription factors, which enables their accumulation and promotion of photomorphogenesis (Ponnu and Hoecker, 2022). One of the mechanisms through which cry prevents COP1 from degrading its substrates is by binding to COP1 through the WD-repeat domain, where COP1 substrates bind. This competitively displaces substrates from the COP1 WD-repeat domain in response to light, allowing the expression of light-regulated genes (Lau et al., 2019, Ponnu et al., 2019, Ponnu and Hoecker, 2022).

2.2 Phototropins

Phototropins are BL photoreceptors present in all green algae and land plants (Christie et al., 2018). *A. thaliana* includes two phot (phot1 and phot2) involved in phototropism, chloroplasts movement, and stomata opening (Figure 2). They contain an N-terminal light-sensing portion constituted of two Light Oxygen Voltage (LOV) domains, each binding a Flavin mononucleotide (FMN) chromophore, and a C-terminal Ser/Thr protein kinase domain involved in signal transduction (Figure 3c) (Christie, 2007, Tokutomi et al., 2008). They belong to the AGC family of protein

kinases (cAMP-dependent protein kinase, cGMP-dependent protein kinase G, and phospholipid-dependent protein kinase C) and are members of the AGC-VIIIb subfamily (Christie, 2007).

In the dark, phot are inactive with their LOV domains non-covalently binding oxidized FMN. BL irradiation on the LOV domains leads to the formation of a covalent bond between the C4a carbon of the FMN and the sulfur atom of a conserved Cysteine amino acid (Cys), which is essential for this photochemical reaction. The FMN-cysteinyl adduct is formed within microseconds and can no longer absorb BL, representing the active signaling state leading to photoreceptor activation (Christie et al., 2015). This adduct causes conformational changes in the LOV2 domain and two helical structures (A'α and Jα) flanking it, which liberates the C-terminal kinase domain from the inhibitory activity of the photosensory domain (Harper et al., 2003, Tokutomi et al., 2008). The photochemical reactions can be reverted by the transition to darkness, a process taking a bit longer than the activation.

The primary step of phot activation is autophosphorylation. Several BL-induced phosphorylation sites have been identified in phot1 and phot2 photosensory and kinase domains, but only the phosphorylation in the activation loop of the protein kinase domain is essential for all the tested phot-dependent physiological responses (Inoue et al., 2008, Sullivan et al., 2008, Inoue et al., 2011). Following these common initial signaling events, the subsequent signaling steps differ depending on the physiological response. For instance, molecular signaling leading to stomata opening requires the phosphorylation of the Ser/Thr kinase BLUE LIGHT SIGNALING1 (BLUS1) for the activation of an H^+-ATPase leading to the swelling of the guard cells (Takemiya et al., 2013). However, phototropism involves phot-induced phosphorylation and dephosphorylation of other key signaling components, which will be described in more detail later (Legris and Boccaccini, 2020).

2.3 Zeituples

ZEITLUPE (ztl), FLAVIN-BINDING, KELCH REPEAT, F-BOX (fkf1) and LOV KELCH PROTEIN2 (lkp2) proteins (collectively named Zeitlupes) are UV-A/BL photoreceptors present in land plants exhibiting overlapping functions. Zeitlupes contain a single FMN-binding LOV domain at their N-terminus followed by an F-box and six Kelch repeats at their C-terminus (Figure 3c). LOV domains bind oxidized FMN and exhibit a similar photochemical reactivity to that of phot, where BL irradiation triggers the formation of an FMN-cysteinyl adduct, although this process occurs much slower than in phot (Christie et al., 2015). F-boxes are associated with Skp Cullin F-box (SCF)-type E3 ubiquitin ligases, which target proteins for degradation, whereas the kelch repeats serve to mediate protein–protein interactions and heterodimerization between lkp2 and ztl and fkf1.

Through a complex interaction network, Zeitlupes have an important function in the photoperiodic control of transition to flowering by controlling gene expression in response to light through its E3 ubiquitin ligase function (Figure 2b) (Galvão and Fankhauser, 2015, Shim et al., 2017). Ztl negatively controls CO in the morning while in the long-day afternoon, BL perception leads to the interaction of FKF1 with GIGANTEA (GI), which recognizes and degrades the CYCLING DOF FACTOR (CDF) transcriptional repressors of CO, allowing CO transcriptional activation (Sawa et al., 2007, Song et al., 2014). ZTL and LKP2 stabilize CIB transcription factors that activate the expression of the florigenic gene FT (Liu et al., 2013).
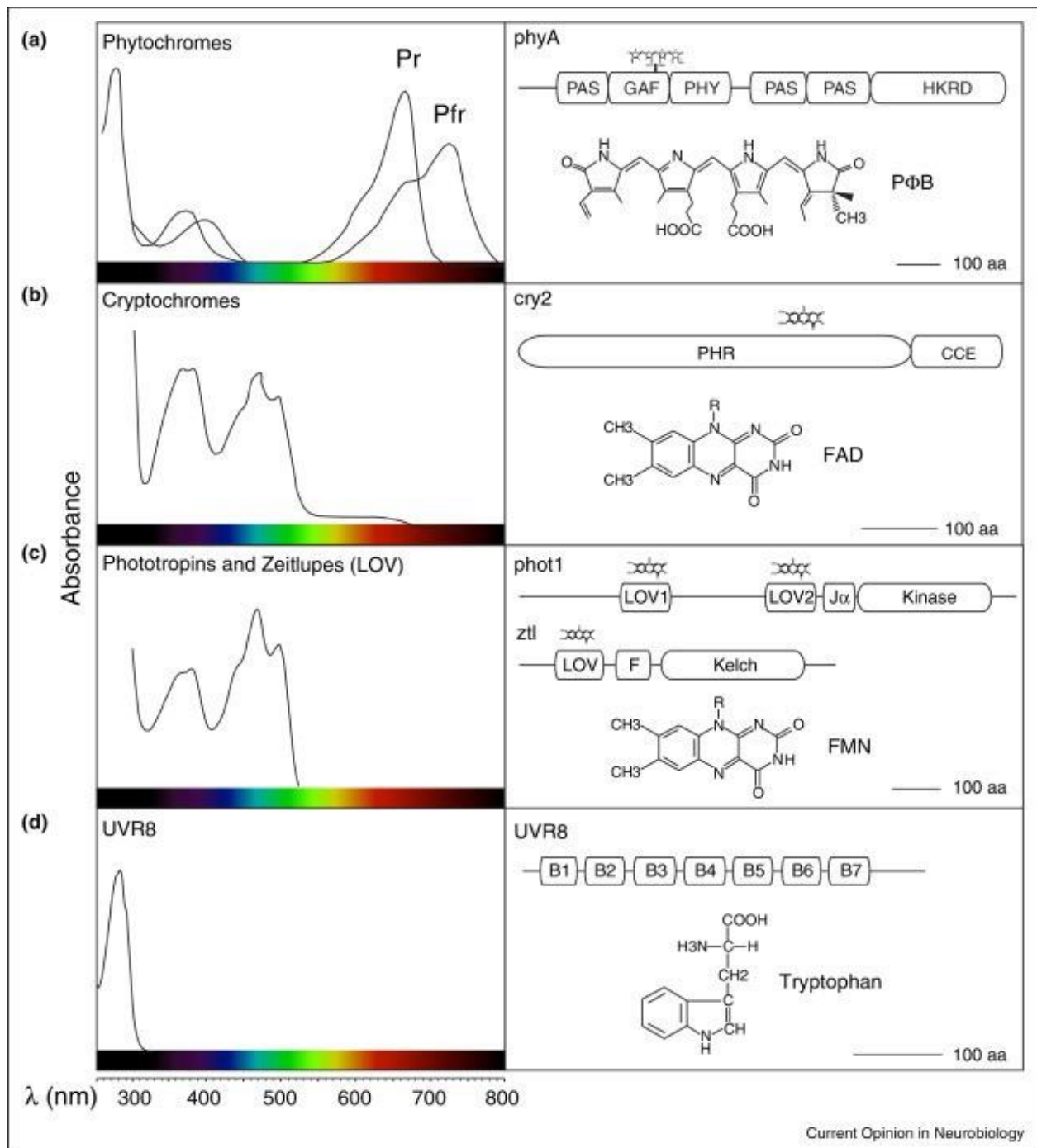
Figure 3. Illustration of the absorption spectra and chromophores of the plant photoreceptors (a) phytochromes, (b) cryptochromes, (c) phototropins and Zeitlupes, and (d) UVR8. Acquired from (Galvão and Fankhauser, 2015).

2.4 Phytochromes

Phytochromes are RL and FRL photoreceptors present in plants, fungi, and prokaryotes. They are important for SAR and developmental transitions such as germination, de-etiolation, and transition to flowering (Figures 2a and 2b). phy are synthesized in the inactive conformation (Pr) and converted to the active conformation (Pfr) upon light absorption. Pfr reverts to the Pr state in response to FRL or through thermal relaxation. They act as dimers, consequently, they can exist in three possible states: Pr-Pr, Pr-Pfr, and Pfr-Pfr. Both conformers Pr and Pfr co-exist in the light, but only after a long period of absolute darkness all the phy are converted to the Pr state, which is relevant because what leads to biological functions is the Pfr/P total ratio (Burgie and Vierstra, 2014). *A. thaliana* contains 5 phytochromes (phyA-E) that can be classified into two groups with similar absorption but different action spectra: type I phy (phyA), which are light labile and can act at very low fluence rates or strong fluence rates of FR light, and type II phy (phyB-E), which are light stable and act in a wide range of fluence rates requiring a higher amount of the active conformer to promote signaling. This relates to the fact that phyA can act as Pfr/Pr heterodimers while phyB needs Pfr/Pfr (Legris et al., 2019).

phy monomers are constituted by the apoprotein PHY covalently bound to its chromophore: a linear tetrapyrrole called phytochromobilin (PϕB). The apoprotein includes an N-terminal photosensory module (PSM) comprising an N-terminal extension (NTE), a period/Arnt/SIM (PAS) domain, a cGMP phosphodiesterase/adenylyl cyclase/FhlA (GAF) domain, and a phy-specific (PHY) domain. The C-terminal module (CTM) includes two PAS domains and a histidine kinase-related domain (HKRD) (Figure 3a). The PSM is mainly involved in light perception, signal transduction, and covalent binding of the chromophore through the GAF domain, while the CTM is involved in phy dimerization and translocation to the nucleus (Burgie and Vierstra, 2014, Li et al., 2022).

phy function requires translocation from the cytosol where they are synthesized to the nucleus, where they act. The light-activated phy (Pfr) conformers interact with members of the PHYTOCHROME-INTERACTING BASIC HELIX-LOOP-HELIX (bHLH) TRANSCRIPTION FACTORS (PIF) family of transcription factors and with E3 ubiquitin ligase complexes (Kikis et al., 2009, Podolec and Ulm, 2018). Pfr interaction with PIFs occurs through their N-terminal APB (Active phyB) or APA (Active phyA) binding domains. *A. thaliana* includes 8 PIF (PIF1-PIF8) that contain an APB domain, while only PIF1 and PIF3 contain an APA domain. PIF interaction with phy generally leads to PIF inactivation, implying changes in transcriptional regulation. PIF inactivation occurs through different mechanisms, among them, preventing PIF binding to the DNA or through PPK-mediated PIF phosphorylation followed by poly-ubiquitination and proteasome degradation (Ni et al., 2014, Ni et al., 2017, Legris et al., 2019).

2.5 UVR8

UV RESISTANCE LOCUS8 (UVR8) is a UV-B photoreceptor present from algae to flowering plants that modulates gene expression driving photomorphogenesis and induction to flowering in addition to the production of anthocyanins and flavonols that act as UV-B protectant "sunscreen". Moreover, UVR8 has a role in phototropism, stomata opening, and the circadian clock (Figure 2) (Galvão and Fankhauser, 2015). Different from other plant photoreceptors, UVR8 does not require an extrinsic chromophore and it instead uses three closely packed tryptophan amino acids (W233, W285, and W337) to perceive light (Figure 3d) (Christie et al., 2012). UVR8 exists as an inactive homodimer mainly in the cytosol in the darkness. Upon UV-B perception, UVR8 is reversibly converted to an active monomer that accumulates in the nucleus where it functions (Podolec et al., 2021).

Active UVR8 binds to the COP1 ubiquitin ligase WD-40 repeat through a beta-propeller core domain in addition to through its VP motif. This interaction leads to the COP1 inactivation and the stabilization of the COP1 target transcription factors, such as the bZIP transcription factors HY5 and HY5-HOMOLOG (HYH), CO, and HFR1, leading to the transcriptional activation of numerous UV-B induced target genes, including REPRESSOR OF UV-B PHOTOMORPHOGENESIS 1/2 (RUP1 and RUP2) and COP1 (Podolec et al., 2021, Shi and Liu, 2021). RUP1 and RUP2 bind UVR8 active monomers with stronger affinity than the homodimer and reverts UVR8 to the inactive homodimer state. UV-B-induced UVR8 monomerization promotes its nuclear translocation via free diffusion, which is counterbalanced with the negative regulation of RUP1 and RUP2, enabling plants to continuously sense and adapt to the light environment (Fang et al., 2022). On the other hand, UVR8 directly binds to specific transcription factors and detaches them from the DNA, promoting gene expression. An example is the WRKY36 transcription factor that regulates HY5 expression at the same time. Moreover, UVR8 activation leads to PIF4 and PIF5 degradation via poly-ubiquitination and proteasome degradation through an unknown E3 ubiquitin ligase (Podolec et al., 2021).

3. Processes leading to hypocotyl growth orientation in response to light

In the cases in which seeds germinate underground, plants invest most of their energy from the seed reserves in promoting rapid growth of the hypocotyl to reach the soil surface and transition to a photoautotrophic lifestyle. During this etiolated development occurring in the dark, seedlings grow following the direction of the constant gravity stimulus: roots grow downwards and shoots grow upwards. When the seedlings emerge from the soil, the plant acquires a de-etiolated development promoting root and cotyledons and arresting the hypocotyl growth. Starting from this developmental transition, the hypocotyl or stem orientation becomes an important adaptive

response to optimize photosynthesis in a continuously changing light environment. During de-etiolated development, the determination of hypocotyl growth orientation results from an integration of responses to gravity and light stimuli, which influence the entire adult plants' physiology and development (Galen et al., 2004). The hypocotyl growth orientation in response to light is driven by the combined action of two main processes: phy-mediated inhibition of gravitropism and phot-mediated phototropism (Correll and Kiss, 2002). Although phototropism and inhibition of gravitropism are independent responses, it was proposed that phy-mediated inhibition of gravitropism enhances phot-mediated phototropism in response to BL (Lariguet and Fankhauser, 2004, Liscum et al., 2014). This study will be centered on these two processes with a special focus on phototropism.

3.1 Inhibition of gravitropism

3.1.1   Hypocotyl gravitropism in darkness

Hypocotyl gravitropism comprises gravity sensing, signal generation, and transduction, and asymmetric growth guided by the regulation of the directional distribution of the plant hormone auxin in the elongation zone (Sack, 1997, Morita and Tasaka, 2004). In flowering plants, gravity sensing in the hypocotyl occurs in specialized endodermal cells called statocytes. Statocytes accumulate starch-filled amyloplasts (also called statoliths) that sediment in the direction of gravity, the bottom of the statocytes in steady-state conditions. Little is known about the mechanisms governing this process except that statoliths' movements are influenced by intracellular components such as actin filaments and the vacuole (Li et al., 2021, Kawamoto and Morita, 2022). However, it is noteworthy to point out that the PIF transcription factors are important for starch accumulation in the amyloplasts to trigger gravitropism in the dark (Oh et al., 2004, Kim et al., 2011).

The process comprising the biophysical signal generation and transduction to the hypocotyl elongation zone, where the differential growth occurs, is not well understood, however, ALTERED RESPONSE TO GRAVITY1 (ARG1) and ARG1-LIKE2 (ARL2) have been suggested to play a role in the signal transduction following amyloplasts sedimentation (Nakamura et al., 2019) (Vandenbrink and Kiss, 2019). Additionally, LAZY1-LIKE (LZY) family has been recently proposed to play an important role in statocytes signal transduction. However, how LZY transmits the signal to the elongation zone to control auxin transport regulating gravitropism requires further investigations (Taniguchi et al., 2017, Nakamura et al., 2019, Furutani et al., 2020).

3.1.2   Phytochromes inhibit hypocotyl gravitropism

Inhibition of hypocotyl gravitropism is a photomorphogenic response affecting hypocotyl growth orientation during seedlings' emergence from the soil. During this process, the gravitropism response established in the dark is disrupted by the perception of RL and FRL, which results in hypocotyls growing with random orientation (Robson and Smith, 1996). In *A. thaliana*, the endodermal statocytes amyloplasts acquire properties of chloroplasts or etioplasts with developed thylakoids and protylakoids upon monochromatic RL and FRL elicitation. Their starch granule size becomes reduced, which diminishes the ability of seedlings to sense gravity, and, as a consequence, hypocotyls show a randomized growth orientation. This process depends on active phyB and phyA in response to RL and FRL respectively (Kim et al., 2011).

PIF transcription factors inhibit the conversion of the amyloplasts into other plastids in hypocotyl endodermal statocytes in the dark (Kim et al., 2011). However, RL triggers the activation of phyB that can transduce the signal from the epidermis to the endodermis to promote PIF degradation, which releases the PIF-mediated inhibition of the amyloplasts conversion (Kim et al., 2016a). Complementation of the *pif1pif3pif4pif5* quadruple mutant by expressing PIF1 in the endodermis

suggests a significant role of PIF1 in this response (Kim et al., 2011). Although little is known about the PIF-mediated mechanisms in this response, PIF1 directly targeting REPRESSOR OF PHOTOSYNTHETIC GENES1 (RPGE1) has been proposed to act in the regulation of amyloplasts conversion (Kim et al., 2016b). Different from most of the PIF transcription factors, PIF8 is degraded in the dark but accumulates in response to FRL. A recent study has proposed that PIF8 suppresses phyA-mediated inhibition of hypocotyl gravitropism in response to FRL by inhibiting the reduced starch composition of amyloplasts, however, the underlying mechanisms remain elusive (Oh et al., 2020).

In addition to the function of phy and PIF in the inhibition of hypocotyl gravitropism, the PHYTOCHROME KINASE SUBSTRATES (PKS) protein family has an important role (Schepens et al., 2008). PKS proteins were found as interactors of phyA and phyB binding to their C-terminal region that shares homology with the histidine kinases domain (Fankhauser et al., 1999). They also act in phy signaling to regulate other RL and FRL-mediated growth responses: de-etiolation (Fankhauser et al., 1999, Lariguet et al., 2003). Among the PKS protein family members, PKS4 is the most important to mediate inhibition of gravitropism in response to both RL and FRL, however, PKS1 also has a more discrete function only in response to RL (Schepens et al., 2008). Hypocotyl gravitropism in darkness is normal in *pks* mutants, suggesting a PKS light-specific function in hypocotyl growth orientation. However, the mechanism through which PKS proteins act in this process remains unknown.

3.2 **Phototropism**

In natural environments, the hypocotyl growth orientation is not merely the result of the randomization induced by RL and FRL, but plant hypocotyl orientates according to the directionality of the incoming light. This process known as phototropism is mainly mediated by

the BL photoreceptors phot. During positive phototropism, plants orient their photosynthetic organs toward the light to increase light capture to do photosynthesis (Holland et al., 2009). The phototropic curvature is mediated by an increase in growth on the shaded side of the stem resulting from an accumulation of the plant growth hormone auxin (Hohm et al., 2013). Generally, the first positive phototropism is referred to as the curvature that is produced in response to low fluence and short irradiation times, while the second positive phototropism is referred to as the increased curvature at higher fluence and longer irradiation times (Janoudi and Poff, 1990). However, plants can also avoid light under high light conditions to prevent photo-damage, a process known as negative phototropism (Strong and Ray, 1975).

3.2.1   Phototropins functions in different responses

In addition to phototropism, phot control other physiological responses in *A. thaliana* such as leaf positioning and flattening, chloroplast movements, and opening of stomata (Figure 4). In *A. thaliana* phot1 and phot2 exhibit both overlapping and unique functions in controlling these responses. For instance, phot1 and phot2 regulate hypocotyl phototropism in response to high BL (HBL), however, upon low BL (LBL) irradiation, this response is only mediated by phot1. This is consistent with the fact that phot1 is light-labile and the protein levels decrease in response to light, while phot2 abundance increases in response to light (Liscum et al., 2014). Comparably, phot1 and phot2 mediate the chloroplast movement in LBL while the chloroplast avoidance movement in HBL is promoted only by phot2. Moreover, phot1 and phot2 contribute equally to the opening of stomata response upon a range of light intensities (Christie, 2007).
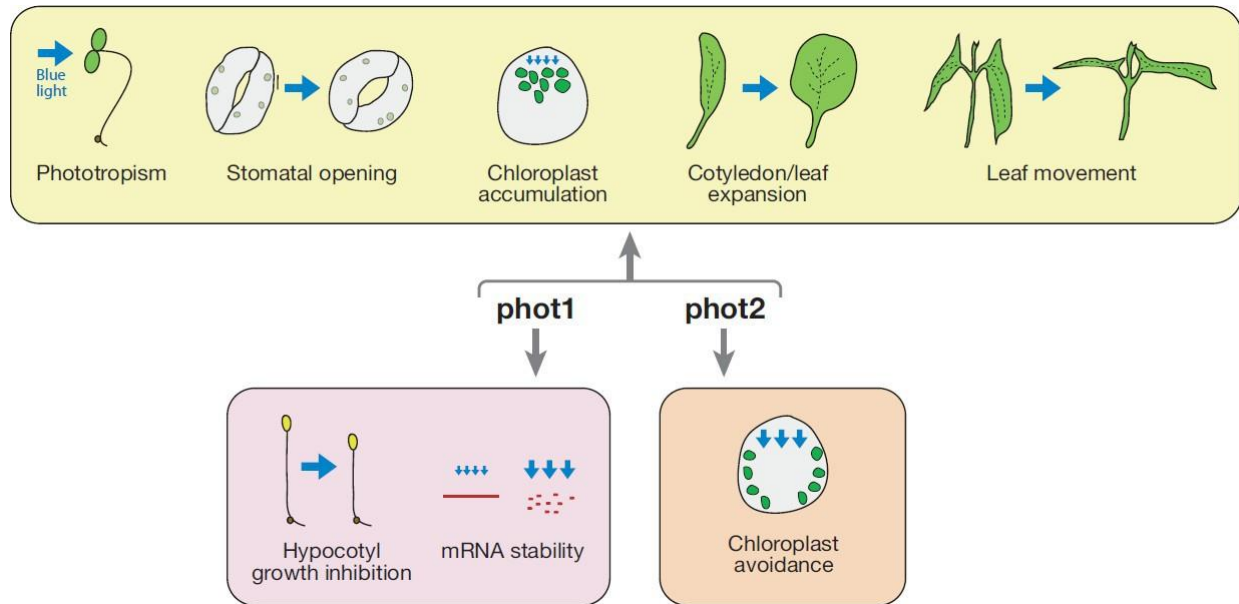
Figure 4. Phototropin-induced responses in higher plants. Adapted from (Christie, 2007).

3.2.2   Phototropins function in phototropism

Despite their hydrophilic properties, phot are proteins associated with the plasma membrane (PM). Upon BL irradiance, a fraction of phot1 rapidly migrates to the cytoplasm, while phot2 relocates to the Golgi (Sakamoto, 2002, Kong et al., 2006). Despite this prompt re-localization, phot1-dependent signaling is initiated at the PM (Preuten et al., 2015). In the darkness, phot1 exists mainly as inactive monomers at the PM, and upon BL activation phot1 form dimers in a BL fluence-dependent manner. Following this dimerization event, a functional phot1 kinase domain is required for the translocation of phot1 to membrane microdomains, where the phot1 signal transduction is activated (Xue et al., 2018).

In angiosperms, phototropic curvature in young seedlings is proposed to occur because of higher activation of phot1 on the irradiated than on the shaded side of the stem, however, how this phot1-

activation gradient across the stem leads to a lateral gradient of auxin remains poorly understood. In *A. thaliana*, phot interact with members of the families NONPHOTOTROPIC HYPOCOTYL 3 (NPH3) and ROOT PHOTOTROPISM 2 (RPT2) -like proteins (NRL) and PKS, which are involved in the early steps of phot-mediated signaling pathway inducing phototropism (Goyal et al., 2013, Boccaccini et al., 2020).
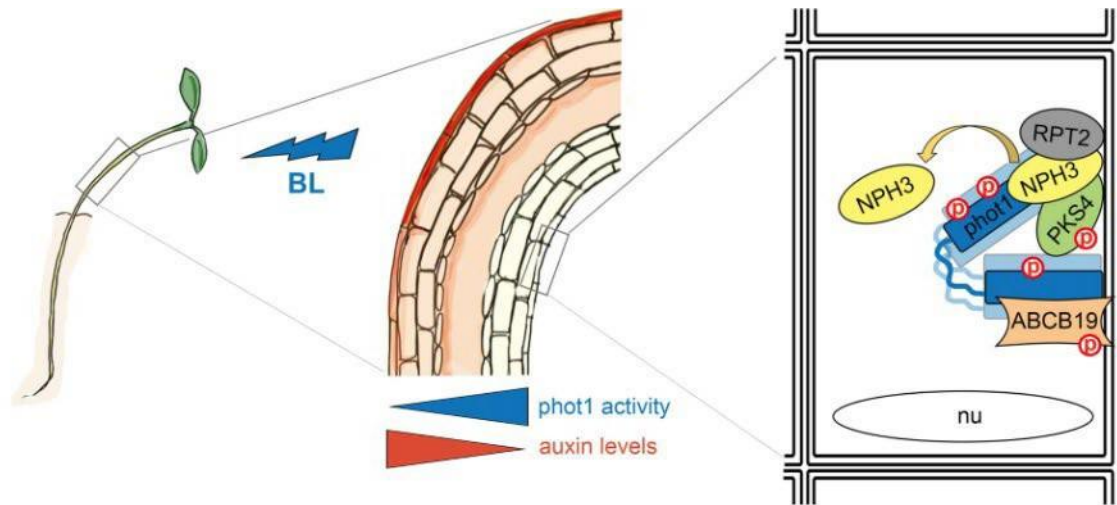
Figure 5. Unilateral BL irradiation triggers hypocotyl curvature through a phot1 activation gradient across the hypocotyl leading to an asymmetric auxin distribution that promotes cell elongation on the shaded side. BL activates phot1 at the PM triggering the molecular signaling cascade leading to phototropism. Acquired from (Legris and Boccaccini, 2020).

3.2.2.1 NPH3 and RPT2 -like proteins (NRL) family

In *A. thaliana,* the NRL family consists of around 30 members. They contain an N-terminal BTB/POZ (broad complex, tram track, and bric à brac/ Poxvirus and Zinc finger) domain involved in protein-protein interaction and four conserved regions. NPH3 interacts with phot1 and phot2 and it is required for hypocotyl and root phototropisms over a broad range of BL conditions. As phot, NPH3 has hydrophilic nature but is localized to the PM (Motchoulski and Liscum, 1999). In the darkness, NPH3 association with the PM is mainly homogeneous across the hypocotyl, however,

in response to unilateral BL, NPH3 internalizes into cytosolic aggregates, which are more abundant in the lit than in the shaded side of the hypocotyl, correlating with the phot1-activation gradient (Sullivan et al., 2019). Recent findings have shown that phototropism requires NPH3 phosphorylation in the C-terminal consensus sequence (RxS) by phot1 in response to BL, which leads to 14-3-3 binding and subsequent NPH3 disassociation from the PM poly-acidic phospholipids where it is bound in the darkness. In darkness, this process is reverted through NPH3 RxS dephosphorylation and re-association with the PM (Reuter et al., 2021, Sullivan et al., 2021). Later events lead to NPH3 dephosphorylation by a PP1-type protein phosphatase (Pedmale and Liscum, 2007). The functional significance of this process had been associated with the desensitization of phot1 signaling during the transition period from first positive phototropism to second positive phototropism (Haga et al., 2015). The NPH3 cycles of disassociation and re-association with the PM depending on the light conditions are important for NPH3 function in phototropism (Reuter et al., 2021, Sullivan et al., 2021).

Additionally, the NPH3 homologous RPT2 is specifically required in HBL- induced hypocotyl phototropism and root phototropism (Sakai et al., 2000, Inada et al., 2004). RPT2 modulates the phosphorylation of NPH3 and promotes the re-association of the phot1-NPH3 complex at the PM, required for second positive phototropism (Haga et al., 2015). NPH3 and RPT2 are also required for leaf flattening and positioning, however, they are not essential for other phot-dependent physiological responses like chloroplast avoidance or opening of stomata (Inoue et al., 2008, de Carbonnel et al., 2010, Harada et al., 2013, Kozuka et al., 2013, Tsutsumi et al., 2013). Moreover, additional members of the NRL family are required for other phot-mediated responses, for instance, RPT2 acts redundantly with the NRL member NRL PROTEIN FOR CHLOROPLAST MOVEMENT1 (NCH1) in chloroplasts accumulation (Suetsugu etal., 2016).

3.2.2.2 PKS family

3.2.2.2.1 PKS proteins function

PKS is a family of basic soluble proteins with no predicted functional domain that was originally identified as phy interactors functioning in phy signaling (Fankhauser et al., 1999, Lariguet et al., 2003, Schepens et al., 2008). In *A. thaliana*, this family includes 4 members (PKS1-PKS4), which seem to exhibit different functions in controlling different phot-mediated responses according to the analysis of the *pks* loss of function mutants' phenotype. Thereby, the phenotype of the *pks1pks2pks4* triple mutant in phototropism, which is comparable to *phot1* phenotype in LBL and more aggravated than the single and double *pks* mutants, indicates that PKS1, PKS2, and PKS4 are important for hypocotyl phototropism (Lariguet et al., 2006, Kami et al., 2014a). According to single *pks* mutants' analysis, PKS4 is the family member with the most remarkable role in phototropism, followed by PKS1 and PKS2. PKS4 synergistically functions with PKS1 to promote phototropism in response to LBL, while PKS2 functions with PKS1 to promote phototropism in response to higher BL fluence rates (Kami et al., 2014b). However, PKS3 has no function in phototropism in response to any BL fluence (Legris Martina, personal communication). In addition to its function in hypocotyl phototropism, PKS1 is also required for root negative phototropism in response to unilateral BL, while no detectable requirement of the other PKS members has been proposed for this response (Boccalandro et al., 2008).

In addition to phototropism, PKS are important in some aspects of leaf development: leaf elevation and leaf flattening. Based on *pks* single mutants' analysis, PKS3 is the PKS family member with the most important function in leaf flattening, given that *pks3* mutant lines mimic the *phot1phot2* leaf flattening phenotype (Legris et al., 2021). Moreover, PKS2, followed by PKS1, also has a role

in leaf flattening, while no function in this response has been described for PKS4 (de Carbonnel et al., 2010). Moreover, based on analysis of the *pks1pks2pks4* and *pks1pks2pks3pks4* mutants' phenotypes, PKS3 has an important role in diurnal leaf elevation response (Legris Martina, personal communication). According to the loss of function *pks* single mutants, PKS2 and PKS1 are also involved in leaf elevation in response to LBL, while PKS4 has almost no function under these conditions (de Carbonnel et al., 2010). However, PKS4 seems to synergistically function with PKS2 in leaf elevation in response to shade and wounding (Fiorucci et al., 2022). The role of PKS proteins in phot signaling appears to be restricted to growth-related responses, given that *pks* mutants are not impaired in BL-induced stomata opening nor chloroplast relocation movement (de Carbonnel et al., 2010).

In addition to their role in phot-mediated responses, PKS are also involved in phy signaling. As presented above, PKS1 and PKS4 are involved in the inhibition of hypocotyl gravitropism in response to RL and FRL (Schepens et al., 2008). Moreover, PKS4, PKS1, and PKS2 are involved in phy-mediated de-etiolation responses such as inhibition of hypocotyl growth and cotyledons unfolding (Fankhauser et al., 1999, Lariguet et al., 2003, Schepens et al., 2008).

3.2.2.2.2 PKS expression patterns

Broadly speaking, there is a good correlation between the tissue expression patterns of *PKS* genes and their main functions in phot signaling. Thereby, PKS4, PKS1, and PKS2 are expressed in the hypocotyl elongation zone of young seedlings, coinciding with their function in hypocotyl phototropism (Lariguet et al., 2003, Schepens et al., 2008, Kami et al., 2014a). PKS1 is also expressed in the root elongation zone, correlating with its function in root phototropism (Boccalandro et al., 2008). Moreover, PKS2 and PKS3 are expressed in the cotyledon and leaf, coinciding with their function in leaf movement and flattening (Lariguet et al., 2003, de Carbonnel

et al., 2010, Legris et al., 2021) (Legris Martina, personal communication). Additionally, PKS expression patterns somehow relate to the light environment in which they function. For instance, PKS4 is mainly expressed in the darkness and its transcripts and protein levels decrease in response to light, coinciding with its main function in LBL-mediated phototropism. However, PKS1 and PKS2 are rather induced by light, consistent with their function in HBL-mediated phototropism and leaf movements (Lariguet et al., 2003, Schepens et al., 2008) Although PKS3 expression patterns are still under study, PKS3 is mainly induced in the cotyledon and leaf in light-grown seedlings, also in accordance to its function in leaf flattening (Legris Martina, persona l communication).

3.2.2.2.3   PKS molecular mechanisms

Little is known about the molecular mechanisms of PKS in phot signaling, except that PKS1, PKS2, and PKS4 can form a protein complex with phot1 and NPH3 at the PM (Lariguet et al., 2006, de Carbonnel et al., 2010, Schumacher et al., 2018). PKS4 is important to promote phototropism in response to LBL, however when the light intensity becomes higher PKS4 is not essential and rather inhibits phototropism (Demarsy et al., 2012, Kami et al., 2012). PKS4 is a phot1 kinase substrate that is rapidly phosphorylated after 30 seconds of phot1 activation by BL treatment in etiolated seedlings. PKS4 is present as the "PKS4D" isoform in darkness whereas, upon BL irradiation, the Serine (Ser) 299 amino acid is transiently phosphorylated, which appears as the hyper-phosphorylated isoform "PKS4L". The appearance of this isoform is dependent on the kinase activity of phot1 and has an inhibitory role on phototropism. PKS4 L isoform progressively decreases within a few hours of BL treatment until completely disappearing around the time in which the PKS4 proteins levels decay (Demarsy et al., 2012, Schumacher et al., 2018). The proportion and duration of hyper-phosphorylated PKS4 isoform increase with the BL fluence. The reversion of the PKS4L to the PKS4D isoform becomes noticeable after several minutes of

exposure in the darkness. This phenomenon is modulated by the activity of the protein phosphatase PP2A which acts in a phot1-dependent manner (Demarsy et al., 2012, Schumacher et al., 2018). Although treatments with other monochromatic light colors do not seem to affect PKS4 phosphorylation status, RL inhibits PKS4 hyper-phosphorylation by phot1 in a process depending on phy, which correlates with phy-mediated inhibition of phototropism in response to LBL (Demarsy et al., 2012).

3.2.3   Auxin transport in phototropism

Downstream phot activation, PKS function enables a controlled asymmetric auxin redistribution across the hypocotyl leading to phototropic curvature (Holland et al., 2009, Demarsy et al., 2012, Kami et al., 2014a). Three families of auxin transporters are involved in this process: PIN-FORMED (PIN) auxin exporters, members of the B subclass of ATP-BINDING CASSETTE (ABCB) efflux carrier, and the AUX/LAX (AUX1) influx carriers, the last one with a minor role in phototropism (Hohm et al., 2013, Liscum et al., 2014).

3.2.3.1 PIN-FORMED (PIN)

PIN-mediated directional auxin flow is important for phototropism (Friml et al., 2002, Ding et al., 2011). *A. thaliana* includes 8 PINs: the canonical PINs (PIN1 to PIN4 and PIN7), which facilitate the auxin efflux from the cytosol to the extracellular space, and PIN5, PIN6, and PIN8, which mediate intracellular auxin movements (Christie and Murphy, 2013b). The canonical PINs often show polar localization at the PM, which facilitates directional auxin transport in tropic responses (Christie and Murphy, 2013a). Based on loss of function mutant analysis, PIN3, PIN2, PIN4, and PIN7 redundantly function during hypocotyl phototropism (Friml et al., 2002, Ding et al., 2011, Wan et al., 2012, Willige et al., 2013). PIN3 is apolarly distributed in hypocotyl endodermal cells in darkness and upon phot1 activation by unilateral BL, it is polarly relocated to the shaded side of

the cell. This process is proposed to occur through a mechanism involving GNOM ARF GTPase GEF (guanine nucleotide exchange factor)-dependent trafficking, which redirects the auxin flow towards the shaded side of the cells (Ding et al., 2011). A similar relocation mechanism had been proposed for PIN1 and PIN2 (Geldner et al., 2001, Geldner et al., 2003). Although with a more predominant role in root phototropism, PIN2 also has a function in hypocotyl phototropism. In the root, light inhibits PIN2 vacuolar degradation. This triggers PIN2 accumulation in the irradiated side of the cells and degradation in the shaded side, and therefore, asymmetric distribution, a process that depends on phot1 and NPH3 (Wan et al., 2012). Although its importance in hypocotyl phototropism remains to be determined, PIN1 localizes at the base of cortical and vasculature cells in the hypocotyl elongation zone and it relocates toward the shaded side of the cell in response to unilateral light (Blakeslee et al., 2004). Interestingly, the D6 PROTEIN KINASE (D6PK) subfamily of AGCVIII kinases is important for PIN3 phosphorylation leading to defects in its relocation in response to light, which affects auxin transport in phototropism (Willige et al., 2013).

3.2.3.2 ATP BINDING CASSETTE B (ABCB)

In addition to PINs, the ATP BINDING CASSETTE B19 (ABCB19) auxin efflux carrier has a role in hypocotyl phototropic bending. ABCB19 transporter activity mediates long-distance auxin transport from the shoot apex, where it is synthesized, to the root by facilitating the auxin efflux towards the extracellular space (Noh et al., 2001). Different from PINs, ABCB19 is homogeneously distributed at the PM and it is inhibited by BL-induced phot1 activation, which leads to enhanced phototropism phenotype, similar to what is observed in the *abcb19* mutants (Christie et al., 2011). These phenotypes can be explained by the accumulation of auxin in the hypocotyl region above the elongation zone, which increases the local auxin lateral redistribution mediated by PINs across the hypocotyl elongation zone, which enhances phototropism (Noh et al., 2003, Christie et al., 2011). These phenotypes are proposed to occur because of the role of ABCB19 in controlling the normal

accumulation of PIN1 on the base of hypocotyl cells, associated with a disrupted basipetal flow of auxin (Noh et al., 2003, Titapiwatanakun et al., 2009).

3.2.3.3 Auxin passive transport

In addition to the facilitated transport, protonated auxin passively diffuses across the PM entering the cell due to a differential pH between the cytoplasmic and apoplastic compartments. Regulation of the apoplastic pH is achieved by the maintenance of a proton gradient across the PM, which requires a controlled activity of the PM localized proton pumps of the AHA family (H+ATPases) (Palmgren, 2001). According to the acid growth theory, acidification of the apoplast through the proton efflux from inside the cell facilitates the uptake of water and solutes and activates the expansins involved in cell wall loosening, which overall leads to cell elongation promoting hypocotyl growth (Li et al., 2021). This process requires the activation of the H+ATPase, whose primary activation step is the phosphorylation of its Threonine (Thr) 947 amino acid (Takahashi et al., 2012). SMALL AUXIN UP-RNA *(*SAUR) and TRANSMEMBRANE KINASE (TMK) proteins are proposed to mediate this activation step through the inactivation of protein phosphatases 2C (PP2C), leading to apoplast acidification and cell expansion (Ren et al., 2018, Du et al., 2020, Li et al., 2021, Lin et al., 2021). Interestingly, BL irradiation leads to increased dephosphorylation of the H+ATPase Thr947, which inhibits its activity. Moreover, controlled H+ATPase activity is required to promote hypocotyl phototropism and lateral auxin gradient establishment in response to unilateral BL (Hohm et al., 2014). Therefore, we could think about a model in which a phot gradient activation across the hypocotyl might lead to an inverse gradient of H+ATPase activation. This would trigger more cell elongation towards the shaded side of the hypocotyl resulting from a reduced inhibition of the H+ATPase, helping the establishment of auxin asymmetric redistribution in response to unilateral BL.

Finally, the auxin gradient across the hypocotyl is perceived by the auxin receptor TRANSPORT INHIBITOR RESISTANT1/AUXIN BINDING F-BOX (TIR1/AFB), which causes the degradation of the repressor auxin-responsive protein IAA19 and liberation of the transcriptional activator NON-PHOTOTROPIC HYPOCOTYL 4 (NPH4) leading to the auxin-responsive genes (Liscum et al., 2014).

AIMS OF THE STUDY

The integration of the auxin passive transport with the PIN-mediated lateral auxin redistribution across the organ facilitated by the ABCB19 transporter provides a comprehensive overview of how the generation of auxin gradients across the stem might occur during phototropism. However, our main question is understanding how the perception of light direction by a plant organ leads to this auxin gradient promoting organ differential growth and orientation in response to light.

In this thesis, we focus on hypocotyl phototropism in response to LBL, a process initiated by the establishment of a phot1-activation gradient across the hypocotyl in response to unilateral LBL that leads to an inverse gradient of auxin accumulation. The main goal of this work is to understand how this phot-activation gradient across the hypocotyl leads to an asymmetric auxin redistribution triggering its orientation toward the light.

To address our main goal, we focus on the analysis of the PKS protein family, which is found at the PM forming a protein complex with phot photoreceptors. Although little is known about how PKS proteins work on a mechanistic level, they are proposed to act downstream phot activation by modulating auxin transport or signaling (de Carbonnel et al., 2010, Demarsy et al., 2012, Kami et al., 2014a). Therefore, understanding the molecular function of PKS proteins, as early players in phot signaling, is important to shed further light on the molecular mechanisms leading to coordinated phototropic growth.

The nature of the PKS family makes this study a big challenge, given that PKS proteins lack a trustable predicted conformational structure. Here, we propose studying the molecular function of PKS4, which has an obvious role in phototropism, allowing us to undertake a structure-function analysis. We identified six evolutionary conserved PKS protein motifs that we hypothesized to be important for PKS function. We mutated them in *PKS4* and tested the resultant variants for

complementation. Our results suggest the requirement of two of the motifs for PKS4 function in phototropic response and we further investigated their mode of action.

In addition to their importance in phototropism, the *A. thaliana* PKS protein family is required in the establishment of several phot-mediated organ growth responses. The expression patterns of the different PKS family members correlate with their function in phot signaling. Thereby, *PKS1* is the only member expressed in the root, where it is essential for negative root phototropism (Boccalandro et al., 2008). Moreover, *PKS2* and *PKS3* are more expressed in leaves and have a prominent role in leaf flattening, while *PKS1* and *PKS4*, which are expressed in the hypocotyl elongation zone, are important for hypocotyl phototropism (Lariguet et al., 2003, Schepens et al., 2008, de Carbonnel et al., 2010, Kami et al., 2014b). However, we do not know how the other PKS work on a mechanistic level in these light-mediated responses. An additional aim of this work is analyzing the diversification of the *A. thaliana* PKS protein family members as well as the conservation of PKS from other organisms, in order to help our understanding about PKS functional conservation across evolution.

BRIEF INTRODUCTION TO RESULTS

The results of this work are presented in three different chapters:

Chapter 1. I present the submitted work on the importance of PKS motif C for function and subcellular localization. I describe my contribution to this work and then presented the submitted manuscript.

Chapter 2. I describe my work on the functional studies of the PKS protein family concerning evolution. Although this work requires a few additional experiments before submission, I present it as a publication manuscript.

Chapter 3. I describe my results on the complementation of the rest of the PKS motifs and focus on the study of motif D and one of its interactors: BPM4. I present it as a paper manuscript although the structure of the future publication might change (depending on additional collaborations).

RESULTS

CHAPTER 1. PKS4 S- acylation controls its activity

OVERVIEW

I led this project where we identified PKS evolutionary conserved motifs through a collaboration with Christophe Dessimoz's lab and addressed the importance of one of the motifs for PKS4 functional activity and mode of association to the PM, under the supervision of Prof. Christian Fankhauser. Our work was submitted to the Plant Cell Journal on July 2022 and it is currently under second revision.

I conceived the original research plans with Laure Allenbach Petrolati and Prof. Christian Fankhauser. I generated all the unpublished transgenic lines used in the experiments that I conducted. I conducted and analyzed the experiments of detection of PKS4 protein levels (Fig. 4a, 4c, 5a, and S2b), phototropism (Fig. 4b, 5b, 5c, S2c, S3a, and S3b), gravitropism (Fig. S2a and S2d), hypocotyl inhibition of gravitropism (Fig. 4d and S2e), and confocal microscopy observations (Fig. 5d, S2f, and S3c). I interpreted the data with the participation of the authors of the manuscripts. Prof. Christian Fankhauser and I wrote the manuscript, with the contribution of all the authors.

SUBMITED MANUSCRIPT

1   **Title page**

2

3   **Author names and affiliations**

4   Ana Lopez Vazquez[a], Laure Allenbach Petrolati[a], Christophe Dessimoz [b, c], Edwin R. Lampugnani

5   [d], Natasha Glover [b, c] and Christian Fankhauser[a*]

6   [a] Centre for Integrative Genomics, Faculty of Biology and Medicine, Génopode Building,

7   University of Lausanne, CH–1015 Lausanne, Switzerland

8   [b] Department of Computational Biology, Faculty of Biology and Medicine, Génopode Building,

9   University of Lausanne, CH–1015 Lausanne, Switzerland

10   [c] Swiss Institute of Bioinformatics, Génopode Building, University of Lausanne, CH–1015

11   Lausanne, Switzerland

12   [d] School of BioScience, University of Melbourne, Parkville, Victoria, Australia 3010.

13   [*] Author for contact: Christian.fankhauser@unil.ch

14

15   **Title**

16   Control of PHYTOCHROME KINASE SUBSTRATE subcellular localization and biological

17   activity by protein S-acylation.

18   **Short title**

19   PKS4 S-acylation controls its activity

20

44

21 **Material distribution**

22 The author responsible for distribution of materials integral to the findings presented in this

23 article in accordance with the policy described in the Instructions for Authors

24 (https://academic.oup.com/plcell/pages/General-Instructions) is: Christian Fankhauser

25 (Christian.fankhauser@unil.ch).

26

27 **ORCID IDs**

28 0000-0001-9661-8451 (A.L.V); 0000-0002-9074-5350 (L.A.P.); 0000-0003-4719-5901

29 (C.F.), 0000-0002-3666-7240 (E.R.L.), 0000-0003-1811-4340 (N.G), 0000-0002-2170-853X

30 (C.D.)

31

32 **ABSTRACT**

33 PHYTOCHROME KINASE SUBSTRATE (PKS) proteins are involved in light-regulated growth

34 orientation responses. They act downstream of phytochromes to control hypocotyl gravitropism in

35 the light and act early in phototropin signaling. Despite their importance for plant development,

36 little is known about their molecular mode of action except that they belong to a protein complex

37 comprising the phototropins at the plasma membrane. Identifying evolutionarily conservation is

38 one approach to reveal biologically important protein motifs. Here, we show that PKS sequences

39 are restricted to seed plants and that these proteins share 6 motifs (A to F from the N- to the C-

40 terminus). While motif D is also found in BIG GRAIN proteins the remining domains are PKS

41 specific. We provide evidence that motif C is S-acylated on highly conserved cysteines, which

42 mediates PKS protein association with the plasma membrane. This motif is also required for PKS4-

43 mediated phototropism and control of hypocotyl gravitropism in the light. Finally, our data

44 suggests that the mode of PKS4 plasma membrane association is important for its biological

45 activity. Our work identifies the mode of plasma membrane association of PKS proteins and

46 strongly suggests that this is their site of action to modulate environmentally regulated organ

47 positioning.

INTRODUCTION

Determination of hypocotyl growth direction is a process occurring from the early seedling establishment that influences the adult plants' physiology and development (Galen et al., 2004). In *Arabidopsis thaliana* (Arabidopsis), etiolated seedlings grow following the direction of the constant gravity stimulus: roots grow downwards while shoots grow upwards. However, in response to light hypocotyls orient their growth following the integration of two main processes: inhibition of gravitropism and phototropism (Correll and Kiss, 2002). Growth against the gravity vector of etiolated hypocotyls is inhibited by red (RL) and far-red (FRL) light perception leading to a random orientation of the hypocotyl growth, which is known as inhibition of gravitropism. This process is mediated by the RL and FRL photoreceptors phytochromes (phy) (Robson and Smith, 1996). Additionally, plants perceive the directionality of blue light (BL) to orient their photosynthetic organs towards the light source to increase light capture, which is known as phototropism. Despite the influence of phytochromes and cryptochromes, phototropism is mainly controlled by the BL photoreceptors phototropins (phot) (Goyal et al., 2013). Although phototropism and inhibition of gravitropism are independent responses, it was proposed that phy-mediated inhibition of gravitropism enhances phototropism in response to BL (Lariguet and Fankhauser, 2004; Liscum et al., 2014).

Gravitropism signaling comprises the perception of the gravity vector that requires the sedimentation of starch-filled amyloplasts for the signal generation and transduction, resulting in hypocotyls growing upwards (Sack, 1997; Nakamura et al., 2019; Vandenbrink and Kiss, 2019). In Arabidopsis, bHLH transcription factors of the PIF (PHYTOCHROME-INTERACTING FRACTORS) family regulate this process in darkness (Oh et al., 2004). In response to RL and FRL, phytochromes convert the hypocotyl amyloplasts into plastids with chloroplasts' properties

71   that show a reduced starch composition, which diminishes the ability of seedlings to sense gravity

72   and, consequently, hypocotyls show a randomized growth orientation (Kim et al., 2011). PIFs

73   inhibit the conversion of amyloplasts to other plastids in the dark, however in response to RL phyB

74   activation in the epidermis promotes the degradation of endodermal PIFs, which releases the PIFs-

75   mediated inhibition of the amyloplasts conversion (Kim et al., 2016a; Kim et al., 2016b). In

76   addition to the phy-PIF module, the phytochrome-interacting PKS (PHYTOCHROME KINASE

77   SUBSTRATES) protein family acts in phytochromes signaling to regulate RL and FRL-mediated

78   growth responses (Fankhauser et al., 1999; Lariguet et al., 2003). PKS1 and more prominently

79   PKS4 regulate the inhibition of gravitropism in response to RL and FRL (Schepens et al., 2008).

80   However, the mechanism through which PKS proteins act in this process remains unknown.

81   Arabidopsis has 2 phototropins, which exhibit specific and partially redundant functions:

82   PHOTOTROPIN1 (phot1) and phot2. Hypocotyl phototropism is mainly mediated by phot1

83   (Christie, 2007). Phototropins form a protein complex with members of the families NRL

84   (NONPHOTOTROPIC HYPOCOTYL 3 (NPH3) and ROOT PHOTOTROPISM 2 (RPT2) -LIKE

85   proteins) and PKS, which are involved in the early steps of phot-mediated signaling (Christie et

86   al., 2018; Harmer and Brooks, 2018). Phototropins are serine/threonine (Ser/Thr) protein kinases

87   belonging to the AGC family (cAMP-DEPENDENT PROTEIN KINASE, cGMP-DEPENDENT

88   PROTEIN KINASE G, and PHOSPHOLIPID-DEPENDENT PROTEIN KINASE C) that

89   phosphorylate NPH3 and PKS4 in response to BL (Demarsy et al., 2012; Christie et al., 2018;

90   Schumacher et al., 2018; Sullivan et al., 2021). Despite their hydrophilic properties, phototropins

91   associate with the plasma membrane (PM) where they initiate the light signaling cascade (Preuten

92   et al., 2015). BL leads to phot1 homodimerization, phosphorylation, and translocation to functional

93   membrane microdomains where the signal transduction is activated (Xue et al., 2018). Phototropic

94   curvature is initiated by a higher activation of phot1 on the irradiated than on the shaded side of

95   the hypocotyl. This leads to asymmetric NPH3 aggregation correlating with the phot1-activation

96   gradient (Sullivan et al., 2019; Legris and Boccaccini, 2020). However, how this phot1-activation

97   gradient across the hypocotyl leads to an auxin gradient finally resulting in growth re-orientation

98   remains poorly understood (Fankhauser and Christie, 2015).

99   PKSs are a family of basic hydrophilic proteins that do not contain domain(s) of known function.

100   They were initially identified as phytochrome binding proteins that regulate phytochrome

101   signaling (Fankhauser et al., 1999). Surprisingly, despite their hydrophilic nature, they are

102   associated with the PM (Lariguet et al., 2006; de Carbonnel et al., 2010; Demarsy et al., 2012).

103   *PKSs* are expressed in the hypocotyl elongation zone, which correlates with their importance

104   during hypocotyl growth regulation (Lariguet et al., 2003; Schepens et al., 2008; Kami et al., 2014).

105   PKS1, PKS2, and PKS4 form a protein complex with phot1 and NPH3 possibly mediating the link

106   between phot1 activation and auxin gradient formation, which ultimately leads to hypocotyl

107   growth towards the light (Lariguet et al., 2006; de Carbonnel et al., 2010; Kami et al., 2014;

108   Schumacher et al., 2018). However, the molecular mode of action of PKSs remains unknown. This

109   led us to conduct a structure-function study of PKS proteins. Although our phylogenetic analyses

110   revealed a low overall similarity among PKS members within seed plants, we identified 6 short

111   regions of protein similarity that we called motifs A to F. We identified motif C as a key

112   determinant of PKS subcellular localization. Further characterization showed that conserved

113   cysteines in this motif are required for S-acylation, subcellular localization and PKS4 function.

114

RESULTS

116 Phylogeny and motif organization of PKS-LIKE proteins

117 The primary amino-acid sequence of PKS proteins does not reveal any protein domain of known

118 function. Moreover, using the protein structure prediction programs Jpred-4 or AlphaFold

119 (Drozdetskiy et al., 2015; Jumper et al., 2021), we found that these proteins are expected to be

120 largely intrinsically disordered. To define functionally important regions of PKS proteins we used

121 a phylogenetic approach to identify evolutionary conserved sequence motifs. We identified 172

122 *PKS* homologs using the Orthologous matrix (OMA) browser (Altenhoff et al., 2021) and manual

123 reciprocal BLASTp searches in NCBI and dedicated plant genome databases (Table S1). This

124 revealed the presence of *PKS* genes in all angiosperms and a few *PKS-LIKE* sequences in

125 gymnosperms (Figure 1A). However, our searches did not reveal *PKS-LIKE* genes in ferns, mosses

126 or the liverwort *Marchantia*. The phylogeny of these genes was determined by creating an

127 alignment of the 172 PKS protein sequences using MAFFT (Katoh and Standley, 2013), removing

128 columns with gaps in more than 20% of the sequences using trimAl (Capella-Gutierrez et al.,

129 2009), and then building a maximum-likelihood tree using IQ-TREE and 1000 ultrafast bootstrap

130 replicates (Trifinopoulos et al., 2016; Hoang et al., 2018). The phylogenetic tree obtained had a

131 number of internodes with ultrafast bootstrap support values <=95, thus are considered unreliable

132 (Minh et al., 2013). However, given the support values we were able to obtain, there is a clear

133 distinction between PKS1 and 3, Brassicaceae PKS1 and PKS2, as well as several basal

134 angiosperm splits (Figure 1A). In the basal angiosperms *Amborella trichopoda*, *Nimphea colorata*

135 and *Persae americana,* we found 2 *PKS* genes, which group into the *PKS4* clade and a clade

136 formed by the ancestors of *PKS1*, *PKS2* and *PKS3* (thereafter referred to the *PKS1/2/3* clade, with

137 names based on the Arabidopsis genes). Based on the limited data available from gymnosperms

138 and the limited bootstrap support throughout the tree, the most parsimonious interpretation of our

139 data is that PKS was present in one copy in the ancestral spermatophyte (seed plants, including

140 gymnosperms and angiosperms). We hypothesize that there was a duplication in the ancestral

141 angiosperm to form two copies: PKS4 and PKS1/2/3. Another duplication occurred after the

142 divergence of *Amborella*, *Persea americana*, and *Nymphaea colorata*, giving rise to PKS1/2 and

143 PKS3 in the ancestral Mesangiospermae. An additional Brassicaceae-specific duplication gave rise

144 to PKS1 and PKS2. The length of tree branches suggests that evolution in the *PKS4* clade is more

145 constrained than in the *PKS1/2/3* clade. *PKS4* genes are present in all analyzed monocots and

146 dicots (Figures 1A and S1A). Eudicots typically possess an additional *PKS3* and a *PKS1-LIKE*

147 gene, while in Brassicacaea the *PKS1* subfamily further duplicated into *PKS1* and *PKS2*. In

148 addition to *PKS4*, monocotyledons genomes often also contain additional *PKS* genes presumably

149 belonging to the *PKS1/2/3* clade. These sequences are not represented here because they are more

150 difficult to identify due to greater sequence divergence. We conclude that *PKS* genes are present

151 in seed plants, basal angiosperms possess *PKS* genes from two subfamilies, and in eudicots the

152 gene family further duplicated leading to the presence of *PKS* genes from at least 3 clades (*PKS4*,

153 *PKS3* and *PKS1*).

154 To define conserved sequences in those genes we used the 172 taxonomically divergent *PKS*

155 sequences from all 4 subfamilies (table S1). We used the PKS protein sequences as input for

156 GLAM2 (Frith et al., 2008) to identify conserved sequence motifs and found that these proteins

157 are characterized by the presence of 6 conserved motifs that we call A to F (from the amino- to the

158 carboxy-terminus) (Figure 1B). In addition, many PKS proteins comprise an additional conserved

159 motif that we call G, which is present between motifs C and D (Figure S1B). Given that this

160 sequence motif is absent from Brassicaceae PKS3 and PKS4 (including *Arabidopsis thaliana*), we

161   do not further consider this motif here. Although the order of the motifs is fully conserved among

162   PKS proteins, the degree of sequence conservation and the spacing between each motif is much

163   less conserved. Finally, we found that motifs C and F are related to each other, in particular, C-

164   terminal to the central Cys residue (Figure 1B). We used hidden Markov Model-based protein

165   searches (Gabler et al., 2020) to determine whether related motives are present in other proteins

166   and found a conserved sequence towards the carboxy-terminus of BIG GRAIN (BG and BG-

167   LIKE) proteins is related to motif D (Mishra et al., 2017). BG and BG-LIKE proteins have a similar

168   taxonomic distribution as PKS proteins. Unfortunately, the molecular function of the conserved

169   carboxy-terminal region of BIG GRAIN proteins that is related to motif D is presently unknown

170   (Mishra et al., 2017). We did not identify proteins containing obvious sequence conservation with

171   any of the other PKS motifs. In summary, our sequence analyses identified six conserved motifs

172   present in PKS proteins and we hypothesize that they correspond to functionally important portions

173   of these proteins.

174   <u>Motif C of PKS proteins is S-acylated and required for their association with the plasma membrane</u>

175   Arabidopsis PKS1 is not an integral membrane protein but it associates with the plasma membrane

176   through unknown mechanisms (Lariguet et al., 2006). Moreover, PKS1, PKS2 and PKS4 are found

177   in a complex with the plasma-membrane-localized phototropins and NPH3 (Lariguet et al., 2006;

178   de Carbonnel et al., 2010; Schumacher et al., 2018). This suggests that plasma membrane

179   localization of PKS proteins is a functionally relevant feature of these proteins. To test whether

180   one of the conserved sequence motifs controls the subcellular localization of PKS1, we determined

181   the subcellular localization of a series of 35S promoter driven PKS1 truncations fused to GFP in

182   hypocotyl epidermal cells of stably transformed Arabidopsis seedlings (Figure 2A). Full length

183   (ABCDEF) PKS1-GFP signal was consistent with the previously reported plasma-membrane

184   localization (Figure 2). Both ABC-GFP and CDEF-GFP colocalized with the FM4-64 dye

185   consistent with plasma-membrane localization (Figure 2B). In contrast, AB-GFP and DEF-GFP

186   largely lost plasma-membrane localization suggesting that motif C plays a central role in mediating

187   association of PKS1 to the plasma membrane. Consistent with this idea, a portion of PKS1

188   comprising conserved motif C alone was sufficient for plasma-membrane localization of a GFP

189   fusion protein (Figure 2B).

190   Highly conserved Cystine (Cys) residues (in particular, Cys at position 12, and less conserved Cys

191   at positions 10 and 8 - see Figure 1B) are a striking feature of motif C. Such residues can be

192   acylated to mediate plasma-membrane association (Hemsley, 2020). To determine their

193   importance in controlling PKS1 subcellular localization we mutated all three Cys to Serine (Ser)

194   residues (Ser cannot be acylated). Mutating these residues in the ABC-GFP, CDEF-GFP or full

195   length PKS1-GFP constructs strongly altered the ability of the protein to associate with the plasma

196   membrane (Figure 3A). To test if the loss of association with the plasma membrane was specific

197   to the conserved Cys residues in the motif C, we also mutated the conserved Cys residue in motif

198   F to Ser. This did not alter the subcellular localization of PKS1-GFP (Figure 3A). This is consistent

199   with our observation that CDEF-GFP but not DEF-GFP associated with the plasma membrane,

200   indicating the central role of motif C in targeting the protein to the plasma membrane, which is

201   apparently mediated by conserved Cys residues (Figure 2B). To determine whether these

202   conserved Cys residues controlling plasma-membrane association of PKS1 are S-acylated, we

203   performed a biochemical assay with the same transgenic plants used for microscopic analysis. The

204   assay consists of exchanging acyl groups covalently bound to Cys residues with biotin which is

205   then revealed by affinity purification (Hemsley, 2013). This assay showed that full length PKS1-

206   GFP and ABC-GFP were both acylated, while mutating the conserved Cys residues in the latter

207 construct prevented acylation. Moreover, the C-GFP construct was acylated as well, consistent

208 with acylation of at least one of the conserved residues of motif C in PKS1. To determine whether

209 the conserved Cys residues in motif C are also important to control the subcellular localization of

210 other PKS proteins, we selected PKS4, a member of the other major subfamily of PKS proteins

211 (Figure 1A). Arabidopsis PKS4 has two Cys residues in motif C, the most highly conserved one

212 at position 12 and a second one at position 10 (Figure 1B). We substituted both residues with Ser

213 residues in the context of full length PKS4-GFP driven by the *35S* promoter and generated stable

214 transgenic Arabidopsis plants in the Col-0 background. While PKS4-GFP was associated with the

215 outline of the cell consistent with the previously reported plasma-membrane association (Figure 3

216 C) (Schumacher et al., 2018), mutations of the conserved Cys residues in motif C strongly impaired

217 plasma-membrane association as observed for PKS1 (Figure 3C). Collectively, these results

218 indicate that conserved Cys residues in motif C are acylated and essential to mediate plasma-

219 membrane association of PKS1 and PKS4.

220 <u>The conserved cysteines in motif C of PKS4 are required for biological activity.</u>

221 To determine whether the conserved Cys residues in motif C are functionally relevant, we used

222 complementation of *pks4*, which is defective in phototropism and phytochrome-mediated

223 inhibition of hypocotyl gravitropism, as a functional assay (Schepens et al., 2008; Kami et al.,

224 2014). This choice was dictated by the fact that amongst *pks* single mutants *pks4* has the strongest

225 phototropism and gravitropism phenotype (Schepens et al., 2008; Kami et al., 2014). We tested

226 the same PKS4 motif C mutant as characterized for subcellular localization studies (Figure 3C)

227 but tagged PKS4 with a carboxyl-terminal triple HA and used a 1.5 kb *PKS4* promoter to control

228 expression of the transgene. We generated transgenic *pks4* plants expressing PKS4 mutated in

229 motif C (termed PKS4 C* lines) and selected three independent single insertion lines expressing

230   PKS4 protein levels comparable to a wild-type PKS4-HA control line (WT-3) (Figure 4A), whose

231   PKS4-HA protein levels were similar to endogenous PKS4 (Schumacher et al., 2018). The PKS4

232   WT-3 line rescued the phototropic phenotype of the *pks4* mutant as previously shown (Schumacher

233   et al., 2018). However, none of the three independent PKS4 C* lines complemented the mutant

234   (Figure 4B). Additionally, we observed that one of these lines (PKS4 C*-2) exhibited an even

235   stronger phototropic defect than the *pks4* line, suggesting that expression of the PKS4 C* variants

236   might interfere with the molecular mechanism underlying phototropism. To look at a rapid

237   phototropin response, we analyzed the light-induced reduction of PKS4 mobility on SDS-PAGE

238   gels triggered by phototropin-mediated PKS4 phosphorylation (Demarsy et al., 2012). This

239   experiment showed that in etiolated seedlings PKS4 C* has a somewhat different migration pattern

240   than the WT showing two isoforms. This modification could be due to the slightly altered amino-

241   acid composition of the mutant and/or a change in protein acylation. In response to blue light, we

242   observed the previously described gradual and transient increase in the appearance of a slower

243   migrating PKS4 isoform for the WT (Figure 4C) (Demarsy et al., 2012). This contrasted with

244   PKS4 C* for which we hardly detected the slower migrating isoform in response to blue light.

245   Collectively, our results show that mutating conserved Cys residues in motif C impairs the ability

246   of PKS4 to promote phototropism and appears to limit the ability of phot1 to phosphorylate PKS4.

247   To determine whether motif C is also important for the function of PKS4 in phytochrome signaling

248   we analyzed light-induced inhibition of hypocotyl gravitropism (Schepens et al., 2008) by

249   analyzing the hypocotyl growth orientation (relative to the vertical) in response to 30 μmol/m2/s

250   of continuous red light. We found that the control PKS4 WT-3 line rescued this light response,

251   while none of the PKS4 C* lines complemented *pks4* (Figure 4D). The phenotype of these lines

252   was more pronounced than the *pks4* phenotype, similar to the *phyB* mutant (Figure 4D). Therefore,

253   expression of PKS4 C* enhances the *pks4* null phenotype suggesting that it interferes with PKS

254   function during phytochrome-mediated inhibition of hypocotyl gravitropism. We then analyzed

255   hypocotyl gravitropism in darkness and found that the WT, *pks4* and all transgenic lines showed

256   the same response (Figure S2A) confirming that the effect of PKS4 on hypocotyl gravitropism is

257   light-dependent. Collectively our data indicates that the highly conserved Cys residues of motif C

258   are essential for the function of PKS4 in phytochrome and phototropin signaling.

259   Our analysis of PKS1 truncations fused to GFP and mutating the conserved cysteine residues in

260   motifs C and F, revealed that motif C is the primary determinant for plasma membrane association

261   (Figures 2 and 3). However, motif F is related to motif C and motif F may contribute to tight

262   plasma membrane association as less intracellular signal is observed in CDEF-GFP than ABC-

263   GFP expressing plants (Figure 2B). We therefore tested the functional importance of motif F by

264   generating a PKS4 motif F mutant by substituting the invariant Cys with a Ser residue and

265   transforming *pks4* mutants as described for the PKS4 C* lines. We selected transgenic lines (PKS4

266   F*1-3), with similar protein levels as in our PKS4 WT control line (Supplemental figure S2B). We

267   found that the three PKS4 F* lines fully complemented the phototropic defect of the *pks4* mutant

268   line (Supplemental figure S2C). Similarly, these PKS4 F* lines also complemented phytochrome-

269   mediated inhibition of hypocotyl gravitropism in red light and showed a normal hypocotyl

270   gravitropic response in darkness (Supplemental figures S2D and S2E). We conclude that mutating

271   the invariant Cys in motif F had no measurable consequences on the analyzed light responses. To

272   confirm the implication of the conserved Cys residues of motif C and motif F in the subcellular

273   localization of PKS4, we generated stable transgenic Arabidopsis plants expressing PKS4-GFP,

274   PKS4 C*-GFP, and PKS4 F*-GFP, driven by the *PKS4* promoter in *pks4*, and we observed their

275   subcellular localization in hypocotyl cortex cells of etiolated seedlings using confocal microscopy

276   (Supplemental figure S2F). PKS4-GFP localized at the plasma membrane while PKS4 C*-GFP

277   signal was apparent inside the cells (Supplemental figure S2F), consistent with our data of the

278   PKS4 WT and C* overexpressing lines (Figure 3C). PKS4 F*-GFP was plasma membrane

279   localized (Supplemental figure S2F), similar to PKS1 F*-GFP (Figure 3A). Collectively, these

280   data indicate that acylation of the highly conserved Cys residues in motif C is essential for the

281   biological functions of PKS4 and plasma membrane localization of the protein, while the role of

282   motif F remains to be determined.

283   <u>The type of lipid mediated PKS4 plasma membrane association affects its biological activity</u>

284   To determine whether the altered subcellular localization and the biological function of PKS4 C*

285   mutants can be rescued by targeting the protein to the plasma membrane through another

286   mechanism, we generated lines comprising an N-terminal myristoylation (myri) sequence. We

287   included a myri-WT PKS4 control construct and generated transgenic plants in the *pks4* mutant

288   background. We selected single insertion lines (myriPKS4 WT 1-4 and myriPKS4 C* 1-3) with

289   comparable protein levels as in our PKS4 WT and C* lines (Figure 5A). We found that the

290   myriPKS4 C* lines did not complement the phototropic phenotype of *pks4* (Figure 5B). However,

291   we observed that myriPKS4 C* lines showed a slightly stronger phototropic response than the

292   PKS4 C* line (Figure 5B). We observed a similar (but not significant) tendency when comparing

293   numerous independent T1 transformants (Supplemental figure S3A). When the myri sequence was

294   added to the WT PKS4 these lines were able to complement the phototropic defect of *pks4* (Figure

295   5C). However, both in the selected T3 lines and when comparing numerous independent T1 lines

296   adding the myri sequence to the WT interfered with the ability of PKS4 to fully complement the

297   phototropic defect of *pks4* (Figures 5C and S3B). To determine whether the myri sequence

298   influenced the subcellular localization of PKS4 and PKS4C* we generated GFP fusions driven by

299   the *PKS4* promoter and analyzed subcellular localization in stably transformed Arabidopsis *pks4*

300   seedlings. This experiment showed that the inclusion of the N-terminal myri sequence restored the

301   plasma-membrane localization of PKS4 C* while it did not visibly alter the localization of WT

302   PKS4. Collectively this data indicates that bringing PKS4 C* to the plasma membrane through an

303   N-terminal myristoylation sequence is not sufficient to restore its biological activity, while adding

304   this sequence to WT PKS4 moderately interferes with PKS4 function.

305   Given that bringing PKS4 to the plasma membrane through an N-terminal lipid modification

306   appears to perturb PKS4 activity, we tried plasma-membrane association through the C-terminus.

307   We used a farnesylation sequence that was included after the triple HA tag of both WT and C*

308   PKS4 and transformed these *PKS4* promoter driven constructs into *pks4* mutants. We then

309   compared the phototropic response of numerous independent T1 transformants expressing either

310   WT, C*, WT-farn or C*-farn PKS4 constructs. This experiment showed that the farnesylation

311   sequence interfered with the ability of the WT PKS4 construct to fully complement *pks4* (Figure

312   S3B). The tendency was the opposite in the context of the C* mutant with the construct containing

313   the farnesylation sequence (C*-farn) displaying a slightly more robust phototropic response than

314   the C* construct (Figure S3B). However, the difference in complementation potential of the C*

315   and C*-farn constructs was not significant and neither construct complemented *pks4* (Figure S3B).

316   To determine whether the inclusion of a C-terminal farnesylation sequence restored plasma-

317   membrane localization of the PKS4 C* mutant we made GFP fusion constructs driven by the *PKS4*

318   promoter and analyzed stably transformed seedlings. This experiment showed that adding a

319   farnesylation sequence after GFP was sufficient to bring PKS4-C*-GFP-farn to the plasma

320   membrane while the same modification in a WT PKS4 construct did not have any obvious effects

321   on subcellular localization (Figure S3C). Collectively these experiments showed that bringing

322   PKS4 C* to the plasma membrane either through N-terminal myristoylation or C-terminal

323   farnesylation was not sufficient to restore the ability of the C* mutant to complement the

324   phototropic defect of *pks4*. However, these results are difficult to interpret given that these

325   modifications also altered the complementation potential of WT PKS4.

326

327   **DISCUSSION**

328   We found PKS-LIKE sequences in seed plants but not in the genomes of mosses, ferns, liverwort

329   or algae indicating that these proteins appeared relatively late in land plants (Fig. 1, S1). This

330   evolutionary history is similar to the one of BIG GRAIN proteins which also share a sequence

331   motif with PKS proteins (Figure 1) (Mishra et al., 2017). In contrast, members of the *NRL* family

332   are present in all land plants while phototropin photoreceptors are present in land plants,

333   charophytes and chlorophytes (Christie et al., 2018). PKS proteins also appear much later than

334   phytochromes which are found in charophytes and land plants (not considering phytochromes in

335   cyanobacteria, bacteria and fungi) (Li and Mathews, 2016). Based on this evolutionary history it

336   is tempting to propose that PKS proteins are required for a seed-plant specific function and/or were

337   required following changes in the light environment triggered by the expansion of seed plants (Li

338   and Mathews, 2016). While a single PKS-LIKE sequence was found in some gymnosperms, basal

339   angiosperms have 2 members of the family that we call PKS1 and PKS4 based on the Arabidopsis

340   nomenclature (Figure 1, S1).

341   PKS proteins share 6 or 7 sequence motifs which are present in the same order and separated by

342   regions of various length and without obvious homology (Figure S1). These motifs appear to be

343   unique to PKS proteins except for motif D that is related to a conserved sequence motif present

344   towards the C-terminus of BIG GRAIN proteins (Mishra et al., 2017). The molecular function of

345   BIG GRAIN proteins is largely unknown, however, similar to PKS proteins they are proposed to

346   regulate auxin transport and/or signaling (de Carbonnel et al., 2010; Kami et al., 2014; Liu et al.,

347   2015). Additional experiments are required to determine if and how these proteins perform such

348   functions and whether the common sequence motif (motif D in PKS) is involved in controlling the

349   distribution of auxin.

350   The plasma membrane is the major site of phototropin action, where these photoreceptors are part

351   of a protein complex comprising PKS proteins (Lariguet et al., 2006; de Carbonnel et al., 2010;

352   Demarsy et al., 2012; Preuten et al., 2015). We therefore tested whether any of the conserved PKS

353   motives are required for plasma-membrane association. We found that motif C is a major

354   determinant for the subcellular localization of PKS1 and PKS4 (Figures 2 and 3). Given that PKS1

355   and PKS4 are representatives of both PKS clades present in angiosperms (Figure 1), this suggests

356   that the function of motif C is broadly shared amongst PKS proteins. Motif C contains highly

357   conserved Cys residues, particularly C12 (12th amino acid of the motif) and to a lesser extent C10

358   (Figure 1D). Mutating all three conserved Cys residues of PKS1 motif C prevented protein

359   acylation *in vivo* and localization of the protein to the plasma membrane (Figure 3). PKS4 has 2

360   Cys residues in motif C (C10 and C12), mutating both prevents plasma-membrane association of

361   the GFP-tagged variant (Figures 3C and S2F). This strongly suggests that S-acylation of at least

362   one of those conserved Cys residues is essential for PKS association with the plasma membrane.

363   Interestingly, motif F, which is related to motif C, does not play a prominent role in the control of

364   PKS protein localization (Figures 1B, 3A and S2F). A recent large-scale analysis of protein

365   acylation in Arabidopsis identified PKS1, PKS2 and PKS3 as S-acylated proteins (Kumar et al.,

366   2022). Moreover, acylation of PKS proteins was mapped to Cys residues in motif C and in motif

367   F (Kumar et al., 2022), independently confirming our data on S-acylation of motif C in PKS1.

368   PKS4 was not identified in this study (Kumar et al., 2022), possibly because light-grown seedlings

369   were used and PKS4 protein levels decline rapidly in etiolated seedlings transferred into the light

370   (Demarsy et al., 2012). While S-acylation is very difficult to predict based on primary amino-acid

371   sequence, lysin residues are often found in the vicinity of S-acylated cysteines (Zaballa and van

372   der Goot, 2018). For some proteins S-acylation was shown to prevent ubiquitination of the nearby

373   lysine and subsequent protein degradation (Zaballa and van der Goot, 2018). We note that in motif

374   F there is an invariant lysine residue, which is much less conserved in motif C (Figure 1B). One

375   possibility is that motif F regulates the stability of PKS proteins. In summary, our data is consistent

376   with S-acylation of highly conserved Cys residues of motif C playing a key role in plasma

377   membrane localization of PKS proteins, while the role of motif F requires further investigations.

378   By testing the ability of PKS4 variants to complement phototropism and hypocotyl gravitropism

379   of *pks4* mutants, we found that the ability of those variants to localize to the plasma membrane

380   correlates with their ability to complement *pks4* (Figures 4 and S2). This data suggests that

381   localization of PKS4 at the plasma membrane is required for PKS4 function in phototropin and

382   phytochrome signaling (Schepens et al., 2008; Kami et al., 2014). Moreover, we find less of the

383   more slowly migrating light-induced isoform in the mislocalized PKS4 C* variant (Figure 4C).

384   These finding are consistent with PKS4 being a phototropin signaling element acting at the plasma

385   membrane and a substrate of phot1 kinase activity (Demarsy et al., 2012). The requirement of

386   plasma-membrane-localized PKS4 to control phytochrome-induced inhibition of gravitropism

387   indicates that PKS4 does not act in the nucleus where the majority of well-characterized

388   phytochrome signaling events occur (Legris et al., 2019; Cheng et al., 2021).

389   To further test the link between PKS4 subcellular localization and its ability to regulate hypocotyl

390   growth orientation, we tethered PKS4 C* variants to the plasma membrane by adding either an N-

391   terminal myristoylation sequence or a C-terminal farnesylation sequence. Both approaches largely

392   restored the subcellular localization of PKS4 C* (Figures 5 and S3). However, these PKS4 variants

393   were not able to complement the phototropic defect of *pks4* (Figures 5 and S3). Interestingly,

394   phototropism in plants expressing the PKS4 C* variant was often less efficient than in *pks4*

395   suggesting that expression of the mislocalized PKS4 C* interferes with phototropism (Figures 4B,

396   5B and S3). Consistent with this idea plants expressing a PKS4 C* variant localized to the plasma

397   membrane (myristoylated or farnesylated PKS4 C*) have a less severe phenotype than those

398   expressing PKS4 C* (Figure 5 and S3). Nevertheless, rescuing the subcellular localization defect

399   of PKS4 C* was insufficient to restore the ability of this construct to promote phototropism

400   (Figures 5 and S3). Importantly, including a myristoylation or farnesylation sequence to PKS4

401   slightly interferes with the ability of wild-type PKS4 to promote phototropism (Figures 5C and

402   S3A, B). This suggests that the mode of plasma membrane attachment of PKS4 influences its

403   ability to work in phototropin signaling. Indeed, the wild-type protein is attached to the plasma

404   membrane through the middle of the protein, which is a distinguishing feature of S-acylation

405   contrasting with N-terminal or C-terminal lipid mediated plasma-membrane association occurring

406   through myristoylation or farnesylation (Turnbull and Hemsley, 2017; Hemsley, 2020). PKS4

407   including myristoylation or farnesylation tags is expected to be associated to the plasma membrane

408   through the C motif and the N- or C-terminus, while PKS4 C* including additional lipid

409   modification sequences either though the N- or the C-terminus alone. This difference in protein

410   attachment to the plasma membrane may explain the observed phenotypes for example because

411   the N- and C-terminus must be free to efficiently engage in protein-protein interactions.

412   Alternatively, while S-acylation is a reversible process allowing regulated association with the

413   plasma membrane, myristoylation or farnesylation are not reversible (Hemsley, 2020). In the case

414   of NPH3 cycles of plasma membrane association and dissociation are functionally important

415   (Sullivan et al., 2021). We do not have evidence for regulated PKS subcellular localization.

416   Moreover, adding either an N-terminal myristoylation or a C-terminal farnesylation sequence to

417   PKS4 only interfered slightly with the ability of these constructs to complement *pks4* (Figures 5

418   and S3). Therefore, our current data do not provide evidence for regulated, S-acylation-mediated

419 PKS localization playing a key functional role. We therefore propose that proper positioning of

420 PKS association with the plasma membrane is functionally important but cannot rule out that Cys

421 to Ser mutations in the conserved C motif alter PKS4 activity through a yet to be discovered

422 mechanism.

423

424 **METHODS**

425 <u>PKS phylogeny and motif discovery</u>

426 The PKS sequences used to make the tree were obtained from multiple sources. The majority were

427 obtained from OMA Hierarchical Orthologous Groups (HOGs) from the Jan2020 version of the

428 OMA browser (Altenhoff et al., 2021). The first three HOGs were found by searching the browser

429 for protein sequences from *Arabidopsis thaliana PKS1*, *2*, *3*, and *4* genes (At2g02950, At1g14280,

430 At1g18810 and At5g04190). *PKS1* and *2* were inferred by OMA to be in the same gene family

431 (rooted at the Magnoliopsida-level), and *PKS3* and *PKS4* were in two other families, rooted at the

432 Pentapetalae and Mesangiospermae levels, respectively. A final, smaller gene family was found in

433 OMA by searching for the *Amborella trichopoda PKS4* gene rooted at the Magnoliopsida level.

434 Seventeen additional *PKS* sequences, selected to increase phylogenetic diversity, were added

435 covering the following: Basal angiosperms *Amborella tricopoda* and *Nymphea colorata*, monocots

436 *Brachypodium distachyon* and *Setaria italica*, magnolid *Persea americana*, asterids *Solanum*

437 *tuberosum and Camellia sinensis*, rosids *Fragaria vesca*, and Caryophyllales *Beta vulgaris*. The

438 aforementioned sequences were obtained by reciprocal blast searches using Arabidopsis PKS1 and

439 PKS4 protein sequences as query (Altschul et al., 1990). Two gymnosperm PKS-LIKE genes were

440 found from PLAZA Gymnosperms 1.0 (Proost et al., 2015). Thus, a total of 172 PKS homologs

441 (protein sequences) were used for the remainder of the analysis (Supplementary Table 1).

442 The 172 sequences were used to make an alignment using MAFFT v7.313 (Katoh and Standley,

443 2013), with the E-INS-i algorithm option. This algorithm was chosen because it uses a

444 "generalized affine gap cost" in the pairwise alignment stage, which is better to use for sequences

445 with long unalignable regions, such as in PKS proteins. The alignment was then filtered to remove

446 unreliable columns: those with gaps in more than 20% of the sequences (gap threshold 0.8),

447　essentially those columns not containing the highly conserved motifs. This resulted in 250 columns

448　in the final alignment.

449　The alignment was used to make a gene tree of all the PKS sequences using IQ-TREE web server

450　version 1.6.12 (Trifinopoulos et al., 2016) with the ModelFinder (Kalyaanamoorthy et al., 2017),

451　tree reconstruction (Nguyen et al., 2015), and ultrafast bootstrap (1000 replicates) (Hoang et al.,

452　2018) options. Ultrafast bootstrap was implemented because it has been shown to be orders of

453　magnitude faster to compute and while maintaining accurate equivalent to standard bootstrap

454　methods (Minh et al., 2013; Hoang et al., 2018). The resulting maximum likelihood tree was

455　visualized with phylo.io (Robinson et al., 2016), and manually rooted using gymnosperm

456　sequences as an outgroup.

457　To identify motifs in the highly gapped alignment GLAM2 was utilized (Frith et al., 2008). Since

458　GLAM2 can only find one motif per alignment, we trimmed the sequences based on manual

459　inspection of the alignment as well as gblocks conserved locations (Talavera and Castresana,

460　2007), and included a flanking 20 amino acids on each side. The parameters were set to "default",

461　except the initial columns to be aligned was set to 10, the maximum columns to be aligned was set

462　to 20, and to shuffle the sequences.

463　<u>Plant material</u>

464　All plants utilized in this study are in the *A. thaliana* Columbia-0 ecotype. The *pks4-2* allele was

465　utilized in this study (Schepens et al., 2008). 35Sp::PKS1-GFP (pCF202), 35Sp::PKS4-GFP

466　(pIS03) and PKS4p:PKS4-3XHA (pPS09) in *pks4-2* were previously described (Lariguet et al.,

467　2006; Demarsy et al., 2012; Schumacher et al., 2018). To obtain PKS1 truncations fused to GFP

468　driven by the 35S promoter PKS1 amplicons were cloned Kpn1-BamH1 into a binary vector

469　designed to generate C-terminal GFP fusions (pCF203). The *PKS1* cDNA from plasmid pCF173

470   was amplified with the following primer combinations (CF129/CF470) corresponding to amino-

471   acids 1-160 of PKS1 (AB); (CF129/CF471) corresponding to amino-acids 1-273 (ABC);

472   (CF472/CF473) corresponding to amino-acids 274-439 (DEF); (CF507/CF471) corresponding to

473   amino-acids 161-273 (C) and (CF507/CF473) corresponding to amino-acids 161-439 (CDEF).

474   The PCR products were digested with Kpn1 and BamH1 and ligated into digested pCF203 to

475   obtain pCF524 (AB), pCF525 (ABC), pCF526 (DEF), pCF534 (C) and pCF535 (CDEF).

476   Mutations of the three conserved Cys residues in motif C were obtained by site directed

477   mutagenesis using CF173 as a template to generate pCF546 (ABC*), pCF547 (ABC*DEF),

478   pCF550 (C*DEF). Mutations of the conserved Cys residues in motif F (Cys 378) was also obtained

479   by site directed mutagenesis using CF173 as a template to obtain pCF393. For PKS4 C* lines, a

480   fragment corresponding to ABC (186 first amino acids of PKS4 with cysteins 143 and 145 mutated

481   into serine) was ordered at Eurofins and after digestion with XmaI/Bpu10I was ligated into a

482   35Sp:PKS4-GFP construct to replace the wild type with the mutant sequence to obtain pCF561.

483   For the generation of the PKS4pro::PKS4 C*-3xHA lines (pAL10), a 517 bp DNA fragment

484   containing the PKS4 C143S and C145S mutations was digested from the pCF561 with the

485   restriction enzymes EcoRV and NruI and replaced in the pPS9 construct (Schumacher et al., 2018)

486   previously digested with the same restriction enzymes to replace the wild type with the mutant

487   sequence. Similarly, for the generation of the PKS4pro:PKS4 F*-3xHAlines (pAL40), a synthetic

488   682 bp DNA fragment of the PKS4 CDS containing the C358S mutation and flanked by the EcoRV

489   and BamHI sites was ordered from Eurofins® and replaced in the pPS9 construct previously

490   digested with the same restriction enzymes to replace the wild type with the mutant sequence. For

491   the generation of the PKS4pro::myriPKS4-3xHA (pAL63) and PKS4pro::myriPKS4 C*-3xHA

492   (pAL64) lines, a synthetic 171 bp DNA fragment of the PKS4 CDS containing the last part of the

493   PKS4 promoter and the myristoylation signal sequence ATGGGAATTTGTATGTCTAGA

494   followed by the beginning of the PKS4 CDS was ordered and digested with the restriction enzymes

495   XhoI and NruI and replaced in the pPS9 and pAL10 constructs previously digested with the same

496   restriction enzymes for that purpose. For the generation of the PKS4pro::PKS4-3xHAfarn

497   (pAL70) and PKS4pro::PKS4 C*-3xHAfarn (pAL71) lines, a synthetic 225 bp DNA fragment

498   including the last part of the PKS4 CDS, the 3xHA tag followed by the farnesylation sequence

499   TCT AAG GAT GGA AAG AAG AAG AAG AAG AAG TCT AAG ACT AAG TGT GTT ATT

500   ATG, and a very short fragment of the backbone vector flanked by the unique restriction enzymes

501   sites BamHI and PstI was replaced in the pPS9 and pAL10 previously digested with the same

502   restriction enzymes for that purpose. For the generation of PKS4pro::PKS4-GFP (pAL43) lines, a

503   DNA fragment containing the PKS4 pro::PKS4-GFP::term in the pED10 (Demarsy et al., 2012)

504   was digested with the restriction enzyme HindIII and cloned into the pFR100 (pFP100-based

505   vector (Bensmihen et al., 2004) carrying the OLE1pro::OLE1-FastRed for selection of transgenic

506   plants) previously digested with the same enzyme for that purpose. For the generation of the

507   PKS4pro::PKS4 C*-GFP (pAL45) and PKS4pro::PKS4 F*-GFP (pAL65) lines, a DNA fragment

508   including the C143S and C145S or the C358S mutations, respectively, was digested from the

509   pAL10 and pAL40 with the restriction enzymes NruI and ZraI and replaced in the pAL43

510   previously digested with the same enzymes for that purpose. For the generation of the

511   PKS4pro::myriPKS4-GFP (pAL61) and PKS4pro::myriPKS4-GFP (pAL62) lines, the same

512   synthetic 171 bp DNA fragment used for the generation of the pAL63 and pAL64 was replaced in

513   the pAL43 and pAL45 previously digested with the same restriction enzymes for that purpose. For

514   the generation of the PKS4pro::PKS4-GFPfarn (pAL67) and PKS4pro::PKS4 C*-GFPfarn

515   (pAL68) lines, the same synthetic 1557 bp DNA fragment used for the generation of the pAL70

516 and pAL71 was replaced in the pAL43 and pAL45 previously digested with the same restriction

517 enzymes for that purpose. All constructs were sequence verified. Transgenic lines were obtained

518 using *Agrobacterium tumefaciens*-mediated transformation. Several single insertion lines

519 expressing each of them were characterized. The use of fluorescent seeds as selection marker also

520 allowed us to perform experiments with large numbers of independent T1 lines.

521 <u>Growth conditions</u>

522 For seeds production, plants were grown on the soil at 22°C with 16h of white light (WL) per day.

523 For physiological experiments, seeds were surface-sterilized in 70% ethanol and 0.05% Triton-X

524 for 5 min and in 100% ethanol for 5 min. Seeds were then sown on Petri dishes containing half-

525 strength Murashige and Skoog medium, 0.8% agar. Plates were stored in the dark for 3 days at

526 4°C for stratification. For dark-grown seedlings experiments, germination was induced by 4-6

527 hours of white light (80µmol/m2/s) at 22°C and plates were put back in the dark at 19°C or 22°C

528 for 3 days before light treatment. For inhibition of gravitropism experiments, germination was

529 induced by 1h of red light (50 µmol/m2/s) at 22°C and plates were put back in the dark at 22°C

530 for 1 day before light treatment.

531 <u>Light treatments</u>

532 For etiolated conditions, seedlings were grown on vertically orientated plates for 3 days in darkness

533 at 19°C or 22°C prior to the light treatment. For phototropism seedlings were irradiated with

534 constant unilateral 0.1 µmol/m2/s BL at 22°C for up to 24h, and for protein extraction, with

535 unilateral 1 µmol/m2/s BL at 22°C during 0, 1, 3, 10, and 20 minutes. For inhibition of

536 gravitropism, seedlings were grown on vertically orientated plates for 1 day in darkness at 22°C

537 prior to the light treatment. Seedlings were irradiated with constant 30 µmol/m2/s RL at 22°C for

538 3 days.

539   Hypocotyl measurements and analysis

540   Plates were pictured using an infra-red CCD camera system at different timepoints. The curvature

541   angles were calculated by subtracting average angle of orientation of upper region (85−95% of

542   total length) of each hypocotyl with respect to vertical after light treatment determined by a

543   customized MATLAB script developed in the Fankhauser Lab. One-way ANOVA (aov) and

544   Compute Tukey's Honest Significance Differences (HSD.test) [agricolae package] using the R

545   software was performed. We considered p values <0.01 significant.

546   Fluorescence microscopy

547   Confocal microscopy images were taken with an Airy confocal microscope (Zeiss), either model

548   LSM 510 or 880. Model LSM 510 was used for all the PKS1 imaging and for 35Spro:PKS4-GFP

549   and 35Spro:PKS4_C*- GFP. Excitation was done using an Argon laser at 488nm and detection

550   used a band pass emission between 505 and 530 nm. For some images, the plasma membrane was

551   stained with FM4-64 dye (Cat. T13320, Invitrogen) at a concentration of 50µM, by soaking the

552   seedlings 1 minute and then washing three times in ½ MS. In that case the signal was detected at

553   a long pass emission from 650nm. Model LSM 880 was used for imaging pPKS4::PKS4-GFP,

554   pPKS4::PKS4 C*-GFP, pPKS4::PKS4 F*-GFP, pPKS4::myriPKS4-GFP WT, pPKS4::myriPKS4

555   C*-GFP, pPKS4::PKS4-GFPfarn, and pPKS4::PKS4 C*-GFPfarn. Samples were excited with an

556   Argon laser (488nm) and detection was done between 495 and 518 nm. In all cases a channel was

557   set to detect chlorophyll, exciting with the laser used for excitation of the fluorophore of interest,

558   and detecting between 607 and 691 nm.

559   Biotin switch assay

560   Palmitoylation of the PKS1 fragments were assayed as described in (Hemsley et al., 2008) with

561   some modifications. Three-day-old etiolated seedlings were ground in cold mortar at 4°C and

562   resuspended in 2x volume of lysis buffer per fresh weight. After the first centrifugation, 1ml of the

563   supernatant was combined to 1ml of lysis buffer and incubation was done during 3h at 4°C on a

564   roller table. All centrifugation steps were performed at 4°C. The loading control was not

565   precipitated. We used 60µl of high capacity neutravidin-agarose beads (Thermo Fisher) instead of

566   15µl.

567   <u>Western blot</u>

568   For the biotin switch assay, proteins extracted in 2x Laemmli buffer were separated on 12%

569   SDS/PAGE gels and transferred onto nitrocellulose in CAPS buffer. Blots were probed with anti-

570   GFP monoclonal antibody JL-8 (632381, Clontech) diluted at 1/3000 in 1X PBS containing 0.1%

571   Tween-20 and 5% non-fat milk. For the other western blots, total proteins (80µl 2× Laemmli buffer

572   for 20mg fresh weight; 10µg per lane) were separated on 4-15% precast polyacrylamide gels and

573   transferred onto nitrocellulose using the Trans-Blot Turbo RTA Transfer Kit. Anti-HA-HRP

574   monoclonal antibody 3F10 was used at 1/4000 (12013819001, Roche), anti-GFP monoclonal

575   antibody JL-8 (632381, Clontech) was used at 1/3000, and anti-DET3 antibody was used at

576   1/20000 dilutions (Schumacher et al., 1999) in 1X PBS containing 0.1% Tween-20 and 5% non-

577   fat milk. Chemiluminescence signals were generated using Immobilon Western HRP Substrate

578   (Millipore). Signals were detected with a Fujifilm ImageQuant LAS 4000 mini CCD camera

579   system and quantifications were performed with ImageQuant TL software (GE Healthcare).

580   <u>Accession Numbers</u>

581   The Arabidopsis Genome Initiative numbers for the genes mentioned in this article are as follows:

582   AT2G02950 (PKS1), AT1G14280 (PKS2), AT1G18810   (PKS3),   AT5G04190   (PKS4),

583   AT5G64330

584

597 **Author contributions**

598 A.L.V., L.A-P and C.F. conceived the original research plans; A.L.V., L.A-P, N.G., E.R.L., C.D.

599 and C.F. performed experiments and/or analyzed the data; A.L.V. and C.F. wrote the article with

600 contributions of all the authors; C.F. agrees to serve as the author responsible for contact and

601 ensures communication.

602

LITERATURE CITED

Altenhoff, A.M., Train, C.M., Gilbert, K.J., Mediratta, I., Mendes de Farias, T., Moi, D., Nevers, Y., Radoykova, H.S., Rossier, V., Warwick Vesztrocy, A., Glover, N.M., and Dessimoz, C. (2021). OMA orthology in 2021: website overhaul, conserved isoforms, ancestral gene order and more. Nucleic Acids Res **49,** D373-D379.

Altschul, S.F., Gish, W., Miller, W., Myers, E.W., and Lipman, D.J. (1990). Basic local alignment search tool. J Mol Biol **215,** 403-410.

Bensmihen, S., To, A., Lambert, G., Kroj, T., Giraudat, J., and Parcy, F. (2004). Analysis of an activated ABI5 allele using a new selection method for transgenic Arabidopsis seeds. FEBS Lett **561,** 127-131.

Capella-Gutierrez, S., Silla-Martinez, J.M., and Gabaldon, T. (2009). trimAl: a tool for automated alignment trimming in large-scale phylogenetic analyses. Bioinformatics **25,** 1972-1973.

Cheng, M.C., Kathare, P.K., Paik, I., and Huq, E. (2021). Phytochrome Signaling Networks. Annu Rev Plant Biol **72,** 217-244.

Christie, J.M. (2007). Phototropin blue-light receptors. Annu Rev Plant Biol **58,** 21-45.

Christie, J.M., Suetsugu, N., Sullivan, S., and Wada, M. (2018). Shining Light on the Function of NPH3/RPT2-Like Proteins in Phototropin Signaling. Plant Physiol **176,** 1015-1024.

Correll, M.J., and Kiss, J.Z. (2002). Interactions between gravitropism and phototropism in plants. J Plant Growth Regul **21,** 89-101.

de Carbonnel, M., Davis, P., Roelfsema, M.R., Inoue, S., Schepens, I., Lariguet, P., Geisler, M., Shimazaki, K., Hangarter, R., and Fankhauser, C. (2010). The Arabidopsis PHYTOCHROME KINASE SUBSTRATE2 protein is a phototropin signaling element that regulates leaf flattening and leaf positioning. Plant Physiol **152,** 1391-1405.

Demarsy, E., Schepens, I., Okajima, K., Hersch, M., Bergmann, S., Christie, J., Shimazaki, K., Tokutomi, S., and Fankhauser, C. (2012). Phytochrome Kinase Substrate 4 is phosphorylated by the phototropin 1 photoreceptor. EMBO J **31,** 3457-3467.

Drozdetskiy, A., Cole, C., Procter, J., and Barton, G.J. (2015). JPred4: a protein secondary structure prediction server. Nucleic Acids Res **43,** W389-394.

Fankhauser, C., and Christie, J.M. (2015). Plant phototropic growth. Curr Biol **25,** R384-389.

Fankhauser, C., Yeh, K.C., Lagarias, J.C., Zhang, H., Elich, T.D., and Chory, J. (1999). PKS1, a substrate phosphorylated by phytochrome that modulates light signaling in Arabidopsis. Science **284,** 1539-1541.

Frith, M.C., Saunders, N.F., Kobe, B., and Bailey, T.L. (2008). Discovering sequence motifs with arbitrary insertions and deletions. PLoS Comput Biol **4,** e1000071.

Gabler, F., Nam, S.Z., Till, S., Mirdita, M., Steinegger, M., Soding, J., Lupas, A.N., and Alva, V. (2020). Protein Sequence Analysis Using the MPI Bioinformatics Toolkit. Curr Protoc Bioinformatics **72,** e108.

Galen, C., Huddle, J., and Liscum, E. (2004). An experimental test of the adaptive evolution of phototropins: blue-light photoreceptors controlling phototropism in Arabidopsis thaliana. Evolution **58,** 515-523.

Goyal, A., Szarzynska, B., and Fankhauser, C. (2013). Phototropism: at the crossroads of light-signaling pathways. Trends Plant Sci **18,** 393-401.

647 **Harmer, S.L., and Brooks, C.J.** (2018). Growth-mediated plant movements: hidden in plain
648 sight. Curr Opin Plant Biol **41,** 89-94.
649 **Hemsley, P.A.** (2013). Assaying protein S-acylation in plants. Methods Mol Biol **1043,** 141-146.
650 **Hemsley, P.A.** (2020). S-acylation in plants: an expanding field. Biochem Soc Trans **48,** 529-536.
651 **Hemsley, P.A., Taylor, L., and Grierson, C.S.** (2008). Assaying protein palmitoylation in plants.
652 Plant Methods **4,** 2.
653 **Hoang, D.T., Chernomor, O., von Haeseler, A., Minh, B.Q., and Vinh, L.S.** (2018). UFBoot2:
654 Improving the Ultrafast Bootstrap Approximation. Mol Biol Evol **35,** 518-522.
655 **Jumper, J., Evans, R., Pritzel, A., Green, T., Figurnov, M., Ronneberger, O.,**
656 **Tunyasuvunakool, K., Bates, R., Zidek, A., Potapenko, A., Bridgland, A., Meyer, C.,**
657 **Kohl, S.A.A., Ballard, A.J., Cowie, A., Romera-Paredes, B., Nikolov, S., Jain, R.,**
658 **Adler, J., Back, T., Petersen, S., Reiman, D., Clancy, E., Zielinski, M., Steinegger, M.,**
659 **Pacholska, M., Berghammer, T., Bodenstein, S., Silver, D., Vinyals, O., Senior, A.W.,**
660 **Kavukcuoglu, K., Kohli, P., and Hassabis, D.** (2021). Highly accurate protein structure
661 prediction with AlphaFold. Nature **596,** 583-589.
662 **Kalyaanamoorthy, S., Minh, B.Q., Wong, T.K.F., von Haeseler, A., and Jermiin, L.S.** (2017).
663 ModelFinder: fast model selection for accurate phylogenetic estimates. Nat Methods **14,**
664 587-589.
665 **Kami, C., Allenbach, L., Zourelidou, M., Ljung, K., Schutz, F., Isono, E., Watahiki, M.K.,**
666 **Yamamoto, K.T., Schwechheimer, C., and Fankhauser, C.** (2014). Reduced
667 phototropism in pks mutants may be due to altered auxin-regulated gene expression or
668 reduced lateral auxin transport. Plant J **77,** 393-403.
669 **Katoh, K., and Standley, D.M.** (2013). MAFFT multiple sequence alignment software version 7:
670 improvements in performance and usability. Mol Biol Evol **30,** 772-780.
671 **Kim, J., Song, K., Park, E., Kim, K., Bae, G., and Choi, G.** (2016a). Epidermal Phytochrome
672 B Inhibits Hypocotyl Negative Gravitropism Non-Cell-Autonomously. Plant Cell **28,**
673 2770-2785.
674 **Kim, K., Shin, J., Lee, S.H., Kweon, H.S., Maloof, J.N., and Choi, G.** (2011). Phytochromes
675 inhibit hypocotyl negative gravitropism by regulating the development of endodermal
676 amyloplasts through phytochrome-interacting factors. Proc Natl Acad Sci U S A **108,**
677 1729-1734.
678 **Kim, K., Jeong, J., Kim, J., Lee, N., Kim, M.E., Lee, S., Chang Kim, S., and Choi, G.** (2016b).
679 PIF1 Regulates Plastid Development by Repressing Photosynthetic Genes in the
680 Endodermis. Mol Plant **9,** 1415-1427.
681 **Kumar, M., Carr, P., and Turner, S.R.** (2022). An atlas of Arabidopsis protein S-acylation
682 reveals its widespread role in plant cell organization and function. Nat Plants **8,** 670-681.
683 **Lariguet, P., and Fankhauser, C.** (2004). Hypocotyl growth orientation in blue light is
684 determined by phytochrome A inhibition of gravitropism and phototropin promotion of
685 phototropism. Plant J **40,** 826-834.
686 **Lariguet, P., Boccalandro, H.E., Alonso, J.M., Ecker, J.R., Chory, J., Casal, J.J., and**
687 **Fankhauser, C.** (2003). A growth regulatory loop that provides homeostasis to
688 phytochrome a signaling. Plant Cell **15,** 2966-2978.
689 **Lariguet, P., Schepens, I., Hodgson, D., Pedmale, U.V., Trevisan, M., Kami, C., de**
690 **Carbonnel, M., Alonso, J.M., Ecker, J.R., Liscum, E., and Fankhauser, C.** (2006).
691 PHYTOCHROME KINASE SUBSTRATE 1 is a phototropin 1 binding protein required
692 for phototropism. Proc Natl Acad Sci U S A **103,** 10134-10139.

693 **Legris, M., and Boccaccini, A.** (2020). Stem phototropism toward blue and ultraviolet light.
694   Physiol Plant **169,** 357-368.
695 **Legris, M., Ince, Y.C., and Fankhauser, C.** (2019). Molecular mechanisms underlying
696   phytochrome-controlled morphogenesis in plants. Nat Commun **10,** 5219.
697 **Li, F.W., and Mathews, S.** (2016). Evolutionary aspects of plant photoreceptors. J Plant Res **129,**
698   115-122.
699 **Liscum, E., Askinosie, S.K., Leuchtman, D.L., Morrow, J., Willenburg, K.T., and Coats, D.R.**
700   (2014). Phototropism: growing towards an understanding of plant movement. Plant Cell
701   **26,** 38-55.
702 **Liu, L., Tong, H., Xiao, Y., Che, R., Xu, F., Hu, B., Liang, C., Chu, J., Li, J., and Chu, C.**
703   (2015). Activation of Big Grain1 significantly improves grain size by regulating auxin
704   transport in rice. Proc Natl Acad Sci U S A **112,** 11102-11107.
705 **Minh, B.Q., Nguyen, M.A., and von Haeseler, A.** (2013). Ultrafast approximation for
706   phylogenetic bootstrap. Mol Biol Evol **30,** 1188-1195.
707 **Mishra, B.S., Jamsheer, K.M., Singh, D., Sharma, M., and Laxmi, A.** (2017). Genome-Wide
708   Identification and Expression, Protein-Protein Interaction and Evolutionary Analysis of the
709   Seed Plant-Specific BIG GRAIN and BIG GRAIN LIKE Gene Family. Front Plant Sci **8,**
710   1812.
711 **Nakamura, M., Nishimura, T., and Morita, M.T.** (2019). Gravity sensing and signal conversion
712   in plant gravitropism. J Exp Bot **70,** 3495-3506.
713 **Nguyen, L.T., Schmidt, H.A., von Haeseler, A., and Minh, B.Q.** (2015). IQ-TREE: a fast and
714   effective stochastic algorithm for estimating maximum-likelihood phylogenies. Mol Biol
715   Evol **32,** 268-274.
716 **Oh, E., Kim, J., Park, E., Kim, J.I., Kang, C., and Choi, G.** (2004). PIL5, a phytochrome-
717   interacting basic helix-loop-helix protein, is a key negative regulator of seed germination
718   in Arabidopsis thaliana. Plant Cell **16,** 3045-3058.
719 **Preuten, T., Blackwood, L., Christie, J.M., and Fankhauser, C.** (2015). Lipid anchoring of
720   Arabidopsis phototropin 1 to assess the functional significance of receptor internalization:
721   should I stay or should I go? New Phytol **206,** 1038-1050.
722 **Proost, S., Van Bel, M., Vaneechoutte, D., Van de Peer, Y., Inze, D., Mueller-Roeber, B., and**
723   **Vandepoele, K.** (2015). PLAZA 3.0: an access point for plant comparative genomics.
724   Nucleic Acids Res **43,** D974-981.
725 **Robinson, O., Dylus, D., and Dessimoz, C.** (2016). Phylo.io: Interactive Viewing and
726   Comparison of Large Phylogenetic Trees on the Web. Mol Biol Evol **33,** 2163-2166.
727 **Robson, P.R., and Smith, H.** (1996). Genetic and transgenic evidence that phytochromes A and
728   B act to modulate the gravitropic orientation of Arabidopsis thaliana hypocotyls. Plant
729   Physiol **110,** 211-216.
730 **Sack, F.D.** (1997). Plastids and gravitropic sensing. Planta **203,** S63-68.
731 **Schepens, I., Boccalandro, H.E., Kami, C., Casal, J.J., and Fankhauser, C.** (2008).
732   PHYTOCHROME KINASE SUBSTRATE4 modulates phytochrome-mediated control of
733   hypocotyl growth orientation. Plant Physiol **147,** 661-671.
734 **Schumacher, P., Demarsy, E., Waridel, P., Petrolati, L.A., Trevisan, M., and Fankhauser, C.**
735   (2018). A phosphorylation switch turns a positive regulator of phototropism into an
736   inhibitor of the process. Nat Commun **9,** 2403.

737   **Sullivan, S., Kharshiing, E., Laird, J., Sakai, T., and Christie, J.M.** (2019). Deetiolation
738   Enhances Phototropism by Modulating NON-PHOTOTROPIC HYPOCOTYL3
739   Phosphorylation Status. Plant Physiol **180,** 1119-1131.
740   **Sullivan, S., Waksman, T., Paliogianni, D., Henderson, L., Lutkemeyer, M., Suetsugu, N.,**
741   **and Christie, J.M.** (2021). Regulation of plant phototropic growth by NPH3/RPT2-like
742   substrate phosphorylation and 14-3-3 binding. Nat Commun **12,** 6129.
743   **Talavera, G., and Castresana, J.** (2007). Improvement of phylogenies after removing divergent
744   and ambiguously aligned blocks from protein sequence alignments. Syst Biol **56,** 564-577.
745   **Trifinopoulos, J., Nguyen, L.T., von Haeseler, A., and Minh, B.Q.** (2016). W-IQ-TREE: a fast
746   online phylogenetic tool for maximum likelihood analysis. Nucleic Acids Res **44,** W232-
747   235.
748   **Turnbull, D., and Hemsley, P.A.** (2017). Fats and function: protein lipid modifications in plant
749   cell signalling. Curr Opin Plant Biol **40,** 63-70.
750   **Vandenbrink, J.P., and Kiss, J.Z.** (2019). Plant responses to gravity. Semin Cell Dev Biol **92,**
751   122-125.
752   **Xue, Y., Xing, J., Wan, Y., Lv, X., Fan, L., Zhang, Y., Song, K., Wang, L., Wang, X., Deng,**
753   **X., Baluska, F., Christie, J.M., and Lin, J.** (2018). Arabidopsis Blue Light Receptor
754   Phototropin 1 Undergoes Blue Light-Induced Activation in Membrane Microdomains. Mol
755   Plant **11,** 846-859.
756   **Zaballa, M.E., and van der Goot, F.G.** (2018). The molecular era of protein S-acylation:
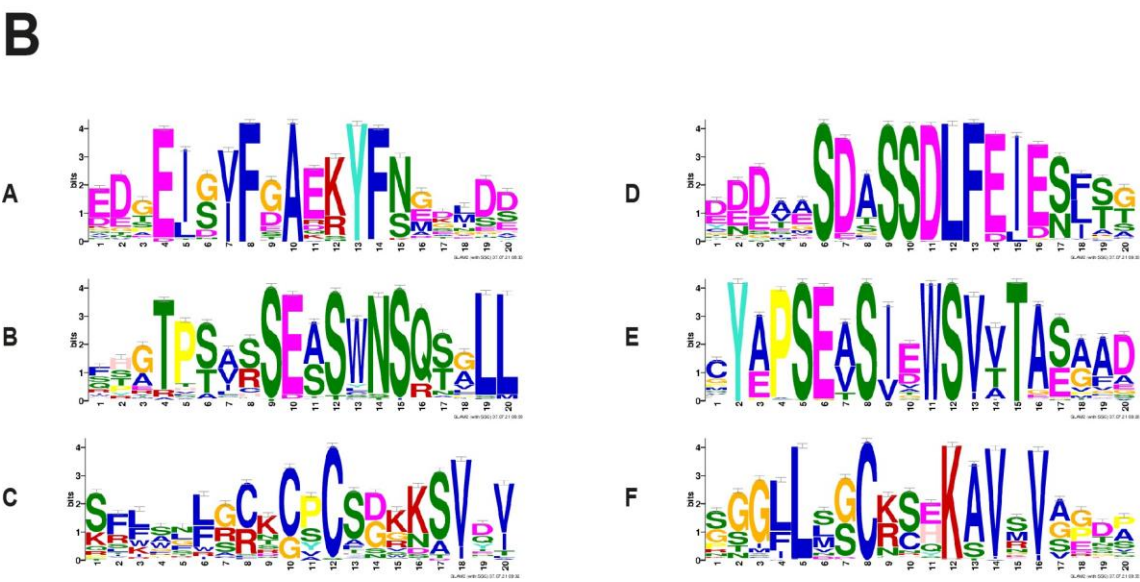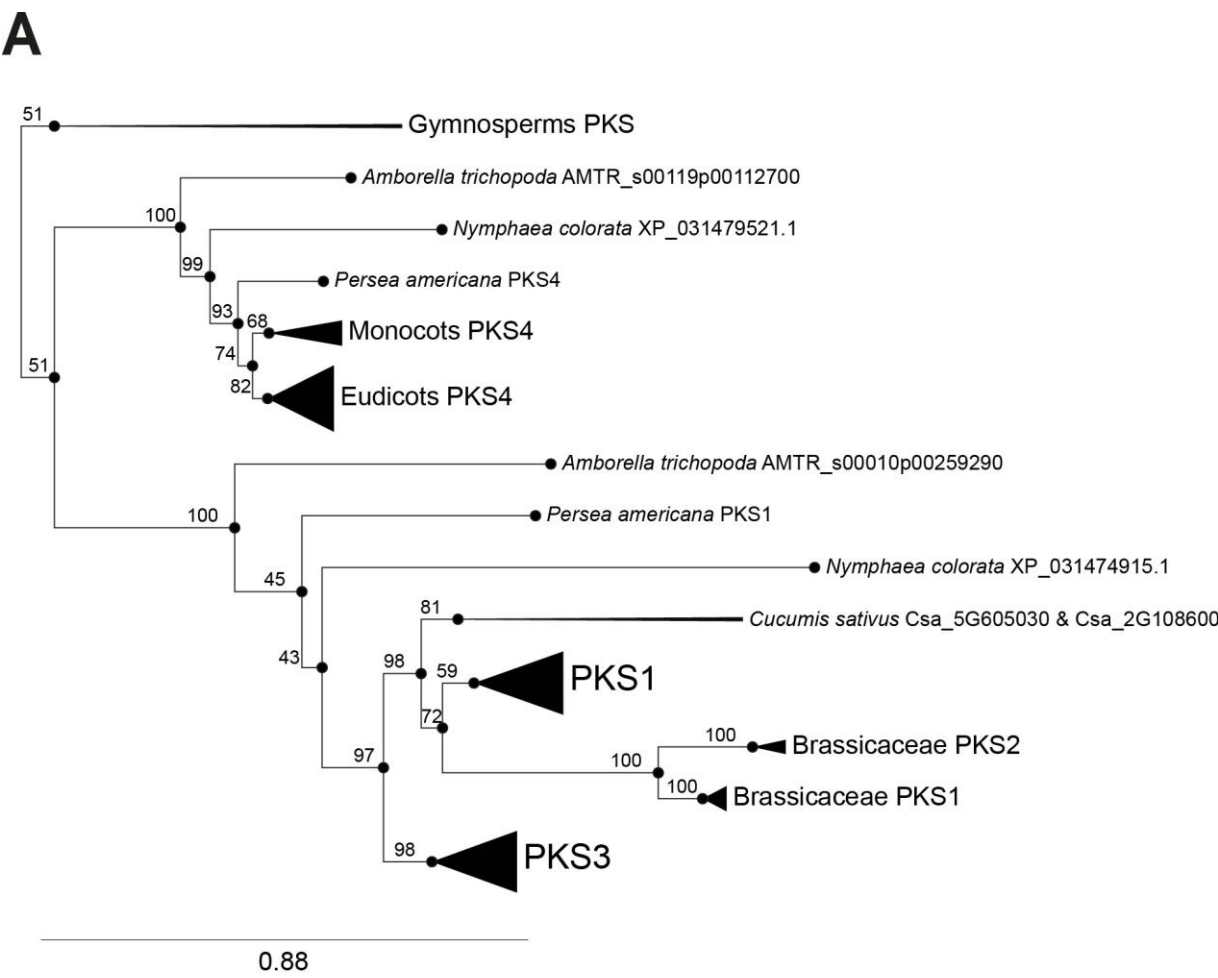757   spotlight on structure, mechanisms, and dynamics. Crit Rev Biochem Mol Biol **53,** 420-
758   451.

759

760

FIGURES

763   **Figure 1.** PKS proteins are present in seed plants and comprise 6 conserved sequence motifs.

764   **(A)** Simplified phylogeny of PKS proteins, obtained using IQ-TREE and the JTT+I+G4 substitution model. Some

765   nodes are collapsed, indicated by triangles at the leaves, and represent multiple genes. Ultrafast bootstrap values are

766   shown at each node. The full version of the tree can be found in Supplemental Figure S1. **(B)** Sequence motifs

767   conserved amongst members of the PKS family. Motifs A to F are found from the N- to the C-terminus of the proteins.

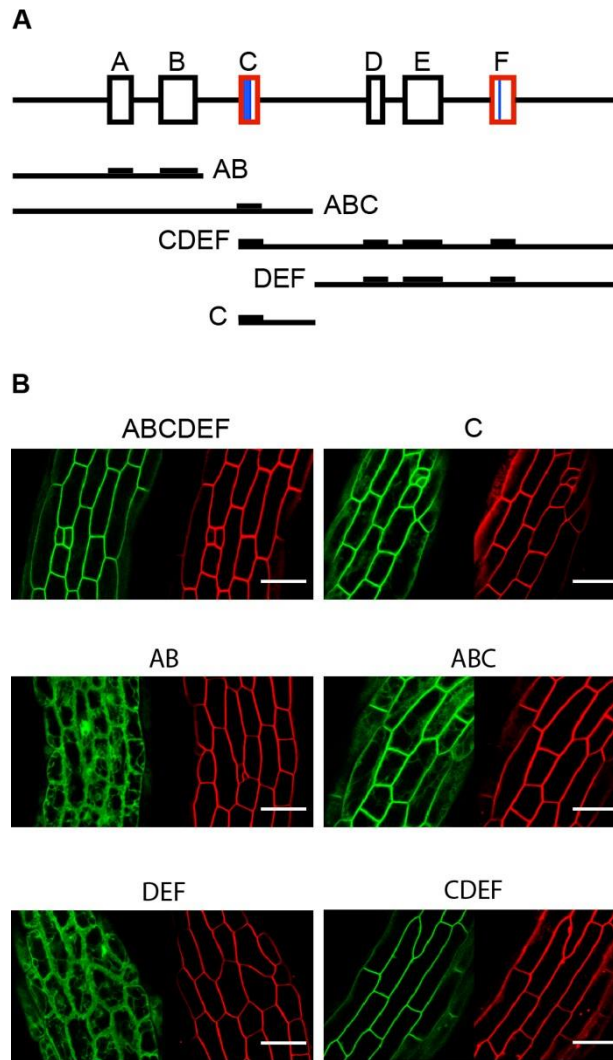768   GLAM2 was used to find the conserved motifs and to create the logos images.

769

A

B

Figure 2. PKS1 is plasma membrane associated and motif C is required for this association.

(**A**) Illustration of PKS1 protein, with the 6 motifs as defined in figure 1. Motifs C and F are shown in red, as they share homologies. Cystein residues are shown as blue lines, one thick line in motif C to represent the 3 cystein residues, one thin line in motif F to represent one cystein residue. (**B**) Confocal images of hypocotyl hooks from 3 days old transgenic etiolated seedlings, expressing GFP-tagged PKS1 either full length or truncated fragments. In red the FM4-64 staining, to show the plasma membrane. Scale bar is 30µm.
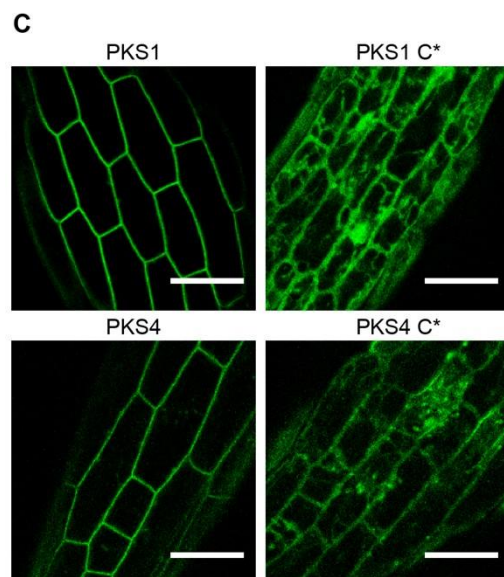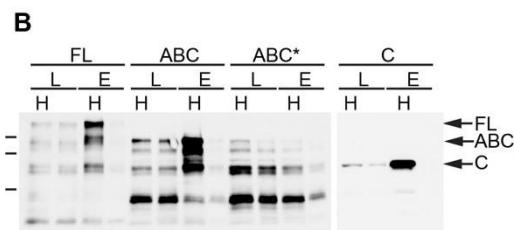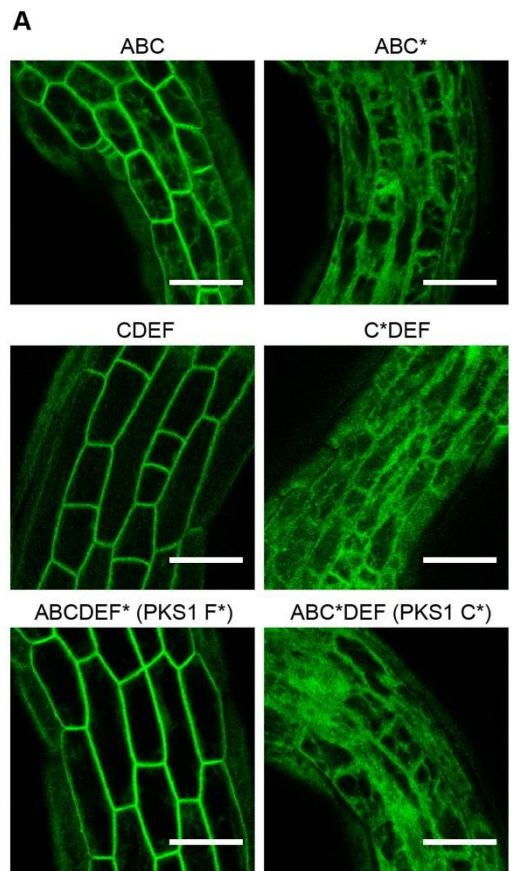
Figure 3. Cysteines of motif C from PKS1 and PKS4 are essential for plasma membrane localization.

(A) Confocal images of hypocotyl hooks from 3 days old transgenic etiolated seedlings, expressing GFP-tagged PKS1 full length or truncated fragments with mutated cysteines either in motif C or F. Scale bar is 30μm. **(B)** Cysteine residues of motif C are S-acylated. Western blots of full length PKS1 or truncated fragments either WT or with mutated cysteines. Protein extracts were used in a biotin switch assay. L = loading, E= elution, H = hydroxylamine-treated. Marker sizes are 72, 55, 36 KDa. **(C)** Confocal images of hypocotyl hooks from 3 days old transgenic etiolated seedlings, expressing GFP-tagged PKS1 or PKS4 full length proteins, either WT or mutated in cysteines of motif C. Scale bar is 30μm.
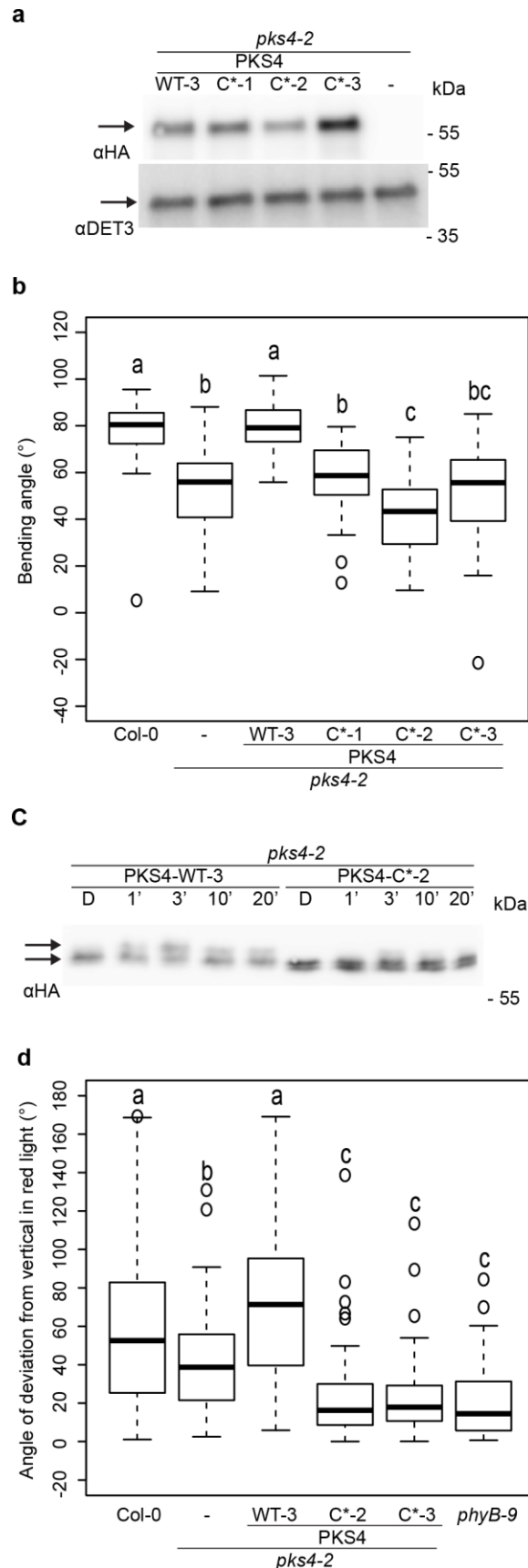
777

Figure 4. Motif C is required for PKS4 function in phototropism and inhibition of gravitropism.

(A) Western blot probed with anti-HA antibody from *pks4-2*, *pks4-2* PKS4 WT-3 and *pks4-2* PKS4 C*-1, C*-2, and C*-3 samples of 3- day- old dark grown seedlings. The same membrane was probed with alpha-DET3 antibody as a loading control. **(B)** Phototropic curvature of 3-day-old dark grown Col-0, *pks4-2*, *pks4-2* PKS4 WT-3 and *pks4-2* PKS4 C* (C*-1, C*-2, and C*-3) lines treated with unidirectional blue light coming from one side. Seedlings were exposed to 0.1 μmol m^{-2} s^{-1} blue light during 24 h prior to measurement of growth reorientation. n= 40 – 60, means with the same letter are not significantly different (p > 0.01, two-way ANOVA with Tukey's HSD test). **(C)** Western blot probed with anti-HA antibody from *pks4-2* PKS4 WT and *pks4-2* PKS4 C*-2 samples of 3- day- old dark grown samples exposed to 1 μmol m^{-2} s^{-1} blue light for 0, 1, 3, 10, and 20 minutes. **(D)** Hypocotyl growth orientation of Col-0, *pks4-2*, *pks4-2* PKS4 WT-3 and *pks4-2* PKS4 C*-1, C*-2, and C*-3 seedlings growing in continuous 30 μmol m^{-2} s^{-1} red light. Seedlings were kept for 24h in darkness prior to 4 days of red light treatment following measurement of growth orientation. 0° represents vertical growth. We consider the absolute value of the angle, no matter if the seedling bends towards the left or the right side. n= 70 – 80, means with the same letter are not significantly different (p > 0.01, two-way ANOVA with Tukey's HSD test).
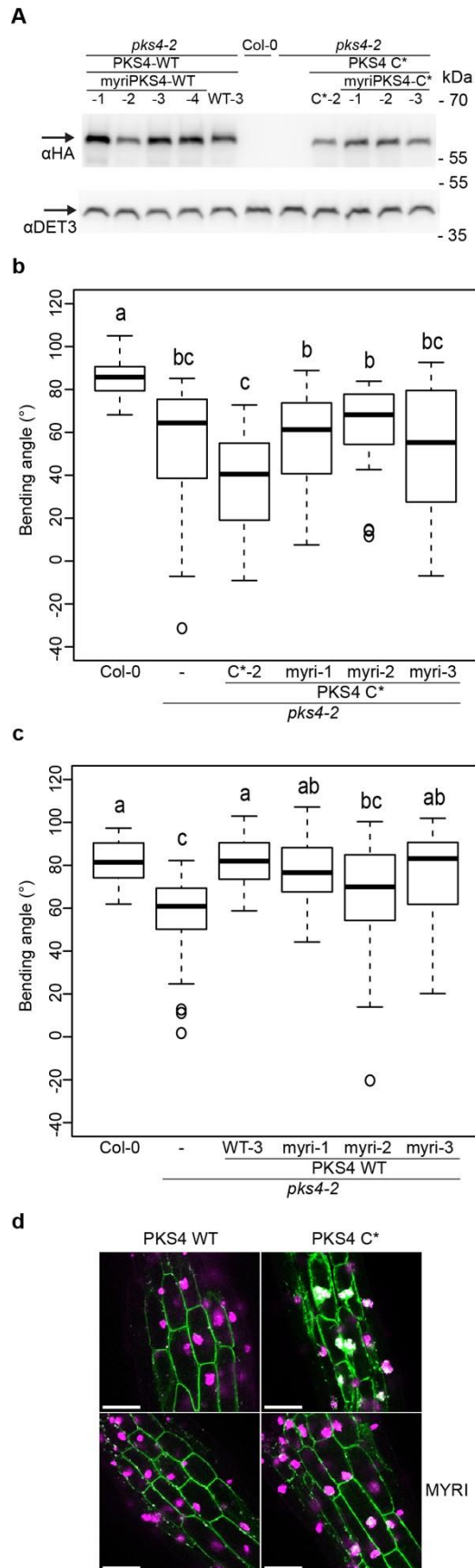
778

A

Figure 5. Targeting PKS4 C* to the PM through myristoylation does not rescue PKS4 function. **(A)** Western blot probed with anti-HA antibody from Col-0, *pks4-2*, *pks4-2* PKS4 WT-3, *pks4-2* PKS4 C*-2, *pks4-2* myriPKS4 WT-1, -2, -3, -4, myriPKS4 C*-1, -2, and -3 samples of 3- day- old dark grown seedlings. The same membrane was probed with alpha-DET3 antibody as a loading control. **(B)** Phototropic curvature of 3-day-old dark grown Col-0, *pks4-2*, *pks4-2* PKS4 C*-2 and *pks4-2* myriPKS4 C* (myriC*-1, myriC*-2, and myriC*-3) lines seedlings treated with unidirectional blue light coming from one side. Seedlings were exposed to 0.1 μmol m^{-2} s^{-1} blue light during 24 h prior to measurement of growth reorientation. n= 25 – 60, means with the same letter are not significantly different (p > 0.01, two-way ANOVA with Tukey's HSD test). **(C)** Phototropic curvature of 3-day-old dark grown Col-0, *pks4-2*, *pks4-2* PKS4 WT-3 and *pks4-2* myriPKS4 WT (myriWT-1, myriWT-2, and myriWT-3) lines seedlings treated with unidirectional blue light coming from one side. Seedlings were assayed as in b. **(D)** Confocal microscopy images of 3-day-old etiolated hypocotyls cortex cells expressing PKS4-GFP, PKS4 C*-GFP, myriPKS4-GFP, and myriPKS4 C*-GFP (green signal) from the PKS4 promoter. Note that these lines also show remaining oily bodies (in magenta) resulting from the expression of OLE1-RFP from the OLE1 promoter, used as a seeds coats selection marker. Scale bar: 50 μm.

779

1   **SUPPLEMENTARY MATERIAL**

2   Control of PHYTOCHROME KINASE SUBSTRATE subcellular localization and biological

3   activity by protein S-acylation.

4

5   Ana Lopez Vazquez[a], Laure Allenbach Petrolati[a], Christophe Dessimoz [b, c], Edwin R. Lampugnani

6   [d], Natasha Glover [b, c] and Christian Fankhauser[a*]

7

13

A

PKS4

PKS1

Brassicaceae PKS2

Brassicaceae PKS1

PKS3

0.38

A B C G D E F
motif

B

motif G

15 **Supplemental figure S1.** PKS protein phylogeny and motif composition.

16 **(A)** phylogeny of PKS proteins and motif composition. The tree was obtained using IQ-TREE and the JTT+I+G4

17 substitution model. The orange, green, and blue boxes highlighting the sequences indicate clades of PKSs 1/2, 3, and

18 4, respectively. The table to the right of the tree corresponds to the phylogeny: each row in the table corresponds to

19 the sequence to its left, and each column is a motif. A black box in the table indicates absence of a motif in a given

20 sequence. **(B)** Conserved motif G that is absent in Brassicacea PKS3 and PKS4 proteins

a

b

c

d

e

f

PKS4 WT   PKS4 C*   PKS4 F*
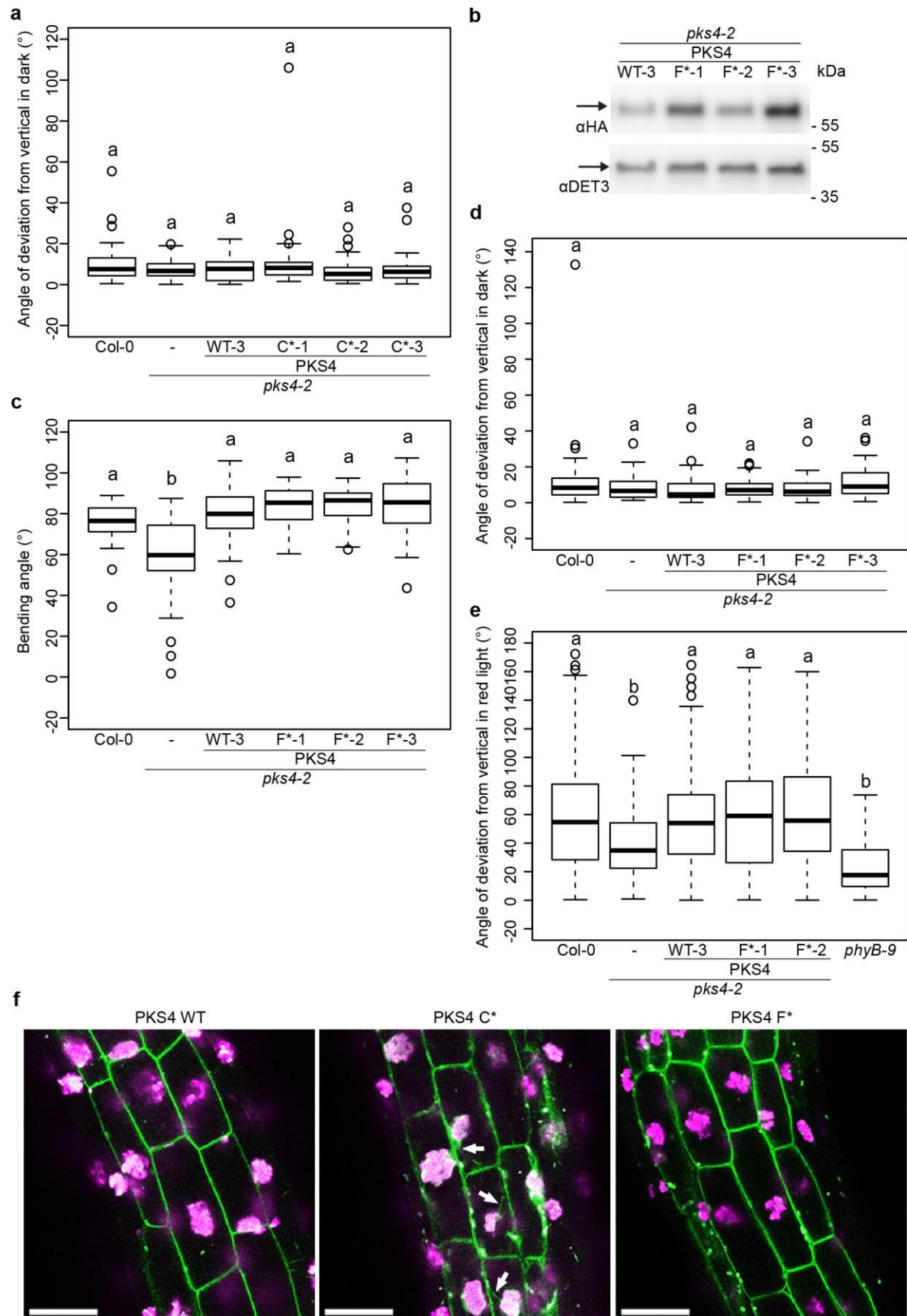
22 **Supplemental figure S2.** The invariant Cys residue of motif F is not required for PKS4 function. **(A)** Hypocotyl

23 growth orientation of 3-day-old Col-0, *pks4-2*, *pks4-2* PKS4 WT-3 and *pks4-2* PKS4 C*-1, C*-2, and C*-3 etiolated

24 seedlings. 0° represents vertical growth. We consider the absolute value of the angle, no matter if the seedling bends

25 towards the left or the right side. n= 50 – 60, means with the same letter are not significantly different (p > 0.01, two-

26 way ANOVA with Tukey's HSD test). **(B)** Western blot probed with anti-HA antibody from *pks4-2* PKS4 WT-3 and

27 *pks4-2* PKS4 F*-1, F*-2, and F*-3 samples of 3- day- old dark grown seedlings. The same membrane was probed

28 with alpha-DET3 antibody as a loading control. **(C)** Phototropic curvature of 3-day-old dark grown Col-0, *pks4-2*,

29 *pks4-2* PKS4 WT-3 and *pks4-2* PKS4 F*-1, F*-2, and F*-3 seedlings treated with unidirectional blue light coming

30 from one side. Seedlings were exposed to 0.1 µmol m^{-2} s^{-1} blue light during 24 h prior to measurement of growth

31 reorientation. n= 40 – 60, means with the same letter are not significantly different (p > 0.01, two-way ANOVA with

32 Tukey's HSD test). **(D)** Hypocotyl growth orientation of 3-day-old Col-0, *pks4-2*, *pks4-2* PKS4 WT-3 and *pks4-2*

33 PKS4 F*-1, F*-2, and F*-3 etiolated seedlings. Considerations and data analysis were as in S2a. **(E)** Hypocotyl growth

34 orientation of Col-0, *pks4-2*, *pks4-2* PKS4 WT-3 and *pks4-2* PKS4 F*-1 and F*-2 seedlings growing in continuous 30

35 µmol m^{-2} s^{-1} red light. Seedlings were kept for 24h in darkness prior to 4 days of red light treatment following

36 measurement of growth orientation. 0° represents vertical growth. We consider the absolute value of the angle, no

37 matter if the seedling bends towards the left or the right side. n= 70 – 80, means with the same letter are not

38 significantly different (p > 0.01, two-way ANOVA with Tukey's HSD test). **(F)** Confocal microscopy images of 4-

39 day- old *pks4-2* dark-grown seedlings expressing *pPKS4:PKS4 WT:GFP, pPKS4:PKS4 C*:GFP* oand *pPKS4:PKS4*

40 *F*:GFP*. Scale bar: 50 µm.

41
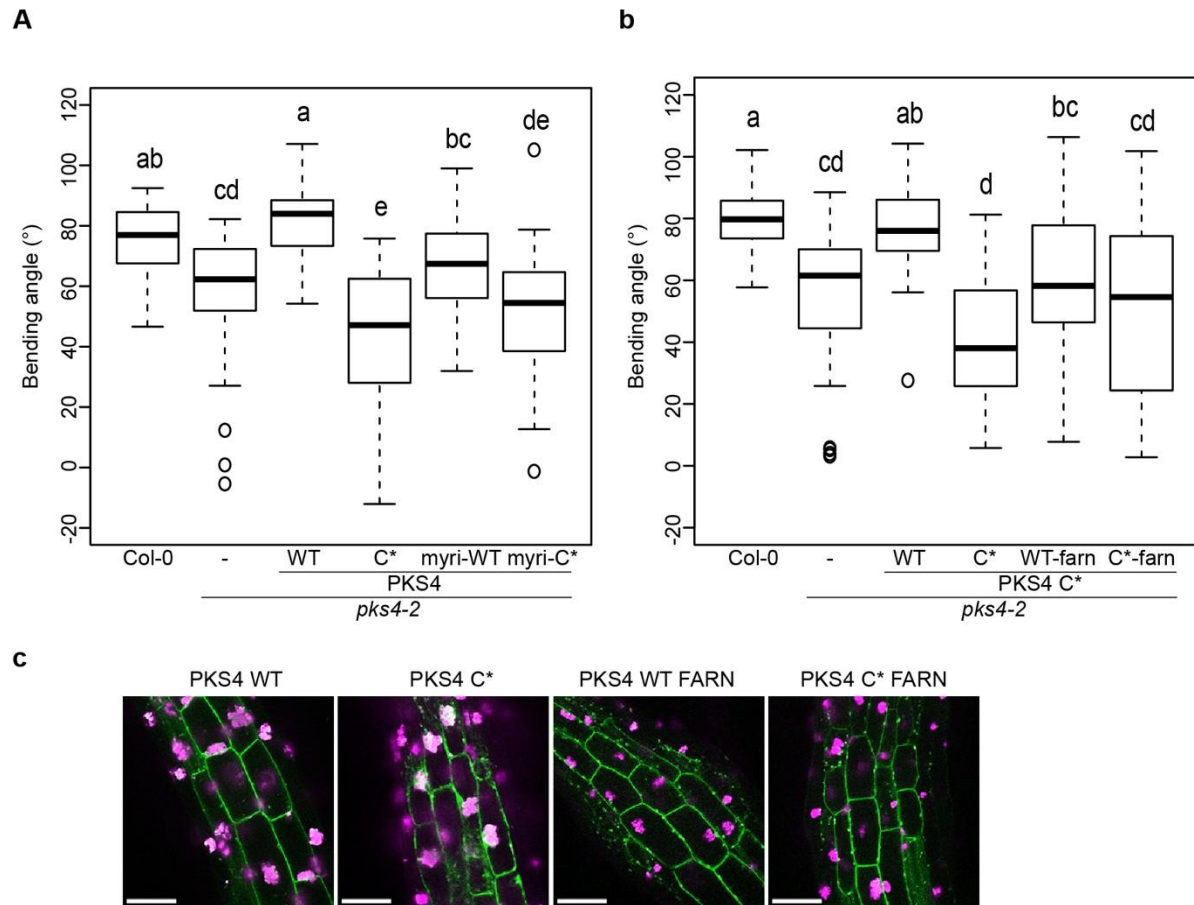
Supplemental figure S3 Targeting PKS4 C* to the PM through farnesylation does not rescue PKS4 function.

(**A**) Phototropic curvature of 3-day-old dark grown Col-0, *pks4-2*, *pks4-2* PKS4 WT-3, *pks4-2* PKS4 C*-2, *pks4-2* myriPKS4 WT and *pks4-2* myriPKS4 C* seedlings treated with unidirectional blue light coming from one side. The *pks4-2* lines expressing the PKS4 WT and the different variants were assayed in the T1 generation. Seedlings were exposed to 0.1 μmol m^{-2} s^{-1} blue light during 24 h prior to measurement of growth reorientation. n= 40 – 60, means with the same letter are not significantly different (p > 0.01, two-way ANOVA with Tukey's HSD test). (**B**) Phototropic curvature of 3-day-old dark grown Col-0, *pks4-2*, *pks4-2* PKS4 C*-2, *pks4-2* PKS4 WTfarn and *pks4-2* myriPKS4 C*farn seedlings treated with unidirectional blue light coming from one side. Considerations, light treatment, and data analysis were as in S3a. (**C**) Confocal microscopy images of 3-day-old etiolated hypocotyls cortex cells expressing PKS4-GFP, PKS4 C*-GFP, PKS4-GFPfarn, and PKS4 C*-GFPfarn (green signal) from the PKS4 promoter. Note that these lines also show remaining oily bodies (in magenta) resulting from the expression of OLE1-RFP from the OLE1 promoter, used as a seeds coats selection marker. Scale bar: 50 μm.

55　**Supplemental table 1.** PKS sequences used in the phylogenetic analysis

56

PKS sequences	Source	Nb sequences
PKS1/2 root HOG	OMA database Jan2020 version	59
PKS3 root HOG	OMA database Jan2020 version	42
PKS4 root HOG	OMA database Jan2020 version	40
HOG with missing PKS4 Amborella gene	OMA database Jan2020 version	14
Other sequences in *Beta vulgaris*, *Nymphea colorata*, *Persea americana*, Setaria, Phalaenopsis, *Fragaria vesca*, *Camellia sinensis* (word doc from Christian)	NCBI	15
Gymnosperm sequences PAB00020933 & PAB00056196 from *Picea abies* (from PLAZA)	Gymno PLAZA 1.0	2

57
58

59 **Supplemental table 2.** Primers used in this study

Name	Sequence
CF129	5'- ggggtaccaaaatggtgacactaacacca-3'
CF470	5'- cgcggatcccctttccttgaaggaactgttg-3'
CF471	5'- cgcggatccctgtgtcgtcctcctctgttc-3'
CF472	5'- cggggtaccaaaatgaagagtgaagggagtgattc-3'
CF473	5'- cgcggatcccctgactataaagaagagatg-3'
CF507	5'- cggggtaccaaaatgaagaacagtaatggtcaga-3'

60
61
62
63
64
65
66
67

CHAPTER 2. Evolutionary analysis of the PKS protein family function

OVERVIEW

I led this project where we made a functional analysis of PKS proteins to help our understanding of their evolutionary history and made an analysis of their subcellular localization to find how it relates with function, under the supervision of Prof. Christian Fankhauser. Our work has not been submitted yet because we are waiting for the generation of transgenic lines to include a few additional experiments.

I conceived the original research plans with Laure Allenbach Petrolati and Prof. Christian Fankhauser. I generated the transgenic lines of the PKS4 orthologs for complementation analysis and confocal microscopy. I also helped in the generation of the CRISPR mutant lines in collaboration with Alja Van der Schuren and Amelia Maria Amiguet Vercher. I conducted and analyzed all the experiments presented in this chapter. I interpreted and discussed the data with the participation of Prof. Christian Fankhauser and the rest of the lab members. I wrote the manuscript about the current available data, with comments from Martina Legris and Prof. Christian Fankhauser.

ABSTRACT

PHYTOCHROME KINASE SUBSTRATE (*PKS*) genes are present in all angiosperms. It is predicted that duplication in the ancestral angiosperm *PKS* gene gave rise to the clades *PKS4*, where evolution was more constrained, and *PKS1/2/3* (names based on the *Arabidopsis thaliana* genes). Later divergence gave rise to the clades *PKS3* and *PKS1/2*, the last one splitting into *PKS1* and *PKS2* within Brassicaceae. *A. thaliana* includes 4 *PKS* genes, among which *PKS4* and *PKS1* are important for hypocotyl orientation in response to light, while *PKS3* and *PKS2* are important for leaf flattening and movement. Although *A. thaliana PKS* divergence can be explained by changes in their expression patterns, it is unknown whether there is also a functional diversification in their coding sequence. Our data show that PKS1 conserves the function of PKS4 while PKS2 and PKS3 functionally diverged. Moreover, PKS2 showed a different subcellular localization than PKS1 and PKS4, which are associated with the plasma membrane to function in phototropin and phytochrome signaling. Moreover, we provide evidence that PKS4 from the basal angiosperm *Amborella trichopoda* can partially function as *A. thaliana*PKS4, suggesting functional conservation across evolution. Additionally, our work shows that PKS4 is required to promote phototropism in *Brachypodium distachyon*, additionally suggesting deep conservation of PKS function in monocots.

INTRODUCTION

Gene families evolve through the processes of speciation, gene duplication, and horizontal gene transfer leading to the appearance of genes related by common ancestry, also called homologs, that are mainly classified into orthologs and paralogs. Orthologs are pairs of genes that started diverging via speciation, while paralogs are pairs of genes that started diverging via gene duplication (Fitch, 1970). Moreover, the connotation homoeologs appeared later to refer to pairs of genes in the same species that started diverging via speciation and were brought back together in the same genome via hybridization and genome doubling, which often occurred in genomes of plant species through the course of evolution (Glover et al., 2016).

The Orthologous Matrix (OMA) browser uses an algorithm to infer orthologs, paralogs, and homoeologs by considering all-against-all alignments between all the genomes in addition to taking into account evolutionary processes such as gene duplication, differential gene loss, chromosomal rearrangements, and genes movements (Glover et al., 2016, Altenhoff et al., 2017, Glover et al., 2021). Therefore, combined with experimental data, OMA can be useful to reconstruct the functional evolutionary story of plant gene families. The study of the plant-specific BRX protein family in root development represents a great example of functional validation where the most ancient BRX ortholog and the *Arabidopsis thaliana* (*A. thaliana*) BRX family members were tested for subcellular localization and functional complementation potential in the *brx* mutant (Briggs et al., 2006, Beuchat et al., 2010, Marhava et al., 2020, Koh et al., 2021).

OMA and other plant genome databases identified *PKS* ortholog and paralog genes that were present in all angiosperms. *PKS* phylogenetic studies predict that one *PKS* gene was present in the ancestral spermatophyte preceding a duplication in the ancestral angiosperm to form two copies: *PKS4* and *PKS1/2/3* (names based on *A. thaliana* genes). Additionally, after the basal angiosperms divergence,

it was predicted that another duplication occurred giving rise to *PKS1/2* and *PKS3*, and an additional Brassicaceae-specific duplication happened to give rise to *PKS1* and *PKS2*. The length of the phylogenetic tree branches suggests that evolution in the *PKS4* clade is more constrained than in the *PKS1/2/3* clade. The *PKS4* gene was present in all analyzed monocots and dicots. Moreover, while eudicots typically possess an additional *PKS3* and *PKS1-* like gene (the last one including *PKS1* and *PKS2* in Brassicaceae), monocots include a diverse number of additional *PKS* genes (Vazquez et al., 2022).

PKS gene expression patterns in *A. thaliana* correlate with their importance in phototropin (phot)-mediated growth responses. Thereby, *PKS1* expresses in the root, where it functions in root phototropism (Boccalandro et al., 2008). Moreover, *PKS2* and *PKS3* are rather expressed in leaves, where they are important for leaf movement and flattening, while *PKS1* and *PKS4* are expressed in the hypocotyl elongation zone, where they are important for hypocotyl growth orientation (Lariguet et al., 2003, Lariguet et al., 2006, Schepens et al., 2008, de Carbonnel et al., 2010, Kami et al., 2014, Legris et al., 2021) (Legris Martina, personal communication). PKS4 functions at the plasma membrane (PM) to mediate hypocotyl phototropism by leading to an auxin gradient across the hypocotyl in response to unilateral blue light (BL) (Lariguet et al., 2006, Demarsy et al., 2012, Kami et al., 2014a, Schumacher et al., 2018, Vazquez et al., 2022). Although PKS1 and PKS3 are also localized at the PM, their capability to function as PKS4 remains elusive (Legris Martina, personal communication) (Lariguet et al., 2006, Vazquez et al., 2022). Here, we compared the subcellular localization of the *A. thaliana* members that belong to the same clade: PKS1 and PKS2, and used complementation of the *pks4* mutant, which is defective in phototropism and inhibition of gravitropism, to test the PKS members' potential to function as PKS4. We additionally tested the complementation of the PKS4 orthologs from a basal angiosperm and a monocot and further provided data suggesting that the function of PKS4 in phototropism is conserved in monocots.

RESULTS

<u>PKS1 retains the function of PKS4 at the plasma membrane to promote hypocotyl growth orientation</u>

A. thaliana possesses 4 *PKS* genes (*PKS1-PKS4*), among which *PKS4* and *PKS1* are the most important ones to promote hypocotyl growth orientation during early seedlings establishment, while *PKS2* and *PKS3* are more important for other adaptative responses such as leaf flattening. The diverse *PKS* expression patterns correlate with their importance in different light-mediated responses, suggesting that functional diversification could be due to changes in the expression patterns (Lariguet et al., 2003, Boccalandro et al., 2008, Schepens et al., 2008, de Carbonnel et al., 2010, Kami et al., 2014). Additionally, we wondered whether there is a functional diversification in the coding sequence (*CDS*) of the *PKS* genes. To address that question, we used complementation of *pks4*, which is defective in hypocotyl phototropism and phytochrome (phy)-mediated inhibition of gravitropism (Schepens et al., 2008, Kami et al., 2014a). Then, we generated transgenic *pks4* plants expressing the *PKS1*, *PKS2*, and *PKS3 CDS* from a 1.5 kb *PKS4* promoter to control the expression of the transgene, PKS tagged with a carboxyl-terminal triple HA. We selected a few independent single insertion lines expressing the protein of interest comparable to the wild-type PKS4-HA control lines WT-3 and WT-2 (Figure 1A), whose PKS4-HA protein levels were similar or lower to endogenous PKS4 respectively (Schumacher et al., 2018). The three *pks4* lines expressing PKS1 could rescue the *pks4* phenotype in phototropism (Figure 1B), comparable to the PKS4 WT-3 line (Schumacher et al., 2018, Vazquez et al., 2022), which demonstrates that PKS1 can function as PKS4 in phototropism. However, none of the independent selected *pks4* lines expressing PKS2 nor PKS3 could complement the *pks4* phenotype as the PKS4 WT-2 line did, suggesting that PKS2 and PKS3 cannot function as PKS4 and PKS1 when they are expressed from

the *PKS4* promoter (Figures 1C and 1D). Additionally, we observed that lines 1 and 2 expressing PKS2 aggravated the *pks4* phenotype, suggesting that expression of PKS2 might interfere with the molecular mechanism underlying phototropism (Figure 1C). Although less pronounced, lines 1 and 2 expressing PKS3 also led to a worse phenotype than *pks4* (Figure 1D), which also suggests an interference of PKS3 with the molecular system.
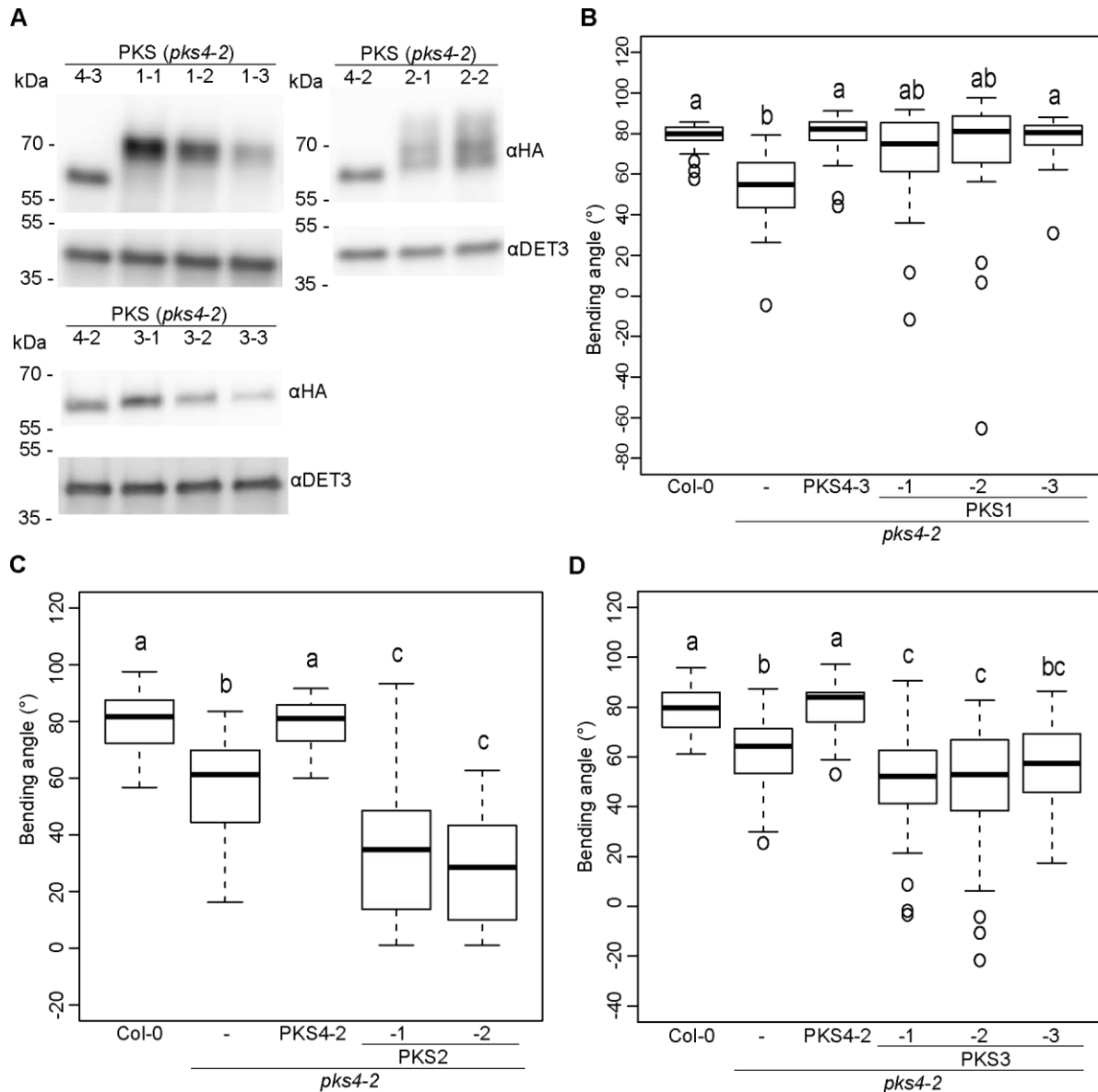

Figure 1. PKS1 but not PKS2 and PKS3 can complement the phototropic defect of *pks4* mutants. (**A**) Western blots probed with an anti-HA antibody from *pks4-2* PKS4-3 and *pks4-2* PKS1 (-1, -2, and -3), *pks4-2* PKS4-2, and *pks4-2* PKS2 (-1 and -2), and *pks4-2* PKS4-2, and *pks4-2* PKS3 (-1, -2,

and -3) samples of 3- day- old dark-grown seedlings. The same membranes were probed with an anti-DET3 antibody as a loading control. (**B**) Phototropic curvature of 3-day-old dark-grown Col-0, *pks4-2*, *pks4-2* PKS4-3, and *pks4-2* PKS1 (-1, -2, and -3) lines treated with BL coming from one side. (**C**) Phototropic curvature of 3-day-old dark-grown Col-0, *pks4-2*, *pks4-2* PKS4-2, and *pks4-2* PKS2 (-1 and -2) lines treated with BL coming from one side. (**D**) Phototropic curvature of 3-day- old dark-grown Col-0, *pks4-2*, *pks4-2* PKS4-2, and *pks4-2* PKS3 (-1, -2, and -3) lines treated with BL coming from one side. In (**B**), (**C**), and (**D**) seedlings were exposed to 0.1 μmol m^{-2} s^{-1} BL for 24h before measurement of growth reorientation. For each experiment, n= 25 – 55, means with the same letter are not significantly different (p > 0.01, two-way ANOVA with Tukey's HSD test).

We then analyzed hypocotyl gravitropism in darkness and observed that Col-0, *pks4,* and all transgenic lines expressing PKS1, PKS2, or PKS3 showed a comparable response (Figures 2A, 2B, and 2C), confirming that the observed phototropic phenotype of the lines expressing the different *A. thaliana PKS* genes from the *PKS4* promoter is light-dependent. Moreover, to determine whether PKS1, PKS2, and PKS3 can complement the *pks4* phenotype in phy signaling we analyzed light-induced inhibition of hypocotyl gravitropism by analyzing the hypocotyl growth orientation relative to the vertical in response to 30 μmol m^{-2} s^{-1} of continuous RL (Schepens et al., 2008). We observed that the control PKS4 WT-3 line rescued the *pks4* phenotype as previously shown (Vazquez et al., 2022) and that the *pks4* lines expressing PKS1 could similarly rescue it (Figure 3A), showing that PKS1 can function as PKS4 in response to RL. We additionally observed that the PKS4 WT-2 line complemented as the PKS4 WT-3 did, however, the lines expressing PKS2 or PKS3 showed a phenotype similar to *pks4* and *phyB*, showing that PKS2 and PKS3 cannot complement *pks4* in response to RL (3C). Altogether our data indicate that PKS1 can complement *pks4* in phy and phot signaling, while PKS2 and PKS3 cannot do it.
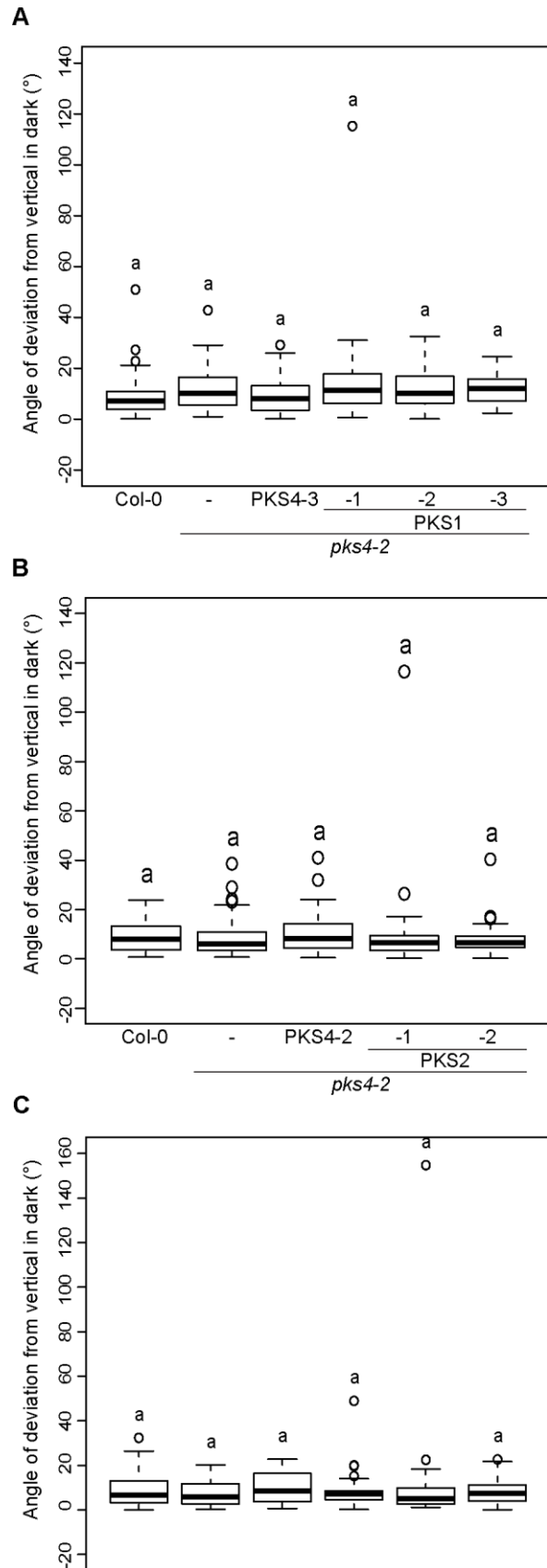
Figure 2. Ectopic expression of PKS1, PKS2, or PKS3 from the *PKS4* promoter does not alter hypocotyl gravitropism in dark-grown seedlings. (**A**) Hypocotyl growth orientation of 3-day-old Col-0, *pks4-2*, *pks4-2* PKS4 WT-3, and *pks4-2* PKS1 (-1, -2, and -3), (**B**) Col-0, *pks4-2*, *pks4-2* PKS4 WT-2, and *pks4-2* PKS2 (-1 and -2), and (**C**) Col-0, *pks4-2*, *pks4-2* PKS4 WT-2, and *pks4-2* PKS3 (-1, -2, and -3) dark-grown seedlings. 0° represents vertical growth and an average of 90° represents a random distribution. We consider the absolute value of the angle, no matter if the seedling bends towards the left or the right side. n= 45 – 60, means with the same letter are not significantly different (p > 0.01, two-way ANOVA with Tukey's HSD test).
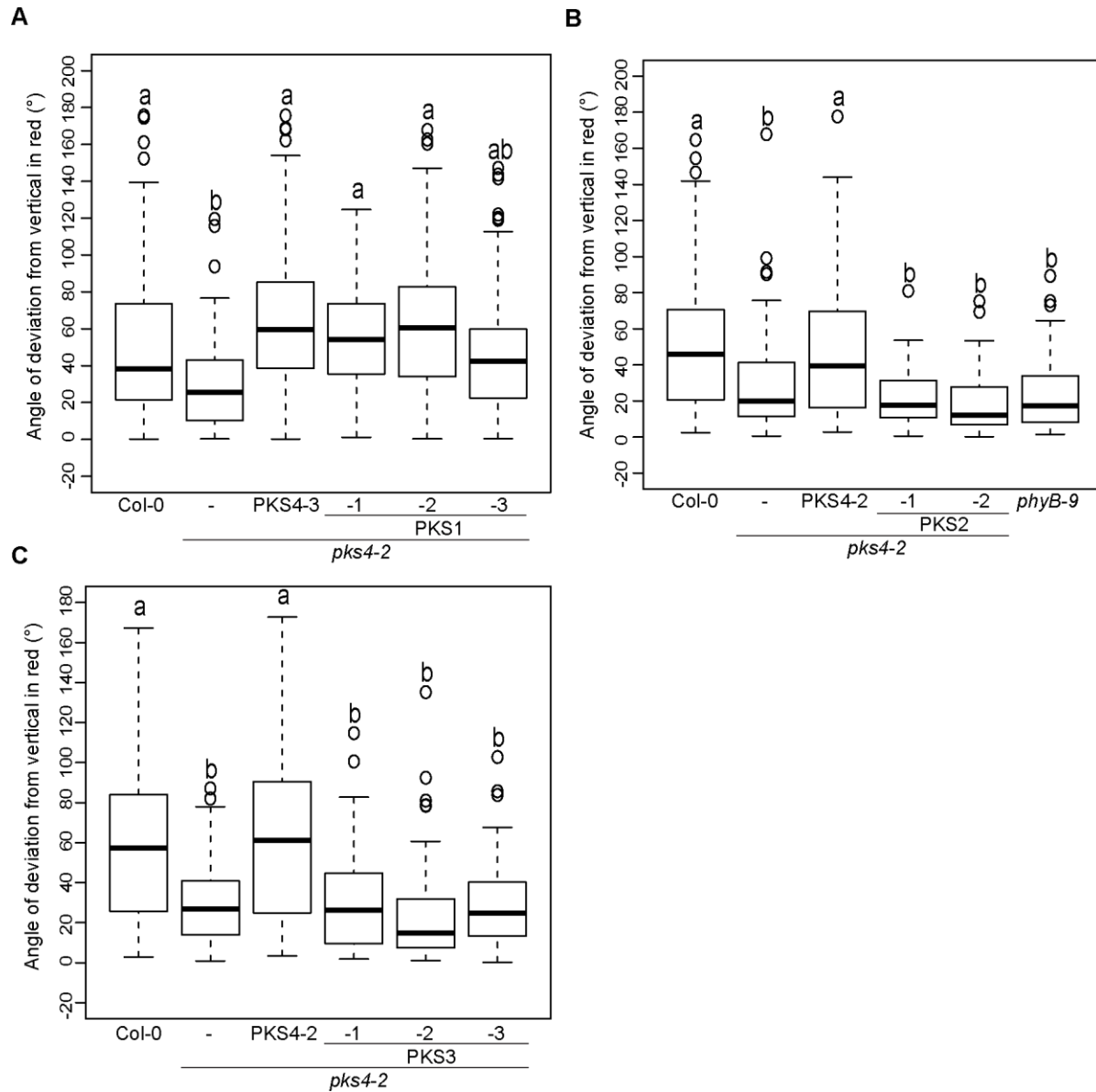
Figure 3. PKS1 but not PKS2 and PKS3 can complement the defect of *pks4* in light-induced inhibition of hypocotyl gravitropism. (**A**) Hypocotyl growth orientation of Col-0, *pks4-2*, *pks4-2* PKS4 WT-3, and *pks4-2* PKS1 (-1, -2, and -3), (**B**) Col-0, *pks4-2*, *pks4-2* PKS4 WT-2, *pks4-2* PKS2 (-1 and -2), and (**C**) *phyB-9*, and Col-0, *pks4-2*, *pks4-2* PKS4 WT-2, and *pks4-2* PKS3 (-1, -2, and -3) seedlings growing in continuous 30 µmol m^{-2} s^{-1} RL. Seedlings were kept for 24h in darkness before 4 days of RL treatment following measurement of growth orientation. 0° represents vertical growth and an average of 90° represents a random distribution. We consider the absolute value of the angle, no matter if the seedling bends towards the left or the right side. n= 70 – 80, means with the same letter are not significantly different (p > 0.01, two-way ANOVA with Tukey's HSD test).

PKS1, PKS2, and PKS4 form a protein complex with the PM-localized phot and NPH3 (Lariguet et al., 2006, de Carbonnel et al., 2010, Schumacher et al., 2018). Given that PKS4 needs to be effectively attached to the PM to functionally mediate hypocotyl growth orientation in response to light (Schumacher et al., 2018, Vazquez et al., 2022), we wondered whether the subcellular localization of the other PKS members might explain the complementation potential of *pks4* when the different *PKS* genes are expressed from the *PKS4* promoter. To answer this question, we compared the subcellular localization of 35S promoter-driven PKS1 and PKS2 fused to GFP in root, hypocotyl, and hook epidermal cells. We observed that, as previously reported (Lariguet et al., 2006, Vazquez et al., 2022), PKS1 localized to the PM in hook epidermal cells (Figure 4A top panel). Moreover, PKS1 also localized to the PM in the hypocotyl and root tissues (Figure 4A top right and middle panels), confirming that PKS1 generally associates with the PM. However, we found that PKS2 was mainly localized at the nucleus and cytoplasm in the epidermal root, hypocotyl, and hook cells (Figure 4A bottom panel). Collectively, our data suggest that PKS1 can complement *pks4* and is localized at the same place as PKS4, while PKS2 cannot complement *pks4* and it appears localized in different subcellular compartments.

A
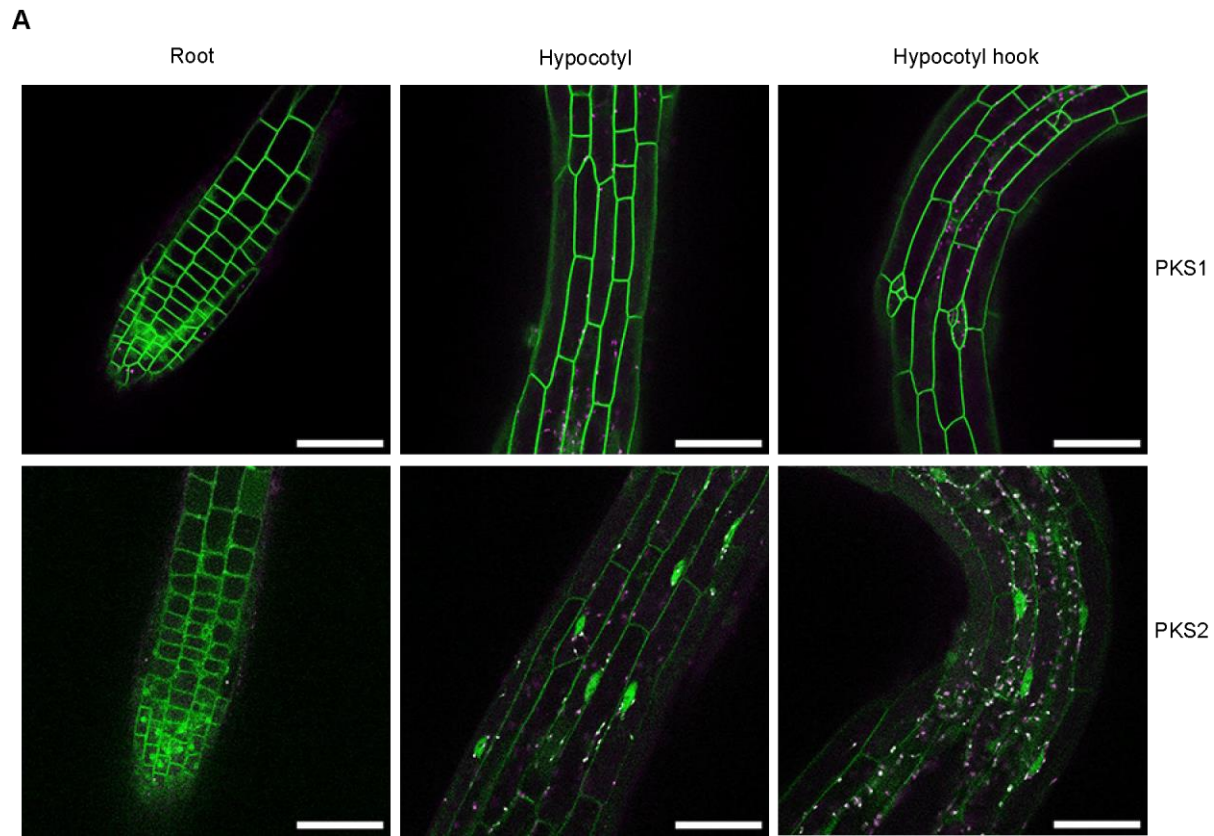
Figure 4. PKS1 localizes to the PM while PKS2 mainly localizes at the nucleus and cytosol. (**A**) Confocal microscopy images of roots, hypocotyls, and hooks from 3-day-old transgenic dark-grown seedlings expressing PKS1-GFP (top) and PKS2-GFP (bottom) from the 35S promoter. Scale bar: 50 μm.

A. trichopoda PKS4 localizes at the plasma membrane and can complement *pks4* in response to red light in *A. thaliana*

Phylogenetic studies revealed that all the angiosperms, including the most basal ones, already possess at least 2 *PKS* genes, one belonging to the PKS4 clade and the rest belonging to the PKS1/2/3 clade. Given these studies suggest a more constrained evolution in the PKS4 clade than in the PKS1/2/3 clade (Vazquez et al., 2022), we first wondered if the PKS4 function has been conserved across evolution. To address that question, we used the complementation of *pks4* with

the PKS4 ortholog from the basal angiosperm *Amborella trichopoda* (*A. trichopoda*) and the monocot *Brachypodium distachyon* (*B. distachyon*). We generated transgenic *A. thaliana pks4* plants expressing an *A. thaliana* codon optimized *CDS* of *A. trichopoda* PKS4 from a 1.5 kb *PKS4* promoter to control the expression of the transgene, *A. trichopoda* PKS4 tagged with a carboxyl-terminal triple HA. Then, we selected a few independent single insertion lines expressing *A. trichopoda* PKS4 (termed PKS4 *Amt* lines) comparable to the wild-type PKS4-HA control line WT-2 (here named as *At-2* for consistency with the rest of the nomenclatures) (Figure 5A), whose PKS4-HA protein levels were lower to endogenous PKS4 (Schumacher et al., 2018). We found that none of the three independent PKS4 *Amt1-3* lines could complement the *pks4* phenotype as the *At-2* did (Figure 5B), showing that *A. trichopoda* PKS4 does not work on promoting phototropism in *A. thaliana.* Similarly, we tested three independent *A. thaliana pks4* lines expressing an *A. thaliana* optimized *CDS* of *B. distachyon* PKS4 (termed PKS4 *Bd* lines) and found that none of these lines could complement the *pks4* phenotype as the PKS4 *At-2* did (Figure 5C). The expression levels of *B. distachyon* PKS4 were equal to or higher than the PKS4 *At-2* complementing line (Figure 5D), suggesting that the lack of complementation is not due to a lower expression of the *B. distachyon* PKS4. Moreover, the PKS4 *Bd* lines showed a much more severe phenotype than *pks4*, suggesting that the expression of *B. distachyon* PKS4 in *A. thaliana* strongly interferes with the molecular mechanism promoting phototropism.
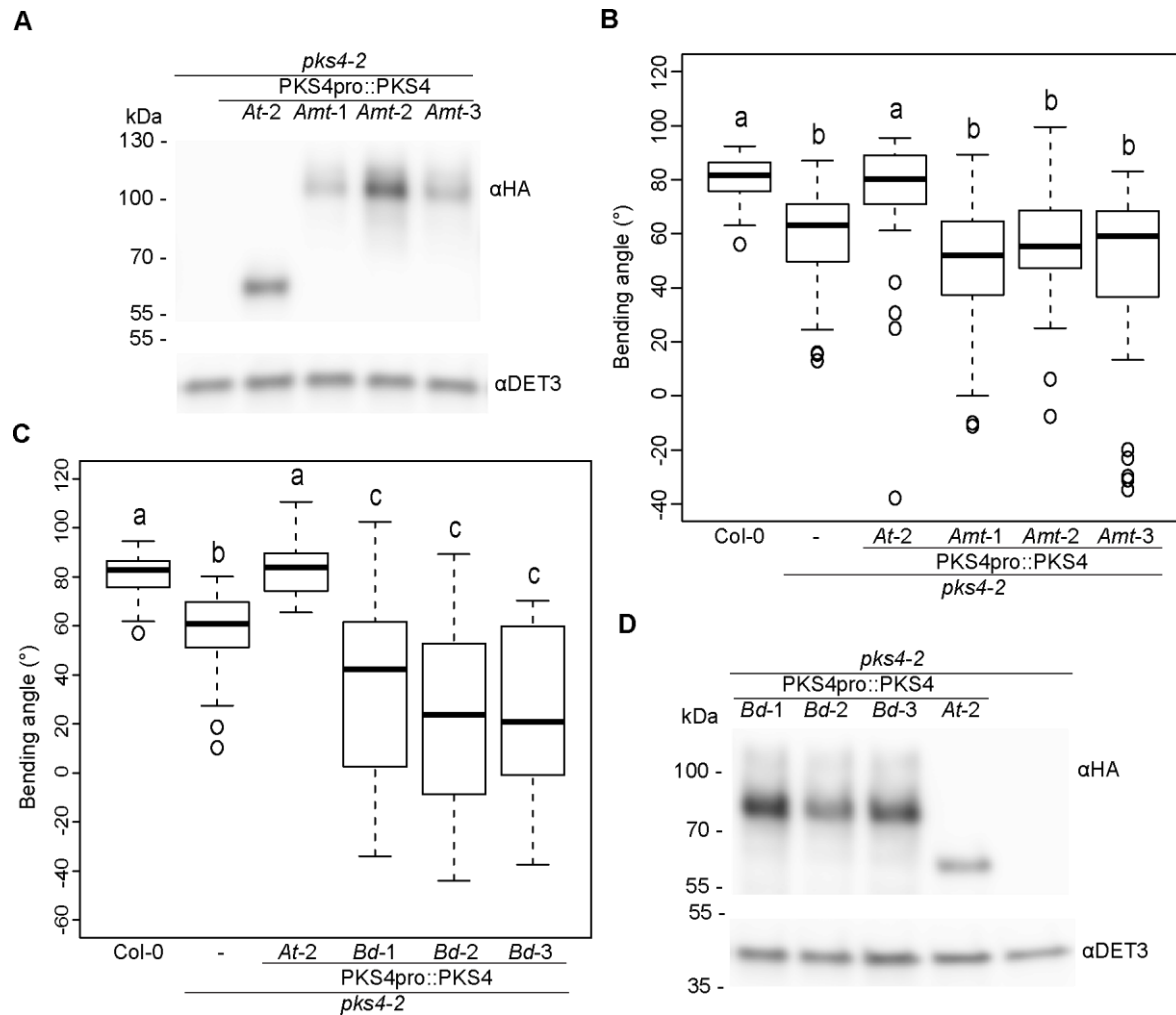
Figure 5. Expression of *A. trichopoda* and *B. distachyon* PKS4 does not rescue the phototropic defect of the *pks4* mutants in *A. thaliana*. (**A**) Western blot probed with an anti-HA antibody from *pks4-2*, *pks4-2 A. thaliana* PKS4 (*At*-2), and *pks4-2 A. trichopoda* PKS4 (*Amt*-1, -2, and -3) sample s of 3-day- old dark-grown seedlings. The same membrane was probed with an anti-DET3 antibody as a loading control. (**B**) Phototropic curvature of 3-day-old dark-grown Col-0, *pks4-2*, *pks4-2 A. thaliana* PKS4 (*At*-2), and *pks4-2 A. trichopoda* PKS4 (*Amt*-1, -2, and -3) lines treated with BL coming from one side. (**C**) Phototropic curvature of 3-day-old dark-grown Col-0, *pks4-2*, *pks4-2 A. thaliana* PKS4 (*At*-2), and *pks4-2 B. distachyon* PKS4 (*Bd*-1, -2, and -3) lines treated with BL coming from one side. In (**B**) and (**C**) seedlings were exposed to 0.1 µmol m^{-2} s^{-1} BL for 24h before measurement of growth reorientation. For each experiment, n= 25 – 55, means with the same letter are not significantly different (p > 0.01, two-way ANOVA with Tukey's HSD test). (**D**) Western blot probed with an anti-HA antibody from *pks4-2*, *pks4-2 A. thaliana* PKS4 (*At*-2), and *pks4-2 B.*

distachyon PKS4 (*Bd*-1, -2, and -3) samples of 3- day- old dark-grown seedlings. The same membrane was probed with an anti-DET3 antibody as a loading control.

To check whether the expression of *A. trichopoda* and *B. distachyon* PKS4 in *A. thaliana* affects the hypocotyl growth orientation independent of light, we analyzed hypocotyl gravitropism in darkness and observed that the WT, *pks4,* and all transgenic lines expressing *A. trichopoda* or *B. distachyon* PKS4 showed the same response (Figures 6A and 6B), which confirms that the observed phenotypes in the hypocotyl orientation are solely due to light.
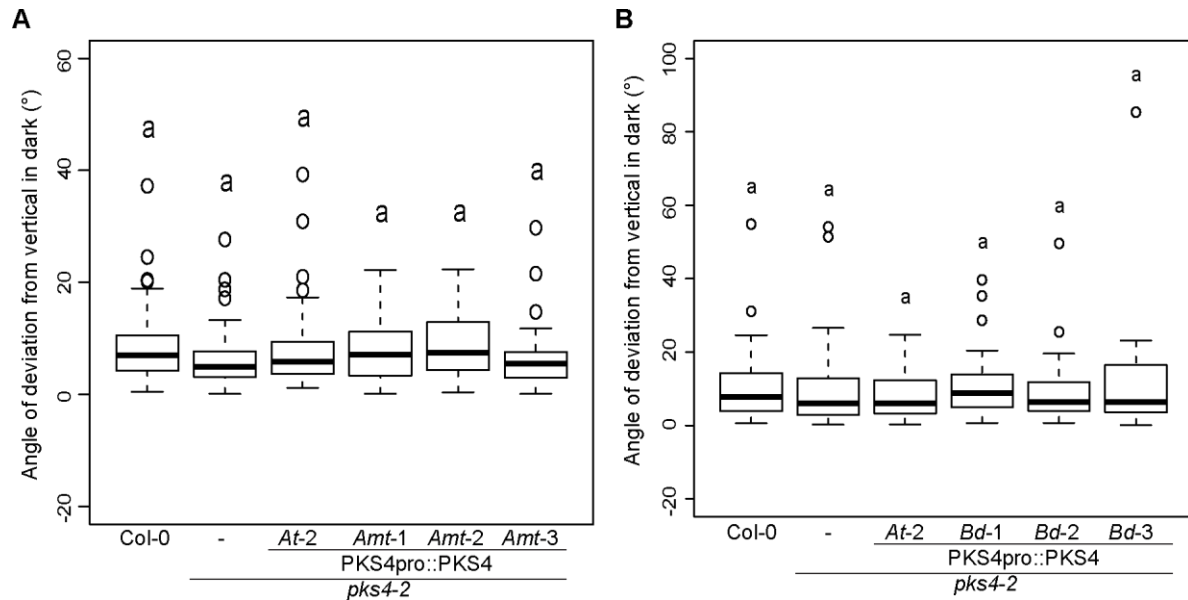
Figure 6. Expression of *A. trichopoda* and *B. distachyon* PKS4 in *A. thaliana* does not alter hypocotyl gravitropism in dark-grown seedlings. (**A**) Hypocotyl growth orientation of 3-day-old Col-0, *pks4-2*, *pks4-2 A. thaliana* PKS4 (*At*-2), and *pks4-2 A. trichopoda* PKS4 (*Amt*-1, -2, and -3) and (**B**) Col-0, *pks4-2*, *pks4-2 A. thaliana* PKS4 (*At*-2), and *pks4-2 B. distachyon* PKS4 (*Bd*-1, -2, and -3) dark-grown seedlings. 0° represents vertical growth and an average of 90° represents a random distribution. We consider the absolute value of the angle, no matter if the seedling bends towards the left or the right side. n= 45 – 60, means with the same letter are not significantly different (p > 0.01, two-way ANOVA with Tukey's HSD test).

To determine whether *A. trichopoda* and *B. distachyon* PKS4 can complement the *pks4* phenotype in phy signaling in *A. thaliana,* we analyzed light-induced inhibition of hypocotyl gravitropism as we did for the *A. thalian*a PKS members. Surprisingly, we found that the PKS4 *Amt* lines rescued the *pks4* phenotype in *A. thaliana*, as the control PKS4 *At-2* line did (Figure 7A). Only the PKS4 *Amt*-1 line showed an intermediate phenotype between Col-0 and *pks4*, which might be because the expression levels of this line were lower than the PKS4 *At-2* line (Figure 5A), which had already lower expression levels compared to the endogenous PKS4 (Schumacher et al 2018). This shows that *A. trichopoda* PKS4 can function as *A. thaliana* PKS4 in RL-induced inhibition of hypocotyl gravitropism. On the contrary, when we tested the PKS4 *Bd* lines in *A. thaliana*, we found that none of the three lines could complement the *pks4* phenotype in response to RL (Figure 7B), suggesting that *B. distachyon* PKS4 cannot function as *A. thaliana* PKS4 in phototropism in *A. thaliana*.
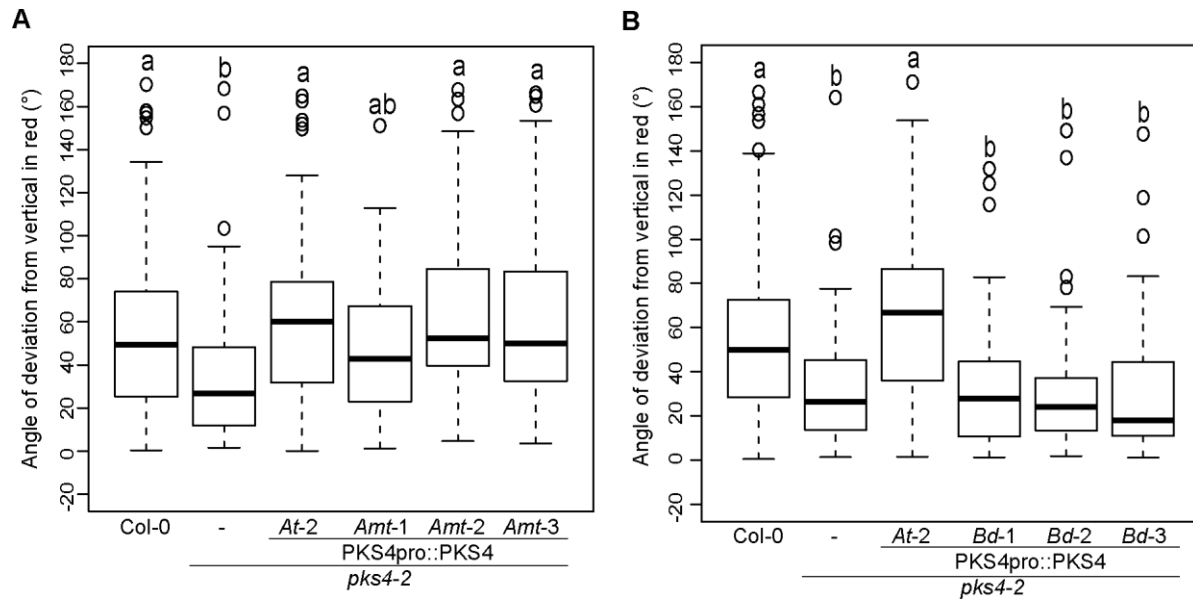
Figure 7. *A. trichopoda* PKS4 complements the defect of *pks4-2* in inhibition of gravitropism in *A. thaliana* while *B. distachyon* PKS4 does not. (**A**) Hypocotyl growth orientation of Col-0, *pks4-2*, *pks4-2 A. thaliana* PKS4 (*At-2*), and *pks4-2 A. trichopoda* PKS4 (*Amt*-1, -2, and -3) and (**B**) Col-0, *pks4-2*, *pks4-2 A. thaliana* PKS4 (*At-2*), and *pks4-2 B. distachyon* PKS4 (*Bd*-1, -2, and -3) seedlings growing in continuous 30 µmol m^{-2} s^{-1} RL. Seedlings were kept for 24h in darkness before 4 days of

RL treatment following measurement of growth orientation. 0° represents vertical growth and an average of 90° represents a random distribution. We consider the absolute value of the angle, no matter if the seedling bends towards the left or the right side. n= 70 – 80, means with the same letter are not significantly different ($p > 0.01$, two-way ANOVA with Tukey's HSD test).

Our data showing that *A. trichopoda* PKS4 can rescue the function of *pks4* in response to RL but not to BL and that *B. distachyon* PKS4 cannot rescue any of the PKS4 function in *A. thaliana* led us to check the subcellular localization of *A. trichopoda* and *B. distachyon* PKS4 in *A. thaliana*. We made *A. trichopoda* and *B. distachyon* PKS4 (*A. thaliana* codon optimized CDS) GFP fusion constructs driven by the 35S promoter and analyzed stably transformed seedlings. We found that while *A. trichopoda* PKS4 localized to the PM as *A. thaliana* PKS4, *B. distachyon* PKS4 mainly localized to the nucleus and cytoplasm (Figure 8A). These data suggest that *A. trichopoda* PKS4 can bind to the PM where *A. thaliana* PKS4 functions and can efficiently complement the *pks4* function in response to RL, although it cannot complement in response to BL. Moreover, *B. distachyon* PKS4 cannot effectively associate with the PM or complement the *pks4* phenotype in response to red nor blue light.
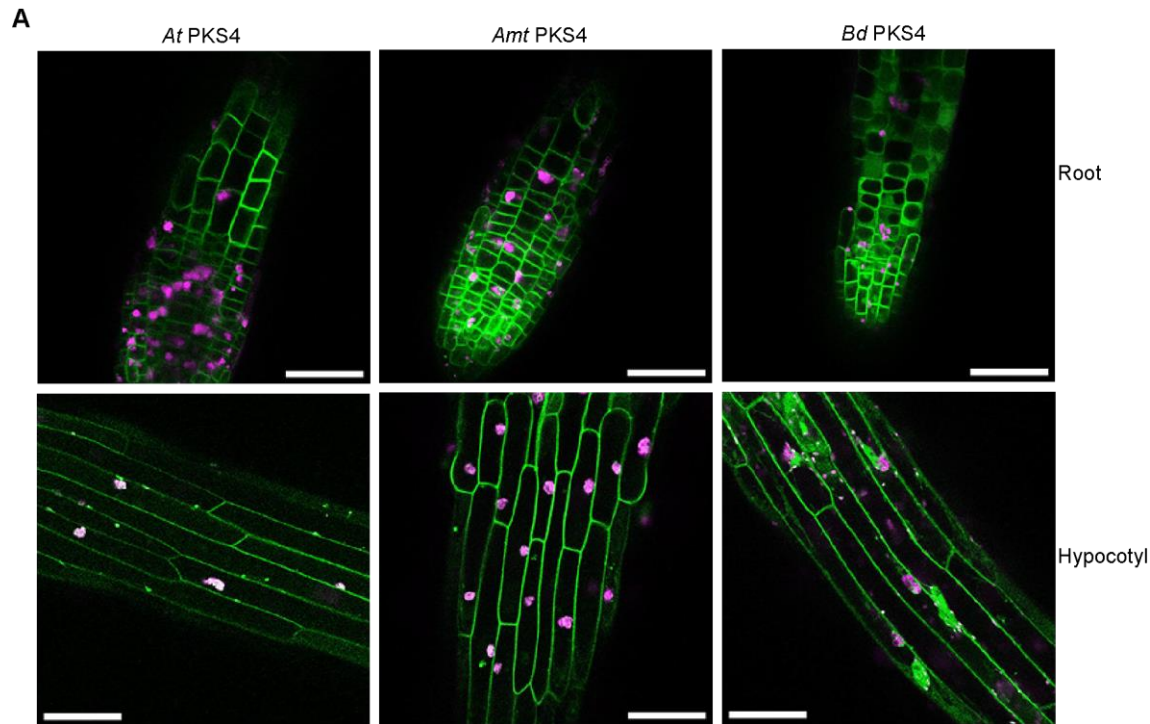
Figure 8. *A. trichopoda* PKS4 localizes at the PM in *A. thaliana* while *B. distachyon* PKS4 localizes at the nucleus and cytosol. (**A)** Confocal microscopy images of roots (top) and hypocotyls (bottom) from 3-day-old transgenic dark-grown *A. thaliana* seedlings expressing *A. thaliana* PKS4- GFP, *A. trichopoda* PKS4-GFP, and *B. distachyon* PKS4 -GFP from the 35S promoter. Note that these lines also show remaining oily bodies (in magenta) resulting from the expression of OLE1- RFP from the *OLE1* promoter, used as a seeds coats selection marker. Scale bar: 50 µm.

The function of PKS4 in phototropism is conserved in *B. dystachion*

Given that the expression of *B. distachyon* PKS4 from the *PKS4* promoter in *A. thaliana* could not rescue the *pks4* phenotype, we wondered whether *B. distachyon* PKS4 is still important to promote phototropism but it does not work in the *A. thaliana* molecular system or whether PKS4 does not have an important function in phototropism in *B. distachyon*. To address that question, we generated three independent *B. distachyon* CRISPR mutant lines in Bradi2g09750v3 (*BdPKS4*). *Bdpks4*-1 lacked the

CDS comprising the nucleotides from 1-26 and from 1565 to 1573, and *Bdpks4*-2 and *Bdpks4*-3 had both the same mutational event: T nucleotide insertion in the position 20 that causes an ORF shift and a premature STOP codon (Figure 9A). This suggests that in *Bdpks4*-1 the *B. distachyon* PKS4 protein is not produced and in the *Bdpks4*-2 and *Bdpks4*-3 lines a very small protein might be produced. We first tested etiolated WT (Bd21-3) and *Bdpks4-2* coleoptiles for phototropism in response to 24h unilateral low BL (LBL) (0.1 μmol m^{-2} s^{-1}) as we did for the previous phototropic experiments shown in this study. We found that Bd21-3 bended towards the BL source with an average angle of 70 degrees (Figure 9B top panel), which is close to the 80 degrees' average angle that *A. thaliana* WT hypocotyls usually showed after 24h in this study (Figures 1 and 5). Moreover, we found that the *Bdpks4*-2 line was significantly impaired in this response, showing almost no bending after 24h unilateral LBL (Figure 9B bottom panel). Then, we tested the three independent *Bdpks4* lines together with Bd21-3 for phototropism in bigger-scale experiments, and we found that the three independent mutant lines were notably impaired in phototropic bending in response to LBL compared to the WT (Figure 9C). These data indicate that the function of PKS4 in phototropism is conserved in *B. distachyon.*
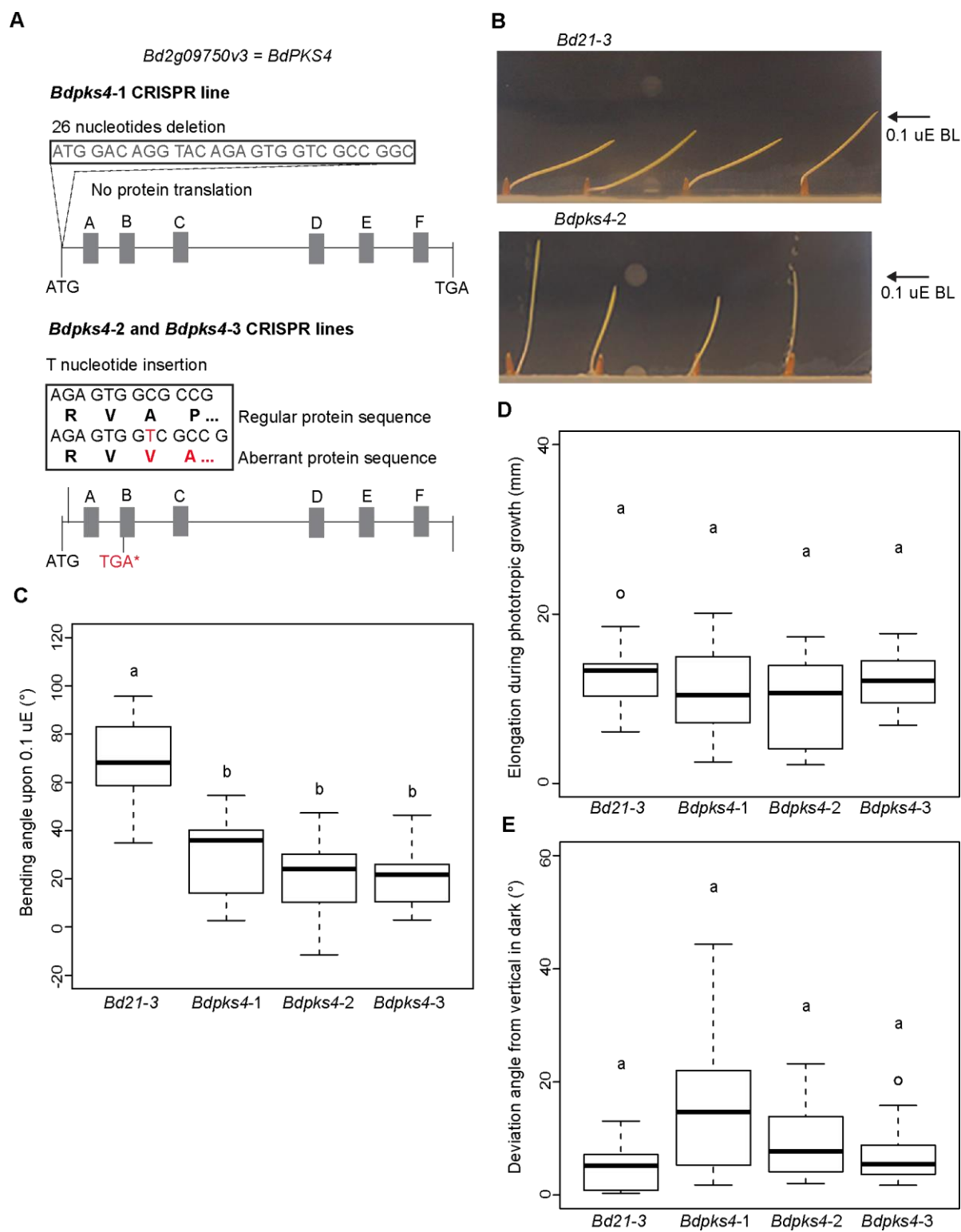
Figure 9. The function of PKS4 in phototropism is conserved in *B. distachyon.* (**A**) Schematic representation of the PKS4 CRISPR mutant independent lines *Bdpks4-1*, *Bdpks4-2,* and *Bdpks4-3*

and consequences in protein translation. (**B**) Pictures showing Bd21-3 (WT) and *Bdpks4-2* 5-day-old dark-grown coleoptiles after 24h treatment with 0.1 µmol m^{-2} s^{-1} BL coming from one side. (**C**) Phototropic curvature of 5-day-old dark-grown Bd21-3, *Bdpks4-1*, *Bdpks4-2,* and *Bdpks4-3* lines treated with BL coming from one side. Seedlings were exposed to 0.1 µmol m^{-2} s^{-1} BL for 24h before measurement of growth reorientation. n= 10 – 20, means with the same letter are not significantly different (p > 0.01, two-way ANOVA with Tukey's HSD test). (**D**) Coleoptiles elongation of the Bd21-3, *Bdpks4-1*, *Bdpks4-2,* and *Bdpks4-3* lines for phototropism in response to 0.1 µmol m^{-2} s^{-1} BL coming from one side. The length of the coleoptiles assayed in C was measured at times 0 and 24h after the BL treatment and the subtracted values were represented. n= 10 – 20, means with the same letter are not significantly different (p > 0.01, two-way ANOVA with Tukey's HSD test). (**E**) Coleoptile growth orientation of 5-day-old Bd21-3, *Bdpks4-1*, *Bdpks4-2,* and *Bdpks4-3* dark-grown seedlings. 0° represents vertical growth. We consider the absolute value of the angle, no matter if the seedling bends towards the left or the right side. n= 10 – 20, means with the same letter are not significantly different (p > 0.01, two-way ANOVA with Tukey's HSD test).

To confirm that the bending phenotype that we observed in the three *Bdpks4* lines is due to unresponsiveness to the light treatment and not because of a difference in coleoptile elongation due to the BL treatment, we measured the coleoptile elongation of these lines during the phototropic experiment. Then, we subtracted the coleoptile length at the start of the experiment from the coleoptile length after 24h of BL treatment. We found no significant difference in the *Bdpks4* lines elongation compared to Bd21-3 (Figure 9D), corroborating that the mutations in *BdPKS4* lead to a defect in phototropism in *B. distachyon*. We also measured the coleoptile gravitropism angle in the WT and the three *Bdpks4* lines in the darkness and we found that all the lines showed the same response (Figure 9E), suggesting that *BdPKS4* is not involved in coleoptile gravitropism in *B. distachyon*. Additionally, we tested coleoptile bending in response to higher BL intensity (10 µmol m^{-2} s^{-1}). We found that while Bd21-3 bent toward the light source with an average angle of around 60 degrees after 24h, the

Bdpks4 lines were significantly impaired (Figure 10A), showing an average bending angle similar to that in response to LBL. As we did when we tested phototropism in response to LBL, to confirm that the bending phenotype that we observed in the three *Bdpks4* is not due to a reduced coleoptile growth in the *Bdpks4* lines, we measured the coleoptile elongation during the phototropic experiment in response to higher BL and we found no significant difference among them (Figure 10B). Collectively these data show that the function of PKS4 in phototropism in young seedlings is conserved in *B. distachyon.*
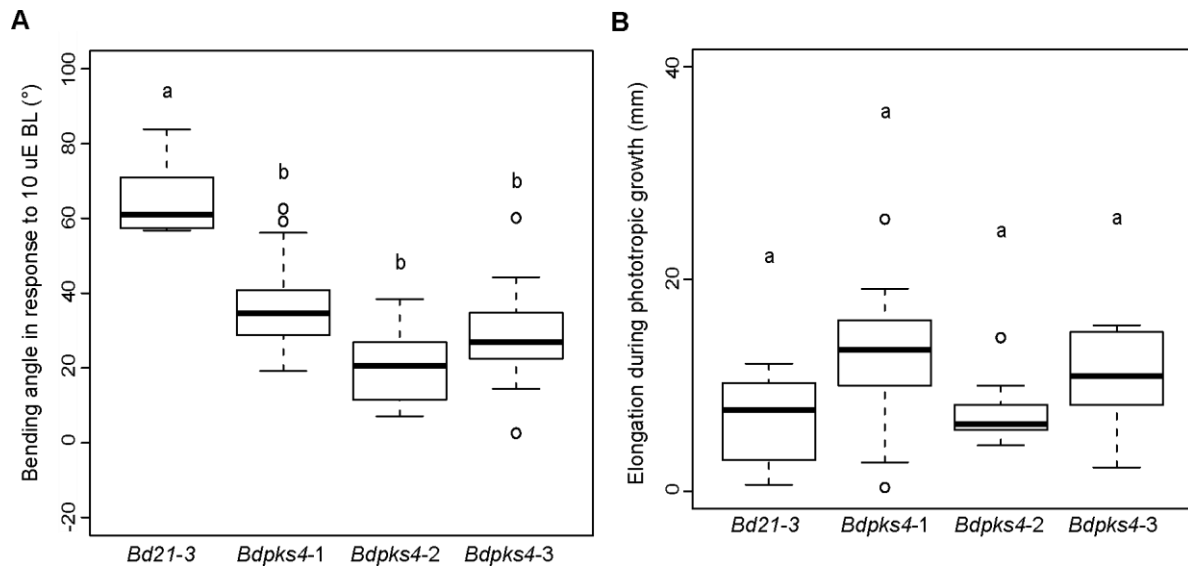
Figure 10. The PKS4 function in phototropism is conserved also in response to higher light fluence. (**A**) Phototropic curvature of 5-day-old dark-grown Bd21-3, *Bdpks4-1*, *Bdpks4-2,* and *Bdpks4-3* lines treated with 10 µmol m^{-2} s^{-1} BL coming from one side for 24h before measurement of growth reorientation. n= 10 – 20, means with the same letter are not significantly different (p > 0.01, two-way ANOVA with Tukey's HSD test). (**B**) Coleoptiles elongation of the Bd21-3, *Bdpks4-1, Bdpks4-2,* and *Bdpks4-3* lines for phototropism in response to 10 µmol m^{-2} s^{-1} BL coming from one side. The length of the coleoptiles assayed in E was measured at times 0 and 24h after the BL treatment and the subtracted values were represented. n= 10 – 20, means with the same letter are not significantly different (p > 0.01, two-way ANOVA with Tukey's HSD test).

DISCUSSION

<u>PKS4 function is conserved in *Brachypodium dystachion*</u>

Numerous studies have addressed the importance of the *A. thaliana* PKS genes, however, the importance of PKS from other organisms had not been investigated to date (Kami et al., 2014a, de Carbonnel et al., 2010, Legris et al., 2021). Although phototropism has been previously studied in monocots, here we showed for the first time that *B. distachyon,* phylogenetically close to the cereal crops, can efficiently perform phototropic curvature in response to unilateral LBL (Figure 9B) (Salomon et al., 1997). Given that they are predicted to be related by common ancestry, we hypothesized that *B. distachyon* PKS4 (*Bd* PKS4) has a similar biological function to *A. thaliana* PKS4. To test that, we generated independent knock-out and loss-of-function mutant lines in *B. distachyon* (*BdPKS4*) using CRISPR and we found that phototropism was significantly impaired in all the tested *BdPKS4* mutant lines compared to the WT (Figure 9B, C, and 10A). Moreover, gravitropism in darkness remained unaltered in the *BdPKS4* lines compared to the WT, indicating that, as in *A. thaliana*, PKS4 function in stem orientation is light-dependent (Figure 9E) (Vazquez et al., 2022). This, together with the fact that the NPH3 ortholog COLEOPTILE PHOTOTROPISM1 (CPT1) in rice is required for auxin distribution across the coleoptile in response to unilateral BL stimulation, suggests that the molecular mechanisms underlying asymmetric auxin redistribution in response to phot activation are conserved in monocots (Haga et al., 2005). Moreover, coleoptile elongation of the *BdPKS4* lines was comparable to WT after the phototropic experiment, suggesting that, as *A. thaliana* PKS4, *Bd* PKS4 is not involved in BL- mediated stem growth inhibition (Figures 9D and F) (Folta and Spalding, 2001, Demarsy et al., 2012, Pedmale et al., 2016). Further complementation analysis by expressing *Bd* PKS4 from its promoter in these defective *BdPKS4* mutant lines would confirm functional conservation.

However, we found that *Bd* PKS4 could not complement the *A. thaliana pks4* phenotype in phototropism nor inhibition of gravitropism and it severely aggravated the *pks4* phototropic phenotype (Figure 5C, 6B, and 7B). These data suggest that *Bd* PKS4 divergence does not allow it to function in *A. thaliana* and it further interferes with *A. thaliana* molecular system leading to phototropism. Although *Bd* PKS4 shares the conserved Cysteine (Cys) amino acids in motif C, it seemed to be mainly localized to the nucleus and cytosol when it was expressed in *A. thaliana* (Figure 8), which might explain why *Bd* PKS4 cannot complement *pks4* in *A. thaliana* (Vazquez et al., 2022). Nevertheless, we do not know whether *Bd* PKS4 functions at the PM in *B. distachyon* as *At* PKS4 does in *A. thaliana*. Future confocal observation of plants expressing *Bd* PKS4 translational reporters from the endogenous promoter in *B. distachyon* might answer this question.

Ancestral PKS function correlates with localization at the PM

Given that they are predicted to originate from the same gene in the common ancestor and share all the conserved PKS protein motifs, we hypothesized that the *PKS4* ortholog from one of the most basal angiosperms, *A. trichopoda* (*Ambt PKS4*), may have a similar biological function to *A. thaliana PKS4* (Vazquez et al., 2022). We found that, despite having appeared later in evolution than phot, *Ambt* PKS4 could not complement the *pks4* phenotype in phototropism (Figure 5B) (Christie et al., 2018). However, *Ambt* PKS4 complements the *pks4* phenotype in the inhibition of gravitropism in response to red light (RL) (Figure 7A), suggesting PKS functional conservation in phy signaling. The different phot and phy predicted gene duplication story might explain the differential complementation potential of *Ambt* PKS4 in response to BL and RL in *A. thaliana* (Li and Mathews, 2016). Our data additionally support the idea of the independence of the signaling events leading to phototropism and inhibition of gravitropism (Lariguet and Fankhauser, 2004, Liscum et al., 2014). However, more studies addressing the importance of PKS proteins in *A. trichopoda* will help to understand PKS functional evolution.

To determine whether the complementation potential of the *Ambt* PKS4 correlates with changes in its subcellular localization, we tested its localization as C-terminal GFP fusions in *A. thaliana*. We observed that *Ambt* PKS4 was localized in the cell periphery, similar to *A. thaliana* PKS4 (Figure 8). Collectively, given that *A. trichopoda* is the sister species to the rest of the angiosperms, our data suggest deep conservation of the association of the ancestral PKS with the cell periphery for biological activity (Soltis et al., 2008).

PKS4 function is conserved in PKS1 but diverged in PKS2 and PKS3 in Brassicaceae

We found that the expression of *A. thaliana PKS1* from the *PKS4* promoter can complement the *pks4* phenotype in phototropism and inhibition of gravitropism (Figures 1B and 3A), suggesting that in addition to being expressed in the hypocotyl as PKS4, PKS1 can perform the same function (Lariguet et al., 2003, Schepens et al., 2008). On the contrary, we observed that the expression of *PKS2*, which is predicted to be the closest homolog to *PKS1*, could not complement the *pks4* phenotype in phototropism nor inhibition of gravitropism, making the phenotype worse especially in phototropism (Figures 1C and 3B) (Vazquez et al., 2022). This suggests that *PKS2*, which is expressed in the leaves in addition to the hypocotyl, has also functionally diverged in the *CDS* and does not retain the same function as *PKS1* and *PKS4* (Lariguet et al., 2003). Our confocal microscopy observations of lines overexpressing *PKS* C-terminal GFP fusions revealed that while PKS4 and PKS1 were localized at the PM, PKS2 was mainly localized to the cytosol and nucleus (Figure 4) (Lariguet et al., 2006, Schumacher et al., 2018, Vazquez et al., 2022). This suggests that the divergence of *PKS2* additionally involved changes in the PKS2 protein subcellular localization, which might explain why PKS2 cannot complement *pks4*. Nevertheless, we should not exclude the possibility that a small fraction of PKS2 is associated with the PM and/or with other endomembrane compartments, which might explain the fact that PKS2 can be found in a protein complex with the PM-associated proteins PKS1, PKS4, phot, and NPH3 (Lariguet et al., 2006, de Carbonnel et al., 2010, Demarsy et al., 2012, Preuten et

al., 2015, Vazquez et al., 2022). Doing a molecular evolution study aimed at finding Single Nucleotide Polymorphisms (SNPs) distinguishing *PKS1* and *PKS2* might give us some hints about amino acids that led to the functional diversification of PKS2 in Brassicaceae.

Moreover, the expression of *PKS3*, whose clade is predicted to have split from the *PKS1/2/3* clade after the divergence of the basal angiosperms, could not complement the *pks4* phenotypes either (Figures 1D and 3C) (Vazquez et al., 2022). Given that PKS3 expression is mainly restricted to the leaf, this suggests that in addition to changes in the expression patterns, *PKS3* divergence includes functional changes in the *CDS* (Legris Martina, personal communication). Although we did not show it in this work, it seems that the divergence of PKS3 does not include changes in subcellular localization, given that PKS3 appeared mainly associated with the PM (Legris Martina, personal communication). Curiously, conserved Cys amino acids in PKS3 motif C did not appear among the identified s-acylated Cys amino acids in the *A. thaliana* s-acylation atlas (Kumar et al., 2022), suggesting that PKS3 conserved Cys in motif C might not be s-acylated. It would be interesting to test whether these Cys are s-acylated in vivo and if not, investigate whether the association with the PM might involve a different mechanism other than the s-acylation of the conserved Cys in motif C. Collectively our functional complementation data together with previous phylogenetic analysis support that *PKS4* and *PKS1*, which are the representatives of the two main clades in which angiosperms *PKS* genes are grouped: *PKS4* and *PKS1/2/3*, conserve the ancestral function of *PKS*. However, *PKS3* and *PKS2* have acquired functional novelty, as it is hypothesized for genes diverged by duplication events (Conant and Wolfe, 2008).

METHODS

<u>Plant material</u>

The plants utilized in this study are in the *A. thaliana* Columbia-0 or the *B. distachyon* Bd21-3 ecotypes. The *pks4-2* and *phyB-9* alleles were utilized in this study (Reed et al., 1993, Schepens et al., 2008). 35Sp::PKS1-GFP (pCF202) and PKS4p:PKS4-3XHA (pPS9) in *pks4-2* were previously described (Lariguet et al., 2006, Schumacher et al., 2018). For the generation of the 35Sp::PKS2- GFP (pMC21) lines, the PKS2 CDS was amplified with the primers PL21 and PL18 from the pCF204 and cloned into a modified pPZP212 with basta resistance to which we added a 35S promoter, GFP and rbcs terminator for C-terminal fusion. For the generation of the PKS4pro::PKS1-3xHA lines (pCF575), PKS4pro::PKS2-3xHA lines (pCF576), and PKS4pro::PKS3-3xHA lines (pCF577), the PKS4 promoter amplified from the pPS9 construct (Schumacher et al., 2018) with the primers LA25 and LA26 was assembled by Gibson assembly with the PKS1 CDS amplified from the pCF202 with the primers LA24 and LA18 into the pCF398* previously digested with the restriction enzymes HindIII and BamHI. For the generation of the PKS4pro::PKS2-3xHA lines (pCF576), the PKS4 promoter amplified from the pPS9 construct (Schumacher et al., 2018) with the primers LA25 and LA29 was assembled by Gibson assembly with the PKS2 CDS amplified from the pMC21 with the primers LA27 and LA28 into the pCF398* previously digested with the restriction enzymes HindIII and BamHI. For the generation of the PKS4pro::PKS3-3xHA lines (pCF577), the PKS4 promoter amplified from the pPS9 construct (Schumacher et al., 2018) with the primers LA25 and LA32 was assembled by Gibson assembly with the PKS3 CDS amplified from the pMT12 with the primers LA30 and LA31 into the pCF398* previously digested with the restriction enzymes HindIII and BamHI. pMT12 is a pJHOON212 where we introduced via KpnI a sequence containing a PKS3 promoter region, PKS3 CDS, and 1.2

kb 3'UTR amplified from the BAC F6A14. For the generation of the PKS4pro::*A. trichopoda* PKS4-3xHA (pAL20) lines, a synthetic DNA fragment of 2159 containing the last part of the *A. thaliana* PKS4 promoter followed by the *A. thaliana* codon optimized PKS4 CDS from *A. trichopoda* (Supl mat) was ordered from Eurofins® and digested with the restriction enzymes XhoI and BamHI and replaced in the pPS9 construct previously digested with the same restriction enzymes for that purpose. Similarly, for the generation of the PKS4pro::*B. distachyon* PKS4-3xHA (pAL33) lines, a synthetic DNA fragment of 1703 bp containing the last part of the *A. thaliana* PKS4 promoter followed by the *A. thaliana* codon optimized PKS4 CDS from *B. distachyon* (Supl mat) was ordered from Eurofins® and digested with the restriction enzymes XhoI and BamHI and replaced in the pPS9 construct previously digested with the same restriction enzymes for that purpose. For the generation of the 35Spro::GFP construct carrying the (pAL73), the GFP sequence was amplified from the pAL43 (Vazquez et al., 2022) with the primers AL60 and AL61 and cloned using the In-fusion HD cloning kit (Cat#639649) into the pFR101 previously digested with the unique restriction site enzyme SalI. For the generation of the 35Spro::*A. thaliana* PKS4-GFP (pAL74), 35Spro:: *B. distachyon* PKS4-GFP (pAL75), and 35Spro:: *A. trichopoda* PKS4-GFP (pAL76) lines, the PKS4 CDS was amplified from the pPS9, pAL33, and pAL20, respectively, with the primers pairs AL62 + AL63, AL64 + AL65, and AL66 + AL67, respectively, and cloned using the In-fusion HD cloning kit into the pAL73 previously digested with the unique restriction site enzyme BamHI for that purpose. For the generation of the CRISPR *Bdpks4-1*, *Bdpks4-2,* and *Bdpks4-3* mutant lines, the BdPKSa (GGACAGGTACAGAGTGGCGC) and BdPKSc (GCCGCGTCCACATGCCGGTC) gRNAs were chosen among the gRNAs proposed by Breaking-Cas (Oliveros et al., 2016) and cloned into the p5Cas via BamHI-HindIII restriction digest (van der Schuren et al., 2018). All constructs were sequence verified. *A. thaliana* transgenic lines were obtained using *Agrobacterium tumefaciens*-mediated transformation. Several single insertion

lines expressing each of them were characterized. The use of fluorescent seeds as a selection marker also allowed us to perform experiments with large numbers of independent T1 lines. *B. distachyon* CRISPR mutant lines were obtained using *Agrobacterium tumefaciens*-mediated transformation (Pacheco-Villalobos et al., 2013). Transformants for the CRISPR/Cas9 *BdPKS4* construct were selected on hygromycin as described (Pacheco-Villalobos et al., 2013) with the addition of 600 µg ml^{-1} copper sulfate (CuSO4) to the regeneration media.

Growth conditions

For *A. thaliana* seeds production, plants were grown on the soil at 22°C with 16h of white light (WL) per day. For physiological experiments, seeds were surface-sterilized in 70% ethanol and 0.05% Triton-X for 5 min and 100% ethanol for 5 min. Seeds were then sown on Petri dishes containing half-strength Murashige and Skoog medium, 0.8% agar. Plates were stored in the dark for 3 days at 4°C for stratification. For dark-grown seedlings experiments, germination was induced by 4-6 hours of white light (80 µmol m^{-2} s^{-1}) at 22°C, and plates were put on vertically orientated position back in the dark at 19°C or 22°C for 3 days before light treatment. For inhibition of gravitropism experiments, germination was induced by 1h of RL (50 µmol m^{-2} s^{-1}) at 22°C, and plates were put back in the dark at 22°C for 1 day before light treatment. For *B. distachyon* seeds production, plants were grown on the soil at 22°C with 20h of white light (WL) per day. For physiological experiments, seeds were surface-sterilized in 70% ethanol and 0.05% Triton-X for 30 secs and 1.3% sodium hypochlorite for 4 mins. Seeds were then sown on boxes containing half-strength Murashige and Skoog medium, 0.7% agar. For dark-grown seedlings experiments, germination was induced by 1 hour of RL (50 µmol m^{-2} s^{-1}) at 22°C and boxes were put in the dark at 22°C for 5 days before light treatment.

Light treatments

For phototropism experiments, seedlings were irradiated with constant unilateral 0.1 µmol m^{-2} s^{-1} or 10 µmol m^{-2} s^{-1} BL at 22°C for up to 24h. For inhibition of gravitropism, seedlings were grown on vertically orientated plates for 1 day in darkness at 22°C before the light treatment. Seedlings were irradiated with constant 30 µmol m^{-2} s^{-1} RL at 22°C for 3 days.

Hypocotyl measurements and analysis

Plates were pictured using an infra-red CCD camera system at different timepoints. The curvature angles were calculated by subtracting the average angle of orientation of the upper region (85−95% of total length) of each hypocotyl to vertical after light treatment determined by a customized MATLAB script developed in the Fankhauser Lab. The curvature angles in *B. distachyon* phototropic experiments were calculated the same way but by subtracting the angle of orientation of the upper region (85−95% of total length) of each coleoptile to the angle of orientation before the light treatment. The *B. distachyon* coleoptile growth was calculated by subtracting the coleoptile length before the start of the experiment to the coleoptile length at 24h after light treatment. The coleoptile length was measured using the 'segmented line' tool in (Fiji Is Just) ImageJ. One-way ANOVA (aov) and Compute Tukey's Honest Significance Differences (HSD.test) [agricolae package] using the R software were performed. We considered p values <0.01 significant.

Fluorescence microscopy

Confocal microscopy images were taken with an Airy confocal microscope (Zeiss), model LSM 880. The samples 35Spro::PKS1-GFP, 35Spro::PKS2-GFP, 35Spro::*A. thaliana* PKS4-GFP, 35Spro::*A. trichopoda* PKS4-GFP, and 35Spro::*B. distachyon* PKS4 -GFP were excited with an Argon laser (488nm) and detection was done between 495 and 518 nm. In all cases a channel was set to detect chlorophyll and OLE1-RFP, exciting with the laser used for excitation of the fluorophore of interest, and detecting between 607 and 691 nm.

Western blot

Total proteins (80µl 2× Laemmli buffer for 20mg fresh weight; 10µg per lane) were separated on 4-15% precast polyacrylamide gels and transferred onto nitrocellulose using the Trans-Blot Turbo RTA Transfer Kit. Anti-HA-HRP monoclonal antibody 3F10 was used at 1/4000 (12013819001, Roche) and anti-DET3 antibody was used at 1/20000 dilutions (Schumacher et al., 1999) in 1X PBS containing 0.1% Tween-20 and 5% non-fat milk. Chemiluminescence signals were generated using Immobilon Western HRP Substrate (Millipore). Signals were detected with a Fujifilm ImageQuant LAS 4000 mini CCD camera system and quantifications were performed with ImageQuant TL software (GE Healthcare).

Accession Numbers

The Arabidopsis Genome Initiative numbers for the genes mentioned in this article are as follows: AT2G02950 (PKS1), AT1G14280 (PKS2), AT1G18810 (PKS3), AT5G04190 (PKS4), AT5G64330, AMBTC04918 (*A. trichopoda* PKS4), Bd2g09750 (*B. distachyon* PKS4).

SUPLEMENTAL MATERIAL

Supplemental material 1. *A. thaliana* codon optimized PKS4 CDS from *A. trichopoda*

ATGGAACGGTATACCGTCAGCGCATCTTTGAATGGTGAATTCCCTTTCAGTCAAAGCAC

TACACACTTGAGAGATGCTTCTTTCTCTTCTTACATTAGCAATCCGCCAGATCCGAAAC

TTCATATCTCGCCCAATAACCTTTCATTGGAGAACCCTCTCTCAGAGTTTAGCCAAATC

CCTAAACTTACTATCTCGTCCAATATCAGTCTCGAAAACCCAGTTAACGAGTCATCACA

AACTCCAAAGCTGACCATCAATTCAAATAATTTGTCACTTCAGAATCCACCTAACGAGT

TCTTTTCCAAACCGAAGTTGACCATTCAGCCAAACTCATTCAGCCTCGAAGATCCTCAC

TCTGAATTTTCCCAGAATCCAAAACTGATAAACAACCCCAACAATCTTACCCTGGAAA

ACCCCATTCCAGCGTCCCTCAGAAAACCGGGGAATGTTGGCAGAACTCGTACCAACTA

TTCTGAAATCTCTATCTTTGATGCGGAGAAGTACTTCAATGGGACCAGCTTGGAGAGAA

TTCCAGAGAAAGGGCTCGTTAGTGAGCTCAGTCGTCCGAAAACAAATGGGGAGAACTT

AAACTTTTCTATTCCAAGGGATTCCTCTGCATCGTCAGCAGATGGATTTAGCCGTAACT

ACCGTAGTGTCTCTTTCCATGCGACTCCAACATCTTCCAGTGAAGCGTCGTGGAACTCA

CAATCAGGCTTGCTATGCAATCCTCCGGGGTCTATATCAGTGACTGTTAGGAATCTTCC

CGTTAAACCACAGAGGAAGGGTGCAAGTAAATGGTCGTTCTCTTGTAGGTGTCCTTGTT

ATGGTAAGAAGTCCGTTGGTGTGAGAGAACGTAAGTCAGAAACGCGTAATGAAGCCTC

TAGTATGGCTGCTTCAACGGAAGGAAGCCCTAGCTCATCCAGAAAGACTTTAGGGCCT

AATGAGAACTCTAACTCCCATGCCTCTGAGAGAGAGAAGAGTCAAGCTAGTGAGACAG

AGATGTCCCATGCATCTGAACGAGAGATGACACAGGCTAGAGGTAGAGAAACGAAAG

TAGTTGCCGGCAAAGTCAAGCCAGCGGGTAATTGGGAAGCACAATCGCCTGAGATTCA

TTTCCGTGCTGAAATAGGCAGAAGAAAGATGAACCCTGATGCTGGATTTTCCTTTCCCA

TTCTTAATCCTATGGCTGGAAAGTTCGCTGGTAAACCTAATGGTCTACCGGAAAAGAG

AATTGATGACAAACCTAGGGATTCTATAGAGGTGTTTCAGCCGTCTAAGGAGCTTCATG

GGCCACCTGAATTCAGAATCTCTGGTGAGGGATTACGACGATCATTCGGCTTTCCAGCA

AGAGGCCTATTAGACAACGAAAGGGATGACGCTGGTTCAGATAGTTCTTCTGACCTGT

TCGAAATCGAATCATTTTCTACAGGAATTACTAGTTCGCTCTATAATATGAGGGATTCT

CTTGACGAACTATCCTCTTGCACGGGTAGCGAATTTCCGGCTCGTAGATTACCTACCAA

TCCAAACGCCTCGTTCTTCAGGCAAGGACCTCACGAGGAAGCTGTCACACCAAGTGCC

TTAAGTGACTGCTATGAGCCAAGTGAGGCTAGCGTAGAGTGGAGCGTAACAACAGCTG

AGGGTTTTGATAGAGGATCGATATCAAACTTCACAGTTGATGGTTTGGAACGAGTATC

GATAGGAAACTTTAGTGCAGCACCAACGGAATGTGGTGATCCGAAAGTCTTTGGTGTG

AGGGGATACTCTGATACTAGAGCTATAGGAGCAAGCCACAAGTCTAAGAACAAATCTA

AATCCGGATTGCTTTGGTGTAAGTGTGAGAAGGCTGTTAATGTGGTTCCCCAACCTATC

AAAGGAGGACCTGATCGGGCTCATCTAGACAGAGGAATGGGACTTGTTCGGGTGCAGG

AAGTGTGCATTACTGACCCTTCAGCACATGTTAATGGAATTATGGATCGAAGAATGTTG

GCCAGATCACCTTCAGAGCACTTTTCTCGGGCGCTGGCTACTCAT

Supplemental material 2. *A. thaliana* codon optimized PKS4 CDS from *B. distachyon*

ATGGATCGATACCGAGTAGCTCCAGCCAGACCGGTTTTCCTTTCATCTGGCGCTACTCA

TCACCACGTTCAAGCTCCACCTCCACCTAGACGTTCTGATGGAGCAGAACTTGACATCT

TTACGGCCGAGAGGTACTTCAATGCCGCAGATGCCACGAAGTATCGTGCTGCATCTGCT

GCAACTCCTGTCCCTGTCGACTCTCCGACTGCTCCGCATTTAGCCATGGATAGCGCGGC

ATCTCAGTCAGGCAGAACAGCTGCTTCTTCCGAAGCTAGTTGGAACTCCAGATCTGGAC

TTCTGGCGTCGAACAATAACAACAACCAGTCAGCATCTGCGCGACAGCAACATGACGG

AAAAGGCGGTTATGGAGGGGTAGGTGTGGGTAACGGAGGTGTTGTAGATGGCACAAG

AGATGAACGATACCACAGAGCTAAGAAACCCGCAGGACAACGGTGGGGACTCTTCTCC

AGAGTAGATTGTCCTTGTGTGGGTCGTAAAGCCGTGACCGTTGGAGTGGCCTCAGAGC

CACCATCGCCAAGAACGCAACATGCAACTTCCAGTGCGGCTACAGACCAAGAGATTTC

AGCTATCTTCAAAGCGAATCGTCTTTTACTGGCTCCTCCCTCACCCACACATGAACCGG

AACCTAGCACAGCCAAGATCATATCTACCACTGGTAGTTGCACCTTTCTCCTTAGAGCA

AACAACAATAGCGGGATGTTGGCACCACCGGGGCCGAATAAGGTCGCTGCATTTAGGG

CTCCAGATATTGGTAGACGGGTTGTGGTTAGCTCCTCAGGAGCAGTAGGGTTTACGTTC

CCCGTGATTGGACCAGCAACCAACGTCGTCATTGATGAACCTCCTAGAGAGTCACTTG

AAGTTTTCCGTCCTATAGACGAGGACAGTGTCCTCTTAGCGGATGAACCTCCACCTCGT

CCTCCATCTCTATCTGCTCCCGGAGCTTTTCTACGTGCGCCTGTTTTGGCAACAGCTGAA

GAAGATGCCATGAGTGATGCTTCGAGTGACTTGTTTGATTTGGAGTCATTTGCGGCTAG

CTCCTCTTACCCGACTACATGTAGAGGTGGGAGGGGTTCATCGAGGCGGAATTCACGA

GAGGAGGATGACAATTTGCCTCCATATGCGGAGGCAATGGCTGCTATGGCTGCAGAGC

CTGCTCTATCGGAATGCATGTATGCCCCATCTGAGGCTTCCGTTGTTTGGTCGGTAGCT

ACTGCCGAAGGTTTTGCACCATACGATGCCGCACCATCTGTGGCTAATTTCAGTAGTGC

AGCAAGCGCTTGTGGGGCAGATGATTTTGCCAGGTTTGTGGTTCAGCCGCCAGCGGCT

GGAGGTGGAGGGTTCACAGCGGCTATGAGTAGATCAGCGGCTGGTAGGAAGAAAGGT

GGAGGTGGATTCCTCAATTCTTGTCGGTGCGAGAAGGCAGTGAGCGTTGGCCCCACTC

CTGTTAGAGTGGCTAGACCAAGACCTCCGGTTCCTGAAGCTAAAACCGCTATGGCTTTC

GAGTCTGGCGGTGCTGCAAGGTATCACCATGGAAGGGTTCATATGCCTGTCAGAACT

Supplemental table 1. Primers used in this study

Name	Sequence
AL60	5'- ctgactctagaggatccgtcgacatgagtaaaggagaagaacttttc -3'

AL61	5'- gaacgatctgcaggtcgacttatttgtatagttcatccatgcca -3'
AL62	5'- gacaagctgactctagaggatccaaaaatggcgcaaactactgtca -3'
AL63	5'- tactcatgtcgacggatccttgccttggtctactcgtca -3'
AL64	5'- gacaagctgactctagaggatccaaaaatggatcgataccgagtagc -3'
AL65	5'- tactcatgtcgacggatccagttctgacaggcatatgaac -3'
AL66	5'- gacaagctgactctagaggatccaaaaatggaacggtataccgtcag -3'
AL67	5'- tactcatgtcgacggatccatgagtagccagcgcccga -3'
LA18	5'- gtatgggtagtcgacggatccctgactataaagaagagatgattg -3'
LA24	5'- aagaagcaaaagatacttcaatggtgacactaacaccatc -3'
LA25	5'-atccaagctcaagctaagctctaagctttaaatagtaatgttctagaatttgg -3'
LA26	5'- gatggtgttagtgtcaccattgaagtatctttttgcttctttttctc -3'
LA27	5'- aagaagcaaaagatacttcaatggtgaccttaacttcatcttc -3'
LA28	5'- gtatgggtagtcgacggatccagtatacaaaaaaggcgattgc -3'
LA29	5'- gatgaagttaaggtcaccattgaagtatctttttgcttctttttctc -3'
LA30	5'- aagaagcaaaagatacttcaatggatgctgaaaagaagagtg -3'
LA31	5'- gtatgggtagtcgacggatccaagaaagctcaagtcttgaatcc -3'
LA32	5'- ctcttcttttcagcatccattgaagtatctttttgcttctttttctc -3'
PL21	5'- ggggtaccaaaatggtgaccttaacttcatc -3'

PL18	5'- cgggatccgtatacaaaaaaggcgattgc -3'

LITERATURE CITED

ALTENHOFF, A. M., GLOVER, N. M., TRAIN, C.-M., KALEB, K., WARWICK VESZTROCY, A., DYLUS, D., DE FARIAS, T. M., ZILE, K., STEVENSON, C. & LONG, J. 2017. The OMA orthology database in 2018: retrieving evolutionary relationships among all domains of life through richer web and programmatic interfaces. *Nucleic acids research,* 46**,** D477-D485.

BEUCHAT, J., LI, S., RAGNI, L., SHINDO, C., KOHN, M. H. & HARDTKE, C. S. 2010. A hyperactive quantitative trait locus allele of Arabidopsis BRX contributes to natural variation in root growth vigor. *Proceedings of the National Academy of Sciences,* 107**,** 8475-8480.

BOCCALANDRO, H. E., DE SIMONE, S. N., BERGMANN-HONSBERGER, A., SCHEPENS, I., FANKHAUSER, C. & CASAL, J. J. 2008. PHYTOCHROME KINASE SUBSTRATE1 regulates root phototropism and gravitropism. *Plant Physiology,* 146**,** 108-15.

BRIGGS, G. C., MOUCHEL, C. F. & HARDTKE, C. S. 2006. Characterization of the plant-specific BREVIS RADIX gene family reveals limited genetic redundancy despite high sequence conservation. *Plant Physiology,* 140**,** 1306-16.

CHRISTIE, J. M., SUETSUGU, N., SULLIVAN, S. & WADA, M. 2018. Shining light on the function of NPH3/RPT2-like proteins in phototropin signaling. *Plant physiology,* 176**,** 1015-1024.

CONANT, G. C. & WOLFE, K. H. 2008. Turning a hobby into a job: how duplicated genes find new functions. *Nature Reviews Genetics,* 9**,** 938-950.

DE CARBONNEL, M., DAVIS, P., ROELFSEMA, M. R., INOUE, S., SCHEPENS, I., LARIGUET, P., GEISLER, M., SHIMAZAKI, K., HANGARTER, R. & FANKHAUSER, C. 2010. The Arabidopsis PHYTOCHROME KINASE SUBSTRATE2 protein is a

phototropin signaling element that regulates leaf flattening and leaf positioning. *Plant Physiology,* 152**,** 1391-405.

DEMARSY, E., SCHEPENS, I., OKAJIMA, K., HERSCH, M., BERGMANN, S., CHRISTIE, J., SHIMAZAKI, K., TOKUTOMI, S. & FANKHAUSER, C. 2012. Phytochrome Kinase Substrate 4 is phosphorylated by the phototropin 1 photoreceptor. The *EMBO Journal,* 31**,** 3457-67.

FITCH, W. M. 1970. Distinguishing homologous from analogous proteins. *Systematic zoology,* 19**,** 99-113.

FOLTA, K. M. & SPALDING, E. P. 2001. Unexpected roles for cryptochrome 2 and phototropin revealed by high-resolution analysis of blue light-mediated hypocotyl growth inhibition. *The Plant Journal,* 26**,** 471-478.

GLOVER, N., SHEPPARD, S. & DESSIMOZ, C. 2021. Homoeolog inference methods requiring bidirectional best hits or syntheny miss many pairs. *Genome biology and evolution,* 13**,** evab077.

GLOVER, N. M., REDESTIG, H. & DESSIMOZ, C. 2016. Homoeologs: what are they and how do we infer them? *Trends in plant science,* 21**,** 609-621.

HAGA, K., TAKANO, M., NEUMANN, R. & IINO, M. 2005. The rice COLEOPTILE PHOTOTROPISM1 gene encoding an ortholog of Arabidopsis NPH3 is required for phototropism of coleoptiles and lateral translocation of auxin. *The Plant Cell,* 17**,** 103-115.

KAMI, C., ALLENBACH, L., ZOURELIDOU, M., LJUNG, K., SCHÜTZ, F., ISONO, E., WATAHIKI, M. K., YAMAMOTO, K. T., SCHWECHHEIMER, C. & FANKHAUSER, C. 2014. Reduced phototropism in pks mutants may be due to altered auxin-regulated gene expression or reduced lateral auxin transport. *The Plant Journal,* 77**,** 393-403.

KOH, S. W., MARHAVA, P., RANA, S., GRAF, A., MORET, B., BASSUKAS, A. E.,

ZOURELIDOU, M., KOLB, M., HAMMES, U. Z. & SCHWECHHEIMER, C. 2021. Mapping and engineering of auxin-induced plasma membrane dissociation in BRX family proteins. *The Plant Cell,* 33**,** 1945-1960.

KUMAR, M., CARR, P. & TURNER, S. R. 2022. An atlas of Arabidopsis protein S-acylation reveals its widespread role in plant cell organization and function. *Nature Plants*, 8, 670-681.

LARIGUET, P., BOCCALANDRO, H. E., ALONSO, J. M., ECKER, J. R., CHORY, J., CASAL, J. J. & FANKHAUSER, C. 2003. A growth regulatory loop that provides homeostasis to phytochrome a signaling. *The Plant Cell,* 15**,** 2966-2978.

LARIGUET, P. & FANKHAUSER, C. 2004. Hypocotyl growth orientation in blue light is determined by phytochrome A inhibition of gravitropism and phototropin promotion of phototropism. *The Plant Journal,* 40**,** 826-834.

LARIGUET, P., SCHEPENS, I., HODGSON, D., PEDMALE, U. V., TREVISAN, M., KAMI, C., DE CARBONNEL, M., ALONSO, J. M., ECKER, J. R. & LISCUM, E. 2006. PHYTOCHROME KINASE SUBSTRATE 1 is a phototropin 1 binding protein required for phototropism. *Proceedings of the National Academy of Sciences,* 103**,** 10134-10139.

LEGRIS, M., SZARZYNSKA-ERDEN, B. M., TREVISAN, M., ALLENBACH PETROLATI, L. & FANKHAUSER, C. 2021. Phototropin-mediated perception of light direction in leaves regulates blade flattening. *Plant physiology,* 187**,** 1235-1249.

LI, F.-W. & MATHEWS, S. 2016. Evolutionary aspects of plant photoreceptors. *Journal of plant research,* 129**,** 115-122.

LISCUM, E., ASKINOSIE, S. K., LEUCHTMAN, D. L., MORROW, J., WILLENBURG, K. T. & COATS, D. R. 2014. Phototropism: growing towards an understanding of plant movement. *The Plant Cell,* 26**,** 38-55.

MARHAVA, P., FANDINO, A. C. A., KOH, S. W., JELÍNKOVÁ, A., KOLB, M., JANACEK, D. P., BREDA, A. S., CATTANEO, P., HAMMES, U. Z. & PETRÁŠEK, J. 2020. Plasma membrane domain patterning and self-reinforcing polarity in Arabidopsis. *Developmental cell,* 52**,** 223-235. e5.

OLIVEROS, J. C., FRANCH, M., TABAS-MADRID, D., SAN-LEÓN, D., MONTOLIU, L., CUBAS, P. & PAZOS, F. 2016. Breaking-Cas—interactive design of guide RNAs for CRISPR-Cas experiments for ENSEMBL genomes. *Nucleic acids research,* 44**,** W267-W271.

PACHECO-VILLALOBOS, D., SANKAR, M., LJUNG, K. & HARDTKE, C. S. 2013. Disturbed local auxin homeostasis enhances cellular anisotropy and reveals alternative wiring of auxin-ethylene crosstalk in Brachypodium distachyon seminal roots. *PLoS Genetics,* 9**,** e1003564.

PEDMALE, U. V., HUANG, S.-S. C., ZANDER, M., COLE, B. J., HETZEL, J., LJUNG, K., REIS, P. A., SRIDEVI, P., NITO, K. & NERY, J. R. 2016. Cryptochromes interact directly with PIFs to control plant growth in limiting blue light. *Cell,* 164**,** 233-245.

PREUTEN, T., BLACKWOOD, L., CHRISTIE, J. M. & FANKHAUSER, C. 2015. Lipid anchoring of Arabidopsis phototropin 1 to assess the functional significance of receptor internalization: should I stay or should I go? *New Phytologist,* 206**,** 1038-1050.

REED, J. W., NAGPAL, P., POOLE, D. S., FURUYA, M. & CHORY, J. 1993. Mutations in the gene for the red/far-red light receptor phytochrome B alter cell elongation and physiological responses throughout Arabidopsis development. *The Plant Cell,* 5**,** 147-157.

SALOMON, M., MARKUS, Z. & RÜDIGER, W. 1997. Asymmetric, Blue Light-Dependent Phosphorylation of a 116-Kilodalton Plasma Membrane Protein Can Be Correlated with the First- and Second-Positive Phototropic Curvature of Oat Coleoptiles. *Plant Physiology,* 115**,**

485-491.

SCHEPENS, I., BOCCALANDRO, H. E., KAMI, C., CASAL, J. J. & FANKHAUSER, C. 2008. PHYTOCHROME KINASE SUBSTRATE4 modulates phytochrome-mediated control of hypocotyl growth orientation. *Plant Physiology,* 147**,** 661-71.

SCHUMACHER, K., VAFEADOS, D., MCCARTHY, M., SZE, H., WILKINS, T. & CHORY, J. 1999. The Arabidopsis det3 mutant reveals a central role for the vacuolar H+–ATPase in plant growth and development. *Genes & development,* 13**,** 3259-3270.

SCHUMACHER, P., DEMARSY, E., WARIDEL, P., PETROLATI, L. A., TREVISAN, M. & FANKHAUSER, C. 2018. A phosphorylation switch turns a positive regulator of phototropism into an inhibitor of the process. *Nature Communications,* 9, 1-9.

SOLTIS, D. E., ALBERT, V. A., LEEBENS-MACK, J., PALMER, J. D., WING, R. A., DEPAMPHILIS, C. W., MA, H., CARLSON, J. E., ALTMAN, N. & KIM, S. 2008. The Amborellagenome: an evolutionary reference for plant biology. *Genome biology,* 9**,** 1-6.

VAN DER SCHUREN, A., VOINICIUC, C., BRAGG, J., LJUNG, K., VOGEL, J., PAULY, M. & HARDTKE, C. S. 2018. Broad spectrum developmental role of Brachypodium AUX 1. *New Phytologist,* 219**,** 1216-1223.

VAZQUEZ, A. L., PETROLATI, L. A., DESSIMOZ, C., LAMPUGNANI, E. R., GLOVER, N. & FANKHAUSER, C. 2022. Control of PHYTOCHROME KINASE SUBSTRATE subcellular localization and biological activity by protein S-acylation. *bioRxiv*.

ACKNOWLEDGEMENTS

CHAPTER 3. Evolutionary conserved PKS proteins motif D is required for biological activity

OVERVIEW

I led this project where we tested the functional importance of the PKS motifs A, B, D, and E, and focused on motif D, under the supervision of Prof. Christian Fankhauser. Our work has not been submitted yet because we are aiming to include additional experiments to complete our work. Depending on the progress of additional collaborations, we might include some of the data presented in this chapter in a different manuscript for another publication.

I conceived the original research plans with Prof. Christian Fankhauser. I generated all the Arabidopsis unpublished transgenic lines and the Y2H clones concerning PKS family. Alexandre Dudt, master student in the Fankhauser lab under my supervision, generated the Arabidopsis unpublished transgenic lines and the Y2H clones concerning BPM family, under my supervision. I conducted and analyzed all the experiments presented in this chapter, except the experiments presented in Fig. 10B and 11A, which were conducted by Alexandre Dudt, under my supervision. I interpreted and discussed the data with the participation of Prof. Christian Fankhauser and the rest of the lab members. I wrote the manuscript about the current available data, with comments from Martina Legris and Prof. Christian Fankhauser.

ABSTRACT

PHYTOCHROME KINASE SUBSTRATE (PKS) proteins regulate plant growth in response to light. They control hypocotyl growth orientation by integrating the processes of phytochrome- mediated inhibition of gravitropism and phototropins (phot)-mediated phototropism. Phototropism arises from a gradient of phot1 activation across the hypocotyl, which leads to an increase in growth on the shaded side of the hypocotyl resulting from asymmetric auxin accumulation. Little is known about the molecular mechanisms of PKS in this process except that they share six protein motifs (A to F), among which motif C is required for function and association with the plasma membrane, where PKS form a protein complex with phot. Here, we show that the conserved protein sequence DLFEIE in PKS motif D is required for PKS4-mediated hypocotyl phototropism and control of gravitropism in response to light. Our work identifies six candidates that interact with PKS4 motif D in yeast and addresses the importance of some of the conserved amino acids for the interactions. We provide evidence that the central F amino acid is fundamental for all the tested interactions and PKS4 biological activity. Finally, our work suggests that PKS4 and PKS2 interact with members of the BTB/POZ AND MATH DOMAIN (BPM) family through its MATH domain to control phototropism.

INTRODUCTION

In *A. thaliana,* phototropins (phot1 and phot2) control numerous physiological responses such as phototropism, leaf positioning and flattening, chloroplast movements, and stomata opening (Christie, 2007). PKS proteins are part of the phototropins complex and are required for the establishment of several light adaptative growth responses: *PKS1* is essential for negative root phototropism while *PKS2* and *PKS3* are more important for leaf movement and flattening (Lariguet et al., 2003, Lariguet et al., 2006, Boccalandro et al., 2008, de Carbonnel et al., 2010, Legris et al., 2021) Moreover, *PKS1* and *PKS4* are important for hypocotyl phototropism and inhibition of gravitropism (Schepens et al., 2008, Kami et al., 2014a).

In angiosperms, phototropism arises from a phototropins activation gradient across the hypocotyl in response to unilateral BL irradiation, which leads to a gradient of concentration of the plant growth hormone auxin that is accumulated on the shaded side of the hypocotyl. Phototropins form a protein complex at the plasma membrane (PM) with NPH3 and PKS4, PKS1, and PKS2, however, the molecular mechanisms of PKS leading to a lateral auxin gradient are not well understood (Goyal et al., 2013, Legris and Boccaccini, 2020). *A. thaliana* includes 4 PKS protein family members (PKS1-PKS4), among which PKS4 is the most important in phototropism, followed by PKS1 and PKS2. PKS4 and PKS1 promote phototropism in response to LBL, while PKS2 together with PKS1 promote phototropism in HBL (Kami et al., 2014b). PKS3 does not promote phototropism in response to any BL fluence (Legris Martina, personal communication). Although it is not required to promote phototropism in HBL, PKS4 is a negative regulator of the process at higher fluence rates (Kami et al., 2014a, Schumacher et al., 2018). In addition to phototropism, PKS4 and PKS1 are involved in phy-mediated inhibition of hypocotyl gravitropism, a process depending on RL and FRL (Schepens et al., 2008).

PKS primary amino acid sequence does not reveal any protein domain of a known function. Moreover, protein structure prediction programs reveal that PKS proteins are expected to be largely intrinsically disordered, which makes the study of their molecular mechanism a big challenge (Vazquez et al., 2022). Phylogenetic studies based on protein sequence alignments of all the PKS found in plants allowed the identification of 6 evolutionary conserved protein motifs that are present in all the existing PKS proteins (motifs A to F). Structure-function analysis of the PKS motifs C and F revealed the requirement of PKS4 motif C for PKS4 localization at the PM and function in phototropism and inhibition of hypocotyl gravitropism, while the PKS4 motif F is not required (Vazquez et al., 2022). PKS4 associates with the PM through the s-acylation of the conserved Cysteine (Cys) amino acids in motif C, and this type of lipid-mediated association to the PM is essential for the biological activity of PKS in mediating hypocotyl growth orientation in response to light (Vazquez et al., 2022).

In this study, we addressed the importance of the rest of the conserved PKS4 motif for function in phototropism and inhibition of gravitropism. According to the hidden Markov Model-based protein searches, PKS motif D is related to a conserved sequence in the carboxy terminus of BIG GRAIN (BG and BG LIKE) proteins (Vazquez et al., 2022). The molecular function of this conserved sequence is currently unknown, however, as PKS, BG proteins are proposed to regulate auxin signaling and/or transport, suggesting that this conserved motif might be involved in auxin-mediated growth regulation (de Carbonnel et al., 2010, Kami et al., 2014a, Liu et al., 2015, Mishra et al., 2017). Interestingly, we found that the PKS4 motif D is essential for PKS4 function while it does not have an apparent role in bringing PKS4 to the PM, which led us to make a deeper analysis of motif D to investigate its molecular mechanisms. We further found several candidates that appear to interact with PKS through motif D and here we followed up on one of them: BPM4.

RESULTS

<u>The conserved motif D of PKS4 is required for biological activity.</u>

PKS form a protein complex with phot1 and NPH3 at the PM to promote phototropism, however little is known about PKS molecular mode of action (Lariguet et al., 2006, Schumacher et al., 2018, Christie et al., 2018). To determine the functional importance of the rest of the PKS conserved motifs whose function in hypocotyl growth orientation had not been previously addressed, we used complementation of *pks4*, which is defective in phototropism and phytochrome (phy)-mediated inhibition of hypocotyl gravitropism, as we did for the analysis of motifs C and F (Schepens et al., 2008, Kami et al., 2014a, Vazquez et al., 2022). First, we analyzed the PKS4 protein motifs sequence (Figure 1A).
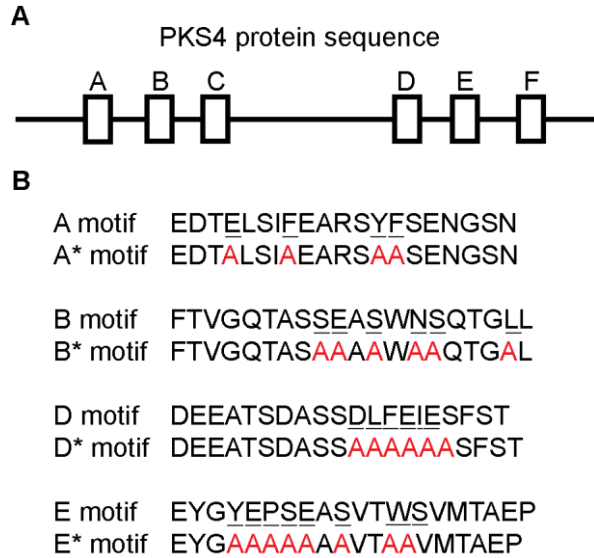
Figure 1. Illustration of the PKS4 motifs A, B, D, and E and mutant variants. (**A**) Schematic representation of the *A. thaliana* PKS4 protein sequence. The square boxes represent the PKS motifs (A to F) as described (Vazquez et al., 2022). The length of the boxes and the spaces between them are proportional to the length of the protein motifs and the spacing among them. (**B**) Primary structure of the PKS4 protein motifs A, B, D, and E and the designed variants A*, B*, D*, and E*. Underlined letters indicate the selected amino acids to be replaced with the ones in red color.

We selected the highly conserved amino acids of motifs A and B, the highly conserved hydrophobic and negatively charged amino acids of motif D, and a combination of highly conserved, hydrophobic, polar, and negatively charged amino acids of motif E. We designed the variants PKS4 A*, B*, D*, and E* motifs in which the selected amino acids were replaced with Alanine (A) (Figure 1B). We then tested the functional importance of motifs A, B, D, and E by generating PKS4 motifs A*, B*, D*, and E* mutants where the selected amino acids were replaced with Alanine and transforming *pks4* mutants as described for the PKS4 C* and F* lines. To test the importance of motifs A and B, we first selected transgenic lines (PKS4 A*1-2 and PKS4 B*1-4) with protein levels comparable to the PKS4 WT-3 control line (Figure 2A). We found that both PKS4 A* lines fully complemented the phototropic defect of the *pks4* mutant line as the PKS4 WT-3 did in response to blue light (BL) (Figure 2B). Similarly, the PKS4 B*-2 and B*-4 lines fully complemented the phototropic defect of the *pks4* mutant line (Figure 2C). Only the PKS4 B*-1 line did not complement, however, given that the expression level of the PKS4 B*-1 line was lower compared to the WT and the rest of the lines (Figure 2 A), these data overall suggest that the motifs A and B are not required for the function of PKS4 in phototropism in the tested conditions. To test the importance of motifs D and E, we similarly selected transgenic lines (PKS4 D*1-3 and PKS4 E*1-3) with comparable protein levels to the PKS4 WT-3 control line (Figure 2D). We found that none of the PKS4 D* lines complemented the phototropic defect of the *pks4* mutant line. Moreover, these lines notably aggravated the phototropic phenotype of *pks4*, particularly the lines PKS4 D*-1 and D*-2 which showed higher expression levels than the rest (Figures 2D and 2E).
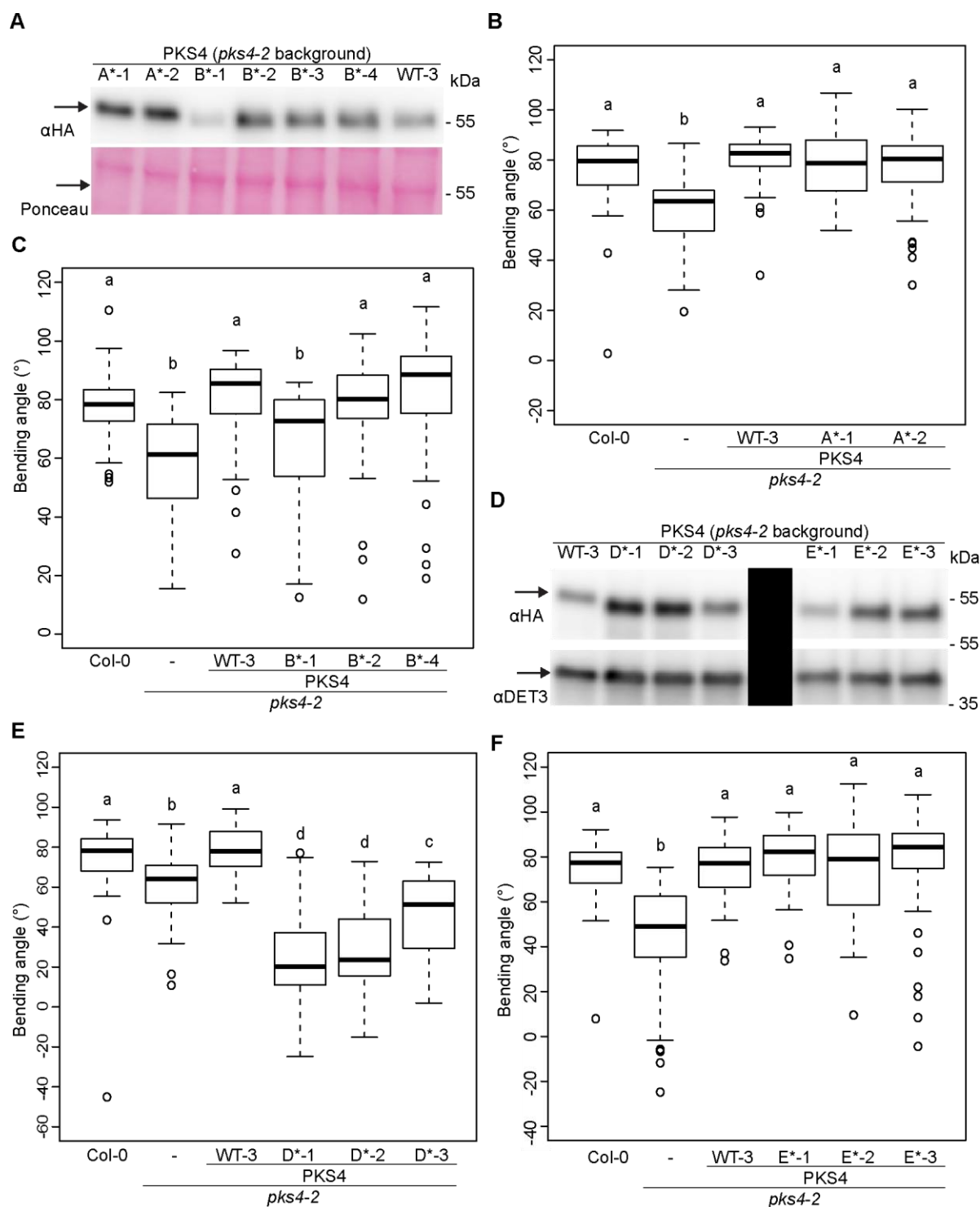
Figure 2. PKS4 A*, B*, and E* complement the phototropic phenotype of *pks4* while PKS4 D* do not. (**A**) Western blot probed with anti-HA antibody from *pks4-2* PKS4 WT-3, A*-1, A*-2, B*-1, B*-2, B*-3, and B*-4 samples of 3- day- old dark-grown seedlings. The same membrane was stained with Ponceau as a loading control. (**B**) Phototropic curvature of 3-day-old dark-grown Col-0, *pks4-2*, *pks4-2* PKS4 WT-3, and *pks4-2* PKS4 A* (A*-1 and A*-2) lines treated with BL coming from one

side. (**C**) Phototropic curvature of 3-day-old dark-grown Col-0, *pks4-2*, *pks4-2* PKS4 WT- 3, and *pks4-2* PKS4 B* (B*-1, B*-2, and B*-4) lines treated with BL coming from one side. (**D**) Western blot probed with anti-HA antibody from *pks4-2* PKS4 WT-3, *pks4-2* PKS4 D*-1, D*-2, and D*-3, and *pks4-2* PKS4 E*-1, E*-2, and E*-3 samples of 3- day- old dark-grown seedlings. The same membrane was probed with an anti-DET3 antibody as a loading control. The black box marks a region of the membrane that is not shown. (**E**) Phototropic curvature of 3-day-old dark-grown Col-0, *pks4-2*, *pks4-2* PKS4 WT-3, and *pks4-2* PKS4 D* (D*-1, D*-2, and D*-3) lines treated with BL coming from one side. (**F**) Phototropic curvature of 3-day-old dark-grown Col-0, *pks4-2*, *pks4-2* PKS4 WT-3, and *pks4-2* PKS4 E* (E*-1, E*-2, and E*-3) lines treated with BL coming from one side. In (**B**), (**C**), (**E**), and (**F**) seedlings were exposed to 0.1 µmol m^{-2} s^{-1} BL for 24h before measurement of growth reorientation. In each experiment, n= 40 – 60, means with the same letter are not significantly different (p > 0.01, two-way ANOVA with Tukey's HSD test).

This indicates that the motif D is important for the function of PKS4 and that mutating this motif significantly interferes with the molecular mechanism leading to phototropism. On the contrary, all the PKS4 E* lines complemented the phototropic defect of the *pks4* mutant line (Figure 2F), suggesting that this motif is not required for phototropism.

We analyzed hypocotyl gravitropism in darkness and observed that Col-0, *pks4,* and transgenic lines expressing PKS4 WT, A*, B*, or D* showed the same response (Figures 3A, 3B, and 3C), showing that the expression of PKS4 WT, A*, B*, or D* did not lead to an unusual gravitropism response in darkness and that the observed phenotype of the PKS4 D* lines is light-dependent. Although the line PKS4 E*-3 showed more randomized growth orientation than Col-0, *pks4*, and PKS4 WT-3, the lines PKS4 E*-1 and -2 showed a similar orientation compared to the control lines (Figure 3D), indicating that the expression of PKS4 E* does not lead to an unusual gravitropism response in darkness either. Collectively our data indicate that the conserved amino acids DLFEIE in PKS4 motif D are important to promote phototropism, while the motifs A, B, and E are not important, and that the expression of PKS4 A*, B*, D*, or E* does not lead to a defective gravitropism response in darkness.
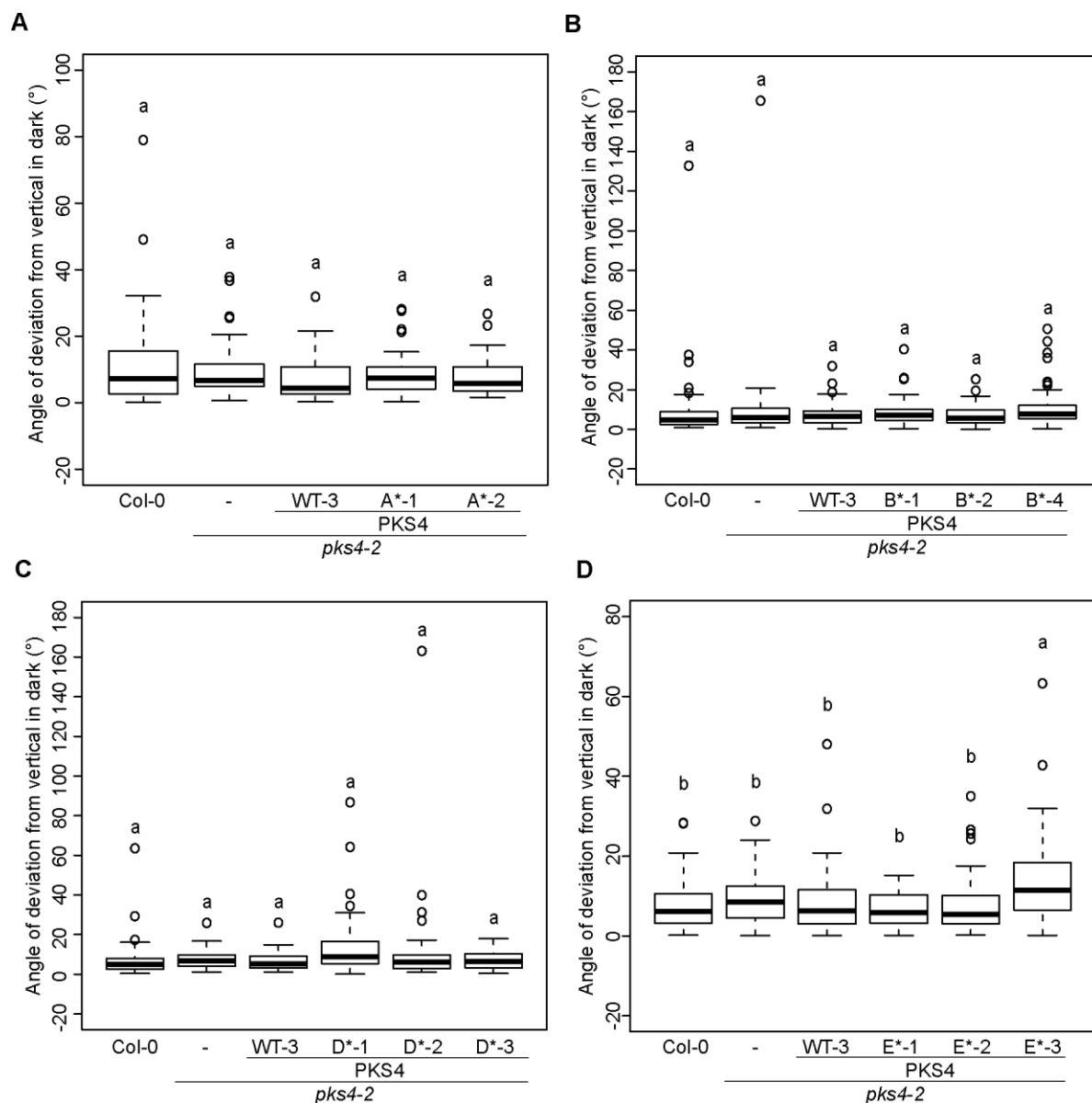
Figure 3. Expression of the PKS4 A*, B*, D*, or E* mutants does not alter hypocotyl gravitropism in dark-grown seedlings. (**A**) Hypocotyl growth orientation of 3-day-old Col-0, *pks4-2*, *pks4-2* PKS4 WT-3 and *pks4-2* PKS4 A* (A*-1 and A*-2), (**B**) Col-0, *pks4-2*, *pks4-2* PKS4 WT-3, and *pks4-2* PKS4 B* (B*-1, B*-2, and B*-4), (**C**) Col-0, *pks4-2*, *pks4-2* PKS4 WT-3, and *pks4-2* PKS4 D* (D*-1, D*-2, and D*-3), and (**D**) Col-0, *pks4-2*, *pks4-2* PKS4 WT-3, and *pks4-2* PKS4 E* (E*- 1, E*-2, and E*-3) dark-grown seedlings. 0° represents vertical growth and an average of 90° represents a random distribution. We consider the absolute value of the angle, no matter if the seedling bends towards the left or the right side. In each experiment, n= 50 – 60, means with the same letter are not significantly different (p > 0.01, two-way ANOVA with Tukey's HSD test).

To determine the importance of these motifs in phy signaling we analyzed light-induced inhibition of hypocotyl gravitropism by measuring the hypocotyl growth orientation relative to the vertical in response to 30 µmol m^{-2} s^{-1} of continuous red light (RL) (Schepens et al., 2008, Vazquez et al., 2022). We found that similar to the control PKS4 WT-3 line, the PKS4 A* lines complemented the *pks4* phenotype in response to this light treatment (Figure 4A), suggesting that motif A is not important for this function. Comparably, the PKS4 B* lines complemented the *pks4* phenotype and further showed an overall bigger deviation angle from the vertical compared to the WT (Figure 4B). However, the PKS4 D* lines did not complement *pks4* and they often showed a phenotype similar to *phyB*-9 (Figure 4C), indicating the relevance of motif D for PKS4 function in the inhibition of gravitropism. Similar to the lines expressing PKS4 A* and PKS4 B*, the PKS4 E* lines complemented the *pks4* phenotype (Figure 4D).
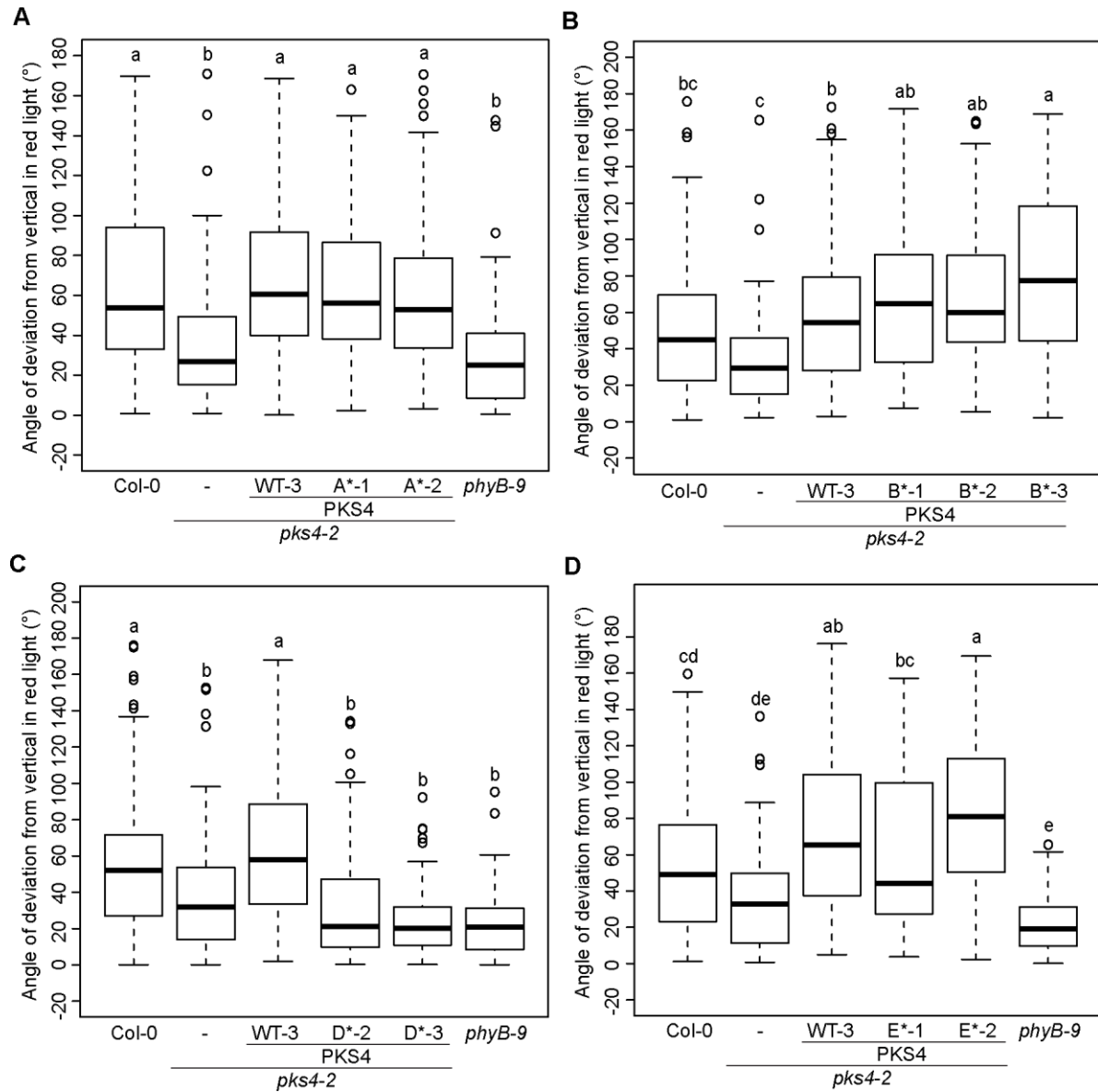
Figure 4. PKS4 A*, B*, and E* complement the phenotype of *pks4* in the inhibition of gravitropism while PKS4 D* do not. (**A**) Hypocotyl growth orientation of Col-0, *pks4-2*, *pks4-2* PKS4 WT-3, and *pks4-2* PKS4 A* (A*-1 and A*-2), (**B**) Col-0, *pks4-2*, *pks4-2* PKS4 WT-3, and *pks4-2* PKS4 B* (B*-1, B*-2, and B*-4), (**C**) Col-0, *pks4-2*, *pks4-2* PKS4 WT-3, and *pks4-2* PKS4 D* (D*-1, D*-2, and D*-3), and (**D**) Col-0, *pks4-2*, *pks4-2* PKS4 WT-3, and *pks4-2* PKS4 E* (E*- 1, E*-2, and E*-3) seedlings growing in continuous 30 µmol m^{-2} s^{-1} red light. Seedlings were kept for 24h in darkness before 4 days of red light treatment following measurement of growth orientation. 0° represents vertical growth and an average of 90° represents random distribution. We consider the absolute value of the angle, no matter if the seedling bends towards the left or the right side. n= 70 – 80, means with the same letter are not significantly different (p > 0.01, two-way ANOVA with Tukey's HSD test).

Given that PKS4 requires to be associated with the PM to function in response to blue light BL and RL, we wondered whether the lack of complementation of the lines expressing PKS4 D* could be due to altered subcellular localization of PKS4 D* (Vazquez et al., 2022). To address that question, we generated stable transgenic Arabidopsis plants expressing PKS4 D*-GFP driven by the *PKS4* promoter in *pks4*, and we determined their subcellular localization compared with that of plants expressing PKS4 WT-GFP in etiolated seedlings using confocal microscopy (Figure 5A). These results suggested that PKS4 D*-GFP maintains the same subcellular localization as the WT. This finding aroused our interest in making a more extended analysis of motif D.

A
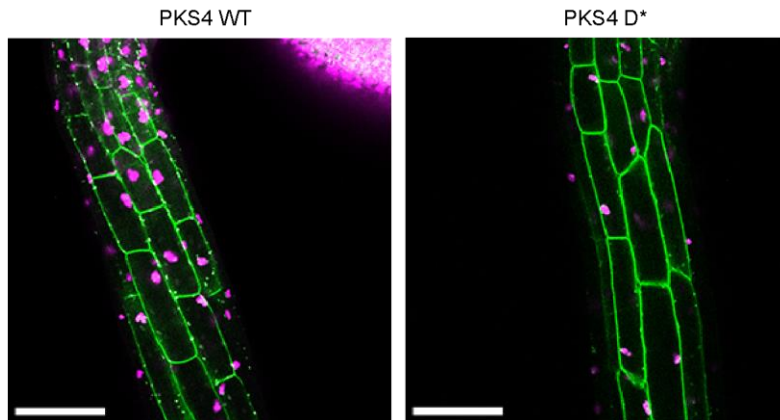
Figure 5. PKS4 motif D is not required for the association of PKS4 to the PM. (**A**) Confocal microscopy images of 3-day-old dark-grown hypocotyls cortex cells expressing PKS4-GFP and PKS4 D*-GFP (green signal) from the *PKS4* promoter. Note that these lines also show remaining oily bodies (in magenta) resulting from the expression of OLE1-RFP from the *OLE1* promoter, used as seeds coats selection marker. Scale bar: 100 μm.

We selected mutant combinations including one or two negatively charged and/or hydrophobic

amino acids to design the variants PKS4 D1*, D2*, D3*, D4*, and D5* in which the selected amino acids were replaced with Alanine (Figure 6A). To test the importance of these amino acids, we started by looking at the expression levels of the transgenic lines expressing PKS4 D1* and PKS4 D2* (PKS4 D*1-6 and PKS4 D2*1-6) and selected those with expression levels more similar to the PKS4 WT-3 control line: PKS4 D1*-1 and PKS4 D1*-6 and PKS4 D2*-3 and PKS4 D2*-4 (Figure 6B). We found that none of the PKS4 D1* lines could complement the phototropic phenotype of *pks4* and they further aggravated the phenotype (Figure 6C). This was supported by the phenotype of the progeny of the D1* lines that did not carry the transgene (shown with "-"), which was comparable to *pks4* (Figure 6C). This suggests that the highly conserved negatively charged amino acids D276 and E279 are important for the function of PKS4, and mutating them interferes with the molecular system leading to phototropism. Similarly, the PKS4 D2*-3 and D2*-4 lines could not complement the phototropic phenotype of *pks4* as the PKS4 WT-3 did and they remarkably aggravated the *pks4* phenotype (figure 6D), suggesting that the central F278 and E279 amino acids are important for PKS4 function and their mutation notably interfere with the molecular mechanism of PKS4 leading to phototropism. Later, we wondered which amino acids, among the ones that had been replaced in the PKS4 D1* or D2* variants, are key for PKS4 function, therefore, we generated PKS4 D3* and D4* mutants where the selected amino acids were replaced with Alanine and transformed *pks4* as done for the rest of the variants in this study. Although stable transgenic single insertion lines expressing PKS4 D3* or D4* were not available at the moment, we could preliminarily test how mutating the single amino acids F278 (D3*) or E279 (D4*) affected phototropism in populations integrated by more than 50 seedlings with independent transgene insertion events. Although these results have not been repeated yet, we observed that the expression of the D3* and D4* variants could not complement the phototropic phenotype of *pks4* and notably enhanced the phenotype (Figure 6E).

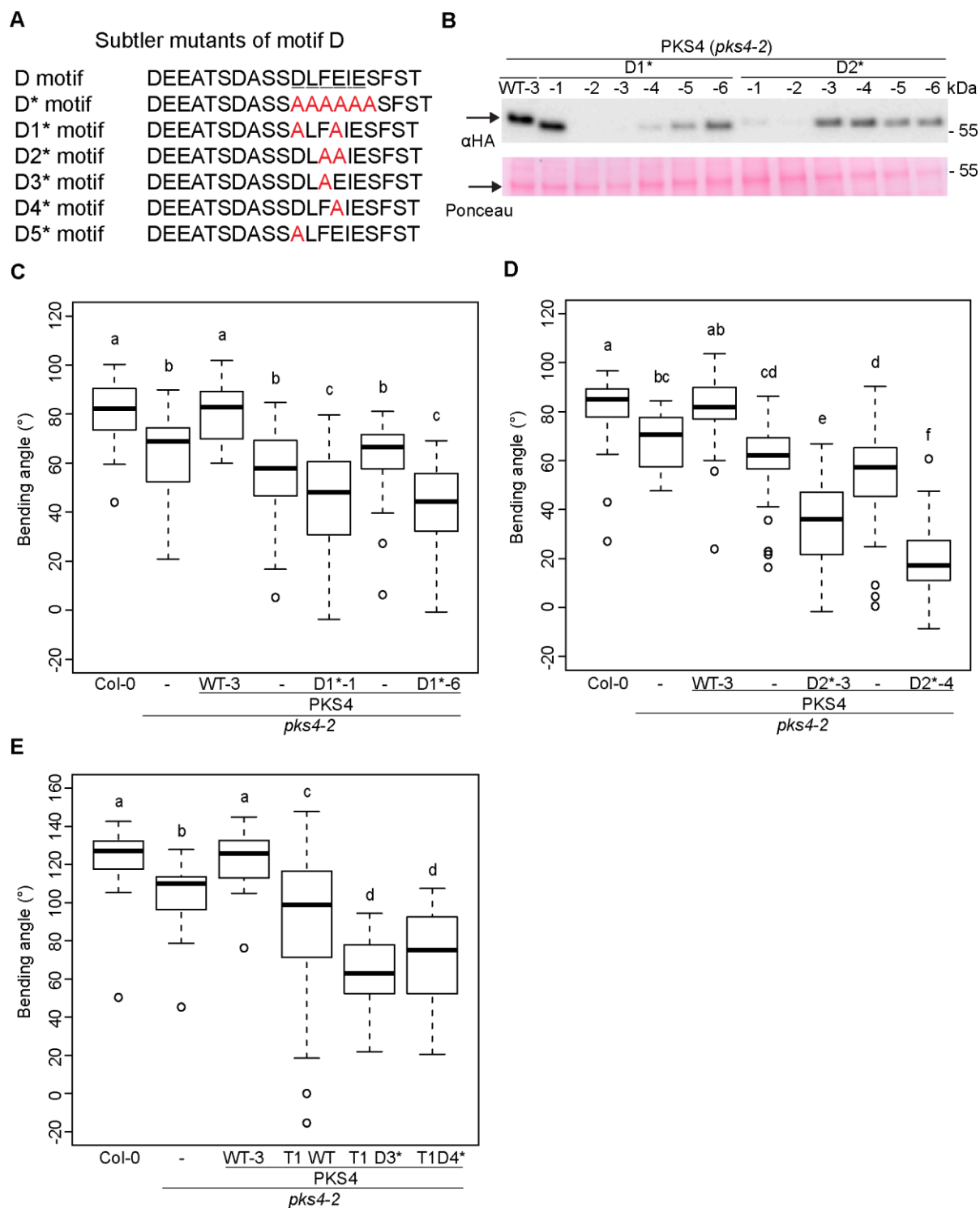**Figure 6**. Subtler mutations in PKS4 motif D led to a strong phototropic defect. (**A**) Illustration of the primary structure of the PKS4 protein motif D and the designed mutant variants D*, D1*, D2*, D3*, D4*, and D5*. Underlined letters indicate the selected amino acids to be replaced with the ones in red color. (**B**) Western blot probed with anti-HA antibody from *pks4-2* PKS4 WT-3, *pks4-2*
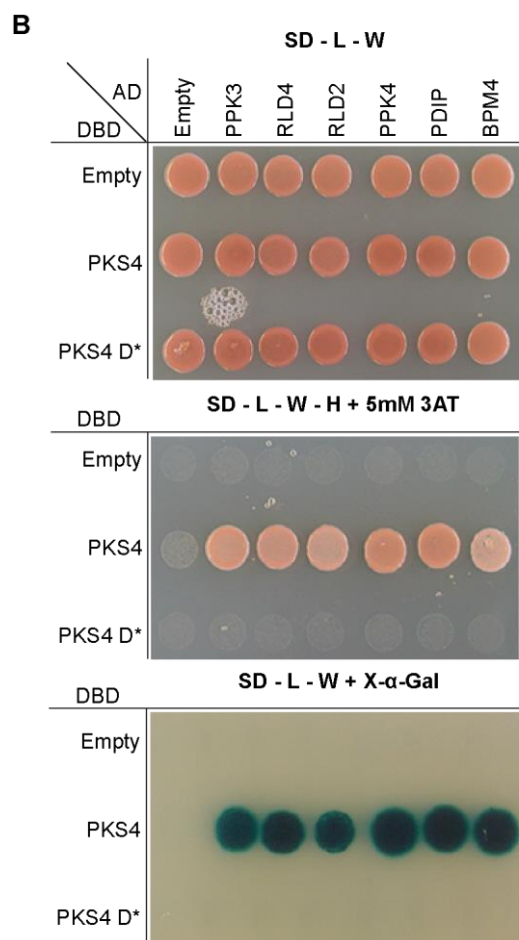
PKS4 D1*-1, D1*-2, D1*-3, D1*-4, D1*-5, D1*-6, D2*-1, D2*-2, D2*-3, D2*-4, D2*-5, and D2*-6 samples of 3- day- old dark-grown seedlings. All the D1* and D2* samples come from 3:1 ratio segregating independent transgenic lines that carried the transgene. The same membrane was stained with Ponceau as a loading control. (**C**) Phototropic curvature of 3-day-old dark-grown Col- 0, *pks4-2*, *pks4-2* PKS4 WT-3, and *pks4-2* PKS4 D1* (D1*-1 and D1*-6) lines treated with BL coming from one side. Segregating lines D1*-1 and D1*-6 were split into a population carrying at least one copy of the transgene (D1*-) and a population without carrying the transgene (-), which were separated from the ones carrying the transgene by screening the seeds coat fluorescence marker before the experiment (**D**) Phototropic curvature of 3-day-old dark-grown Col-0, *pks4-2*, *pks4-2* PKS4 WT-3, and *pks4-2* PKS4 D2* (D2*-3 and D2*-4) lines treated with BL coming from one side. Segregating lines D2*-3 and D2*-4 were split into a population carrying at least one copy of the transgene (D2*-) and a population without carrying the transgene (-) the same way as for D1* lines. In (**C**) and (**D**), seedlings were exposed to 0.1 µmol m^{-2} s^{-1} BL for 24h before measurement of growth reorientation. In each experiment, n= 40 – 60, means with the same letter are not significantly different (p > 0.01, two-way ANOVA with Tukey's HSD test). (**E**) Phototropic curvature of 3-day-old dark-grown Col-0, *pks4-2*, *pks4-2* PKS4 WT-3, *pks4-2* T1 PKS4 WT, *pks4-2* T1 PKS4 D3*, and *pks4-2* T1 PKS4 D4* lines treated with BL coming from one side. Seedlings were exposed to 0.1 µmol m^{-2} s^{-1} BL for 24h before measurement of growth reorientation. The population of T1 results from independent events of transgene insertion. n= 40 – 60, means with the same letter are not significantly different (p > 0.05, two-way ANOVA with Tukey's HSD test).

Collectively, our data suggest that the charged and hydrophobic conserved amino acids D276, F278, and E279 in motif D are essential for PKS4 biological activity.

Identification of PKS motif D interactors

Our study of the PKS4 motifs revealed the striking importance of motif D for PKS4 function and excluded the possibility of this motif having an apparent role in PKS4 PM association. To elucidate the molecular mechanisms underlying motif D function, we looked for PKS4 motif D interactors in the Yeast two-hybrid (Y2H) system. We first designed a PKS4 WT bait from amino acids 250 to

308 that included the D motif (Figure 7A). With the help of Hybrigenics services, we made a Y2H screening against an *A. thaliana* light-grown seedlings cDNA library with this PKS4 bait that was tested for 146 million interactions. Among those, we selected six candidates to interact with our bait which we further tested in the lab. We generated an additional PKS4 D* bait of the same length as the PKS4 WT where the DLFEIE amino acids were replaced with AAAAAA (Figure 7A), and we tested the six candidates that we found with our PKS4 WT and D* baits in the Y2H system to address the importance of motif D for those interactions. We found that our PKS4 WT bait interacted with the 6 candidates: PHOTOREGULATORY PROTEIN KINASES 3 and 4 (PPK3 and PPK4), RCC1-like domain proteins 2 and 4 (RLD2 and RLD4), BTB/POZ AND MATH DOMAIN 4 (BPM4), and a candidate belonging to the BTB/POZ protein domain superfamily that has an Ankyrin repeats domain and that we described as PKS MOTIF D INTERACTING PROTEIN (PDIP) (Figure 7B) (Gingerich et al., 2007, Liu et al., 2017, Furutani et al., 2020). On the contrary, we observed that our PKS4 D* bait did not interact with any of the candidates in the HIS assay nor the β-galactosidase system (Figure 7B), suggesting that the PKS4 motif D is required for the interaction with the six candidates.

Figure 7. Identification of interactors of PKS4 motif D. (**A**) Illustration of the PKS4 bait that was used for a Y2H screening (PKS4 amino acid from 250 to 308) and the PKS4 D* bait. In red are the amino acids that were replaced with the underlined ones from the WT protein sequence. (**B**) Interaction between the identified candidates PPK3, PPK4, RLD2, RLD4, PDIP, and BPM4 and the WT and D* forms of PKS4 in the Y2H system.

The functional complementation analysis of *pks4* used in this study revealed the importance of the amino acids D276, F278, and E279 in motif D for the function of PKS4 in phototropism (Figures 6C, 6D, and 6E). We then wondered about their relevance to mediate the interaction with the different candidates we found. To address this question, we designed PKS4 D1*, D2*, D3*, D4*,

and D5* baits of the same length as WT but including the described amino acids replaced with Alanine (Figure 8A). We tested the designed baits with the different candidates and found that while PKS4 D1* could interact with only PPK4, PKS4 D2* did not interact with any (Figure 8B), suggesting that the negatively charged D276 and E279 amino acids are important for the interaction with all the candidates except PPK4 and that the central part of the conserved DLFEIE represented by F278 and E279 is essential for all the interactions. The analysis of the single amino acid substitutions revealed that PKS4 D3* prevented the interaction with all the candidates except with BPM4, PKS4 D4* prevented the interaction with all the candidates except with PPK4, and PKS4 D5* interacted only with PPK3, PPK4, and RLD2 (Figure 8B). These data suggested that the F278 is required for the interaction with all the candidates except BPM4, that the E279 is required for the interaction with all the candidates except PPK4, and that D276 is required for the interaction with RLD4, PDIP, and BPM4. We randomly selected the cotransformants with PPK3 and BPM4 to test the expression of the WT and all the mutant baits and we observed that all the cotransformants comparably expressed the bait (Figure 8C), suggesting that the lack of interaction of the D* and D2* is not due to a lack of expression of the bait.
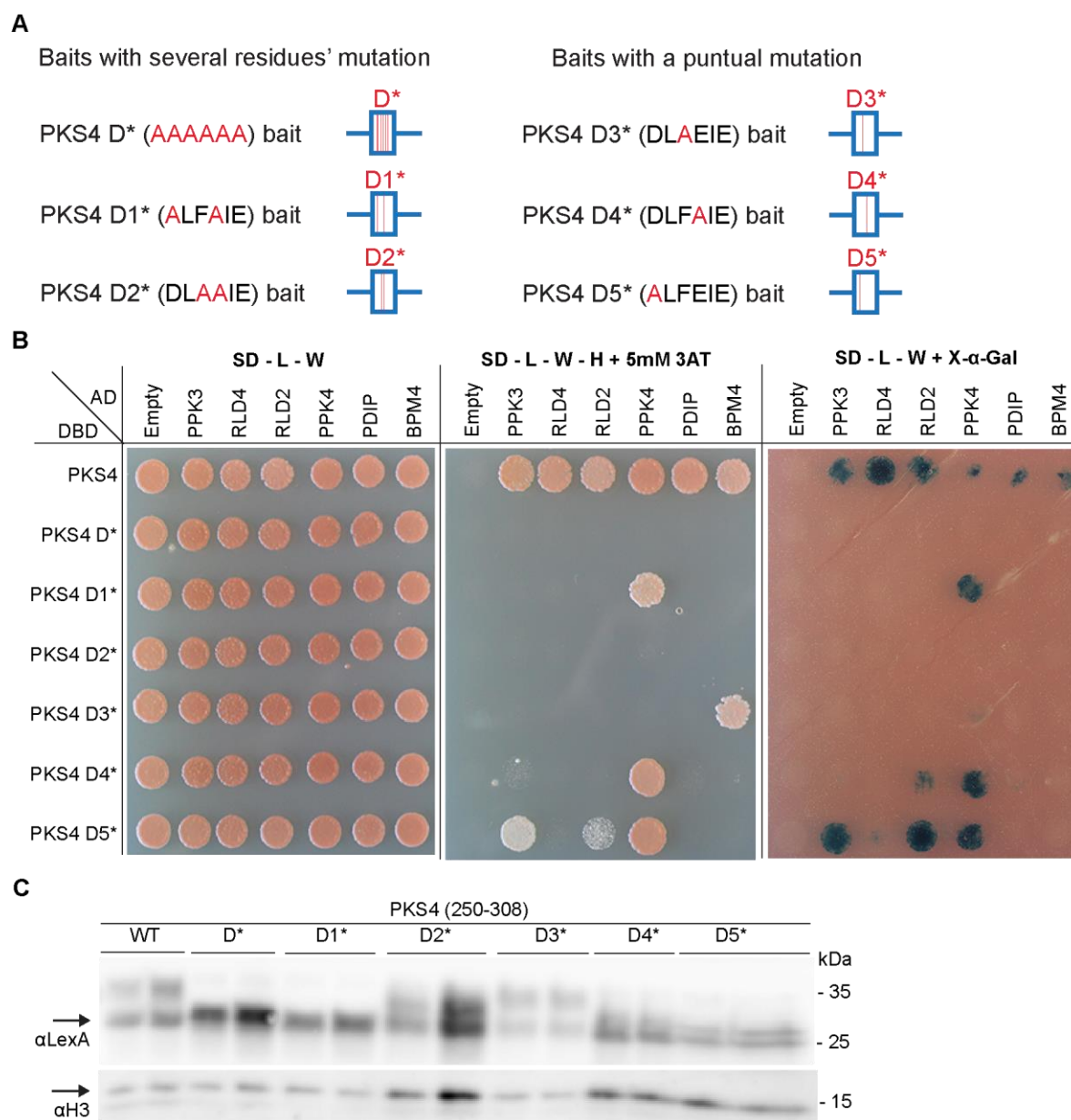
Figure 8. Interaction between the PKS4 motif D interactors and subtler PKS4 motif D mutant forms. (**A**) Illustration of the PKS4 baits D*, D1*, and D2* comprising several amino acids mutated (left) and the PKS4 baits D3*, D4*, and D5* comprising a single amino acid mutated (right). In black are the WT amino acids and in red are the amino acids that they were replaced with. (**B**) Interaction between PPK3, PPK4, RLD2, RLD4, PDIP, and BPM4 and the PKS4 WT, D*, D1*, D2*, D3*, D4*, and D5* mutant forms in the Y2H system. (**C**) Western blot probed with an anti- LexA antibody from samples of yeast culture cotransformed with the PKS4 WT, D*, D1*, D2*, D3*, D4*, and D5* baits, and the PPK3 and BPM4 preys. The same membrane was probed with an anti-H3 antibody as a loading control.

153

Given that we found that the DLFEIE sequence in motif D is conserved in all the Arabidopsis PKS protein family members and that it is required for the biological function of PKS4 and the interaction with all the found candidates, we wondered about the capability of the other Arabidopsis PKS protein family members to interact with the PKS4 interactors. To address that, we generated a PKS1, a PKS2, and a PKS3 bait including an equivalent protein sequence to the one of the PKS4 bait, and tested them for interaction with the PKS4 interactors. We found that while RLD2 and RLD4 interacted with all the PKS members, PPK3 and PPK4 did not interact with any other than PKS4 (Figure 9A). Additionally, BPM4 interacted with PKS2 in addition to PKS4, and PDIP had the capability of interacting with PKS1 in addition to PKS4 (Figure 9A). We tested the expression levels of the PKS4 WT, D*, PKS1, PKS2, and PKS3 baits in the cotransformants with PPK3 and RLD4 preys and they were comparable (Figure 9B).
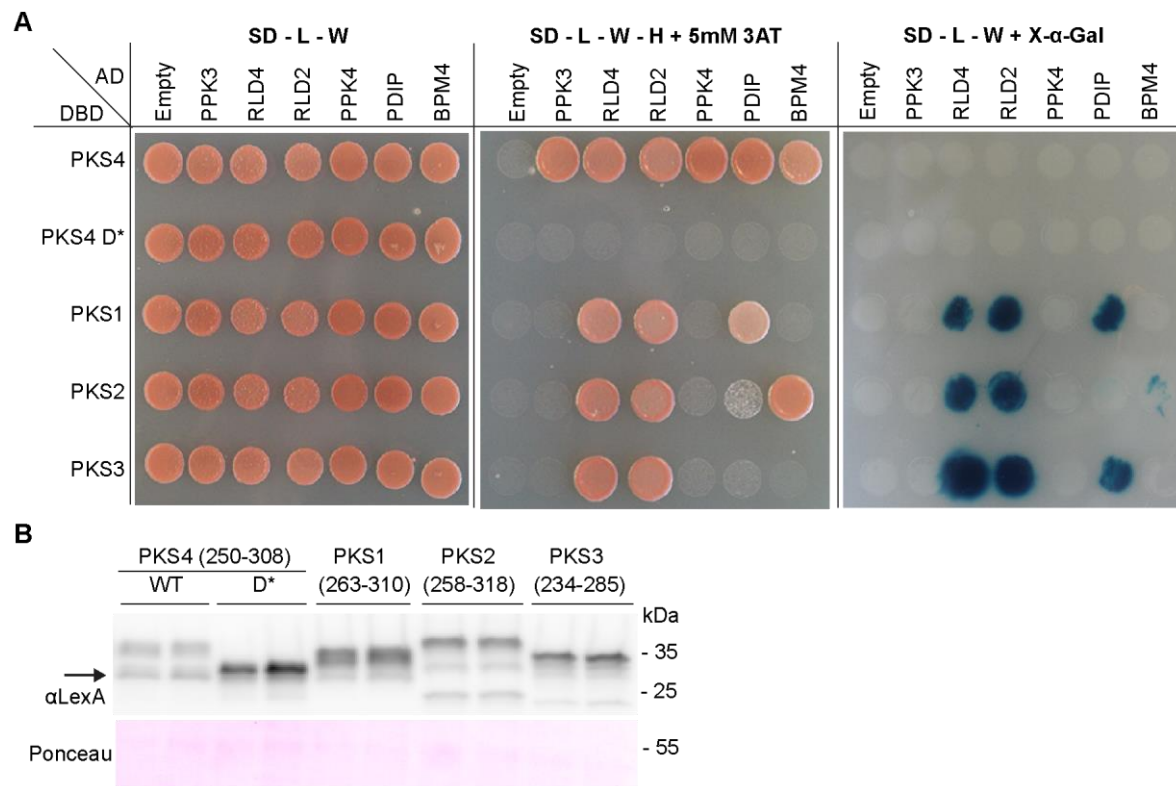
Figure 9. Interaction between the PKS4 motif D interactors and the PKS protein family members. (**A**) Interaction between PPK3, PPK4, RLD2, RLD4, PDIP, and BPM4 and the PKS1, PKS2, and PKS3 including motif D forms in the Y2H system. PKS1 (from amino acid 263 to 310), PKS2 (from amino acid 258 to 318), and PKS3 (from amino acid 234 to 285) baits comprise an equivalent portion of protein sequence to the one of the PKS4 bait. (**B**) Western blot probed with anti-LexA antibody from samples of yeast culture cotransformed with the PKS members' baits and the PPK3 and RLD4 preys. The same membrane was stained with Ponceau as a loading control.

BPM4 interacts with PKS through the MATH domain and has a role in phototropism

In this study, we found that the negatively charged amino acids D276 and E279 are strictly required for the interaction of PKS4 with BPM4 through the motif D (Figure 8), and we further observed that in addition to PKS4, BPM4 can interact with PKS2 (Figure 9). BPM proteins are constituted by an N-terminal Meprin and TRAF homology (MATH) domain, a Broad Complex/Poz virus and Zinc finger (BTB/POZ) domain, and a C-terminal domain (Weber et al., 2005). Several studies suggested BPM as substrate adaptors of Cullin-RING E3 Ubiquitin Ligases (CRLs) interacting through the BTB/POZ domain with the Cullin of the CRL and with the substrate through their MATH domain to regulate substrate ubiquitination and degradation (Weber and Hellmann, 2009, Zhuang et al., 2009, Julian et al., 2019, Chico et al., 2020). To find out the part of BPM4 protein that interacts with PKS motif D, we generated three different preys expressing: the BPM4 N-terminal part that includes the MATH domain (BPM4 MATH prey), the middle part of the protein that includes the BTB/POZ domain (BPM4 BTB/POZ prey), and the C-terminal part of BPM4 (BPM4 C-terminal prey) (Figure 10A). We tested them for interaction with the PKS4 and PKS2 baits and we found that in addition to the BPM4 full length, the N-terminal prey containing the MATH domain also interacted with the PKS4 and PKS2 baits, however, the middle prey containing the BTB/POZ domain and the C-terminal prey did not interact (Figure 10B). These data suggested that PKS4 and PKS2 interact with BPM4 through
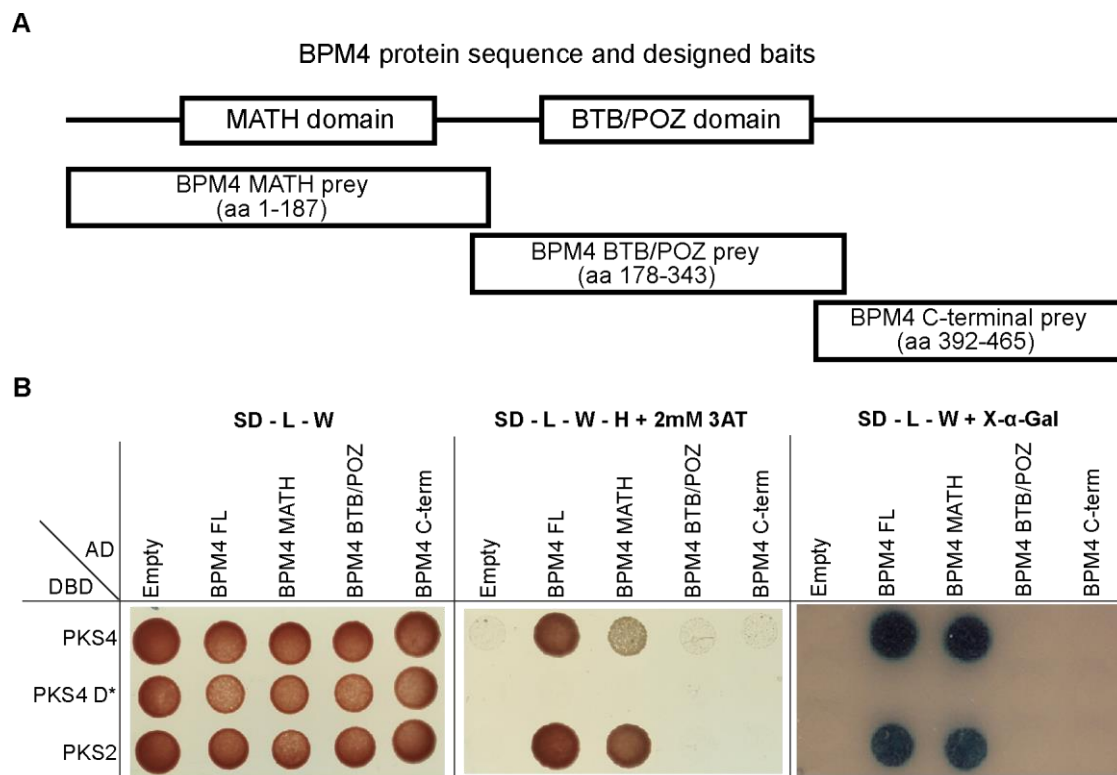
its MATH domain.

Figure 10. Interaction between PKS and BPM4 protein regions. (**A**) Schematic representation of the *A. thaliana* BPM4 protein sequence. The square boxes represent the MATH and BTB/POZ protein domains. The length of the boxes and the spaces between them are proportional to the length of the protein domains and the spacing among them. On the bottom, an illustration of the designed BPM4 preys including the MATH domain (from amino acid 1 to 187), the BTB/POZ domain (from amino acid 178 to 343), or the C-terminal part (from amino acid 392 to 465) of the BPM4 protein sequence. (**B**) Interaction between PKS4 and PKS2 including motif D forms and the BPM4 full length, MATH domain, BTB/POZ domain, and C-terminal forms in the Y2H system.

We then wondered whether the other BPM protein family members could also interact with PKS4 and PKS2. To address that question, we generated BPM1, BPM2, BPM3, BPM5, and BPM6 N-terminal preys including an equivalent protein sequence to the one of the BPM4 that included the MATH domain, and tested them for the interaction with all the PKS protein family members. We

found that, in addition to interacting with the BPM4 MATH prey, PKS2 interacted with the BPM2 MATH prey and PKS4 with the BPM2 MATH and BPM6 MATH preys (Figure 11A). The xgal assay additionally suggested the interaction of PKS4 with BPM1 and BPM5 preys (Figure 11A). These data indicated that different PKSs can potentially interact with different BPMs through the MATH domain in yeast.
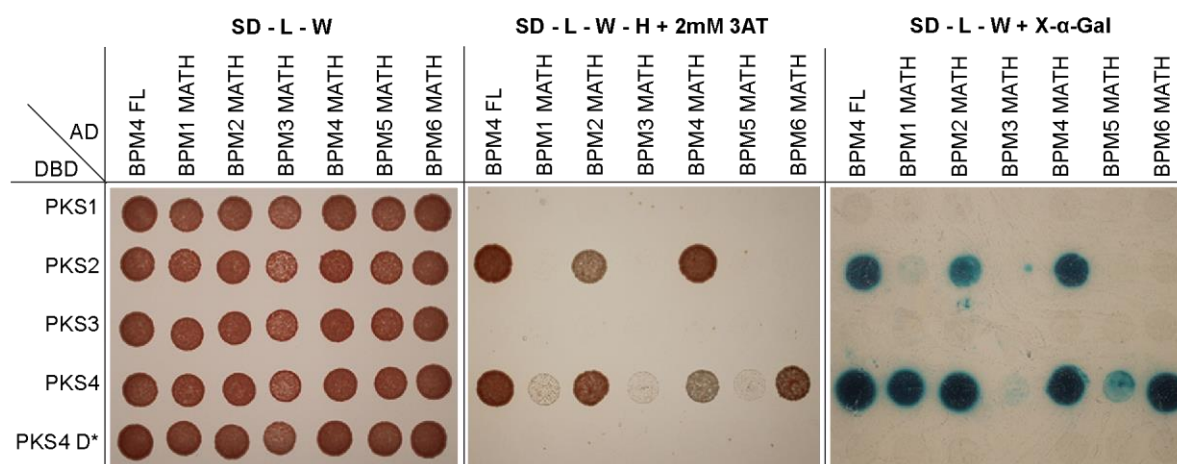
Figure 11. Interaction between the PKS protein family members and the N-terminal region including the MATH domain of the BPM protein family members. (**A**) Interaction between PKS1, PKS2, PKS3, PKS4, and PKS4 D* and BPM1 (from amino acid 1 to 174), BPM2 (from amino acid 1 to 173), BPM3 (from amino acid 1 to 165), BPM4 (from amino acid 1 to 187), BPM5 (from amino acid 1 to 169), and BPM6 (from amino acid 1 to 176) MATH domain forms in the Y2H system.

Given that our studies demonstrate that the PKS-BPM interaction occurs through the MATH domain, we hypothesized that PKS4 could be a potential substrate of BPM4 bringing it to the CLR[BPM] complex for poly-ubiquitination and proteasomal degradation. To test our first hypothesis, we generated transgenic Arabidopsis plants expressing 3xHA-BPM4 and BPM4-3xHA from the strong constitutive *35S* promoter and we determined the PKS4 protein abundance by western blot (Figure 12A). We found that different lines of etiolated seedlings expressing 3xHA-BPM4 and BPM4-3xHA at

different levels showed similar PKS4 protein abundance compared to Col-0 (Figure 12A), suggesting that the overexpression of BPM4 does not enhance PKS4 degradation in etiolated seedlings. Additionally, given that BPM interaction with PKS seems to depend on the motif D (Figure 7), we wondered whether the PKS4 D* variant, which is not expected to interact with BPM, shows higher PKS4 protein abundance compared to PKS4 WT in response to light treatment (Demarsy et al., 2012). To test this hypothesis, we tested the PKS4 protein levels in the dark, 2, and 4 hours after continuous white light treatment in the *pks4* lines expressing PKS4 WT and PKS4 D*, and we found that the pattern of PKS4 protein levels was not altered in the PKS4 D* lines in comparison with the PKS4 WT lines (Figure 12B), suggesting that the observed decrease of PKS4 protein levels in response to light does not occur because of the interaction with BPM. Altogether, these data suggest that the regulation of PKS4 protein abundance in response to light is not controlled by BPM.
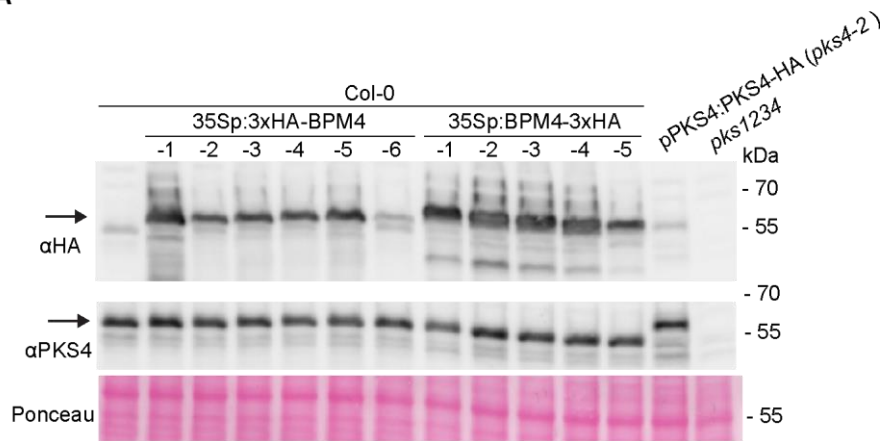
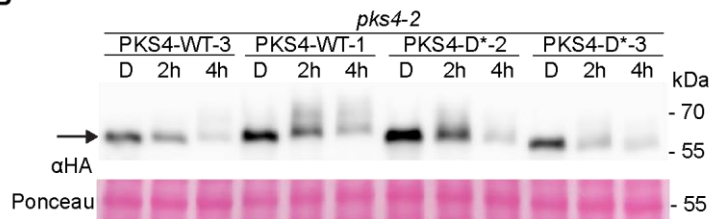**Figure 12**. PKS4 protein abundance does not depend on BPM4. (**A**) Western blot probed with anti-HA antibody (top) and anti-PKS4 antibody (bottom) from Col-0, Col-0 35Spro::3xHA-BPM4 (-1,

-2, -3, -4, -5, -6), Col- 35Spro::BPM4-3xHA (-1, -2, -3, -4, -5), *pks4-2* PKS4pro::PKS4-3xHA, and *pks1234* samples of 3- day-old dark-grown seedlings. The same membrane was stained with Ponceau as a loading control. (**B**) Western blot probed with anti-HA antibody from *pks4-2* PKS4 WT-3, *pks4-2* PKS4 WT-1, *pks4-2* PKS4 D*-2, and *pks4-2* PKS4 D*-3 samples of 3- day- old dark- grown seedlings treated with continuous white light during 0, 2, and 4 h. The same membrane was stained with Ponceau as a loading control.

The fact that BPMs interact with PKS4 and PKS2, the PKS members "specialized" in promoting phototropism in response to low and high BL (HBL) respectively (Kami et al., 2014a), led us to analyze the importance of BPM in phototropism. In this study, we analyzed the kinetics of hypocotyl bending in response to low BL (LBL) in *bpm4* and *bpm34* mutant alleles. Our data showed that the hypocotyl orientation with respect to the vertical in the darkness in the *bpm* mutants was comparable to Col-0 and *pks4* (Figure 13A). However, *bpm4* and *bpm34* were impaired in phototropism in comparison to Col-0 after 4 h of BL treatment, showing *bpm34* a phenotype comparable to *pks4* and *bpm4* an intermediate phenotype between Col-0 and *pks4* (Figures 13B). After 6h of BL treatment, the phenotype of the *bpm4* and *bpm34* lines remained impaired, showing an intermediate phenotype between Col-0 and *pks4* (Figure 13C). However, *bpm4* and *bpm34* behaved as Col-0 after 24h of BL treatment while *pks4* was impaired as previously shown (Figure 13E). These data suggested that BPMs have a role at least in the early phases of phototropism while they are dispensable to promote the response after 24h.
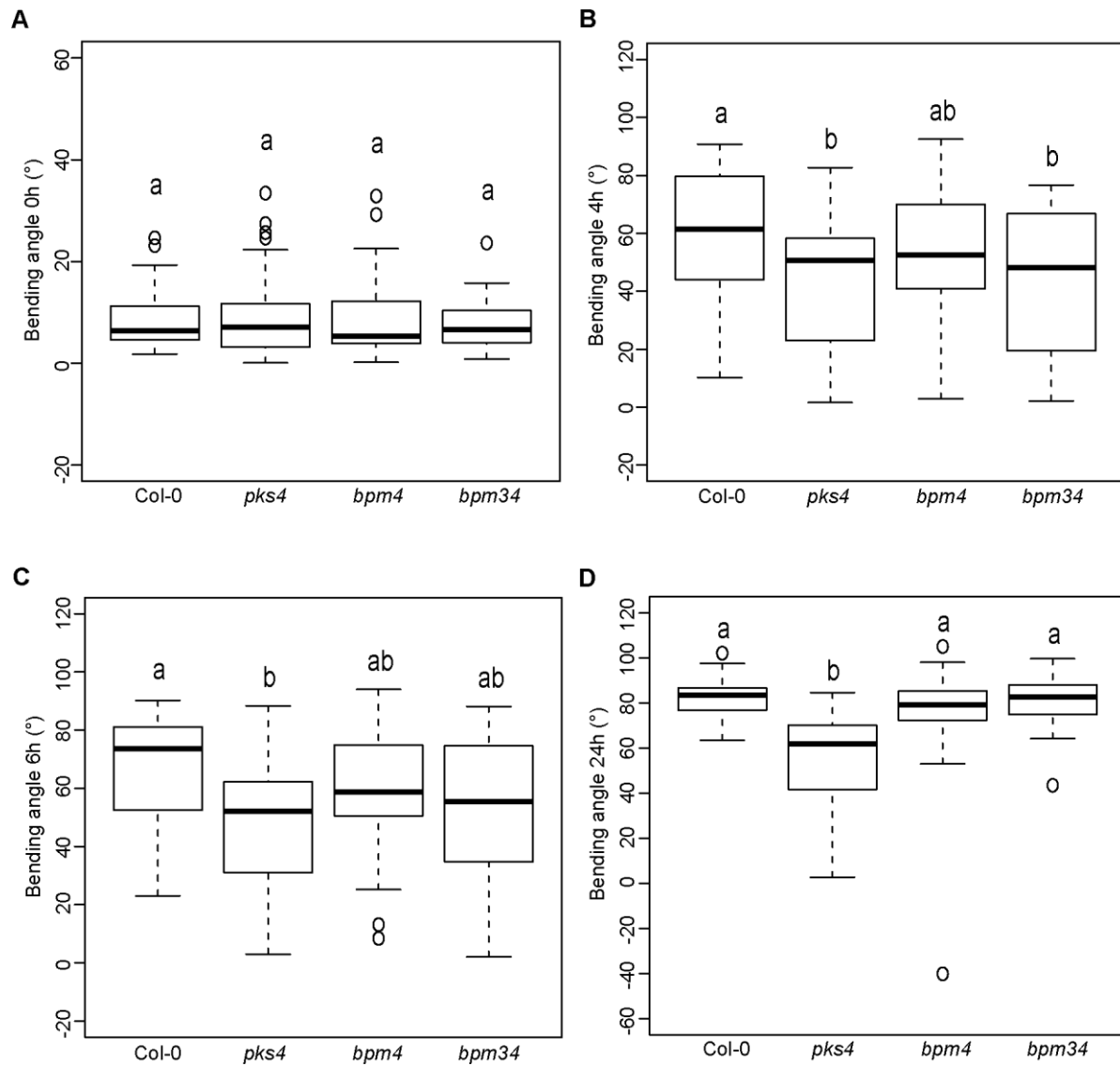
Figure 13. BPM is involved in hypocotyl phototropism. (**A**) Hypocotyl growth orientation of 3- day-old Col-0, *pks4-2*, *bpm4*, and *bpm34* dark-grown seedlings. 0° represents vertical growth and an average of 90° represents a random distribution. (**B**) Phototropic curvature of 3-day-old dark- grown Col-0, *pks4*, *bpm4*, and *bpm34* lines treated with BL coming from one side for 4 hours, (**C**) 6 hours, and (**D**) 24 hours. In (**B**), (**C**), and (**D**) seedlings were exposed to 0.1 μmol m^{-2} s^{-1} BL for 24h before to measurement of growth reorientation. For each experiment, n= 25 – 45, means with the same letter are not significantly different (p > 0.01, two-way ANOVA with Tukey's HSD test).

Our data suggested that PKS4 and BPM4 interact in yeast (Figure 7B), therefore we wondered

whether they could associate with each other *in vivo* in the plant. To test that, we generated transgenic Arabidopsis plants expressing EYFP-BPM4 and BPM4-EYFP driven by the strong constitutive *35S* promoter and we observed the subcellular localization in etiolated seedlings using confocal microscopy. We observed that EYFP-BPM4 was mainly localized in the cytosol in roots, hypocotyls, and hook epidermal cells and also in the nucleus in roots and hook tissues (Figure 14A).
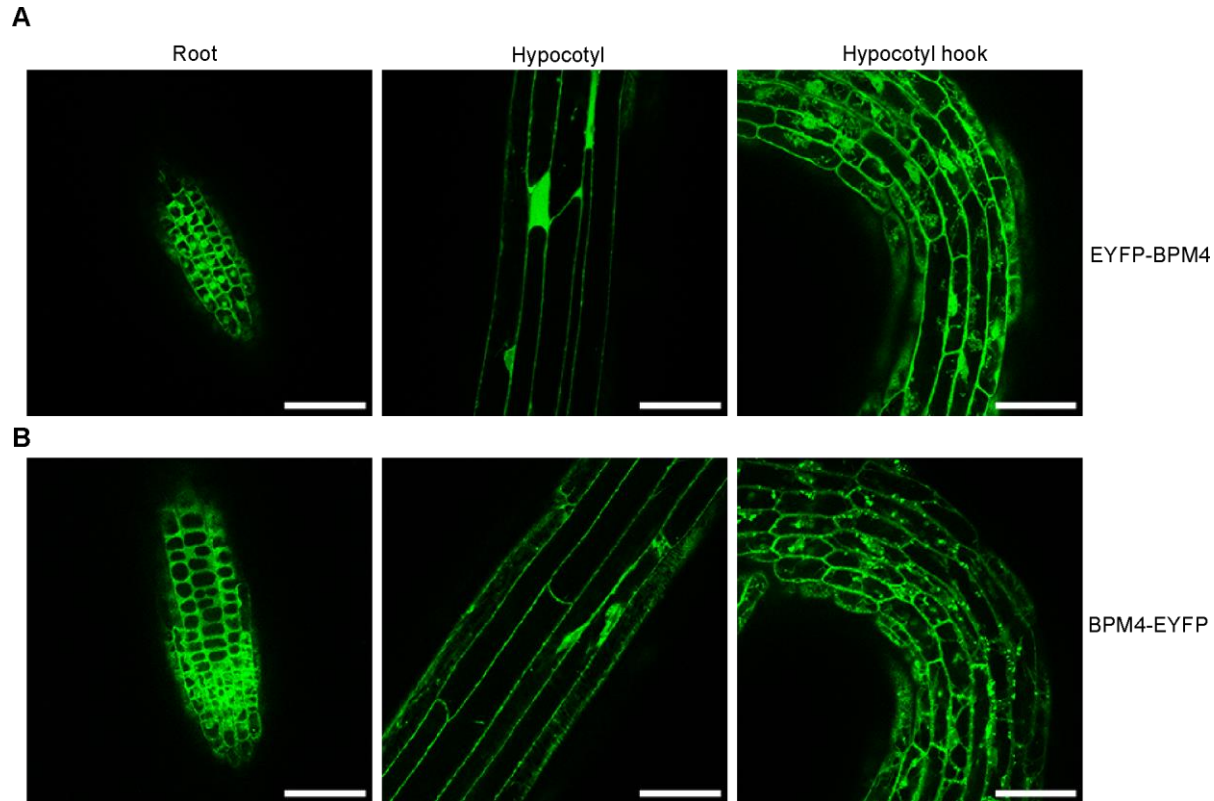
Figure 14. BPM4 localizes at the cytosol and nucleus in dark-grown seedlings. (**A**) Confocal microscopy images of roots, hypocotyls, and hooks from 3-day-old transgenic dark-grown seedlings expressing EYFP-BPM4 (top) and BPM4-EYFP (bottom) from the 35S promoter. Scale bar: 50 µm.

Similarly, we observed that BPM4-EYFP was localized mainly in the cytosol of epidermal cells in those tissues (Figure 14B) (Weber and Hellmann, 2009). Collectively, our data suggested that BPM4 could potentially interact with PKS4 motif D through the MATH domain to promote early

phototropism.

DISCUSSION

PKS motif D is essential for biological activity

PKS proteins share 6 motifs (A to F from the N- to the C-terminus) that appear in the same order in all the angiosperms. While s-acylation of the conserved Cys amino acids of Motif C is required for PKS1 and PKS4 association with the PM and biological function, the role of its related motif F remains to be determined (Vazquez et al., 2022). To determine the functional importance of the rest of PKS motifs, we generated the PKS4 A*, B*, D*, and E* variants in which the highly conserved amino acids of each motif were replaced with Alanine. Here, we found that PKS4 D* variant, in which the highly conserved amino acids DLFEIE (D276, L277, F278, E279, I280, and E281) were replaced with Alanine, did not complement *pks4* in phototropism nor inhibition of gravitropism, showing that motif D is essential to trigger these responses (Figures 2E, 3C, and 4C). While the PKS4 C* variant failed to function and to associate with the PM, where PKS function with phot to mediate phototropism, we found that the PKS4 D* variant was localized at the cell periphery similar to PKS4 WT (Figure 5) (Lariguet et al., 2006, de Carbonnel et al., 2010, Preuten et al., 2015, Vazquez et al., 2022). This suggests that the mutation in motif D does not alter the subcellular localization of PKS4.

Additionally, we found that the PKS4 A*, B*, and E* variants complemented the hypocotyl phototropism phenotype of *pks4* mutants after 24h of BL treatment, suggesting that motifs A, B, and E are not essential for PKS4 function in phototropism (Figures 2B, 2C, and 2F and 3A, 3B, and 3D) (Kami et al., 2014a). Moreover, these variants complemented the *pks4* phenotype in the inhibition of gravitropism, showing that they are not essential to trigger this response either (Figures 4A, 4B, and 4D) (Schepens et al., 2008). However, a more careful analysis of the bending kinetics

from the start of the light treatment will be required to determine whether these motifs have a role in phototropism. Collectively, our functional studies indicate that among all the conserved PKS motifs, motifs C and D appeared to be essential for function, and motif C is additionally required for the association of PKS with the PM (Vazquez et al., 2022).

To determine a more specific importance of the conserved amino acids comprising motif D (DLFEIE), we generated the PKS4 D1* (D276A and E279A), D2* (F278A and E279A), D3* (F278A), D4* (E279A), and D5* (D276A) variants and tested their ability to complement the *pks4* phenotype in phototropism. We found that the expression of D1* and D2* in individuals from the second generation of transgenic lines aggravated the *pks4* phenotype, suggesting the importance of maintaining the motif D negative charge and the central Phenylalanine 278 for function (Figures 6C and 6D). Moreover, *pks4* mutants expressing the D3* and D4* variants aggravated the *pks4* phenotype (Figure 6E). This suggests that each of the amino acids comprising the middle part of the conserved DLFEIE sequence: F278 and E279, are required for PKS biological activity, additionally supporting the importance of the central Phenylalanine 278 and the charged Glutamic acid 279 for function.

PKS4 motif D interactors

We performed a Y2H screening against an *A. thaliana* light-grown seedlings cDNA library by using a short sequence of PKS4 protein (58 amino acids) that included motif D as bait. Among the 146 million tested interactions, we confirmed that PKS4 interacts with PPK3 and PPK4, RLD2 and RLD4, BPM4, and PDIP (Figure 7) (Gingerich et al., 2007, Wywial and Singh, 2010, Ni et al., 2017). The replacement of the conserved DLFEIE sequence with Alanine (PKS4 D* variant) prevented the interaction of PKS4 with all the candidates, showing the requirement of this sequence for all the tested interactions in yeast (Figure 7). We performed a more detailed analysis of these

interactions by generating equivalent baits including the PKS4 D1* (D276A and E279A), D2* (F278A and E279A), D3* (F278A), D4* (E279A), and D5* (D276A) modifications (Figure 8A). Among them, PKS4 D2* could not interact with any of the candidates, suggesting that the central F278 and E279 amino acids of the conserved DLFEIE sequence are important for all the tested interactions, in addition, to being required for biological activity (Figures 6D and 8B). The rest of the motif D mutant variants prevented the interaction with most of the candidates, only PKS4 D5* could interact with PPKs and RLD2, suggesting that among the single tested amino acids, the D276 might be overall the less important for all the interactions. Testing the interaction of PKS4 with these candidates in Arabidopsis will confirm whether these interactions happen *in vivo*.

<u>PKS4 interacts with BPM through the MATH domain</u>

We found that BPM4 does not interact with any of the PKS4 variants in which at least one negatively charged amino acid was mutated (D1*, D2*, D4*, and D5*), however, it could interact with the variant in which the F278 was mutated (D3*). This suggests that the interaction of PKS with BPM4 might be electrostatic and different from the rest of the motif D interactions, which require the Phenylalanine 278 (Figure 8). We further showed that PKS4 bait interacts with BPM4 through the N-terminal part of the protein containing the MATH domain (Figure 10). The next steps to follow up on the characterization of this interaction in yeast might involve searching conserved positively charged amino acids in the MATH domain and mutating them in the N-terminal prey to test the interaction.

The interaction through the MATH domain led us to wonder whether the PKS4 protein abundance might depend on BPM. This was based on a model proposing BPM as substrate adaptors of CRLs interacting with the substrate through their MATH domain to regulate substrate ubiquitination and degradation (Weber and Hellmann, 2009, Zhuang et al., 2009, Julian et al., 2019, Chico et al.,

2020). However, we found that the PKS4 protein levels remained unaltered in numerous transgenic 35S promoter-driven lines that expressed BPM4 at different levels in the dark (Figure 12A). Given that PKS4 protein abundance is regulated by light, we additionally checked the PKS4 levels in lines expressing PKS4 WT vs. the PKS4 D* variant, which is expected to not interact with BPM (Demarsy et al., 2012). We found no difference between PKS4 WT and D* in the dark and upon 2 and 4 hours of light treatment, suggesting that light-mediated PKS4 abundance does not depend on BPM interaction (Figure 12B). This would need to be confirmed by analyzing the light-controlled PKS4 levels in the *bpm* mutants. Although our data suggest that PKS4 protein abundance does not seem to be controlled by BPM, it does not exclude the possibility of PKS4 being a BPM substrate for ubiquitination, which could lead to changes in function, other posttranslational modifications, or subcellular localization, as it has been previously reported for phot1 in response to BL (Christie et al., 2018). In response to BL, overall PKS4, phot1, and NPH3 phosphorylation status changes, therefore, testing these modifications in the *bpm* mutants and BPM overexpressing lines would help to determine BPM importance in the early phot signaling events (Pedmale and Liscum, 2007, Sullivan et al., 2008, Demarsy et al., 2012, Schumacher et al., 2018).

To determine the importance of BPM4 in phototropism, we analyzed the hypocotyl bending kinetics of the *bpm4* and *bpm34* mutants in response to LBL. Both mutants showed an intermediate phenotype between Col-0 and *pks4* after 4 and 6 hours of BL treatment, however, they behaved as Col-0 after 24h (Figure 13). This suggests a mild role of BPM4 in the early stages of phototropins (phot) signaling. However, given that PKS4 can also interact with BPM2 and BPM6 in yeast, we should not exclude a possible role of other BPM proteins in the process (Figure 11). To test this, we are currently obtaining higher-order mutants, particularly those with mutations in *BPM4* and *BPM2*, whose expression levels are significantly higher than those of *BPM6* in the hypocotyl (Sun et al., 2016). Moreover, we plan testing higher-order *bpm* mutants in response to HBL given that BPM

can also interact with PKS2, which promotes phototropism in HBL (Figure 11) (Kami et al., 2014a).

As previously reported, we found BPM4 localized mainly at the cytosol and nucleus, suggesting that, although it is not mainly associated with the PM as PKS and phot1, BPM4 might potentially interact with PKS4 motif D to promote phototropism (Figure 14) (Lariguet et al., 2006, de Carbonnel et al., 2010, Demarsy et al., 2012, Preuten et al., 2015, Vazquez et al., 2022, Weber and Hellmann, 2009, Morimoto et al., 2017). However, given that BPM also interacts with PKS2, which is also localized in the cytosol and the nucleus, we should not exclude the possibility of BPM functioning with PKS2 in the nucleus, where BPM have been previously pointed out to work in modulating transcriptional regulation (Holland et al., 2009, Lechner et al., 2011, Chico et al., 2020).

METHODS

<u>Plant material</u>

All plants utilized in this study are in the *A. thaliana* Columbia-0 ecotype. The *pks4-2*, *phyB-9, bpm4,* and *bpm34* alleles were utilized in this study (Reed et al., 1993, Schepens et al., 2008, Chico et al., 2020). PKS4p:PKS4-3XHA (pPS9) in *pks4-2* was previously described (Schumacher et al., 2018). For the generation of the PKS4p::PKS4 A*-3xHA lines (pAL30), a 523 bp DNA fragment containing the PKS4 motif A sequence ELSIFEARSYF mutated to ALSIAEARSAA was ordered from Eurofins® and digested with the restriction enzymes NruI and EcoRV and replaced in the pPS9 construct previously digested with the same restriction enzymes to replace the wild type with the mutant sequence. For the generation of the PKS4p::PKS4 B*-3xHA lines (pAL31), a 523 bp DNA fragment containing the PKS4 motif A sequence SEASWNSQTGL mutated to AAAAWAAQTGA was ordered from Eurofins® and digested with the restriction enzymes NruI and EcoRV and replaced in the pPS9 construct previously digested with the same restriction enzymes to replace the wild type with the mutant sequence. For the generation of the PKS4p::PKS4 D*-3xHA lines (pAL9), a 682 bp DNA fragment containing the PKS4 motif D sequence DLFEIE mutated to AAAAAA was ordered from Eurofins® and digested with the restriction enzymes EcoRV and BamHI and replaced in the pPS9 construct previously digested with the same restriction enzymes to replace the wild type with the mutant sequence. For the generation of the PKS4p::PKS4 E*-3xHA lines (pAL14), a 682 bp DNA fragment containing the PKS4 motif E sequence YEPSEASVTWS mutated to AAAAAAAVTAA was ordered from Eurofins® and digested with the restriction enzymes EcoRV and BamHI and replaced in the pPS9 construct previously digested with the same restriction enzymes to replace the wild type with the mutant sequence. For the generation of the PKS4p::PKS4 D1*-3xHA (pAL38), PKS4pro::PKS4 D2*-3xHA (pAL39),

PKS4p::PKS4 D3*-3xHA (pAL49), PKS4p::PKS4 D4*-3xHA (pAL50), and PKS4p::PKS4 D5*-3xHA (pAL51) lines, a 682 bp DNA fragment containing the PKS4 motif D sequence DLFEIE mutated to ALFAIE, DLAAIE, DLAEIE, DLFAIE, or ALFEIE, respectively, were ordered from Eurofins® and digested with the restriction enzymes EcoRV and BamHI and replaced in the pPS9 construct previously digested with the same restriction enzymes to replace the wild type with the mutant sequences. For the generation of the PKS4p::PKS4 D*-GFP (pAL44) lines, a DNA fragment including the DLFEIE sequence mutated to AAAAAA was digested from the pAL9 with the restriction enzymes NruI and ZraI and replaced in the pAL43 (Vazquez et al., 2022) previously digested with the same enzymes for that purpose. For the generation of the 35Sp::3xHA-BPM4 (pAD1) and 35Sp::BPM4-3xHA (pAD2) lines, the BPM4 CDS was cloned BamH-I into a binary vector designed to generate N-terminal 3xHA (pFP101-HA) (Bensmihen et al., 2004) and C-terminal 3xHA (inverted pCF398) (Schumacher et al., 2018) fusions using the In-fusion HD cloning kit Cat#639649. The BPM4 CDS was amplified from the pGAD424 gateway-BPM4 (provided by Pascal Genschik's lab) with the primers AD001 and AD002 and AD003 and AD004, respectively. For the generation of the 35Spro::EYFP-BPM4 (pAD3) and 35Spro::BPM4-EYFP (pAD4) lines, the BPM4 CDS was cloned BamH-I into a binary vector designed to generate N-terminal EYFP (pCF499) or C-terminal EYFP (pCF497) fusions using the In-fusion HD cloning kit. The BPM4 CDS was amplified from the pGAD424 gateway-BPM4 with the primers AD005 and AD006 and AD007 and AD008, respectively. The pCF499 and pCF497 come from pPZP312, a modified pPZP200 with a basta resistance to which we added a 35S promoter, EYFP, and rbcs terminator for either N- or C- terminal fusion (Hajdukiewicz et al., 1994). All constructs were sequence verified. Transgenic lines were obtained using *Agrobacterium tumefaciens*-mediated transformation. Several single insertion lines expressing each of them were characterized. The use of fluorescent seeds as a selection marker also allowed us to perform experiments with large numbers of independent

T1 lines.

<u>Yeast material</u>

The empty bait expression vector containing the LexA DNA binding domain and the tryptophan-auxotrophic marker *TRP1* (pB27), the empty prey expression vector containing the *GAL4* activation domain and the leucine-auxotrophic marker *LEU2* (pP6), and the PPK3 (pB27_B-24), RLD4 (pB27_B-35), RLD2 (pB27_B-46), PPK4 (pB27_B-75), PDIP (pB27_B-84), and BPM4 (pB27_B-98) prey expression vectors containing the *GAL4* activation domain and the leucine-auxotrophic marker *LEU2* were provided by Hybrigenics services. For the generation of the PKS4 WT (hgx5115v5_pB27), D* (pAL34), D1* (pAL41), D2* (pAL42), D3* (pAL52), D4* (pAL53), and D5* (pAL54) bait expression vectors, the PKS4 CDS was amplified from the ISA_Topo1_MT, pAL09, pAL38, pAL39, pAL49, pAL50, and pAL51, respectively, with the primers pair AL6 + AL7 and digested with the restriction enzyme Sfi-I and cloned into the pB27 previously digested with the same enzyme for that purpose. For the generation of the PKS1 (pAL57), PKS2 (pAL58), and PKS3 (pAL59) bait expression vectors, the CDS was amplified from the pCF575, pCF576, and pCF577 (chapter 2 of this work), respectively, with the primers pairs AL43 + AL44, AL45 + AL46, and AL47 + AL48, respectively, and digested with the restriction enzyme Sfi-I and cloned into the pB27 previously digested with the same restriction enzyme for that purpose. For the generation of the BPM4 MATH (pAD6), BPM4 BTB/POZ (pAD7), and BPM4 C-terminal (pAD8) prey expression vectors, the BPM4 CDS was amplified from the pGAD424 gateway-BPM4 with the primers pairs AD11 + AD12, AD13 + AD14, and AD15 + AD16, respectively, and cloned Sfi-I into pB27 using the In-fusion HD cloning kit. For the generation of the BPM1 MATH (pAD9), BPM2 MATH (pAD10), BPM3 MATH (pAD11), BPM5 MATH (pAD13), and BPM6 MATH (pAD14) prey expression vectors, the CDS was amplified from the Arabidopsis Biological Resource Center

(ABRC) U24902, U10745, U16043, U82612, and U87547, respectively, with the primers pairs AD17 + AD18, AD19 + AD20, AD21 + AD22, AD23 + AD24, and AD25 + AD26, respectively, and cloned Sfi-I into pB27 using the In-fusion HD cloning kit. The bait and prey vectors were co-transformed into the diploid yeast strain TATA provided by Hybrigenics services and whose phenotype is MATa/a, gal4::loxP-kanMX-loxP/Gal4D, ade2-101/ade2-101::loxP-kanMX-loxP, leu2-3,112/ leu2-3,-112, his3D200/ his3D200, trp1-901/trp1-901, LYS2/LYS2::(lexAop)4-HIS3, ura3-52::URA3(lexAop)8-lacZ/ ura3-52 URA3::UASGAL1-LacZ. Transformants were selected on solid yeast extract nitrogen base (YNB) synthetic Drop-out (SD) media containing appropriate auxotrophic supplements.

Plant growth conditions

For seed production, plants were grown on the soil at 22°C with 16h of white light (WL) per day. For physiological experiments, seeds were surface-sterilized in 70% ethanol and 0.05% Triton-X for 5 min and 100% ethanol for 5 min. Seeds were then sown on Petri dishes containing half- strength Murashige and Skoog medium, 0.8% agar. Plates were stored in the dark for 3 days at 4°C for stratification. For dark-grown seedlings experiments, germination was induced by 4-6 hours of white light (80 µmol m^{-2} s^{-1}) at 22°C, and plates were put on a vertically orientated position in the dark at 19°C or 22°C for 3 days before light treatment. For inhibition of gravitropism experiments, germination was induced by 1h of red light (50 µmol m^{-2} s^{-1}) at 22°C, and plates were put back in the dark at 22°C for 1 day before light treatment.

Light treatments

For etiolated conditions, seedlings were grown on vertically orientated plates for 3 days in darkness at 19°C or 22°C before the light treatment. For phototropism seedlings were irradiated with constant unilateral 0.1 µmol m^{-2} s^{-1} BL at 22°C for up to 24h, and for protein extraction, with 80 µmol m^{-2} s^{-1}

white light at 22°C during 0, 2, and 4 hours. For inhibition of gravitropism, seedlings were grown on vertically orientated plates for 1 day in darkness at 22°C before the light treatment. Seedlings were irradiated with constant 30 µmol m^{-2} s^{-1} RL at 22°C for 3 days.

Hypocotyl measurements and analysis

Plates were pictured using an infra-red CCD camera system at different timepoints. The curvature angles were calculated by subtracting the average angle of orientation of the upper region (85−95% of total length) of each hypocotyl to vertical after light treatment determined by a customized MATLAB script developed in the Fankhauser Lab. One-way ANOVA (aov) and Compute Tukey's Honest Significance Differences (HSD.test) [agricolae package] using the R software was performed. We considered p values <0.01 (0.05 in T1 lines) significant.

Fluorescence microscopy

Confocal microscopy images were taken with an Airy confocal microscope (Zeiss), model LSM 880. The samples PKS4p::PKS4-GFP and PKS4p::PKS4 D*-GFP were excited with an Argon laser (488nm) and detection was done between 495 and 518 nm. The samples 35Sp::GFP- BPM4 and 35Sp::BPM4-GFP were excited with the same laser and detection was done between 495 and 525 nm. In all cases a channel was set to detect chlorophyll and OLE1-RFP, exciting with the laser used for excitation of the fluorophore of interest, and detecting between 607 and 691 nm.

Yeast-Two-Hybrid experiments

Screening with PKS4 against a plant cDNA library was performed at Hybrigenics Services per their standard protocols. The screen parameters are as follow: (1) Nature: cDNA; (2) Reference Bait Fragment: *Arabidopsis thaliana* - PKS4 (aa250-308); hgx5115v5; (3) Prey Library: *Arabidopsis thaliana* seedlings_RP3; (4) Vectors: pB27 (N-LexA-bait-C fusion); (5) Processed Clones: 111 (pB27_B); Analyzed Interactions: 146 millions (pB27_B), and (6) histidine-antagonist 171

3-aminotriazole (3AT) concentration: 5.0 mM. Double transformants were selected as cells growing in solid SD media in the absence of L and W. Cells bearing interacting proteins were selected on media lacking L, W, and H, but containing 5mM of 3AT, and tested for β-galactosidase activity as described (Duttweiler, 1996).

<u>Western blot</u>

For plant material, total proteins (80µl 2× Laemmli buffer for 20mg fresh weight; 10µg per lane) were separated on 4-15% precast polyacrylamide gels and transferred onto nitrocellulose using the Trans-Blot Turbo RTA Transfer Kit. For yeast material, total proteins (80µl 2× Laemmli buffer; 0.5 OD600-units per lane) were separated and transferred following the same. Yeast lysis buffer: 50 mM Tris–HCl pH 7.5, 5 mM MgCl2, 150 mM NaCl, 1 mM DTT, 0.1% Triton X-100, 2 mM PMSF. Anti-HA-HRP monoclonal 3F10 was used at 1/4000 (12013819001, Roche), anti-LexA (Cat No PA1-4966) was used at 1/2500 dilutions, anti-PKS4 was used at 1/300 (Demarsy et al., 2012), and anti-DET3 was used at 1/20000 dilutions (Schumacher et al., 1999) in 1X PBS containing 0.1% Tween-20 and 5% non-fat milk. Chemiluminescence signals were generated using Immobilon Western HRP Substrate (Millipore). Signals were detected with a Fujifilm ImageQuant LAS 4000 mini CCD camera system and quantifications were performed with ImageQuant TL software (GE Healthcare).

<u>Accession Numbers</u>

The Arabidopsis Genome Initiative numbers for the genes mentioned in this study are as follows: AT2G02950 (PKS1), AT1G14280 (PKS2), AT1G18810 (PKS3), AT5G04190 (PKS4), AT3G03940 (PPK3), AT2G25760 (PPK4), AT5G12350 (RLD2), AT5G42140 (RLD4), AT2G04740 (PDIP), AT5G19000 (BPM1), AT3G06190 (BPM2), AT2G39760 (BPM3), AT3G03740 (BPM4), AT5G21010 (BPM5), and AT3G43700 (BPM6).

Supplemental table 1. Primers used in this study

Name	Sequence
AD1	5'- gcagatatctctagagcggatccaatgaaatctgtcattttcacagag -3'
AD2	5'- ctgcaggtcgacttggatcctcaatcttctagttctgccattg -3'
AD3	5'- gctgacaagctgactctagaggatccaaaaatgaaatctgtcattttcacag -3'
AD4	5'- gtatgggtagtcgacggatccatcttctagttctgccattgg -3'
AD5	5'- tggacgagctgtacaaggcggatccaatgaaatctgtcattttcacagag -3'
AD6	5'- tatctagagccctaggatcctcaatcttctagttctgccattg -3'
AD7	5'- gacgagctcggtacccggggatccaaaaatgaaatctgtcattttcacagag -3'
AD8	5'- caccattctagagcgggatccatcttctagttctgccattgg -3'
AD11	5'- ctagccatggccgcaggggccacgaagatgaaatctgtcattttcacagag -3'
AD12	5'- gctactcgaggggccccaggggccacgaactatttctgagaccacaactcc -3'
AD13	5'- ctagccatggccgcaggggccacgaagtgcaccgtgggagttg -3'
AD14	5'- gctactcgaggggccccaggggccacgaacgtaacggtcagcaagcg -3'
AD15	5'- ctagccatggccgcaggggccacgaagtcagtagattccgttgcaaatattttg -3'
AD16	5'- gctactcgaggggccccaggggccacgaacatcttctagttctgccattgg -3'
AD17	5'- ctagccatggccgcaggggccacgaagatgggcacaactagggtc -3'
AD18	5'- gctactcgaggggccccaggggccacgaaccgtaactgacttcaccacac -3'

AD19	5'- ctagccatggccgcaggggccacgaagatggacacaattagggtttcc -3'
AD20	5'- gctactcgagggcccccaggggccacgaactgtgcgtgacttcaccac -3'
AD21	5'- ctagccatggccgcaggggccacgaagatgagtaccgtcggagg -3'
AD22	5'- gctactcgaggggcccccaggggccacgaacgagtcgggctctaacaac -3'
AD23	5'- ctagccatggccgcaggggccacgaagatgtcagaatcagtgattcagg -3'
AD24	5'- gctactcgaggggcccccaggggccacgaactatttctgaaaccacaactccaac -3'
AD25	5'- ctagccatggccgcaggggccacgaagatgtcaaagctaatgaccagaac -3'
AD26	5'- ctactcgaggggcccccaggggccacgaaccatttctgaaacgacaactcc -3'
AL6	5'- tggaattcggggccggacgggcccccgattaaaccggttctgaatcct-3'
AL7	5'- aggtcgaggggcccccagtggcctcaaccgtactcagacacggtctcttc-3'
AL43	5'- tggaattcggggccggacgggcccccatggaaatcgagaacagaggag-3'
AL44	5'- aggtcgaggggcccccagtggcctcaacacgtaggtgaagctggatcact-3'
AL45	5'- tggaattcggggccggacgggcccccatgggaatactcgagctctgcg-3'
AL46	5'- aggtcgaggggcccccagtggcctcaaccatctggtgagtctggatcact-3'
AL47	5'- tggaattcggggccggacgggccacatgggacgcaataccaaaccaa-3'
AL48	5'- aggtcgaggggcccccagtggcctcagacactgctcgttatgttctcaat-3'

LITERATURE CITED

BENSMIHEN, S., TO, A., LAMBERT, G., KROJ, T., GIRAUDAT, J. & PARCY, F. 2004.
Analysis of an activated ABI5 allele using a new selection method for transgenic
Arabidopsis seeds. *FEBS letters,* 561**,** 127-131.

BOCCALANDRO, H. E., DE SIMONE, S. N., BERGMANN-HONSBERGER, A., SCHEPENS,
I., FANKHAUSER, C. & CASAL, J. J. 2008. PHYTOCHROME KINASE SUBSTRATE1
regulates root phototropism and gravitropism. *Plant Physiology,* 146**,** 108-15.

CHICO, J. M., LECHNER, E., FERNANDEZ-BARBERO, G., CANIBANO, E., GARCÍA-
CASADO, G., FRANCO-ZORRILLA, J. M., HAMMANN, P., ZAMARREÑO, A. M.,
GARCÍA-MINA, J. M. & RUBIO, V. 2020. CUL3BPM E3 ubiquitin ligases regulate
MYC2, MYC3, and MYC4 stability and JA responses. *Proceedings of the National
Academy of Sciences,* 117**,** 6205-6215.

CHRISTIE, J. M. 2007. Phototropin blue-light receptors. *Annu Rev Plant Biol,* 58**,** 21-45.

CHRISTIE, J. M., SUETSUGU, N., SULLIVAN, S. & WADA, M. 2018. Shining Light on the
Function of NPH3/RPT2-Like Proteins in Phototropin Signaling. *Plant Physiology,*
176**,** 1015-1024.

DE CARBONNEL, M., DAVIS, P., ROELFSEMA, M. R., INOUE, S., SCHEPENS, I.,
LARIGUET, P., GEISLER, M., SHIMAZAKI, K., HANGARTER, R. & FANKHAUSER,
C. 2010. The Arabidopsis PHYTOCHROME KINASE SUBSTRATE2 protein is a
phototropin signaling element that regulates leaf flattening and leaf positioning. *Plant
Physiology,* 152**,** 1391-405.

DEMARSY, E., SCHEPENS, I., OKAJIMA, K., HERSCH, M., BERGMANN, S., CHRISTIE, J.,
SHIMAZAKI, K., TOKUTOMI, S. & FANKHAUSER, C. 2012. Phytochrome Kinase

Substrate 4 is phosphorylated by the phototropin 1 photoreceptor. *The EMBO journal,* 31**,** 3457-3467.

DUTTWEILER, H. M. J. T. I. G. 1996. A highly sensitive and non-lethal beta-galactosidase plate assay for yeast. *Trends in Genetics,* 12**,** 340-341.

FURUTANI, M., HIRANO, Y., NISHIMURA, T., NAKAMURA, M., TANIGUCHI, M., SUZUKI, K., OSHIDA, R., KONDO, C., SUN, S. & KATO, K. 2020. Polar recruitment of RLD by LAZY1-like protein during gravity signaling in root branch angle control. *Nature Communications,* 11**,** 1-13.

GINGERICH, D. J., HANADA, K., SHIU, S.-H. & VIERSTRA, R. D. 2007. Large-scale, lineage-specific expansion of a bric-a-brac/tramtrack/broad complex ubiquitin-ligase gene family in rice. *The Plant Cell,* 19**,** 2329-2348.

GOYAL, A., SZARZYNSKA, B. & FANKHAUSER, C. 2013. Phototropism: at the crossroads of light-signaling pathways. *Trends in plant science,* 18**,** 393-401.

HAJDUKIEWICZ, P., SVAB, Z. & MALIGA, P. 1994. The small, versatile pPZP family of Agrobacterium binary vectors for plant transformation. *Plant molecular biology,* 25**,** 989-994.

HOLLAND, J. J., ROBERTS, D. & LISCUM, E. 2009. Understanding phototropism: from Darwin to today. *Journal of experimental botany,* 60**,** 1969-1978.

JULIAN, J., COEGO, A., LOZANO-JUSTE, J., LECHNER, E., WU, Q., ZHANG, X., MERILO, E., BELDA-PALAZON, B., PARK, S.-Y. & CUTLER, S. R. 2019. The MATH-BTB BPM3 and BPM5 subunits of Cullin3-RING E3 ubiquitin ligases target PP2CA and other clade A PP2Cs for degradation. *Proceedings of the National Academy of Sciences,* 116**,** 15725-15734.

KAMI, C., ALLENBACH, L., ZOURELIDOU, M., LJUNG, K., SCHÜTZ, F., ISONO, E.,

WATAHIKI, M. K., YAMAMOTO, K. T., SCHWECHHEIMER, C. & FANKHAUSER, C. 2014. Reduced phototropism in pks mutants may be due to altered auxin-regulated gene expression or reduced lateral auxin transport. *The Plant Journal,* 77**,** 393-403.

LARIGUET, P., BOCCALANDRO, H. E., ALONSO, J. M., ECKER, J. R., CHORY, J., CASAL, J. J. & FANKHAUSER, C. 2003. A growth regulatory loop that provides homeostasis to phytochrome a signaling. *The Plant Cell,* 15**,** 2966-2978.

LARIGUET, P., SCHEPENS, I., HODGSON, D., PEDMALE, U. V., TREVISAN, M., KAMI, C., DE CARBONNEL, M., ALONSO, J. M., ECKER, J. R. & LISCUM, E.2006. PHYTOCHROME KINASE SUBSTRATE 1 is a phototropin 1 binding protein required for phototropism. *Proceedings of the National Academy of Sciences,* 103**,** 10134-10139.

LECHNER, E., LEONHARDT, N., EISLER, H., PARMENTIER, Y., ALIOUA, M., JACQUET, H., LEUNG, J. & GENSCHIK, P. 2011. MATH/BTB CRL3 receptors target the homeodomain-leucine zipper ATHB6 to modulate abscisic acid signaling. *Developmental cell,* 21**,** 1116-1128.

LEGRIS, M. & BOCCACCINI, A. 2020. Stem phototropism toward blue and ultraviolet light. *Physiologia plantarum,* 169**,** 357-368.

LEGRIS, M., SZARZYNSKA-ERDEN, B. M., TREVISAN, M., ALLENBACH PETROLATI, L. & FANKHAUSER, C. 2021. Phototropin-mediated perception of light direction in leaves regulates blade flattening. *Plant physiology,* 187**,** 1235-1249.

LIU, L., TONG, H., XIAO, Y., CHE, R., XU, F., HU, B., LIANG, C., CHU, J., LI, J. & CHU, C. 2015. Activation of Big Grain1 significantly improves grain size by regulating auxin transport in rice. *Proceedings of the National Academy of Sciences,* 112**,** 11102-11107.

LIU, Q., WANG, Q., DENG, W., WANG, X., PIAO, M., CAI, D., LI, Y., BARSHOP, W. D., YU, X. & ZHOU, T. 2017. Molecular basis for blue light-dependent phosphorylation of

Arabidopsis cryptochrome 2. *Nature communications,* 8**,** 1-12.

MISHRA, B. S., JAMSHEER, K. M., SINGH, D., SHARMA, M. & LAXMI, A. 2017. Genome-Wide Identification and Expression, Protein-Protein Interaction and Evolutionary Analysis of the Seed Plant-Specific BIG GRAIN and BIG GRAIN LIKE Gene Family. *Frontiers in Plant Science,* 8**,** 1812.

MORIMOTO, K., OHAMA, N., KIDOKORO, S., MIZOI, J., TAKAHASHI, F., TODAKA, D., MOGAMI, J., SATO, H., QIN, F. & KIM, J.-S. 2017. BPM-CUL3 E3 ligase modulates thermotolerance by facilitating negative regulatory domain-mediated degradation of DREB2A in Arabidopsis. *Proceedings of the National Academy of Sciences,* 114**,** E8528-E8536.

NI, W., XU, S.-L., GONZÁLEZ-GRANDÍO, E., CHALKLEY, R. J., HUHMER, A. F., BURLINGAME, A. L., WANG, Z.-Y. & QUAIL, P. H. 2017. PPKs mediate direct signal transfer from phytochrome photoreceptors to transcription factor PIF3. *Nature Communications,* 8**,** 1-11.

PEDMALE, U. V. & LISCUM, E. 2007. Regulation of phototropic signaling in Arabidopsis via phosphorylation state changes in the phototropin 1-interacting protein NPH3. *Journal Biological Chemistry,* 282**,** 19992-20001.

PREUTEN, T., BLACKWOOD, L., CHRISTIE, J. M. & FANKHAUSER, C. 2015. Lipid anchoring of Arabidopsis phototropin 1 to assess the functional significance of receptor internalization: should I stay or should I go? *New Phytologist,* 206**,** 1038-1050.

REED, J. W., NAGPAL, P., POOLE, D. S., FURUYA, M. & CHORY, J. 1993. Mutations in the gene for the red/far-red light receptor phytochrome B alter cell elongation and physiological responses throughout Arabidopsis development. *The Plant Cell,* 5**,** 147-157.

SCHEPENS, I., BOCCALANDRO, H. E., KAMI, C., CASAL, J. J. & FANKHAUSER, C. 2008.

PHYTOCHROME KINASE SUBSTRATE4 modulates phytochrome-mediated control of hypocotyl growth orientation. *Plant Physiology,* 147**,** 661-671.

SCHUMACHER, K., VAFEADOS, D., MCCARTHY, M., SZE, H., WILKINS, T. & CHORY, J. 1999. The Arabidopsis det3 mutant reveals a central role for the vacuolar H+–ATPase in plant growth and development. *Genes & development,* 13**,** 3259-3270.

SCHUMACHER, P., DEMARSY, E., WARIDEL, P., PETROLATI, L. A., TREVISAN, M. & FANKHAUSER, C. 2018. A phosphorylation switch turns a positive regulator of phototropism into an inhibitor of the process. *Nature Communications,* 9**,** 1-9.

SULLIVAN, S., THOMSON, C. E., LAMONT, D. J., JONES, M. A. & CHRISTIE, J. M. 2008. In vivo phosphorylation site mapping and functional characterization of Arabidopsis phototropin 1. *Molecular Plant,* 1**,** 178-194.

SUN, N., WANG, J., GAO, Z., DONG, J., HE, H., TERZAGHI, W., WEI, N., DENG, X. W. & CHEN, H. 2016. Arabidopsis SAURs are critical for differential light regulation of the development of various organs. *Proceedings of the National Academy of Sciences,* 113**,** 6071-6076.

VAZQUEZ, A. L., PETROLATI, L. A., DESSIMOZ, C., LAMPUGNANI, E. R., GLOVER, N. & FANKHAUSER, C. 2022. Control of PHYTOCHROME KINASE SUBSTRATE subcellular localization and biological activity by protein S-acylation. *bioRxiv*.

WEBER, H., BERNHARDT, A., DIETERLE, M., HANO, P., MUTLU, A., ESTELLE, M., GENSCHIK, P. & HELLMANN, H. 2005. Arabidopsis AtCUL3a and AtCUL3b form complexes with members of the BTB/POZ-MATH protein family. *Plant Physiology,* 137**,** 83-93.

WEBER, H. & HELLMANN, H. 2009. Arabidopsis thaliana BTB/ POZ-MATH proteins interact with members of the ERF/AP2 transcription factor family. *The FEBS Journal,* 276**,** 6624-

6635.

WYWIAL, E. & SINGH, S. M. 2010. Identification and structural characterization of FYVE
domain-containing proteins of Arabidopsis thaliana. *BMC Plant Biology,* 10**,** 1-15.

ZHUANG, M., CALABRESE, M. F., LIU, J., WADDELL, M. B., NOURSE, A., HAMMEL, M.,
MILLER, D. J., WALDEN, H., DUDA, D. M. & SEYEDIN, S. N. 2009. Structures of
SPOP-substrate complexes: insights into molecular architectures of BTB-Cul3 ubiquitin
ligases. *Molecular cell,* 36**,** 39-50.

ACKNOWLEDGEMENTS

GENERAL DISCUSSION AND OUTLOOK

In the present work, we identified PKS genes in all angiosperms and a few gymnosperms but we could not find them in earlier appearing organisms in the green lineage, suggesting that the PKS proteins appeared in evolution later than their associated phot and phy photoreceptors (Ch 1, Fig. 1a) (Li and Mathews, 2016, Christie et al., 2018). A combined phylogenetic and experimental analysis suggested that PKS4 is the family member appearing the earliest in evolution and whose function in phototropism is conserved in *B. distachyon,* suggesting PKS4 conservation in monocots (Ch 2, Fig. 9, and 10). We could complement *pks4* with the PKS4 ortholog from the basal angiosperm *A. trichopoda* in response to RL, suggesting a co-evolution of PKS4 and phyB signaling components (Ch 2, Fig. 7A).

Our main goal of unrevealing how PKS proteins work to trigger organ differential growth led us to undertake a PKS structure-function analysis. Our phylogenetic studies identified 6 evolutionary conserved motifs shared by all the angiosperms PKS (motifs A to F) that we hypothesized to be functionally important (Ch 1, Fig.1b). Therefore, we mutated the highly conserved amino acids of each of these motifs in PKS4 to test their complementation potential. Our data showed that conserved motifs C and D are essential for PKS4 function in phototropism in response to unilateral LBL (Ch 1, Fig 4, Ch 3, Fig. 2D, 2E, 4C). Additionally, motifs C and D are also required for inhibition of hypocotyl gravitropism in response to RL, suggesting the common importance of these motifs in hypocotyl growth orientation in response to BL and RL (Ch 1, Fig. 4D and Ch 3, Fig. 4C).

In chapter 1, we studied the mode of action of PKS4 motif C. Our studies showed that conserved PKS4 and PKS1 motif C Cys amino acids are s-acylated and required for association with the PM

(Fig. 3) (Kumar et al., 2022). PKS4 contains 2 conserved Cys whose replacement to Serine (Ser) prevented PKS4 function (Fig. 4). We did not test the functional relevance of PKS1 motif C, which contains an additional conserved Cys, but given that PKS1 can function as PKS4, we propose that PKS1 shares the mechanism of action concerning motif C. Nevertheless, it will be interesting to test whether the conserved Cys are also required for function and subcellular localization of PKS2 and PKS3, whose divergence included changes in subcellular localization and function, in addition to expression patterns (Ch 2, Fig. 1C and 1D, and 4) (Schepens et al., 2008, de Carbonnel et al., 2010) (Legris Martina, personal communication). Our data did not reveal a role of the invariant Cys in motif F in function nor subcellular localization, however, a deeper analysis of this Cys might reveal a yet to be discovered role (Ch 1, Fig S2c and S2e). Moreover, the importance of the rest of the highly conserved amino acids in motif F has not been addressed.

Our data further proposed that the mode of association with the PM affects PKS4 function, given that bringing the PKS4 C* variant to the PM by the addition of N-terminal myristoylation (myri-) or a C-terminal farnesylation (-farn) sequence did not complement the *pks4* phenotype (Fig. 5 and S3). In the discussion of chapter 1, we hypothesized that the permanent attachment to the PM through myri- or -farn might affect PKS4 N- or C-terminal freedom to engage with potential protein interactions to function. However, WT PKS4 associated with the PM through myri- or -farn only slightly interfered with function (Fig. 5 and S3). Therefore, we should not exclude the possibility that motif C Cys s-acylation might have an additional function other than associating PKS with the PM. For instance, internalization, as it has been reported for NPH3 in response to light (Sullivan et al., 2021). Other possible roles might include mediating some protein dynamics at the PM in response to light, as it has been proposed for phot1 functioning in specific lipid regions (Xue et al., 2018). However, we did not observe light-regulated dynamics of PKS proteins. More detailed

observations would be needed to determine whether there are some differences in subcellular localization in response to light. Moreover, given that PKS4, PKS1, and PKS2 can be found in a protein complex, an additional hypothesis could be that the conserved Cys in PKS motif C are involved in forming disulfide bonds to interact with each other (Ch 2, Fig. 4) (Lariguet et al., 2006, de Carbonnel et al., 2010, Schumacher et al., 2018, Vazquez et al., 2022). A working model involving direct interaction of PKS proteins might explain the more aggravated phenotypes shown in the higher-order *pks* mutants in comparison with the added effect of the single mutant phenotypes (Kami et al., 2014a). Moreover, identifying and studying the enzymes that mediate these Cys s-acylation and de-s-acylation might be helpful to our understanding of the molecular mechanisms concerning motif C.

In chapter 3, we showed that the strictly conserved DLFEIE amino acids comprising motif D are essential for PKS4 function in phot and phy signaling, given that mutating them abolished the function (Fig. 2E and 4C). Moreover, a detailed functional analysis revealed that mutating the D276, F278, and/or E279 amino acids was enough to abolish the function in phototropism and further aggravate the phenotype (Fig. 6). This, together with the fact that mutating the F278 and E279 together prevented the interaction with all the candidates found to interact with PKS4 motif D, suggest a central role of the F278 E279 amino acids in the molecular mechanisms concerning PKS motif D (Fig. 7 and 8). Interestingly, the F278 E279 amino acids in PKS motif D are shared by all the BG protein family members. Therefore, it will be interesting to study whether, in addition to participating in auxin signaling and/or transport, BG proteins have a role in response to light (Liu et al., 2015, Mishra et al., 2017).

Our Y2H screening identified two motif D interacting candidates: BPM4 and a member that we described as PDIP, both containing a BTB domain as NPH3, which is required for phototropism

over a broad range of BL intensities (Gingerich et al., 2007, Christie et al., 2018). Interestingly, our data showed that PDIP can interact with PKS4 and PKS1, while BPM4 can interact with PKS4 and PKS2 (Fig. 9A). Given that PKS4 works with PKS1 to promote phototropism in LBL, and PKS2 rather functions in HBL, we could speculate that PDIP might work with NPH3, PKS4, and PKS1 in LBL while BPM might act with NPH3, PKS2, and PKS4 in HBL (Kami et al., 2014a). We should not rule out the possibility of BPM having a role in leaf elevation response, where PKS2 has a function. We are currently analyzing the importance of BPM and PDIP for phototropism to determine the conditions in which they are important. The phototropic curvature defect in the *bpm4* and *bpm34* mutants in LBL was very mild and only observable in the early stages of phototropism (Fig. 13). Higher-order mutants of BPM will need to be tested to determine the functional importance of BPM in LBL and HBL. We found PKS motif D to interact with BPM through its MATH domain, which is proposed to act as a substrate adaptor of E3 ubiquitin ligases (Fig. 10) (Weber et al., 2005). Therefore, although we did not find an obvious role of BPM in PKS4 protein abundance regulation, it is still to be determined whether PKS4 is ubiquitinated.

Our work also identified the photo-regulatory protein kinases PPK4 and PPK3 to interact with PKS4 motif D, however, they did not interact with any of the other *A. thaliana* PKS protein family members (Figure 9). As for cry interaction with PPK, our Y2H screening revealed that PKS4 interacts with PPK through the C-terminal part that does not contain the PPK catalytic kinase domain (Liu et al., 2017). Therefore, we hypothesize that PPK could regulate phototropism through the interaction with PKS4 by controlling important phosphorylation changes in phot1 signaling components like PKS4, phot1, or NPH3, similar to the mechanisms through which PPK proteins control cry2 activity in response to BL (Sullivan et al., 2008, Demarsy et al., 2012, Liu et al., 2017, Schumacher et al., 2018, Sullivan et al., 2021). Given that our data showed no BPM-mediated regulation of PKS4 protein abundance, we could speculate that PPK proteins might be involved in

PKS4 degradation in response to light through a similar mechanism through which cry2 is degraded by the LRB E3 ubiquitin ligases in a PPK-dependent manner (Fig. 12B) (Chen et al., 2021). Additionally, given that PPKs also play a role in RL signaling by inducing PIF3 phosphorylation and degradation, we should not exclude a possible role of PPK in controlling inhibition of gravitropism, where PKS4 also has a function, through PIFs-degradation (Schepens et al., 2008, Christie et al., 2011, Dong et al., 2017, Ni et al., 2017). The lab is currently addressing the importance of PPK in BL and RL signaling.

Moreover, we show that RLD2 and RLD4 interact with all the PKS protein family members' motif D (Fig. 7, 8, and 9). The analysis of the Y2H screening determined that this interaction occurred in PKS4 through the RLD C-terminal BRX domain. Through a collaboration with Miyo Morita's lab, which is analyzing the co-crystal structure of motif D-BRX, we are currently making a functional characterization of the RLD family to determine their importance in hypocotyl growth orientation. Importantly, LZY recruits RLD at the PM through the BRX domain to regulate auxin transport by relocating PIN3 in response to gravity stimuli (Furutani et al., 2020). Therefore, we can hypothesize a model in which, similarly to LZY, PKS recruits RLD through the BRX domain to control auxin transport in response to light stimuli.

Although this work focused on the study of the mode of action of PKS motifs C and D, the role of motifs A, B, E, and F remains to be determined (Ch 3, Fig. 2 and 4). Our functional studies were based on phototropism experiments in which we analyzed the response after 24h of LBL. Measuring the hypocotyl bending kinetics from the start of the light treatment might suggest an influence earlier in the phototropic curvature. Given that we found that PKS1 can function as PKS4 in phototropism and inhibition of gravitropism, it could be possible that we did not observe a phenotype in the PKS4 mutated motifs variants because PKS1 might take over the function of the

PKS4 mutated motifs. Complementation of the *pks1pks4* double mutant with the mutated motif PKS4 variants might be a good strategy to help our understanding of the role of these motifs in promoting phototropism in LBL. Moreover, we should not exclude a possible role of these motifs in the regulation of phototropism at higher light fluence, where PKS4 has an inhibitory role (Demarsy et al., 2012, Schumacher et al., 2018). An additional motif called G appears in many PKS proteins between motifs C and D, but it is absent in Brassicaceae PKS4 and PKS3, so we did not test its requirement in this work (Vazquez et al., 2022). The high conservation of these motifs in PKS proteins suggests that they were under positive selection, so it would be interesting to test their importance in other phot- mediated responses in which other PKS family members are involved.

LITERATURE CITED

BALLARÉ, C. L. & PIERIK, R. 2017. The shade-avoidance syndrome: Multiple signals and ecological consequences. *Plant, cell & environment,* 40**,** 2530-2543.

BLAKESLEE, J. J., BANDYOPADHYAY, A., PEER, W. A., MAKAM, S. N. & MURPHY, A. S. 2004. Relocalization of the PIN1 auxin efflux facilitator plays a role in phototropic responses. *Plant Physiology,* 134**,** 28-31.

BOCCACCINI, A., LEGRIS, M., KRAHMER, J., ALLENBACH-PETROLATI, L., GOYAL, A., GALVAN-AMPUDIA, C., VERNOUX, T., KARAYEKOV, E., CASAL, J. J. & FANKHAUSER, C. 2020. Low blue light enhances phototropism by releasing cryptochrome1-mediated inhibition of PIF4 expression. *Plant Physiology,* 183**,** 1780-1793.

BOCCALANDRO, H. E., DE SIMONE, S. N., BERGMANN-HONSBERGER, A., SCHEPENS, I., FANKHAUSER, C. & CASAL, J. J. 2008. PHYTOCHROME KINASE SUBSTRATE1 regulates root phototropism and gravitropism. *Plant Physiology,* 146**,** 108-115.

BURGIE, E. S. & VIERSTRA, R. D. 2014. Phytochromes: an atomic perspective on photoactivation and signaling. *The Plant Cell,* 26**,** 4568-4583.

CHEN, M., CHORY, J. & FANKHAUSER, C. 2004. Light signal transduction in higher plants. *Annual review of genetics,* 38**,** 87-117.

CHEN, Y., HU, X., LIU, S., SU, T., HUANG, H., REN, H., GAO, Z., WANG, X., LIN, D. & WOHLSCHLEGEL, J. A. 2021. Regulation of Arabidopsis photoreceptor CRY2 by two distinct E3 ubiquitin ligases. *Nature communications,* 12**,** 1-14.

CHRISTIE, J. M. 2007. Phototropin blue-light receptors. *Annual review of Plant Biology,*

58**,** 21-45.

CHRISTIE, J. M., ARVAI, A. S., BAXTER, K. J., HEILMANN, M., PRATT, A. J., O'HARA, A., KELLY, S. M., HOTHORN, M., SMITH, B. O. & HITOMI, K. 2012. Plant UVR8 photoreceptor senses UV-B by tryptophan-mediated disruption of cross-dimer salt bridges. *Science,* 335**,** 1492-1496.

CHRISTIE, J. M., BLACKWOOD, L., PETERSEN, J. & SULLIVAN, S. 2015. Plant flavoprotein photoreceptors. *Plant and Cell Physiology,* 56**,** 401-413.

CHRISTIE, J. M. & MURPHY, A. S. 2013. Shoot phototropism in higher plants: new light through old concepts. *American journal of botany,* 100 1**,** 35-46.

CHRISTIE, J. M., SUETSUGU, N., SULLIVAN, S. & WADA, M. 2018. Shining Light on the Function of NPH3/RPT2-Like Proteins in Phototropin Signaling. *Plant Physiology,* 176**,** 1015-1024.

CHRISTIE, J. M., YANG, H., RICHTER, G. L., SULLIVAN, S., THOMSON, C. E., LIN, J., TITAPIWATANAKUN, B., ENNIS, M., KAISERLI, E., LEE, O. R., ADAMEC, J., PEER, W. A. & MURPHY, A. S. 2011. phot1 inhibition of ABCB19 primes lateral auxin fluxes in the shoot apex required for phototropism. *PLoS Biology,* 9**,** e1001076.

CORRELL, M. J. & KISS, J. Z. 2002. Interactions between gravitropism and phototropism in plants. *Journal of plant growth regulation,* 21, 89-101.

DE CARBONNEL, M., DAVIS, P., ROELFSEMA, M. R., INOUE, S., SCHEPENS, I., LARIGUET, P., GEISLER, M., SHIMAZAKI, K., HANGARTER, R. & FANKHAUSER, C. 2010. The Arabidopsis PHYTOCHROME KINASE SUBSTRATE2 protein is a phototropin signaling element that regulates leaf flattening and leaf positioning. *Plant Physiology,* 152**,** 1391-405.

DEMARSY, E., SCHEPENS, I., OKAJIMA, K., HERSCH, M., BERGMANN, S., CHRISTIE, J., SHIMAZAKI, K., TOKUTOMI, S. & FANKHAUSER, C. 2012. Phytochrome Kinase Substrate 4 is phosphorylated by the phototropin 1 photoreceptor. *The EMBO journal,* 31**,** 3457-3467.

DING, Z., GALVAN-AMPUDIA, C. S., DEMARSY, E., LANGOWSKI, L., KLEINE-VEHN, J., FAN, Y., MORITA, M. T., TASAKA, M., FANKHAUSER, C., OFFRINGA, R. & FRIML, J. 2011. Light-mediated polarization of the PIN3 auxin transporter for the phototropic response in Arabidopsis. *Nature Cell Biology,* 13**,** 447-52.

DONG, J., NI, W., YU, R., DENG, X. W., CHEN, H. & WEI, N. 2017. Light-dependent degradation of PIF3 by SCFEBF1/2 promotes a photomorphogenic response in Arabidopsis. *Current Biology,* 27**,** 2420-2430. e6.

DU, M., SPALDING, E. P. & GRAY, W. M. 2020. Rapid auxin-mediated cell expansion. *Annual review of plant biology,* 71**,** 379-402.

FANG, F., LIN, L., ZHANG, Q., LU, M., SKVORTSOVA, M. Y., PODOLEC, R., ZHANG, Q., PI, J., ZHANG, C. & ULM, R. 2022. Mechanisms of UV-B light-induced photoreceptor UVR8 nuclear localization dynamics. *New Phytologist*, 236, 1824-1837.

FANKHAUSER, C. & CHRISTIE, J. M. 2015. Plant phototropic growth. *Current Biology,* 25**,** R384-R389.

FANKHAUSER, C., YEH, K.-C., CLARK, J., ZHANG, H., ELICH, T. D. & CHORY, J. 1999. PKS1, a substrate phosphorylated by phytochrome that modulates light signaling in Arabidopsis. *Science*, 284**,** 1539-1541.

FIORUCCI, A.-S. & FANKHAUSER, C. 2017. Plant strategies for enhancing access to sunlight. *Current Biology,* 27**,** R931-R940.

FIORUCCI, A.-S., MICHAUD, O., SCHMID-SIEGERT, E., TREVISAN, M., ALLENBACH

PETROLATI, L., ÇAKA INCE, Y. & FANKHAUSER, C. 2022. Shade suppresses wound-induced leaf repositioning through a mechanism involving PHYTOCHROME KINASE SUBSTRATE (PKS) genes. *PLoS Genetics,* 18**,** e1010213.

FRANKLIN, K. A. 2008. Shade avoidance. *New Phytologist,* 179**,** 930-944.

FRANKLIN, K. A. & QUAIL, P. H. 2010. Phytochrome functions in Arabidopsis development. *Journal of experimental botany,* 61**,** 11-24.

FRIML, J., WIŚNIEWSKA, J., BENKOVÁ, E., MENDGEN, K. & PALME, K. 2002. Lateral relocation of auxin efflux regulator PIN3 mediates tropism in Arabidopsis. *Nature*, 415**,** 806-809.

FURUTANI, M., HIRANO, Y., NISHIMURA, T., NAKAMURA, M., TANIGUCHI, M., SUZUKI, K., OSHIDA, R., KONDO, C., SUN, S. & KATO, K. 2020. Polar recruitment of RLD by LAZY1-like protein during gravity signaling in root branch angle control. *Nature Communications,* 11**,** 1-13.

GALEN, C., HUDDLE, J. & LISCUM, E. 2004. An experimental test of the adaptive evolution of phototropins: blue-light photoreceptors controlling phototropism in Arabidopsis thaliana. *Evolution,* 58**,** 515-523.

GALVÃO, V. C. & FANKHAUSER, C. 2015. Sensing the light environment in plants: photoreceptors and early signaling steps. *Current opinion in neurobiology,* 34**,** 46-53.

GELDNER, N., ANDERS, N., WOLTERS, H., KEICHER, J., KORNBERGER, W., MULLER, P., DELBARRE, A., UEDA, T., NAKANO, A. & JÜRGENS, G. 2003. The Arabidopsis GNOM ARF-GEF mediates endosomal recycling, auxin transport, and auxin-dependent plant growth. *Cell,* 112**,** 219-230.

GELDNER, N., FRIML, J., STIERHOF, Y.-D., JÜRGENS, G. & PALME, K. 2001. Auxin transport inhibitors block PIN1 cycling and vesicle trafficking. *Nature,* 413**,** 425-428.

GINGERICH, D. J., HANADA, K., SHIU, S.-H. & VIERSTRA, R. D. 2007. Large-scale, lineage-specific expansion of a bric-a-brac/tramtrack/broad complex ubiquitin-ligase gene family in rice. *The Plant Cell,* 19**,** 2329-2348.

GOMMERS, C. M. & MONTE, E. 2018. Seedling establishment: a dimmer switch-regulated process between dark and light signaling. *Plant physiology,* 176**,** 1061-1074.

GOYAL, A., SZARZYNSKA, B. & FANKHAUSER, C. 2013. Phototropism: at the crossroads of light-signaling pathways. *Trends in plant science,* 18**,** 393-401.

HAGA, K., TSUCHIDA-MAYAMA, T., YAMADA, M. & SAKAI, T. 2015. Arabidopsis ROOT PHOTOTROPISM2 Contributes to the Adaptation to High-Intensity Light in Phototropic Responses. *The Plant Cell,* 27**,** 1098-112.

HARADA, A., TAKEMIYA, A., INOUE, S., SAKAI, T. & SHIMAZAKI, K. 2013. Role of RPT2 in leaf positioning and flattening and a possible inhibition of phot2 signaling by phot1. *Plant and Cell Physiology,* 54**,** 36-47.

HARPER, S. M., NEIL, L. C. & GARDNER, K. H. 2003. Structural basis of a phototropin light switch. *Science*, 301**,** 1541-1544.

HOHM, T., DEMARSY, E., QUAN, C., ALLENBACH PETROLATI, L., PREUTEN, T., VERNOUX, T., BERGMANN, S. & FANKHAUSER, C. 2014. Plasma membrane H(+) - ATPase regulation is required for auxin gradient formation preceding phototropic growth. *Molecular Systems Biology,* 10**,** 751.

HOHM, T., PREUTEN, T. & FANKHAUSER, C. 2013. Phototropism: translating light into directional growth. *American Journal of Botany,* 100**,** 47-59.

HOLLAND, J. J., ROBERTS, D. & LISCUM, E. 2009. Understanding phototropism: from Darwin to today. *Journal of Experimental Botany,* 60**,** 1969-1978.

INADA, S., OHGISHI, M., MAYAMA, T., OKADA, K. & SAKAI, T. 2004. RPT2 is a signal transducer involved in phototropic response and stomatal opening by association with phototropin 1 in Arabidopsis thaliana. *Plant Cell,* 16**,** 887-896.

INOUE, S., KINOSHITA, T., TAKEMIYA, A., DOI, M. & SHIMAZAKI, K. 2008. Leaf positioning of Arabidopsis in response to blue light. *Molecular Plant,* 1**,** 15-26.

INOUE, S., MATSUSHITA, T., TOMOKIYO, Y., MATSUMOTO, M., NAKAYAMA, K. I., KINOSHITA, T. & SHIMAZAKI, K. 2011. Functional analyses of the activation loop of phototropin2 in Arabidopsis. *Plant Physiology,* 156**,** 117-28.

JANOUDI, A. & POFF, K. L. 1990. A common fluence threshold for first positive and second positive phototropism in Arabidopsis thaliana. *Plant physiology,* 94**,** 1605-1608.

KAMI, C., ALLENBACH, L., ZOURELIDOU, M., LJUNG, K., SCHÜTZ, F., ISONO, E., WATAHIKI, M. K., YAMAMOTO, K. T., SCHWECHHEIMER, C. & FANKHAUSER, C. 2014. Reduced phototropism in pks mutants may be due to altered auxin-regulated gene expression or reduced lateral auxin transport. *The Plant Journal,* 77**,** 393-403.

KAMI, C., HERSCH, M., TREVISAN, M., GENOUD, T., HILTBRUNNER, A., BERGMANN, S. & FANKHAUSER, C. 2012. Nuclear phytochrome A signaling promotes phototropism in Arabidopsis. *The Plant Cell,* 24**,** 566-576.

KAMI, C., LORRAIN, S., HORNITSCHEK, P. & FANKHAUSER, C. 2010. Light-regulated plant growth and development. *Current topics in developmental biology,* 91, 29-66.

KAWAMOTO, N. & MORITA, M. T. 2022. Gravity sensing and responses in the coordination of the shoot gravitropic set point angle. *New Phytologist*, 236, 1637-1654.

KIKIS, E. A., OKA, Y., HUDSON, M. E., NAGATANI, A. & QUAIL, P. H. 2009. Residues clustered in the light-sensing knot of phytochrome B are necessary for conformer-specific binding to signaling partner PIF3. *PLoS genetics,* 5**,** e1000352.

KIM, J., SONG, K., PARK, E., KIM, K., BAE, G. & CHOI, G. 2016a. Epidermal phytochrome B inhibits hypocotyl negative gravitropism non-cell-autonomously. *The Plant Cell,* 28**,** 2770-2785.

KIM, K., JEONG, J., KIM, J., LEE, N., KIM, M. E., LEE, S., KIM, S. C. & CHOI, G. 2016b. PIF1 regulates plastid development by repressing photosynthetic genes in the endodermis. *Molecular plant,* 9**,** 1415-1427.

KIM, K., SHIN, J., LEE, S.-H., KWEON, H.-S., MALOOF, J. N. & CHOI, G. 2011. Phytochromes inhibit hypocotyl negative gravitropism by regulating the development of endodermal amyloplasts through phytochrome-interacting factors. *Proceedings of the National Academy of Sciences,* 108**,** 1729-1734.

KONG, S. G., SUZUKI, T., TAMURA, K., MOCHIZUKI, N., HARA-NISHIMURA, I. & NAGATANI, A. 2006. Blue light-induced association of phototropin 2 with the Golgi apparatus. *The Plant Journal,* 45**,** 994-1005.

KOZUKA, T., SUETSUGU, N., WADA, M. & NAGATANI, A. 2013. Antagonistic regulation of leaf flattening by phytochrome B and phototropin in Arabidopsis thaliana. *Plant Cell Physiology,* 54**,** 69-79.

LARIGUET, P., BOCCALANDRO, H. E., ALONSO, J. M., ECKER, J. R., CHORY, J., CASAL, J. J. & FANKHAUSER, C. 2003. A growth regulatory loop that provides homeostasis to phytochrome a signaling. *The Plant Cell,* 15**,** 2966-2978.

LARIGUET, P. & FANKHAUSER, C. 2004. Hypocotyl growth orientation in blue light is determined by phytochrome A inhibition of gravitropism and phototropin promotion of phototropism. *The Plant Journal,* 40**,** 826-834.

LARIGUET, P., SCHEPENS, I., HODGSON, D., PEDMALE, U. V., TREVISAN, M., KAMI, C., DE CARBONNEL, M., ALONSO, J. M., ECKER, J. R. & LISCUM, E. 2006.

PHYTOCHROME KINASE SUBSTRATE 1 is a phototropin 1 binding protein required for phototropism. *Proceedings of the National Academy of Sciences,* 103**,** 10134-10139.

LAU, K., PODOLEC, R., CHAPPUIS, R., ULM, R. & HOTHORN, M. 2019. Plant photoreceptors and their signaling components compete for COP1 binding via VP peptide motifs. *The EMBO journal,* 38**,** e102140.

LEGRIS, M. & BOCCACCINI, A. 2020. Stem phototropism toward blue and ultraviolet light. *Physiologia plantarum,* 169**,** 357-368.

LEGRIS, M., INCE, Y. Ç. & FANKHAUSER, C. 2019. Molecular mechanisms underlying phytochrome-controlled morphogenesis in plants. *Nature communications,* 10**,** 1-15.

LEGRIS, M., SZARZYNSKA-ERDEN, B. M., TREVISAN, M., ALLENBACH PETROLATI, L. & FANKHAUSER, C. 2021. Phototropin-mediated perception of light direction in leaves regulates blade flattening. *Plant physiology,* 187**,** 1235-1249.

LI, F.-W. & MATHEWS, S. 2016. Evolutionary aspects of plant photoreceptors. *Journal of plant research,* 129**,** 115-122.

LI, H., BURGIE, E. S., GANNAM, Z. T., LI, H. & VIERSTRA, R. D. 2022. Plant phytochrome B is an asymmetric dimer with unique signalling potential. *Nature,* 604**,** 127-133.

LI, L., GALLEI, M. & FRIML, J. 2021. Bending to auxin: fast acid growth for tropisms. *Trends in Plant Science,* 27, 440-449.

LIN, C., YANG, H., GUO, H., MOCKLER, T., CHEN, J. & CASHMORE, A. R. 1998. Enhancement of blue-light sensitivity of Arabidopsis seedlings by a blue light receptor cryptochrome 2. *Proceedings of the National Academy of Sciences,* 95**,** 2686-2690.

LIN, W., ZHOU, X., TANG, W., TAKAHASHI, K., PAN, X., DAI, J., REN, H., ZHU, X., PAN, S. & ZHENG, H. 2021. TMK-based cell-surface auxin signalling activates cell-wall acidification. *Nature,* 599**,** 278-282.

LISCUM, E., ASKINOSIE, S. K., LEUCHTMAN, D. L., MORROW, J., WILLENBURG, K. T. & COATS, D. R. 2014. Phototropism: growing towards an understanding of plant movement. *Plant Cell,* 26**,** 38-55.

LIU, H., WANG, Q., LIU, Y., ZHAO, X., IMAIZUMI, T., SOMERS, D. E., TOBIN, E. M. & LIN, C. 2013. Arabidopsis CRY2 and ZTL mediate blue-light regulation of the transcription factor CIB1 by distinct mechanisms. *Proceedings of the National Academy of Sciences,* 110**,** 17582-17587.

LIU, L., TONG, H., XIAO, Y., CHE, R., XU, F., HU, B., LIANG, C., CHU, J., LI, J. & CHU, C. 2015. Activation of Big Grain1 significantly improves grain size by regulating auxin transport in rice. *Proceedings of the National Academy of Sciences,* 112**,** 11102-11107.

LIU, Q., SU, T., HE, W., REN, H., LIU, S., CHEN, Y., GAO, L., HU, X., LU, H. & CAO, S. 2020. Photooligomerization determines photosensitivity and photoreactivity of plant cryptochromes. *Molecular plant,* 13**,** 398-413.

LIU, Q., WANG, Q., DENG, W., WANG, X., PIAO, M., CAI, D., LI, Y., BARSHOP, W. D., YU, X. & ZHOU, T. 2017. Molecular basis for blue light-dependent phosphorylation of Arabidopsis cryptochrome 2. *Nature communications,* 8**,** 1-12.

MIAO, L., ZHAO, J., YANG, G., XU, P., CAO, X., DU, S., XU, F., JIANG, L., ZHANG, S. & WEI, X. 2022. Arabidopsis cryptochrome 1 undergoes COP1 and LRBs-dependent degradation in response to high blue light. *New Phytologist,* 234**,** 1347-1362.

MILLENAAR, F. F., VAN ZANTEN, M., COX, M. C., PIERIK, R., VOESENEK, L. A. & PEETERS, A. J. 2009. Differential petiole growth in Arabidopsis thaliana: photocontrol and hormonal regulation. *New Phytologist,* 184**,** 141-152.

MISHRA, B. S., JAMSHEER, K. M., SINGH, D., SHARMA, M. & LAXMI, A. 2017. Genome-Wide Identification and Expression, Protein-Protein Interaction and Evolutionary

Analysis of the Seed Plant-Specific BIG GRAIN and BIG GRAIN LIKE Gene Family. *Frontiers in Plant Science,* 8**,** 1812.

MORITA, M. T. & TASAKA, M. 2004. Gravity sensing and signaling. *Current opinion in plant biology,* 7**,** 712-718.

MOTCHOULSKI, A. & LISCUM, E. 1999. Arabidopsis NPH3: a NPH1 photoreceptor- interacting protein essential for phototropism. *Science*, 286**,** 961-964.

NAKAMURA, M., NISHIMURA, T. & MORITA, M. T. 2019. Gravity sensing and signal conversion in plant gravitropism. *Journal of experimental botany,* 70**,** 3495-3506.

NI, W., XU, S.-L., GONZÁLEZ-GRANDÍO, E., CHALKLEY, R. J., HUHMER, A. F., BURLINGAME, A. L., WANG, Z.-Y. & QUAIL, P. H. 2017. PPKs mediate direct signal transfer from phytochrome photoreceptors to transcription factor PIF3. *Nature Communications,* 8**,** 1-11.

NI, W., XU, S.-L., TEPPERMAN, J. M., STANLEY, D. J., MALTBY, D. A., GROSS, J. D., BURLINGAME, A. L., WANG, Z.-Y. & QUAIL, P. H. 2014. A mutually assured destruction mechanism attenuates light signaling in Arabidopsis. *Science,* 344**,** 1160-1164.

NOH, B., BANDYOPADHYAY, A., PEER, W. A., SPALDING, E. P. & MURPHY, A. S. 2003. Enhanced gravi-and phototropism in plant mdr mutants mislocalizing the auxin efflux protein PIN1. *Nature*, 423**,** 999-1002.

NOH, B., MURPHY, A. S. & SPALDING, E. P. 2001. Multidrug resistance–like genes of Arabidopsis required for auxin transport and auxin-mediated development. *The Plant Cell,* 13**,** 2441-2454.

OH, E., KIM, J., PARK, E., KIM, J.-I., KANG, C. & CHOI, G. 2004. PIL5, a phytochrome-interacting basic helix-loop-helix protein, is a key negative regulator of seed germination

in Arabidopsis thaliana. *The Plant Cell,* 16**,** 3045-3058.

OH, J., PARK, E., SONG, K., BAE, G. & CHOI, G. 2020. PHYTOCHROME INTERACTING FACTOR8 inhibits phytochrome A-mediated far-red light responses in Arabidopsis. *The Plant Cell,* 32**,** 186-205.

PALMGREN, M. G. 2001. Plant plasma membrane H+-ATPases: powerhouses for nutrient uptake. *Annual review of plant physiology and plant molecular biology,* 52**,** 817-845.

PEDMALE, U. V. & LISCUM, E. 2007. Regulation of phototropic signaling in Arabidopsis via phosphorylation state changes in the phototropin 1-interacting protein NPH3. *J Biol Chem,* 282**,** 19992-20001.

PODOLEC, R., DEMARSY, E. & ULM, R. 2021. Perception and signaling of ultraviolet-B radiation in plants. *Annual Review of Plant Biology,* 72**,** 793-822.

PODOLEC, R. & ULM, R. 2018. Photoreceptor-mediated regulation of the COP1/SPA E3 ubiquitin ligase. *Current Opinion in Plant Biology,* 45**,** 18-25.

PONNU, J. & HOECKER, U. 2022. Signaling mechanisms by Arabidopsis cryptochromes. *Frontiers in Plant Science***,** 415.

PONNU, J., RIEDEL, T., PENNER, E., SCHRADER, A. & HOECKER, U. 2019. Cryptochrome 2 competes with COP1 substrates to repress COP1 ubiquitin ligase activity during Arabidopsis photomorphogenesis. *Proceedings of the National Academy of Sciences,* 116**,** 27133-27141.

PREUTEN, T., BLACKWOOD, L., CHRISTIE, J. M. & FANKHAUSER, C. 2015. Lipid anchoring of Arabidopsis phototropin 1 to assess the functional significance of receptor internalization: should I stay or should I go? *New Phytologist,* 206**,** 1038-1050.

REN, H., PARK, M. Y., SPARTZ, A. K., WONG, J. H. & GRAY, W. M. 2018. A subset of plasma membrane-localized PP2C.D phosphatases negatively regulate SAUR-mediated

cell expansion in Arabidopsis. *PLoS genetics,* 14**,** e1007455.

REUTER, L., SCHMIDT, T., MANISHANKAR, P.,THROM, C., KEICHER, J., BOCK, A., DROSTE-BOREL, I. & OECKING, C. 2021. Light-triggered and phosphorylation-dependent 14-3-3 association with NON-PHOTOTROPIC HYPOCOTYL 3 is required for hypocotyl phototropism. *Nature Communications,* 12**,** 1-15.

RIZZINI, L., FAVORY, J.-J., CLOIX, C., FAGGIONATO, D., O'HARA, A., KAISERLI, E., BAUMEISTER, R., SCHÄFER, E., NAGY, F. & JENKINS, G. I. 2011. Perception of UV-B by the Arabidopsis UVR8 protein. *Science*, 332**,** 103-106.

ROBSON, P. R. & SMITH, H. 1996. Genetic and transgenic evidence that phytochromes A and B act to modulate the gravitropic orientation of Arabidopsis thaliana hypocotyls. *Plant Physiology,* 110**,** 211-216.

SACK, F. D. 1997. Plastids and gravitropic sensing. *Planta,* 203**,** S63-S68.

SAKAI, T., WADA, T., ISHIGURO, S. & OKADA, K. J. T. P. C. 2000. RPT2: a signal transducer of the phototropic response in Arabidopsis. *The Plant Cell*, 12**,** 225-236.

SAKAMOTO, K. 2002. Cellular and Subcellular Localization of Phototropin 1. *The Plant Cell,* 14**,** 1723-1735.

SAWA, M., NUSINOW, D. A., KAY, S. A. & IMAIZUMI, T. 2007. FKF1 and GIGANTEA complex formation is required for day-length measurement in Arabidopsis. *Science,* 318**,** 261-265.

SCHEPENS, I., BOCCALANDRO, H. E., KAMI, C., CASAL, J. J. & FANKHAUSER, C. 2008. PHYTOCHROME KINASE SUBSTRATE 4 modulates phytochrome-mediated control of hypocotyl growth orientation. *Plant Physiology,* 147**,** 661-671.

SCHUMACHER, P.,DEMARSY, E., WARIDEL, P.,PETROLATI, L. A., TREVISAN, M. &

FANKHAUSER, C. 2018. A phosphorylation switch turns a positive regulator of phototropism into an inhibitor of the process. *Nature Communications,* 9**,** 1-9.

SHI, C. & LIU, H. 2021. How plants protect themselves from ultraviolet-B radiation stress. *Plant Physiology,* 187**,** 1096-1103.

SHIM, J. S., KUBOTA, A. & IMAIZUMI, T. 2017. Circadian clock and photoperiodic flowering in Arabidopsis: CONSTANS is a hub for signal integration. *Plant Physiology,* 173**,** 5-15.

SONG, Y. H., ESTRADA, D. A., JOHNSON, R. S., KIM, S. K., LEE, S. Y., MACCOSS, M. J. & IMAIZUMI, T. 2014. Distinct roles of FKF1, GIGANTEA, and ZEITLUPE proteins in the regulation of CONSTANS stability in Arabidopsis photoperiodic flowering. *Proceedings of the National Academy of Sciences,* 111**,** 17672-17677.

STRONG, D. R. & RAY, T. S. 1975. Host Tree Location Behavior of a Tropical Vine (Monstera gigantea) by Skototropism. *Science,* 190**,** 804-806.

SUETSUGU, N., TAKEMIYA, A., KONG, S. G., HIGA, T., KOMATSU, A., SHIMAZAKI, K., KOHCHI, T. & WADA, M. 2016. RPT2/NCH1 subfamily of NPH3-like proteins is essential for the chloroplast accumulation response in land plants. *Proceedings of the National Academy of Sciences,* 113**,** 10424-10429.

SULLIVAN, S., KHARSHIING, E., LAIRD, J., SAKAI, T. & CHRISTIE, J. M. 2019. Deetiolation Enhances Phototropism by Modulating NON-PHOTOTROPIC HYPOCOTYL3 Phosphorylation Status. *Plant Physiology*, 180**,** 1119-1131.

SULLIVAN, S., THOMSON, C. E., LAMONT, D. J., JONES, M. A. & CHRISTIE, J. M. 2008. In vivo phosphorylation site mapping and functional characterization of Arabidopsis phototropin 1. *Molecular Plant,* 1**,** 178-194.

SULLIVAN, S., WAKSMAN, T., PALIOGIANNI, D., HENDERSON, L., LÜTKEMEYER, M., SUETSUGU, N. & CHRISTIE, J. M. 2021. Regulation of plant phototropic growth by

NPH3/RPT2-like substrate phosphorylation and 14-3-3 binding. *Nature communications,* 12**,** 1-13.

TAKAHASHI, K., HAYASHI, K.-I. & KINOSHITA, T. 2012. Auxin activates the plasma membrane H+-ATPase by phosphorylation during hypocotyl elongation in Arabidopsis. *Plant physiology,* 159**,** 632-641.

TAKEMIYA, A., SUGIYAMA, N., FUJIMOTO, H., TSUTSUMI, T., YAMAUCHI, S., HIYAMA, A., TADA, Y., CHRISTIE, J. M. & SHIMAZAKI, K.-I. 2013. Phosphorylation of BLUS1 kinase by phototropins is a primary step in stomatal opening. *Nature communications,* 4**,** 1-8.

TANIGUCHI, M., FURUTANI, M., NISHIMURA, T., NAKAMURA, M., FUSHITA, T., IIJIMA, K., BABA, K., TANAKA, H., TOYOTA, M. & TASAKA, M. 2017. The Arabidopsis LAZY1 family plays a key role in gravity signaling within statocytes and in branch angle control of roots and shoots. *The Plant Cell,* 29**,** 1984-1999.

TITAPIWATANAKUN, B., BLAKESLEE, J. J., BANDYOPADHYAY, A., YANG, H., MRAVEC, J., SAUER, M., CHENG, Y., ADAMEC, J., NAGASHIMA, A. & GEISLER, M. 2009. ABCB19/PGP19 stabilises PIN1 in membrane microdomains in Arabidopsis. *The Plant Journal,* 57**,** 27-44.

TOKUTOMI, S., MATSUOKA, D. & ZIKIHARA, K. 2008. Molecular structure and regulation of phototropin kinase by blue light. *Biochimica et Biophysica Acta,* 1784**,** 133-42.

TSUTSUMI, T., TAKEMIYA, A., HARADA, A. & SHIMAZAKI, K. 2013. Disruption of ROOT PHOTOTROPISM2 gene does not affect phototropin-mediated stomatal opening. *Plant Science,* 201-202**,** 93-7.

VANDENBRINK, J. P. & KISS, J. Z. Plant responses to gravity. 2019. *Seminars in cell & developmental biology*, 92, 122-125.

VANDENBUSSCHE, F., PIERIK, R., MILLENAAR, F. F., VOESENEK, L. A. & VAN DER
STRAETEN, D. 2005. Reaching out of the shade. *Current opinion in plant biology,*
8**,** 462-468.

VANHAELEWYN, L., VICZIÁN, A., PRINSEN, E., BERNULA, P., SERRANO, A. M.,
ARANA, M. V., BALLARÉ, C. L., NAGY, F., VAN DER STRAETEN, D. &
VANDENBUSSCHE, F. 2019. Differential UVR8 signal across the stem controls UV-B–
induced inflorescence phototropism. *The Plant Cell,* 31**,** 2070-2088.

VAZQUEZ, A. L., PETROLATI, L. A., DESSIMOZ, C., LAMPUGNANI, E. R., GLOVER, N.
& FANKHAUSER, C. 2022. Control of PHYTOCHROME KINASE SUBSTRATE
subcellular localization and biological activity by protein S-acylation. *bioRxiv*.

WAN, Y., JASIK, J., WANG, L., HAO, H., VOLKMANN, D., MENZEL, D., MANCUSO, S.,
BALUSKA, F. & LIN, J. 2012. The signal transducer NPH3 integrates the phototropin1
photosensor with PIN2-based polar auxin transport in Arabidopsis root phototropism.
The Plant Cell, 24**,** 551-65.

WANG, Q., BARSHOP, W. D., BIAN, M., VASHISHT, A. A., HE, R., YU, X., LIU, B.,
NGUYEN, P., LIU, X. & ZHAO, X. 2015. The blue light-dependent phosphorylation of
the CCE domain determines the photosensitivity of Arabidopsis CRY2. *Molecular plant,*
8**,** 631-643.

WANG, Q. & LIN, C. 2020. Mechanisms of cryptochrome-mediated photoresponses in plants.
Annual Review of Plant Biology, 71**,** 103-129.

WANG, Q., ZUO, Z., WANG, X., GU, L., YOSHIZUMI, T., YANG, Z., YANG, L., LIU, Q.,
LIU, W. & HAN, Y.-J. 2016. Photoactivation and inactivation of Arabidopsis
cryptochrome 2. *Science,* 354**,** 343-347.

WEBER, H., BERNHARDT, A., DIETERLE, M., HANO, P., MUTLU, A., ESTELLE, M.,

GENSCHIK, P. & HELLMANN, H. 2005. Arabidopsis AtCUL3a and AtCUL3b form complexes with members of the BTB/POZ-MATH protein family. *Plant Physiology,* 137**,** 83-93.

WILLIGE, B. C., AHLERS, S., ZOURELIDOU, M., BARBOSA, I. C., DEMARSY, E., TREVISAN, M., DAVIS, P. A., ROELFSEMA, M. R., HANGARTER, R., FANKHAUSER, C. & SCHWECHHEIMER, C. 2013. D6PK AGCVIII kinases are required for auxin transport and phototropic hypocotyl bending in Arabidopsis. *Plant Cell,* 25**,** 1674-1688.

XUE, Y., XING, J., WAN, Y., LV, X., FAN, L., ZHANG, Y., SONG, K., WANG, L., WANG, X., DENG, X., BALUSKA, F., CHRISTIE, J. M. & LIN, J. 2018. Arabidopsis Blue Light Receptor Phototropin 1 Undergoes Blue Light-Induced Activation in Membrane Microdomains. *Molecular Plant,* 11**,** 846-859.